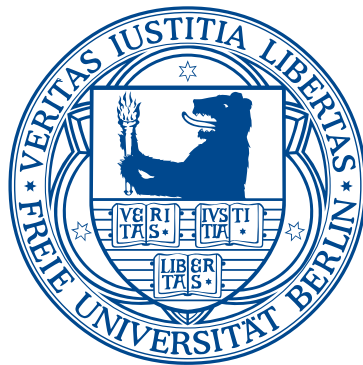


# **Quantum Phase Transition of Light in the Jaynes-Cummings Lattice**

**Diploma Thesis  
by  
Christian Nietner**



**Main Referee: Priv.-Doz. Dr. Axel Pelster**

**Submitted to the  
Department of Physics  
Freie Universität Berlin  
on September 28, 2010**



*“Catch the light, if you can  
Oh, hold it in your hands”*

FLY MY PRETTIES



# Contents

<b>1</b>	<b>Introduction</b>	<b>1</b>
1.1	Quantum Simulators . . . . .	1
1.2	Optical Lattices . . . . .	2
1.3	Cavity QED Lattices . . . . .	4
1.4	Outline of the Thesis . . . . .	7
<b>2</b>	<b>Jaynes-Cummings Model</b>	<b>9</b>
2.1	Quantization of the Free Electromagnetic Field . . . . .	9
2.2	Hamiltonian of a Two-Level System . . . . .	18
2.3	Interaction Hamiltonian . . . . .	20
2.4	Symmetry of the Interaction Hamiltonian . . . . .	22
2.5	Jaynes-Cummings Hamiltonian . . . . .	24
2.6	Polariton Mapping . . . . .	34
<b>3</b>	<b>Jaynes-Cummings-Hubbard Model</b>	<b>37</b>
3.1	Coupled Cavity Lattice . . . . .	38
3.2	Jaynes-Cummings-Hubbard Hamiltonian . . . . .	41
3.3	Atomic Limit . . . . .	42
3.4	Hopping Limit . . . . .	44
3.5	Mean-Field Theory . . . . .	47
3.6	Schrödinger Perturbation Theory . . . . .	49
3.7	Phase Boundary at Zero Temperature . . . . .	55
<b>4</b>	<b>Thermodynamic Properties</b>	<b>61</b>
4.1	Dirac Interaction Picture . . . . .	62
4.2	Mean-Field Theory for Finite Temperatures . . . . .	65
4.3	Strong-Coupling Perturbation Theory . . . . .	74
4.4	Cumulant Expansion . . . . .	77
4.5	Diagrammatic Expansion . . . . .	80
4.5.1	Diagrammatic Rules . . . . .	80
4.5.2	Diagram Weights . . . . .	82
4.6	Expansion of the Free Energy . . . . .	82
4.6.1	Second Order in the Currents . . . . .	84
4.6.2	Fourth Order in the Currents . . . . .	86
4.7	Ginzburg-Landau Action . . . . .	96

## Contents

---

<b>5 Results from Ginzburg-Landau Action</b>	<b>101</b>
5.1 Static Case . . . . .	101
5.2 Dynamic Case . . . . .	102
5.3 Excitation Spectra in the Mott Phase . . . . .	104
5.4 Energy Gap . . . . .	110
5.5 Effective Mass . . . . .	112
<b>6 Summary and Outlook</b>	<b>115</b>
<b>Bibliography</b>	<b>119</b>
<b>List of Figures</b>	<b>133</b>
<b>Danksagung</b>	<b>135</b>

# Chapter 1

## Introduction

When Max Planck introduced his famous quantum of action he could not possibly foresee the impact this would have on the further developments in physics. This “act of desperation“ as he put it, led to a completely new world view and subsequently to *quantum theory*, the most effective and accurate physical theory ever formulated by mankind. Although this theory describes an abstract subatomic world far from every day experience, its impact on our daily life could hardly be any greater. In fact, it enables and boosts spectacular advances in essentially every kind of science one can think of, and its influence is still increasing.

### 1.1 Quantum Simulators

Especially in the fields of information processing, material science, superfluidity and the relatively new field of quantum information theory, a profound understanding of strongly correlated quantum many-body systems is of striking importance in order to further improve existing applications and invent new ones [1–3]. This is due to the fact that, these research fields mainly use solid state systems in which strongly correlated systems appear quite naturally. However, it is experimentally very challenging to access the microscopic properties of such systems, due to the short time- and length scales involved. Therefore, motivated by Feynman’s conjecture of the quantum simulator [4], artificial structures have been considered to create effective many-body systems, which can be investigated more easily. One of the most important theoretical models for such systems is the Hubbard model proposed by John Hubbard in 1963 for strongly correlated electronic lattice systems [5]. Subsequently, this approach has been successfully applied to strongly correlated bosonic lattice systems as well, leading to the seminal Bose-Hubbard theory [6]. In this theoretical model, the bosonic many-particle system in the grand-canonical ensemble is described by the Hamiltonian

$$\hat{H}^{\text{BH}} = \frac{U}{2} \sum_i \hat{b}_i^\dagger \hat{b}_i (\hat{b}_i^\dagger \hat{b}_i - 1) - \mu \sum_i \hat{b}_i^\dagger \hat{b}_i - \kappa \sum_{\langle i,j \rangle} \hat{b}_i^\dagger \hat{b}_j. \quad (1.1)$$

Here, the operators  $\hat{b}_i^\dagger, \hat{b}_i$  are bosonic creation and annihilation operators. The parameter  $U$  characterises the on-site interaction strength and  $\mu$  is the grand-canonical chemical potential. The last term in equation (1.1) specifies the dynamics on the lattice, since the notation  $\langle i, j \rangle$  denotes a sum over next neighbouring lattice sites and  $\kappa$  represents the required energy for a particle to hop from one site to a neighbouring one. An interesting fact about this model is, that it includes a phase transition from a so called Mott insulator, where all particles are pinned to their respective lattice site, to a superfluid phase. This transition arises from the competitive influence of the on-site interaction and the next-neighbour hopping term. Since this kind of transition is driven by quantum fluctuations rather than thermal fluctuations, it is fundamentally different from ordinary thermodynamic phase transitions [7] and is, therefore, often referred to as a *quantum phase transition* [8].

## 1.2 Optical Lattices

The first attempts to build up artificial many-body structures used Josephson junction arrays [9, 10], which proved to be capable of simulating properties of the Bose-Hubbard model [11]. Additionally, over the last two decades, the advances in producing and controlling ultra cold atoms has presented a new experimental realization, which has raised a huge amount of interest and research. Indeed, ultra cold atoms are a very hot topic at the moment.

These new kind of systems are based on one of the most intriguing features of quantum mechanics, which has been the abolition of the classical, distinct views of light and matter in favour of a duality of both. This paradigm shift evolved to a whole new understanding of the fundamental constituents of matter. In consequence of this new theoretical insight Albert Einstein and Satyendranath Bose argued in 1924 that there exists a fourth state of matter [12, 13], which is significantly different to a gas, a solid or a liquid that we can perceive in our every day life. In fact, they conjectured that, if a dilute gas of bosons is cooled down to temperatures very close to absolute zero, all atoms condense into the same ground state and, thus, behave collectively as if they were one particle. This new state of matter is, indeed, so exotic, that it took 71 years before in 1995 the experimental groups of Eric Allin Cornell and Carl Edwin Wiemann in Boulder, Colorado [14] and Wolfgang Ketterle at the Massachusetts Institute of Technology in Cambridge, Massachusetts [15] could create such a so called *Bose-Einstein-Condensate* (BEC) for the first time. This fabulous experimental success, which was honoured with a Nobel prize in 2001, has been followed up by a variety of experiments investigating the properties of BEC's under different conditions. For example one investigated the interference of BEC clouds [16, 17], studied rotating BEC's [18, 19], observed spinor condensates [20], where BEC occurs in different hyperfine states, analysed Bose-Fermi mixtures [21], where a pure BEC is contaminated with fermions and, more recently, tried to probe the

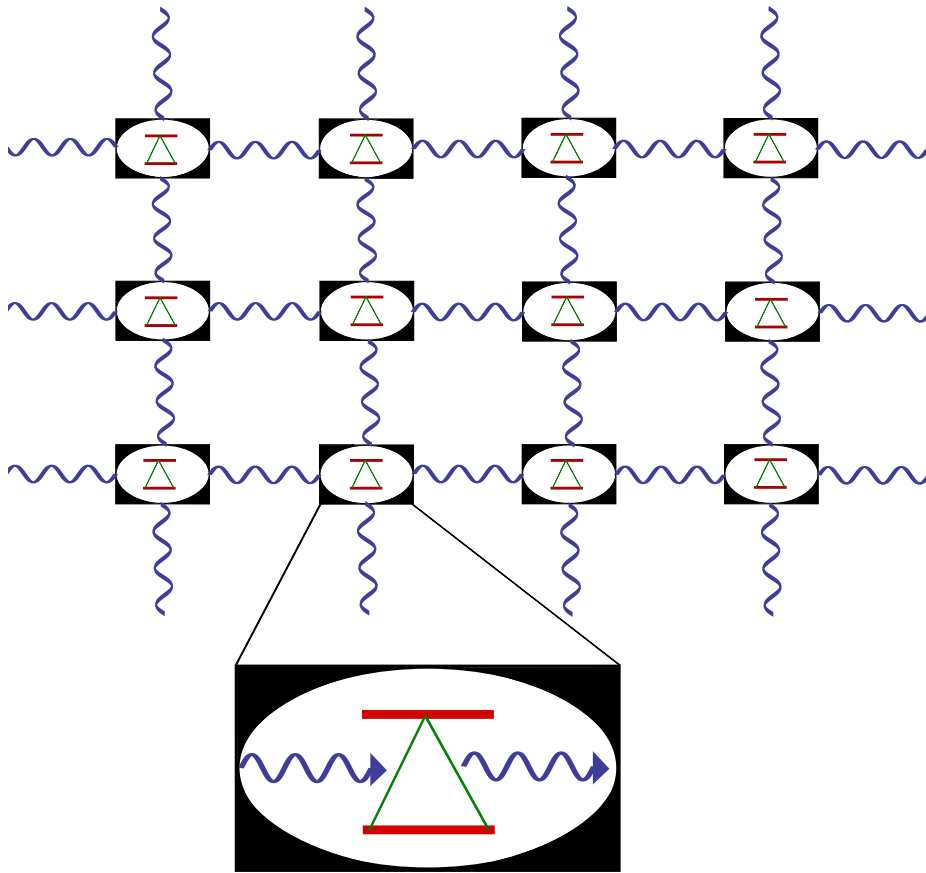


Figure 1.1: **Lattice built up of optical micro cavities.** In this special realization each micro cavity contains one atom exhibiting a two-level energy structure (red lines). The inter-atomic transition is indicated by the green lines. The blue lines correspond to the cavity light field coupled into the system.

properties of BEC's in zero gravity [22]. Of particular interest for the simulation of strongly correlated quantum many body systems, has been the realization of BEC's trapped in optical lattices [23, 24]. Here, the BEC cloud is loaded into an optical periodic potential created by standing laser fields. A non-vanishing probability for each boson to hop from one lattice site to a neighbouring site establishes a strong correlation throughout the lattice. This fact, together with a good experimental control of all important parameters, as well as the possibility to produce different lattice geometries in 1D, 2D or 3D, makes this kind of systems an excellent candidate for the simulation of strongly correlated bosonic systems [25]. Since their experimental realization, optical-lattice systems have initiated intensive studies and led to a multitude of new applications such as entanglement of atoms [26, 27], quantum teleportation [28], Bell state experiments [29], disorder [30–33] and ultra cold molecules [34, 35], to name but a few.

### 1.3 Cavity QED Lattices

Unfortunately, the experimental approaches discussed so far face some crucial limitations. On the one hand, it is necessary to cool down the considered system to some nano Kelvin above absolute zero and, on the other hand, it is experimentally very challenging to control and access single sites individually. For example, in order to obtain the information whether a BEC in an optical lattice is in the Mott or in the superfluid phase, one normally switches off the trap and observes the expansion of the BEC cloud. This leads to the desired information but for the cost of destroying the system under investigation. Recently, a new experimental approach has been established, where fluorescence imaging techniques allow to directly observe atoms in the Mott phase [38]. However, this technique still leads to a depletion of the cold atoms in the lattice and, thus, destroys the system.

These facts strongly restrict their utility as quantum simulators and their application in quantum information technology [39–41]. Especially in the latter, local on-site manipulation is absolutely necessary. For these reasons and encouraged by the latest progress in the fabrication and manipulation of micro cavities [37, 42, 43], Philippe Grangier and others [44–49] proposed a new experimental setup using cavity quantum electrodynamics (QED) schemes.

The underlying idea behind this new approach is pictured in Figure 1.1. Basically, one builds up a lattice from micro cavities and places some real or artificial atoms in each cavity, for example Josephson junctions or quantum dots. Subsequently, light is coupled into the system in such a way, that it can interact with the atoms. As a result, the coupling between the light field and the atomic transitions leads to the formation of bosonic quasi particles, so called polaritons. These quasi particles effectively behave just as real bosonic particles on the lattice. That means, for each polariton there exists a non-vanishing hopping probability to tunnel from one cavity to a neighbouring one, which is proportional to the wave function overlap between neighbouring sites. Furthermore, Kerr non-linearities, known in litera-

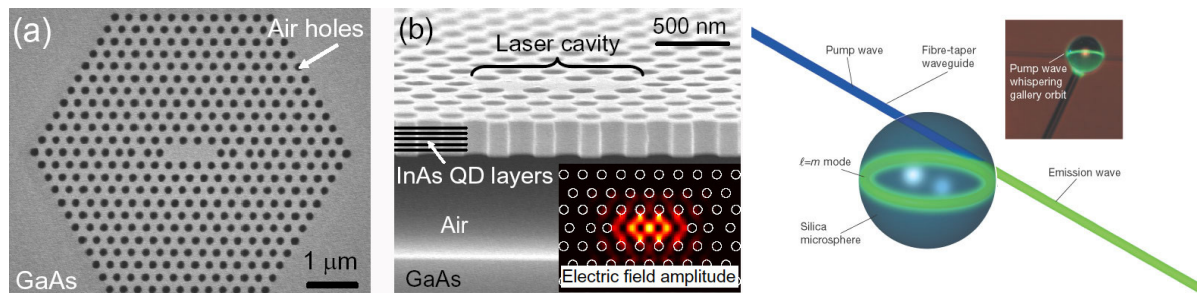


Figure 1.2: **Possible experimental setups** (1) from left to right: 1) – 2) photonic band-gap cavity with quantum dot defect region in the centre [36], 3) micro-sphere cavity filled with nano-crystal defect and coupled to an optical fibre [37].

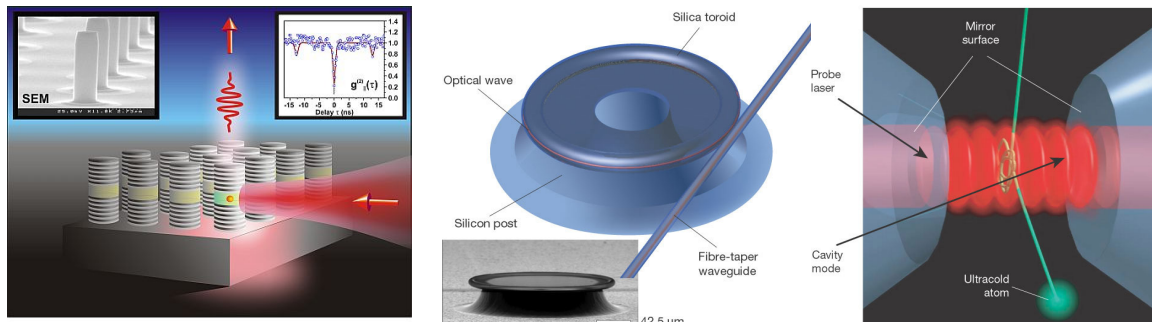


Figure 1.3: **Possible experimental setups (2)** from left to right: 1) array of micro-pillar cavities with intrinsic quantum box defects [50], 2) micro-toroid cavity coupled to optical fibre [37], 3) Fabry-Pérot cavity coupled to atom on the fly [37].

ture as *photon blockade* [52–56], effectively provide a repulsive or attractive on-site interaction, which has intensively been studied in the context of electromagnetically induced transparency (EIT) [57–61]. Therefore, these systems are also capable to simulate the Bose-Hubbard model. In fact, Bose-Einstein condensation of polaritons was recently experimentally achieved in semi-conductor cavities filled with quantum wells [62–64] and superfluidity could be observed [65, 66].

This new idea for a quantum simulator based on cavity QED does not share the limitations of the optical lattice approach. On the contrary, due to relatively huge distances between the cavities, local control and accessibility emerges quite naturally for these systems. Hence, it is possible to analyse these systems without destroying them. Since the atoms are trapped inside the cavities right from the start and their thermal motion does not quantitatively disturb the polariton dynamics [68, 69], BEC experiments with cavity QED setups can be performed even at room temperatures [70]. However, in order to facilitate stable experiments with this setup, there is a

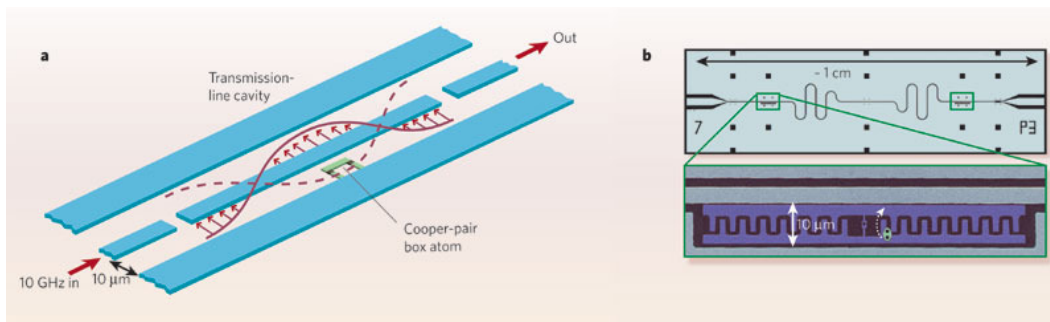


Figure 1.4: **Possible experimental setups (3)** from left to right: 1) – 2) transmission line cavity filled with Cooper-pair box [51].

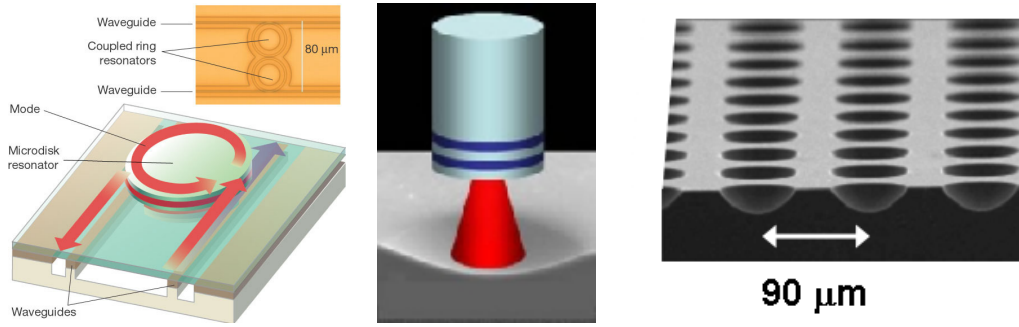


Figure 1.5: **Possible experimental setups** (4) from left to right: 1) micro-disc cavity coupled to wave-guides [37], 2) single on-chip Fabry-Pérot cavity [67], 3) corrie matrix for multiple on-chip Fabry-Pérot cavities [67].

major obstacle to overcome. Namely, it is necessary to minimize unwanted losses, like spontaneous emission or photons leaking out of the cavity, in order to reach a strong coupling between the atoms and the light field. Fortunately, over the past few years, this so called *strong-coupling regime* [71–73] has become experimentally accessible for a large number of different setups. For example, possible building blocks for such a lattice could be: micro-wire cavities [70, 74], micro-pillar cavities [50, 75–79], micro-sphere cavities [80–82], photonic band-gap cavities [83–93], transmission line cavities [51, 94–103], micro-disc and micro-toroid cavities [104–111], photonic-crystal fibres [112, 113] or on-chip Fabry-Pérot cavities [114–118]. Proposals for atom-like defects, that could be injected into those cavities, reach from real atoms or ions over quantum boxes, quantum dots and nano-crystals to superconducting SQUID’s and Cooper-pair boxes. Some of these examples are illustrated in the Figures 1.2–1.5.

Other parameters, which can be tuned by the experimentalist, are the number of atom-like systems placed in each cavity and the spectrum of the light field coupled to the lattice. Both parameters will qualitatively and quantitatively influence the behaviour of the system. In general there are three popular theoretical models, describing their local effects on each lattice site. First, there is the so called Dicke model [119–121], which describes the interaction of atom-like systems with a multi-mode light field. Then, there is the Jaynes-Cummings model [122], which describes the coupling of a single light mode with a two-level system. Generalizing this approach to cover situations, where  $N$  two-level systems couple to a single field-mode, leads to the Tavis-Cummings model [123–127]. From the experimental point of view it is favourable to work with more than one defect in the cavity. Raising the number of atom-like systems increases the interaction possibility as well as the coupling strength. On the other hand, even though the coupling to a multi-mode field leads to interesting new phenomena, such as super-radiance [128–130], the single field-mode implementation is probably the better choice in terms of controllability, which is especially desired for quantum information applications. Since the

fundamental properties can be derived considering only a single two-level system in the cavity, I focus on systems with Jaynes-Cummings-like on-site potentials in the present diploma thesis.

## 1.4 Outline of the Thesis

The main goal of the present thesis is to derive the Jaynes-Cummings-Hubbard model and to study its thermodynamic properties in the grand-canonical ensemble. For this purpose this thesis is structured as follows.

In **Chapter 2**, I derive the Jaynes-Cummings (JC) model which provides the on-site potential in the considered lattice model. Subsequently, I discuss the JC eigenstates and their energy spectrum and introduce polaritons whose number is the conserved quantity in this model.

In **Chapter 3**, I go ahead and generalize the JC model to the Jaynes-Cummings-Hubbard (JCH) model describing a lattice of cavities, each filled with a single two-level system. For a first rough analysis of this model, I subsequently consider the limits of no dynamics at all and the opposite extreme of hopping domination. This approximative treatment qualitatively shows the existence of a quantum phase transition from a Mott insulator to a superfluid phase in the considered model. Afterwards, in order to obtain a more quantitative description of this phase transition, I establish a mean-field theory, which eventually leads to the mean-field phase boundary at zero temperature.

The investigation of temperature effects on the JCH model is then accomplished in **Chapter 4**. To this end, I shortly review the Dirac interaction picture, in which the partition function of the system is expressed. Using a current approach to break the symmetry of the system, which is essential for describing a quantum phase transition, the partition function is then expanded in terms of cumulants. This procedure yields a perturbative expansion of the grand-canonical free energy, which is then Legendre-transformed to an effective Ginzburg-Landau action.

Finally, in **Chapter 5**, I derive the excitation spectra and effective masses of the polaritons in the Mott phase for finite temperature from this Ginzburg-Landau action. A summary of this thesis and an outlook on further investigations is given in **Chapter 6**.



# Chapter 2

## Jaynes-Cummings Model

In 1963, the two American physicists Edwin Jaynes and Fred Cummings proposed a theoretical model in order to investigate the relation between quantum theory and the semi-classical theory of radiation. In fact, they were motivated by describing the process of spontaneous emission [131]. Within their approach they analysed the interaction of a monochromatic electromagnetic field mode with a quantum mechanical two-level system. Although this model is obviously an approximation, it turned out to be of crucial importance for understanding the fundamental interaction between light and matter. The fact that Jaynes and Cummings found a quantum mechanical description of light-matter interaction that showed a very good quantitative agreement with experiments, strongly enhanced the progress in the field of *Quantum Optics* and has been a corner stone especially of this field of physics ever since. In the following years and decades the further developments, based on their model, led to multiple applications and improvements such as masers, lasers and optical trapping and cooling techniques [132–134].

A derivation of this model can be found in almost every physics book concerning quantum optics, see for instance the Refs. [122, 135–138]. Within this thesis the Jaynes-Cummings model is fundamentally important because it describes the potential energy of photons on each lattice site. As mentioned before, I assume this model to be experimentally realized as an optical micro cavity, filled with a two-level system and a monochromatic photon field. To find the quantum mechanical description of this system, I start by deriving the Hamiltonian of the intra-cavity photon field in the following section.

### 2.1 Quantization of the Free Electromagnetic Field

An electromagnetic field is classically described by a set of four equations named after their discoverer James Clerk Maxwell. These Maxwell equations read in SI units in the vacuum:

$$\nabla \cdot \mathbf{B}(\mathbf{r}, t) = 0, \tag{2.1a}$$

$$\nabla \cdot \mathbf{D}(\mathbf{r}, t) = \rho(\mathbf{r}, t), \tag{2.1b}$$

$$\nabla \times \mathbf{E}(\mathbf{r}, t) = -\frac{\partial \mathbf{B}(\mathbf{r}, t)}{\partial t}, \quad (2.1c)$$

$$\nabla \times \mathbf{H}(\mathbf{r}, t) = \mathbf{j}(\mathbf{r}, t) + \frac{\partial \mathbf{D}(\mathbf{r}, t)}{\partial t}, \quad (2.1d)$$

where the respective electric and magnetic fields are linked via the relations

$$\mathbf{B}(\mathbf{r}, t) = \mu_0 \mathbf{H}(\mathbf{r}, t), \quad \mathbf{D}(\mathbf{r}, t) = \epsilon_0 \mathbf{E}(\mathbf{r}, t). \quad (2.2)$$

Considering equation (2.1a), one uses the fact that the divergence of a rotation always vanishes to define the magnetic induction  $\mathbf{B}(\mathbf{r}, t)$  as the rotation of a vector potential  $\mathbf{A}(\mathbf{r}, t)$ :

$$\mathbf{B}(\mathbf{r}, t) = \nabla \times \mathbf{A}(\mathbf{r}, t). \quad (2.3)$$

Plugging this ansatz into equation (2.1c) yields the following expression

$$\nabla \times \left( \mathbf{E}(\mathbf{r}, t) + \frac{\partial \mathbf{A}(\mathbf{r}, t)}{\partial t} \right) = 0. \quad (2.4)$$

This means that the quantity with vanishing curl in equation (2.4) can be written as the gradient of some scalar function, namely, a scalar potential  $\Phi(\mathbf{r}, t)$ :

$$\mathbf{E}(\mathbf{r}, t) + \frac{\partial \mathbf{A}(\mathbf{r}, t)}{\partial t} = -\nabla \Phi(\mathbf{r}, t), \quad (2.5)$$

which leads to the general formula for the electric field:

$$\mathbf{E}(\mathbf{r}, t) = -\nabla \Phi(\mathbf{r}, t) - \frac{\partial \mathbf{A}(\mathbf{r}, t)}{\partial t}. \quad (2.6)$$

Plugging these results into the inhomogeneous Maxwell equations (2.1b) and (2.1d) yields the following coupled differential equations

$$-\frac{\rho(\mathbf{r}, t)}{\epsilon_0} = \nabla^2 \Phi(\mathbf{r}, t) + \frac{\partial}{\partial t} \nabla \cdot \mathbf{A}(\mathbf{r}, t), \quad (2.7)$$

$$-\mu_0 \mathbf{j}(\mathbf{r}, t) = \nabla^2 \mathbf{A}(\mathbf{r}, t) - \frac{1}{c^2} \frac{\partial^2 \mathbf{A}(\mathbf{r}, t)}{\partial t^2} - \nabla \left[ \nabla \cdot \mathbf{A}(\mathbf{r}, t) + \frac{1}{c^2} \frac{\partial^2 \Phi(\mathbf{r}, t)}{\partial t^2} \right], \quad (2.8)$$

where I used the fact that  $\sqrt{\epsilon_0 \mu_0} = c^{-1}$ . So far I reduced the four Maxwell equations (2.1a) – (2.1d) to two equations. However, these equations are still coupled. In order to uncouple them, one can use the arbitrariness involved in the definition of the scalar and the vector potential. Since  $\mathbf{B}(\mathbf{r}, t)$  is defined via (2.3) in terms of  $\mathbf{A}(\mathbf{r}, t)$ , one can add the gradient of an arbitrary scalar function  $\Lambda(\mathbf{r}, t)$  to the vector potential. Thus, one finds that the magnetic field as well as the electric field is unchanged under simultaneous transformations of the form

$$\mathbf{A}(\mathbf{r}, t) \rightarrow \mathbf{A}'(\mathbf{r}, t) + \nabla \Lambda(\mathbf{r}, t), \quad (2.9)$$

$$\Phi(\mathbf{r}, t) \rightarrow \Phi'(\mathbf{r}, t) - \frac{\partial \Lambda(\mathbf{r}, t)}{\partial t}. \quad (2.10)$$

## 2.1 Quantization of the Free Electromagnetic Field

---

These transformations are commonly referred to as *gauge transformations*. The resulting freedom of choice allows to choose a set of potentials  $\{\mathbf{A}(\mathbf{r}, t), \Phi(\mathbf{r}, t)\}$  that uncouple the equations (2.7) and (2.8). In the following calculations I explicitly make use of the so called *Coulomb gauge* which reads

$$\nabla \cdot \mathbf{A}(\mathbf{r}, t) = 0. \quad (2.11)$$

Using this ansatz together with equation (2.7) yields the Poisson equation

$$\nabla^2 \Phi(\mathbf{r}, t) = -\frac{\rho(\mathbf{r}, t)}{\epsilon_0}, \quad (2.12)$$

with the general solution

$$\Phi(\mathbf{r}, t) = \frac{1}{4\pi\epsilon_0} \int \frac{\rho(\mathbf{r}', t)}{|\mathbf{r} - \mathbf{r}'|} d^3r'. \quad (2.13)$$

In principle one can now explicitly determine the dynamics of the potentials according to equations (2.7) and (2.8). However, for now I am just interested in the free electromagnetic fields and, thus, I assume that no sources are present in the system, i.e.  $\rho(\mathbf{r}, t) = 0$  and  $\mathbf{j}(\mathbf{r}, t) = 0$ . This assumption leads, according to equation (2.13), to the statement

$$\Phi(\mathbf{r}, t) = 0, \quad (2.14)$$

and hence one finds from (2.6) for the free electromagnetic field the expression

$$\mathbf{E}(\mathbf{r}, t) = -\frac{\partial \mathbf{A}(\mathbf{r}, t)}{\partial t}. \quad (2.15)$$

All these assumptions simplify the differential equation (2.8) and result in a wave equation for the vector potential:

$$\left( \nabla^2 - \frac{1}{c^2} \frac{\partial^2}{\partial t^2} \right) \mathbf{A}(\mathbf{r}, t) = 0. \quad (2.16)$$

This is a homogeneous wave equation, where the general solution is known to be a superposition of an in- and an outgoing plane wave. Taking this fact into consideration, I choose the following ansatz for the vector potential

$$\mathbf{A}(\mathbf{r}, t) = \mathbf{A}^+(\mathbf{r}, t) + \mathbf{A}^-(\mathbf{r}, t), \quad (2.17)$$

with the two terms representing in- and outgoing waves. Furthermore, the introduced quantities fulfil the relation  $\mathbf{A}^-(\mathbf{r}, t) = [(\mathbf{A}^+(\mathbf{r}, t))]^*$ . Therefore, I can focus my analysis on one of the terms, i.e.  $\mathbf{A}^+(\mathbf{r}, t)$ , keeping in mind that the other is simply the complex conjugate. Using a very general ansatz for the two components of the

vector potential, I express them as a discrete superposition of the respective mode functions in the cavity volume

$$\mathbf{A}^+(\mathbf{r}, t) = \sum_{\rho} \sum_{\sigma=\pm 1} a_{\sigma}(\mathbf{k}_{\rho}) \mathbf{u}_{\sigma}(\mathbf{k}_{\rho}, \mathbf{r}) e^{-i\omega_{\rho}t}. \quad (2.18)$$

The index  $\rho = (\rho_x, \rho_y, \rho_z)$  is the mode index, which specifies the three components of the wave vector  $\mathbf{k}_{\rho}$  and the index  $\sigma$  labels the two possible polarizations of the plane wave. The expressions  $\mathbf{u}_{\sigma}(\mathbf{k}_{\rho}, \mathbf{r})$  are the respective mode functions,  $a_{\sigma}(\mathbf{k}_{\rho})$  are the mode amplitudes and  $\omega_{\rho}$  is the mode frequency. Since the mode functions carry the spatial character of plane waves, I assume them to have the form

$$\mathbf{u}_{\sigma}(\mathbf{k}_{\rho}, \mathbf{r}) = \frac{1}{\sqrt{L^3}} \mathbf{e}_{\sigma}(\mathbf{k}_{\rho}) e^{i\mathbf{k}_{\rho}\mathbf{r}}, \quad (2.19)$$

in which the unity vectors  $\mathbf{e}_{\sigma}(\mathbf{k}_{\rho})$  correspond to the two possible polarizations of a wave with wave vector  $\mathbf{k}_{\rho}$ . Note that, the pre-factor of these mode functions emerges due to the normalization of the modes over the cavity volume, which is assumed to be cubic and of length  $L$ . Thus I explicitly consider a finite volume which is necessary in order to discretely label the electromagnetic wave modes.

Another important fact is, that since the mode functions inherited the whole spatial character of the vector potential, they also have to fulfil the Coulomb gauge (2.11). Demanding this special property, leads to the transversality relation between the polarizations and the wave vector  $\mathbf{k}_{\rho}$ :

$$\mathbf{e}_{\sigma}(\mathbf{k}_{\rho}) \mathbf{k}_{\rho} = 0. \quad (2.20)$$

This equation describes a very important feature of electromagnetic waves, namely that the wave vector, which corresponds to the direction of propagation of the wave, is always orthogonal to the polarizations which are orthogonal to each other as well. Hence,  $\mathbf{e}_{+1}(\mathbf{k}_{\rho}), \mathbf{e}_{-1}(\mathbf{k}_{\rho}), \mathbf{k}_{\rho}$  are all orthogonal to each other and form a right hand-system.

Inserting ansatz (2.17) and relation (2.18) in the wave equation (2.16), leads to a homogeneous differential equation of second order for the mode function and its complex conjugate. Both functions have to fulfil the same differential equation, which reads for the mode function

$$\left( \nabla^2 + \frac{\omega_{\rho}^2}{c^2} \right) \mathbf{u}_{\sigma}(\mathbf{k}_{\rho}, \mathbf{r}) = 0. \quad (2.21)$$

Plugging expression (2.19) into this equation and assuming periodic boundary conditions yields the relation

$$\mathbf{k}_{\rho}^2 = \frac{\omega_{\rho}^2}{c^2}, \quad (2.22)$$

where the components of the wave vector are now quantized as follows

$$k_{\rho,i} = \frac{2\pi\rho_i}{L}, \quad i = x, y, z, \quad \rho_i \in \mathbb{Z}. \quad (2.23)$$

Expression (2.22) can be transformed to give the dispersion relation of the mode function

$$\omega_\rho = c|\mathbf{k}_\rho|. \quad (2.24)$$

Thus, the mode frequency  $\omega_\rho$  has the following property:

$$\omega_{-\rho} = c|\mathbf{k}_{-\rho}| = c|-\mathbf{k}_\rho| = \omega_\rho, \quad (2.25)$$

where I introduced the convention, that a negative mode index  $-\rho$  corresponds to the opposite wave vector  $\mathbf{k}_{-\rho} = -\mathbf{k}_\rho$ .

In general, I have now determined the specific form of the vector potential following from ansatz (2.18) and, thus, am also able to derive the electric field vector using relation (2.15). However, in order to quantize the vector potential  $\mathbf{A}(\mathbf{r}, t)$ , I want to derive a more convenient form, where the respective amplitudes of the mode functions  $a_\sigma(\mathbf{k}_\rho)$  are dimensionless. To find the appropriate pre-factors, I use the definition of the energy of an electromagnetic field, which is defined as

$$E = \frac{1}{2} \int dV \left[ \frac{1}{\mu_0} \mathbf{B}^2(\mathbf{r}, t) + \epsilon_0 \mathbf{E}^2(\mathbf{r}, t) \right]. \quad (2.26)$$

In the following, I do not exactly solve this expression but rather estimate the emerging physical dimensions. Therefore, I neglect the specific  $\mathbf{r}$  dependence of the vector fields in the volume integral above. Hence, considering the physical dimension of the field energy one can conclude

$$[E]_{\text{Dim}} \cong \frac{L^3}{2} \left\{ \frac{1}{\mu_0} [\mathbf{B}^2]_{\text{Dim}} + \epsilon_0 [\mathbf{E}^2]_{\text{Dim}} \right\}. \quad (2.27)$$

Using the definition (2.2) – (2.15) leads to

$$[E]_{\text{Dim}} \cong \frac{L^3}{2} \left\{ \frac{1}{\mu_0} [(\nabla \times \mathbf{A})^2]_{\text{Dim}} + \frac{4\epsilon_0}{L^3} [a_{\text{E}}^2]_{\text{Dim}} \right\}, \quad (2.28)$$

where the index E indicates that the respective mode amplitude  $a_{\text{E}} \hat{=} a_\sigma(\mathbf{k}_\rho)$  belongs to the electric field. Note that, the denominator  $L^3$  in the second term of equation (2.28) emerges from the normalization of the mode function. Furthermore, I do not have to distinguish between  $a_\sigma(\mathbf{k}_\rho)$  and  $a_\sigma^*(\mathbf{k}_\rho)$ , if I only consider the physical dimension of the amplitudes. Therefore, the pre-factor 4 of the last term corresponds to the number of terms proportional to the square of the electric field amplitude. Inserting ansatz (2.18) for the vector potential yields

$$[E]_{\text{Dim}} \cong \frac{L^3}{2} \left\{ \frac{4}{\mu_0} [(a_{\text{A}} \nabla \times \mathbf{u})^2]_{\text{Dim}} + \frac{4\epsilon_0}{L^3} [a_{\text{E}}^2]_{\text{Dim}} \right\}. \quad (2.29)$$

Here, the index A indicates, analogue to the case considered before, the affiliation of the amplitudes  $a_A \hat{=} a_\sigma(\mathbf{k}_\rho)$  to the vector potential. This distinction is necessary, since the physical dimension of the vector-potential amplitude differs from the physical dimension of the electric-field amplitude according to relation (2.15). For a more precise determination of the physical dimension of the magnetic contribution to the energy, it is necessary to calculate the curl of the mode function. Using definition (2.19) leads to the following relation

$$\nabla \times \mathbf{u}_\sigma(\mathbf{k}_\rho, \mathbf{r}) = \frac{1}{\sqrt{L^3}} [(\nabla \times \mathbf{e}_\sigma(\mathbf{k}_\rho)) e^{i\mathbf{k}_\rho \cdot \mathbf{r}} + \nabla e^{i\mathbf{k}_\rho \cdot \mathbf{r}} \times \mathbf{e}_\sigma(\mathbf{k}_\rho)] \quad (2.30)$$

$$= \frac{i}{\sqrt{L^3}} \mathbf{k}_\rho \times \mathbf{e}_\sigma(\mathbf{k}_\rho) e^{i\mathbf{k}_\rho \cdot \mathbf{r}} = \frac{i k_\rho}{\sqrt{L^3}} \mathbf{e}_{-\sigma}(\mathbf{k}_\rho) e^{i\mathbf{k}_\rho \cdot \mathbf{r}}. \quad (2.31)$$

Thus, the curl of the mode function essentially results in the same mode function. Nevertheless, it differs in the opposite polarization and a pre-factor  $i k_\rho$ , where  $k_\rho = |\mathbf{k}_\rho|$  is the modulus of the wave vector. Thus, considering the physical dimension, all one has to take into account is the pre-factor  $i k_\rho / \sqrt{L^3}$ . As a result, one finds

$$[E]_{\text{Dim}} \cong \frac{2}{\mu_0} k_\rho^2 ([a_A]_{\text{Dim}})^2 + 2 \epsilon_0 ([a_E]_{\text{Dim}})^2. \quad (2.32)$$

In quantum mechanics the dimension of the energy of an electromagnetic wave is of the order  $\hbar \omega_\rho$ . Since the dimension of *each* of the two terms in the above equation has to be the dimension of energy, one can derive the following expressions:

$$[a_E]_{\text{Dim}} = \sqrt{\frac{\hbar \omega_\rho}{2 \epsilon_0}}, \quad (2.33)$$

$$[a_A]_{\text{Dim}} = \sqrt{\frac{\hbar}{2 \epsilon_0 \omega_\rho}}, \quad (2.34)$$

where I additionally used relation (2.22). Thus, I reached the point where I can write down the expressions for the vector potential and the electric field vector in the desired dimensionless form:

$$\mathbf{A}(\mathbf{r}, t) = \sum_\rho \sum_{\sigma=\pm 1} \left( \frac{\hbar}{2 \epsilon_0 \omega_\rho} \right)^{1/2} [a_\sigma(\mathbf{k}_\rho) \mathbf{u}_\sigma(\mathbf{k}_\rho, \mathbf{r}) e^{-i\omega_\rho t} + c.c.], \quad (2.35)$$

$$\mathbf{E}(\mathbf{r}, t) = i \sum_\rho \sum_{\sigma=\pm 1} \left( \frac{\hbar \omega_\rho}{2 \epsilon_0} \right)^{1/2} [a_\sigma(\mathbf{k}_\rho) \mathbf{u}_\sigma(\mathbf{k}_\rho, \mathbf{r}) e^{-i\omega_\rho t} - c.c.]. \quad (2.36)$$

Up till now, I have derived a semi-classical description of the intra-cavity field quantities  $\mathbf{A}(\mathbf{r}, t)$  and  $\mathbf{E}(\mathbf{r}, t)$  for the general case of a multi-mode field with all polarizations. I still need to fully quantize this expression. This last step is known in literature as the *second quantization*. This quantization is performed by simply mapping

the dimensionless mode amplitudes to quantum mechanical ladder operators, raising and lowering the number of excitations of a given field mode:

$$a_\sigma(\mathbf{k}_\rho) \longmapsto \hat{a}_\sigma(\mathbf{k}_\rho), \quad (2.37a)$$

$$a_\sigma^*(\mathbf{k}_\rho) \longmapsto \hat{a}_\sigma^\dagger(\mathbf{k}_\rho). \quad (2.37b)$$

Since these operators describe photons, which are bosonic particles, they satisfy the bosonic commutation relations:

$$[\hat{a}_\sigma(\mathbf{k}_\rho), \hat{a}_{\sigma'}^\dagger(\mathbf{k}_{\rho'})] = \delta_{\rho, \rho'} \delta_{\sigma, \sigma'}, \quad [\hat{a}_\sigma(\mathbf{k}_\rho), \hat{a}_{\sigma'}(\mathbf{k}_{\rho'})] = [\hat{a}_\sigma^\dagger(\mathbf{k}_\rho), \hat{a}_{\sigma'}^\dagger(\mathbf{k}_{\rho'})] = 0. \quad (2.38)$$

The fully quantized field vectors are, therefore, given by

$$\hat{\mathbf{A}}(\mathbf{r}, t) = \sum_\rho \sum_{\sigma=\pm 1} \left( \frac{\hbar}{2\epsilon_0 \omega_\rho} \right)^{1/2} [\hat{a}_\sigma(\mathbf{k}_\rho) \mathbf{u}_\sigma(\mathbf{k}_\rho, \mathbf{r}) e^{-i\omega_\rho t} + \text{h.c.}], \quad (2.39)$$

$$\hat{\mathbf{E}}(\mathbf{r}, t) = i \sum_\rho \sum_{\sigma=\pm 1} \left( \frac{\hbar \omega_\rho}{2\epsilon_0} \right)^{1/2} [\hat{a}_\sigma(\mathbf{k}_\rho) \mathbf{u}_\sigma(\mathbf{k}_\rho, \mathbf{r}) e^{-i\omega_\rho t} - \text{h.c.}]. \quad (2.40)$$

In quantum mechanics, all dynamic properties of a system can be deduced from its Hamiltonian. To find the respective Hamiltonian for the free electromagnetic field, I follow equation (2.26). Therefore, I need the quantized expression for the magnetic field  $\hat{\mathbf{B}}(\mathbf{r}, t)$ , which can be derived from equation (2.3) with the help of the relations (2.39) and (2.31). This yields

$$\hat{\mathbf{B}}(\mathbf{r}, t) = i \sum_\rho \sum_{\sigma=\pm 1} \left( \frac{\hbar}{2\epsilon_0 \omega_\rho} \right)^{1/2} k_\rho [\hat{a}_\sigma(\mathbf{k}_\rho) \mathbf{u}_{-\sigma}(\mathbf{k}_\rho, \mathbf{r}) e^{-i\omega_\rho t} - \text{h.c.}]. \quad (2.41)$$

According to equation (2.26) the Hamiltonian can be calculated via the formula

$$\hat{H}(t) = \frac{1}{2} \int dV \left[ \epsilon_0 \hat{\mathbf{E}}^2(\mathbf{r}, t) + \frac{1}{\mu_0} \hat{\mathbf{B}}^2(\mathbf{r}, t) \right] \quad (2.42)$$

Inserting the expression (2.40) for the electric fields into the first term of definition (2.42) and using of the definition of the mode function (2.19) leads to

$$\begin{aligned} \epsilon_0 \int_V dV \hat{\mathbf{E}}^2(\mathbf{r}, t) &= - \sum_{\rho, \rho'} \sum_{\sigma, \sigma'=\pm 1} \frac{\hbar}{2L^3} (\omega_\rho \omega_{\rho'})^{1/2} \int_V dV [\hat{a}_\sigma(\mathbf{k}_\rho) \mathbf{e}_\sigma(\mathbf{k}_\rho) e^{i\mathbf{k}_\rho \mathbf{r}} e^{-i\omega_\rho t} - \text{h.c.}] \\ &\quad \times [\hat{a}_{\sigma'}(\mathbf{k}_{\rho'}) \mathbf{e}_{\sigma'}(\mathbf{k}_{\rho'}) e^{i\mathbf{k}_{\rho'} \mathbf{r}} e^{-i\omega_{\rho'} t} - \text{h.c.}] \\ &= - \sum_{\rho, \rho'} \sum_{\sigma, \sigma'=\pm 1} \frac{\hbar}{2L^3} (\omega_\rho \omega_{\rho'})^{1/2} \int_V dV \\ &\quad \times [\hat{a}_\sigma(\mathbf{k}_\rho) \hat{a}_{\sigma'}(\mathbf{k}_{\rho'}) \mathbf{e}_\sigma(\mathbf{k}_\rho) \mathbf{e}_{\sigma'}(\mathbf{k}_{\rho'}) e^{i(\mathbf{k}_{\rho'} + \mathbf{k}_\rho) \mathbf{r}} e^{-i(\omega_\rho + \omega_{\rho'}) t} \end{aligned}$$

$$\begin{aligned}
 & - \hat{a}_\sigma^\dagger(\mathbf{k}_\rho) \hat{a}_{\sigma'}(\mathbf{k}_{\rho'}) \mathbf{e}_\sigma^*(\mathbf{k}_\rho) \mathbf{e}_{\sigma'}(\mathbf{k}_{\rho'}) e^{i(\mathbf{k}_{\rho'} - \mathbf{k}_\rho)\mathbf{r}} e^{i(\omega_\rho - \omega_{\rho'})t} \\
 & + \hat{a}_\sigma^\dagger(\mathbf{k}_\rho) \hat{a}_{\sigma'}^\dagger(\mathbf{k}_{\rho'}) \mathbf{e}_\sigma^*(\mathbf{k}_\rho) \mathbf{e}_{\sigma'}^*(\mathbf{k}_{\rho'}) e^{-i(\mathbf{k}_\rho + \mathbf{k}_{\rho'})\mathbf{r}} e^{i(\omega_\rho + \omega_{\rho'})t} \\
 & - \hat{a}_\sigma(\mathbf{k}_\rho) \hat{a}_{\sigma'}^\dagger(\mathbf{k}_{\rho'}) \mathbf{e}_\sigma(\mathbf{k}_\rho) \mathbf{e}_{\sigma'}^*(\mathbf{k}_{\rho'}) e^{i(\mathbf{k}_\rho - \mathbf{k}_{\rho'})\mathbf{r}} e^{i(\omega_{\rho'} - \omega_\rho)t} \Big]. \quad (2.43)
 \end{aligned}$$

The volume integral over the second and fourth term in the above expression can be calculated straightforwardly to give

$$\frac{1}{L^3} \int_V dV e^{i(\mathbf{k}_\rho - \mathbf{k}_{\rho'})\mathbf{r}} = \delta_{\rho, \rho'}, \quad (2.44)$$

and the occurring scalar products of the polarization unit vector become

$$\mathbf{e}_\sigma^*(\mathbf{k}_\rho) \mathbf{e}_{\sigma'}(\mathbf{k}_\rho) = \delta_{\sigma, \sigma'}. \quad (2.45)$$

By shifting the mode index  $\rho \rightarrow -\rho$  and using the fact [139] that

$$\mathbf{e}_\sigma(\mathbf{k}_{-\rho}) = \mathbf{e}_\sigma(-\mathbf{k}_\rho) = \mathbf{e}_{-\sigma}(\mathbf{k}_\rho) = \mathbf{e}_\sigma^*(\mathbf{k}_\rho), \quad (2.46)$$

I find for the first term in (2.43) the following result

$$\int_V dV \hat{a}_\sigma(\mathbf{k}_{-\rho}) \hat{a}_{\sigma'}(\mathbf{k}_{\rho'}) \mathbf{e}_\sigma(\mathbf{k}_{-\rho}) \mathbf{e}_{\sigma'}(\mathbf{k}_{\rho'}) e^{i(\mathbf{k}_{\rho'} - \mathbf{k}_\rho)\mathbf{r}} = \hat{a}_\sigma(\mathbf{k}_{-\rho}) \hat{a}_{\sigma'}(\mathbf{k}_{\rho'}) \delta_{\sigma, \sigma'} \delta_{\rho, \rho'}. \quad (2.47)$$

Following the same procedure for the third term in (2.43) yields

$$\int_V dV \hat{a}_\sigma^\dagger(\mathbf{k}_{-\rho}) \hat{a}_{\sigma'}^\dagger(\mathbf{k}_{\rho'}) \mathbf{e}_\sigma^*(\mathbf{k}_{-\rho}) \mathbf{e}_{\sigma'}^*(\mathbf{k}_{\rho'}) e^{-i(\mathbf{k}_{-\rho} + \mathbf{k}_{\rho'})\mathbf{r}} = \hat{a}_\sigma^\dagger(\mathbf{k}_{-\rho}) \hat{a}_{\sigma'}^\dagger(\mathbf{k}_{\rho'}) \delta_{\sigma, \sigma'} \delta_{\rho, \rho'}. \quad (2.48)$$

With these results and the invariance of the mode frequency under the transformation  $\rho \rightarrow -\rho$  from (2.24), equation (2.43) can be simplified to

$$\begin{aligned}
 \epsilon_0 \int_V dV \hat{\mathbf{E}}^2(\mathbf{r}, t) = & \sum_\rho \sum_{\sigma=\pm 1} \frac{\hbar \omega_\rho}{2} [\hat{a}_\sigma(\mathbf{k}_\rho) \hat{a}_\sigma^\dagger(\mathbf{k}_\rho) + \hat{a}_\sigma^\dagger(\mathbf{k}_\rho) \hat{a}_\sigma(\mathbf{k}_\rho) \\
 & - \hat{a}_\sigma^\dagger(\mathbf{k}_{-\rho}) \hat{a}_\sigma^\dagger(\mathbf{k}_\rho) e^{i2\omega_\rho t} - \hat{a}_\sigma(\mathbf{k}_{-\rho}) \hat{a}_\sigma(\mathbf{k}_\rho) e^{-i2\omega_\rho t}]. \quad (2.49)
 \end{aligned}$$

## 2.1 Quantization of the Free Electromagnetic Field

Using the analogue procedure for the magnetic induction, yields the following expression:

$$\begin{aligned}
\frac{1}{\mu_0} \int_V dV \hat{\mathbf{B}}^2(\mathbf{r}, t) &= \sum_{\rho, \rho'} \sum_{\sigma, \sigma' = \pm 1} \frac{\hbar(\omega_\rho \omega_{\rho'})^{1/2}}{2 \epsilon_0 \mu_0} \int_V dV \{ \hat{a}_\sigma(\mathbf{k}_\rho) [\nabla \times \mathbf{u}_\sigma(\mathbf{k}_\rho, \mathbf{r})] e^{-i\omega_\rho t} + \text{h.c.} \} \\
&\quad \times \{ \hat{a}_{\sigma'}(\mathbf{k}_{\rho'}) [\nabla \times \mathbf{u}_{\sigma'}(\mathbf{k}_{\rho'}, \mathbf{r})] e^{-i\omega_{\rho'} t} + \text{h.c.} \} \\
&= - \sum_{\rho, \rho'} \sum_{\sigma, \sigma' = \pm 1} \frac{\hbar k_\rho k_{\rho'}}{2 \epsilon_0 \mu_0} (\omega_\rho \omega_{\rho'})^{1/2} \int_V dV [ \hat{a}_\sigma(\mathbf{k}_\rho) \mathbf{u}_{-\sigma}(\mathbf{k}_\rho, \mathbf{r}) e^{-i\omega_\rho t} - \text{h.c.} ] \\
&\quad \times [ \hat{a}_{\sigma'}(\mathbf{k}_{\rho'}) \mathbf{u}_{-\sigma'}(\mathbf{k}_{\rho'}, \mathbf{r}) e^{-i\omega_{\rho'} t} - \text{h.c.} ] \\
&= \sum_{\rho, \rho'} \sum_{\sigma, \sigma' = \pm 1} \frac{\hbar k_\rho k_{\rho'}}{2 \epsilon_0 \mu_0} (\omega_\rho \omega_{\rho'})^{1/2} \int_V dV [ \hat{a}_\sigma(\mathbf{k}_{-\rho}) \hat{a}_{\sigma'}(\mathbf{k}_{\rho'}) \mathbf{u}_{-\sigma}(\mathbf{k}_{-\rho}, \mathbf{r}) \mathbf{u}_{-\sigma'}(\mathbf{k}_{\rho'}, \mathbf{r}) e^{-i(\omega_\rho + \omega_{\rho'}) t} \\
&\quad + \hat{a}_\sigma(\mathbf{k}_\rho) \hat{a}_{\sigma'}^\dagger(\mathbf{k}_{\rho'}) \mathbf{u}_{-\sigma}(\mathbf{k}_\rho, \mathbf{r}) \mathbf{u}_{-\sigma'}^*(\mathbf{k}_{\rho'}, \mathbf{r}) e^{-i(\omega_\rho - \omega_{\rho'}) t} \\
&\quad + \hat{a}_\sigma^\dagger(\mathbf{k}_\rho) \hat{a}_{\sigma'}(\mathbf{k}_{\rho'}) \mathbf{u}_{-\sigma}^*(\mathbf{k}_\rho, \mathbf{r}) \mathbf{u}_{-\sigma'}(\mathbf{k}_{\rho'}, \mathbf{r}) e^{i(\omega_\rho - \omega_{\rho'}) t} \\
&\quad + \hat{a}_\sigma^\dagger(\mathbf{k}_{-\rho}) \hat{a}_{\sigma'}^\dagger(\mathbf{k}_{\rho'}) \mathbf{u}_{-\sigma}^*(\mathbf{k}_{-\rho}, \mathbf{r}) \mathbf{u}_{-\sigma'}^*(\mathbf{k}_{\rho'}, \mathbf{r}) e^{i(\omega_\rho + \omega_{\rho'}) t} ] \\
&= \sum_{\rho} \sum_{\sigma = \pm 1} \frac{\hbar k_\rho^2}{2 \epsilon_0 \mu_0} \omega_\rho [ \hat{a}_\sigma^\dagger(\mathbf{k}_\rho) \hat{a}_\sigma(\mathbf{k}_\rho) + \hat{a}_\sigma(\mathbf{k}_\rho) \hat{a}_\sigma^\dagger(\mathbf{k}_\rho) + \hat{a}_\sigma^\dagger(\mathbf{k}_{-\rho}) \hat{a}_\sigma^\dagger(\mathbf{k}_\rho) e^{i2\omega_\rho t} \\
&\quad + \hat{a}_\sigma(\mathbf{k}_{-\rho}) \hat{a}_\sigma(\mathbf{k}_\rho) e^{-i2\omega_\rho t} ] . \tag{2.50}
\end{aligned}$$

Hence, using equation (2.22) one finds that the contribution to the energy arising from the magnetic induction is given as:

$$\begin{aligned}
\int_V dV \frac{1}{\mu_0} \hat{\mathbf{B}}^2(\mathbf{r}, t) &= \sum_{\rho} \sum_{\sigma = \pm 1} \frac{\hbar \omega_\rho}{2} [ \hat{a}_\sigma^\dagger(\mathbf{k}_\rho) \hat{a}_\sigma(\mathbf{k}_\rho) + \hat{a}_\sigma(\mathbf{k}_\rho) \hat{a}_\sigma^\dagger(\mathbf{k}_\rho) \\
&\quad + \hat{a}_\sigma^\dagger(\mathbf{k}_{-\rho}) \hat{a}_\sigma^\dagger(\mathbf{k}_\rho) e^{i2\omega_\rho t} + \hat{a}_\sigma^\dagger(\mathbf{k}_{-\rho}) \hat{a}_\sigma^\dagger(\mathbf{k}_\rho) e^{i2\omega_\rho t} ] \tag{2.51}
\end{aligned}$$

Now, one can establish the full Hamiltonian of the system by simply adding the two contributions (2.49) and (2.51), resulting in

$$\hat{H}_{\text{field}} = \frac{1}{2} \sum_{\rho} \sum_{\sigma = \pm 1} \hbar \omega_\rho ( \hat{a}_\sigma(\mathbf{k}_\rho) \hat{a}_\sigma^\dagger(\mathbf{k}_\rho) + \hat{a}_\sigma^\dagger(\mathbf{k}_\rho) \hat{a}_\sigma(\mathbf{k}_\rho) ) . \tag{2.52}$$

Additionally, using the commutator relations for the bosonic ladder operators defined in (2.38), I finally get the full Hamiltonian of the free electromagnetic field, which reads for a *fixed polarization*  $\sigma$ :

$$\hat{H}_{\text{field}} = \sum_{\rho} \hbar \omega_\rho \left( \hat{a}_\sigma^\dagger(\mathbf{k}_\rho) \hat{a}_\sigma(\mathbf{k}_\rho) + \frac{1}{2} \right) = \sum_{\rho} \hbar \omega_\rho \left( \hat{n}_\sigma(\mathbf{k}_\rho) + \frac{1}{2} \right) . \tag{2.53}$$

Here, I defined the occupation number operator  $\hat{n}_\sigma(\mathbf{k}_\rho) = \hat{a}_\sigma^\dagger(\mathbf{k}_\rho) \hat{a}_\sigma(\mathbf{k}_\rho)$  of the intracavity field quantum state corresponding to the quantum number  $\rho$  and polarization  $\sigma$ . I can see from (2.53) that the full Hamiltonian is simply a composition of

harmonic oscillators for each mode frequency and polarization. Hence, if I consider a *monochromatic field with fixed polarization*, the Hamiltonian of the free electromagnetic field is just a harmonic oscillator of frequency  $\omega$ :

$$\hat{H}_{\text{osc}} = \hbar\omega \left( \hat{a}^\dagger \hat{a} + \frac{1}{2} \right). \quad (2.54)$$

The energy spectrum of such a system is well known. It consists of the ground state with energy  $\frac{1}{2}\hbar\omega$ , which represents the zero-point energy of the system. All higher energy levels correspond to increasing occupation numbers and are equally spaced by the amount of  $\hbar\omega$ . The occupation number operator  $\hat{n}$  counts the number of excitations of the fundamental mode  $\omega$ , known as *photons*, and can, therefore, take on integer values between zero and infinity. Furthermore, it is easy to prove that the photonic occupation number operator commutes with the full Hamiltonian (2.53) and, therefore, in this system the number of photons is a conserved quantity.

The form of the Hamiltonian (2.53) is called the occupation number representation. Naturally, the corresponding eigenstates are formed by the set of Fock states  $|n_{\rho,\sigma}\rangle$  satisfying the eigenvalue equation

$$\hat{n}_\sigma(\mathbf{k}_\rho) |n_{\rho,\sigma}\rangle = n_{\rho,\sigma} |n_{\rho,\sigma}\rangle, \quad n_{\rho,\sigma} \in \mathbb{N} \geq 0. \quad (2.55)$$

Therefore, the Hamiltonian for the one-mode electromagnetic field with *fixed polarization* reads:

$$\hat{H}_{\text{field}} = \hbar\omega \left( \hat{n} + \frac{1}{2} \right), \quad (2.56)$$

where I dropped the indexes  $\rho$  and  $\sigma$  as well. From this equation it is to see that, this Hamiltonian is diagonal in the monochromatic Fock basis  $|n\rangle$ .

## 2.2 Hamiltonian of a Two-Level System

Having derived the full Hamiltonian of the free electromagnetic field within the previous section, I now consider the two-level system, placed in the micro cavity and interacting with the intra-cavity field mode. I assume that, the two-level system has an energy structure as depicted in Figure 2.1, consisting of a ground state, labelled  $|g\rangle$ , with energy  $E_0 = 0$  and an excited state, labelled  $|e\rangle$ , with energy  $E_e = \hbar\varepsilon$ . Taking this point of view, I make the most general ansatz to deal with this kind of system, which is applicable to all experimental setups.

Since the energy eigenstates and their respective eigenvalues are known by definition, one can immediately write down the Hamiltonian of this system in the energy representation:

$$\hat{H}_{\text{atom}} = \hbar\varepsilon |e\rangle \langle e| + 0 |g\rangle \langle g|. \quad (2.57)$$

By choosing a specific representation for the abstract eigenstates  $|e\rangle$ ,  $|g\rangle$ , one can transform this Hamiltonian in a more convenient form. Obviously, there are quite a

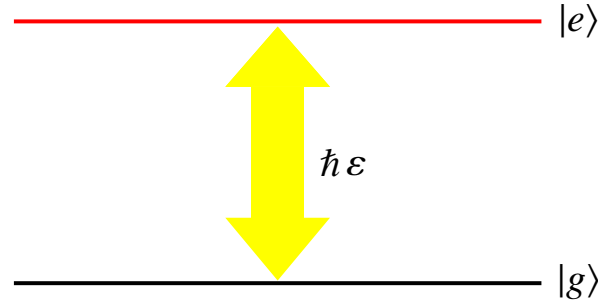


Figure 2.1: **Energy structure of the two-level system.** The two-level system consists of a ground state  $|g\rangle$  with energy  $E_0 = 0$  and an excited state  $|e\rangle$  with energy  $E_e = \hbar\varepsilon$ .

lot of possible representations. I use the simplest representation and associate the kets with the two dimensional Cartesian unit vectors as follows

$$|e\rangle = \begin{pmatrix} 1 \\ 0 \end{pmatrix}, \quad |g\rangle = \begin{pmatrix} 0 \\ 1 \end{pmatrix}. \quad (2.58)$$

Using this representation for the state vectors leads to a matrix representation for the projection operators in the Hamiltonian (2.57). Inserting (2.58) into (2.57) yields

$$\hat{H}_{\text{atom}} = \hbar\varepsilon \begin{pmatrix} 1 & 0 \\ 0 & 0 \end{pmatrix} + 0 \begin{pmatrix} 0 & 0 \\ 0 & 1 \end{pmatrix} = \begin{pmatrix} \hbar\varepsilon & 0 \\ 0 & 0 \end{pmatrix}. \quad (2.59)$$

Furthermore, remembering the definition of the Pauli matrices:

$$\hat{\sigma}_x = \begin{pmatrix} 0 & 1 \\ 1 & 0 \end{pmatrix}, \quad \hat{\sigma}_y = \begin{pmatrix} 0 & -i \\ i & 0 \end{pmatrix}, \quad \hat{\sigma}_z = \begin{pmatrix} 1 & 0 \\ 0 & -1 \end{pmatrix}, \quad (2.60)$$

and their combinations

$$\hat{\sigma}^+ = \frac{1}{2}(\hat{\sigma}_x + i\hat{\sigma}_y) = \begin{pmatrix} 0 & 1 \\ 0 & 0 \end{pmatrix} \quad (2.61a)$$

$$\hat{\sigma}^- = \frac{1}{2}(\hat{\sigma}_x - i\hat{\sigma}_y) = \begin{pmatrix} 0 & 0 \\ 1 & 0 \end{pmatrix}, \quad (2.61b)$$

one finds that, suitable combinations of the state vectors can be expressed in terms of these matrices. In fact, it can be shown that, in this choice of representation, the following relations hold

$$|e\rangle\langle g| = \begin{pmatrix} 0 & 1 \\ 0 & 0 \end{pmatrix} = \hat{\sigma}^+, \quad (2.62a)$$

$$|g\rangle\langle e| = \begin{pmatrix} 0 & 0 \\ 1 & 0 \end{pmatrix} = \hat{\sigma}^-. \quad (2.62b)$$

From the above relations follows, that the operators  $\hat{\sigma}^+$ ,  $\hat{\sigma}^-$  are the creation and annihilation operators of the two-level system, i.e.  $\hat{\sigma}^+$  creates an atomic excitation, whereas  $\hat{\sigma}^-$  destroys it. With the help of these relations, one finds for the remaining projection operators the following form

$$|e\rangle\langle e| = \hat{\sigma}^+\hat{\sigma}^-, \quad (2.63)$$

$$|g\rangle\langle g| = \hat{\sigma}^-\hat{\sigma}^+. \quad (2.64)$$

Hence, one can finally express the projection operators, occurring in the two-level Hamiltonian, in terms of combinations of Pauli matrices. Inserting expressions (2.63) and (2.64) in the Hamiltonian (2.57) yields the desired simplified form

$$\hat{H}_{\text{atom}} = \hbar\varepsilon\hat{\sigma}^+\hat{\sigma}^- = \hbar\varepsilon\hat{n}_a, \quad (2.65)$$

where I introduced the occupation number operator  $\hat{n}_a = \hat{\sigma}^+\hat{\sigma}^-$  for the two-level system. Formally, this Hamiltonian shows quite similarities with the Hamiltonian of the monochromatic free electromagnetic field (2.56). Namely, the Hamiltonian takes on the form of a product of the occupation number of the excited level and the energy of this level. Note that, in literature one often finds other notations for this Hamiltonian corresponding to another choice of energies. Furthermore, one can see that, the Hamiltonian (2.65) commutes with the occupation-number operator  $\hat{n}_a$  and, therefore, the conserved quantities for this Hamiltonian are the excitations of the two-level system.

After having derived the quantum mechanical description of the energy contributions of the intra-cavity photon field and the two-level system, I now investigate the energy contribution arising from the interaction between those two, in the following section.

## 2.3 Interaction Hamiltonian

In the previous section, I derived the Hamiltonian for a two-level system without specifying the actual experimental setup. However, in order to derive the interaction Hamiltonian in the following paragraph, I need to be more precise, since there is a variety of possible realizations of this system, leading to very different interactions. For example, one can implement the two-level system using the spin of an electron, which could be manipulated by a magnetic field. Hence, the interaction Hamiltonian for this case would be proportional to the magnetic field. On the other hand, one can use the electronic transitions in an atom, to realize the system. In this case the electron would couple to the electric field vector.

Within this thesis I focus on the latter case. Hence, the energy states  $|g\rangle$ ,  $|e\rangle$  correspond to electronic states. The transition between these states is characterized by the electronic-transition dipole moment. In this case the interaction is mediated

via the coupling of the electrical field to the transition dipole moment. Assuming that the wavelength of the monochromatic electric field is large compared to the dimension of the atom, one can work in the so called *dipole approximation*. In this approximation, one considers only the field strength at the centre-of-mass position of the atom. Thus, using this approach, the classical interaction Hamilton function takes on the form

$$H_{\text{int}} = -q \mathbf{r} \cdot \mathbf{E}(\mathbf{R}, t), \quad (2.66)$$

where the vector  $\mathbf{R}$  labels the centre-of-mass position of the atom and  $q \mathbf{r}$  is the classical electronic dipole moment. Since I assume that the intra-cavity photon field is monochromatic and has a fixed polarization, I drop the index  $\rho$  and  $\sigma$  in the electric field and, thus, the explicit form of the quantized form of the electric field (2.40) is given by

$$\hat{\mathbf{E}}(\mathbf{R}, t) = i \xi [\hat{a}(t) \mathbf{u}(\mathbf{R}) - \hat{a}^\dagger(t) \mathbf{u}^*(\mathbf{R})], \quad (2.67)$$

where I introduced the abbreviation

$$\xi = \left( \frac{\hbar \omega}{2 \epsilon_0} \right)^{1/2}. \quad (2.68)$$

Note that, the photonic ladder operators  $\hat{a}(t)$ ,  $\hat{a}^\dagger(t)$  in the above equation are now formally time dependent. The reason for this is, that I absorbed the time dependence of the mode function  $\mathbf{u}(\mathbf{R})$  and defined

$$\hat{a}(t) = \hat{a} e^{-i\omega t}. \quad (2.69)$$

To the end of this section, I drop the explicit time dependence for the sake of clarity. In order to write down the fully quantized version of (2.66), one still needs to find the quantum mechanical description of the dipole moment. Trying to use the same procedure as in (2.57), I expand the dipole operator in the energy eigenbasis of the two-level system. This approach leads to

$$q \mathbf{r} = \sum_{i,j} |i\rangle \langle i| q \mathbf{r} |j\rangle \langle j|, \quad (2.70)$$

where the indices  $i$  and  $j$  label the respective energy eigenstates  $|g\rangle$ ,  $|e\rangle$ . Since transition dipole moments can just arise from electronic transition from  $|g\rangle$  to  $|e\rangle$  or vice versa, the terms corresponding to the even transitions  $q \langle e| \mathbf{r} |e\rangle$  and  $q \langle g| \mathbf{r} |g\rangle$ , have to be zero. Hence, I define

$$\begin{aligned} \mathbf{p} &:= q \langle e| \mathbf{r} |g\rangle, \\ \mathbf{p}^* &:= q \langle g| \mathbf{r} |e\rangle. \end{aligned} \quad (2.71)$$

These results yield the following expression for the dipole operator expansion (2.70):

$$q \mathbf{r} = \mathbf{p} |e\rangle \langle g| + \mathbf{p}^* |g\rangle \langle e| = \mathbf{p} \hat{\sigma}^+ + \mathbf{p}^* \hat{\sigma}^-. \quad (2.72)$$

For the last equivalence in (2.72), I used the relation of the state vectors to the Pauli matrices, introduced in (2.62). Subsequently, one can combine expressions (2.67) and (2.72) to give the quantized version of the interaction Hamiltonian (2.66), which reads

$$\hat{H}_{\text{int}} = -i \xi [\hat{a} \mathbf{u}(\mathbf{R}) - \hat{a}^\dagger \mathbf{u}^*(\mathbf{R})] (\mathbf{p} \hat{\sigma}^+ + \mathbf{p}^* \hat{\sigma}^-). \quad (2.73)$$

Expanding this expression yields

$$\begin{aligned} \hat{H}_{\text{int}} = & -i \xi [\hat{a} \mathbf{u}(\mathbf{R}) \cdot \mathbf{p} \hat{\sigma}^+ + \hat{a} \mathbf{u}(\mathbf{R}) \cdot \mathbf{p}^* \hat{\sigma}^- \\ & - \hat{a}^\dagger \mathbf{u}^*(\mathbf{R}) \cdot \mathbf{p} \hat{\sigma}^+ - \hat{a}^\dagger \mathbf{u}^*(\mathbf{R}) \cdot \mathbf{p}^* \hat{\sigma}^-]. \end{aligned} \quad (2.74)$$

Having a closer look at the occurring terms, one can see that, two of them describe rather unphysical processes, that violate conservation laws. In fact, the term proportional to  $\hat{a} \hat{\sigma}^-$  describes the decay of the excited atomic level together with the annihilation of an intra-cavity field photon, whereas the term proportional to  $\hat{a}^\dagger \hat{\sigma}^+$  describes the excitation of the atom together with the creation of a photon. Both processes obviously violate the conservation of energy and particle number in the system and, hence, I neglect them in the further calculations. This approach is known in the literature as the *rotating wave approximation* (RWA) [135, 137, 138] and leads to a Hamiltonian of the form

$$\hat{H}_{\text{int}} = -i \hbar (g \hat{a} \hat{\sigma}^+ - g^* \hat{a}^\dagger \hat{\sigma}^-), \quad (2.75)$$

where I introduced the complex coupling strength  $g$  defined by  $\hbar g = \xi \mathbf{u}(\mathbf{R}) \cdot \mathbf{p}$  and  $\hbar g^* = \xi \mathbf{u}^*(\mathbf{R}) \cdot \mathbf{p}^*$ . Note that the implicit time dependence of the Hamiltonian (2.75) due to relation (2.69) vanishes in a rotating frame and, thus, can be neglected in the following considerations.

At first appearance it seems that, one has arrived at the simplest form for the interaction Hamiltonian. However, I show within the next section that there exists a property of the Hamiltonian (2.75), which leads to an even more compact form.

## 2.4 Symmetry of the Interaction Hamiltonian

Within this section I am going to examine the invariance of the Hamiltonian (2.75) under global  $U(1)$  phase transformations. This symmetry offers the possibility to restrict the complex coupling strength  $g$  to real values and, thus, leads to the final form of the interaction part of the Jaynes-Cummings Hamiltonian.

The standard approach to analyse this property of the Hamiltonian is to apply a global phase transformation to either the state vectors or the appearing operators. I use the first method and perform the following transformation for the two-level eigenstates

$$|e\rangle' \rightarrow e^{i\alpha} |e\rangle, \quad |g\rangle' \rightarrow e^{i\beta} |g\rangle. \quad (2.76)$$

The introduced parameters  $\alpha$  and  $\beta$  are global constants independent of space and time. Using the relations (2.62) I see that this transformation immediately yields new expressions for the annihilation and creation operators of the two-level system, namely

$$\hat{\sigma}^{+'} \rightarrow e^{i(\alpha-\beta)} \hat{\sigma}^+, \quad \hat{\sigma}^{-'} \rightarrow e^{-i(\alpha-\beta)} \hat{\sigma}^-. \quad (2.77)$$

By inserting these expressions into (2.65), it is easy to see that the performed phase transformation leaves the Hamiltonian invariant.

$$\hat{H}'_{\text{atom}} = \hbar \varepsilon \hat{\sigma}^{+'} \hat{\sigma}^{-'} = \hbar \varepsilon e^{i(\alpha-\beta)} \hat{\sigma}^+ e^{-i(\alpha-\beta)} \hat{\sigma}^- = \hbar \varepsilon \hat{\sigma}^+ \hat{\sigma}^- = \hat{H}_{\text{atom}}. \quad (2.78)$$

Following the same procedure, I analyse the symmetry of the Hamilton for the free electromagnetic field (2.53), by performing a global phase transformation on the photonic annihilation and creation operators as follows

$$\hat{a}' \rightarrow e^{i\phi} \hat{a}, \quad \hat{a}^{\dagger'} \rightarrow e^{-i\phi} \hat{a}^\dagger, \quad (2.79)$$

with the global constant  $\phi$ . An investigation of the effect of this transformation on equation (2.53) immediately shows that the Hamiltonian of the intra-cavity photon field stays invariant:

$$\hat{H}'_{\text{field}} = \hbar \omega \left( \hat{a}^{\dagger'} \hat{a}' + \frac{1}{2} \right) = \hbar \omega \left( e^{-i\phi} \hat{a}^\dagger e^{i\phi} \hat{a} + \frac{1}{2} \right) = \hbar \omega \left( \hat{a}^\dagger \hat{a} + \frac{1}{2} \right) = \hat{H}_{\text{field}}. \quad (2.80)$$

Therefore, both the intra-cavity field Hamiltonian as well as the two-level system Hamiltonian, remain invariant under some global phase transformation. The interesting question is: what happens to the interaction part? This can be easily investigated by simultaneously performing both transformations (2.77) and (2.79) on equation (2.75), which results in the modified interaction Hamiltonian:

$$\hat{H}_{\text{int}} = -i\hbar \left[ g \hat{a} \hat{\sigma}^+ e^{i(\phi+\alpha-\beta)} - g^* \hat{a}^\dagger \hat{\sigma}^- e^{-i(\phi+\alpha-\beta)} \right]. \quad (2.81)$$

Furthermore, using the fact that complex numbers can be separated into a real modulus and a complex phase, equation (2.81) can be rewritten as

$$\hat{H}_{\text{int}} = -i\hbar |g| \left[ \hat{a} \hat{\sigma}^+ e^{i(\theta+\phi+\alpha-\beta)} - \hat{a}^\dagger \hat{\sigma}^- e^{-i(\theta+\phi+\alpha-\beta)} \right], \quad (2.82)$$

where I defined  $g = |g|e^{i\theta}$ . The arbitrariness of the introduced parameters  $\alpha$ ,  $\beta$  and  $\phi$  allows to choose their values in such a way as to compensate for the phases of the coupling constant. For this reason, I demand that the following relation has to hold

$$\theta + \phi + \alpha - \beta \stackrel{!}{=} \frac{\pi}{2}. \quad (2.83)$$

Here I choose  $\pi/2$  because I want to use the over determination to get rid of the pre-factor  $i$  in (2.82). With the phase parameters obeying equation (2.83), one finally arrives at the most compact formulation of the interaction Hamiltonian, which reads

$$\hat{H}_{\text{int}} = \hbar g \left( \hat{a} \hat{\sigma}^+ + \hat{a}^\dagger \hat{\sigma}^- \right), \quad (2.84)$$

where the coupling constant  $g$  is now a real quantity defined as

$$\hbar g = \xi |\mathbf{u}(\mathbf{R}) \cdot \mathbf{p}|. \quad (2.85)$$

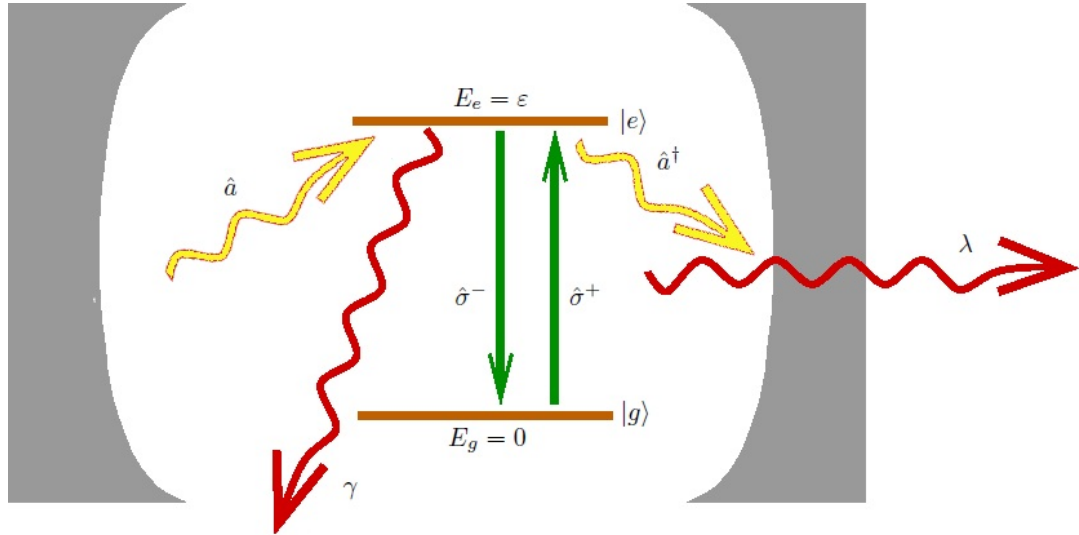


Figure 2.2: **Two-level system in a micro cavity and the most important processes in this system.** Yellow arrows indicate the creation and annihilation of cavity photons, green arrows indicate the excitation and relaxation of the two-level system and the red arrows indicate the loss processes ( $\hbar = 1$ ).

## 2.5 Jaynes-Cummings Hamiltonian

The Jaynes-Cummings (JC) system under consideration is depicted schematically in Figure 2.2. In this picture I have indicated the main processes one has to deal with in the further calculations. In specific there are: the creation and annihilation of intra-cavity photons via the photonic operators  $\hat{a}$ ,  $\hat{a}^\dagger$ , the excitation and relaxation of the two-level system via the electronic operators  $\sigma^+$ ,  $\sigma^-$  and two new processes, that have not been discussed yet. These new processes, which are indicated by the red wavy arrows, correspond to loss processes in the cavity. In a real experiment, there will be two main sources for energy dissipation out of the system. The first one is simply due to the fact that, in general there is a non-vanishing probability for spontaneous emission of a photon from the excited level of the atom. In my formulation this probability is proportional to  $\gamma$ . The second process amounts for the fact, that the cavity itself is not perfectly closed and, therefore, gives rise to the possibility of a photon to leak out of the cavity at a rate  $\lambda$ . However, within the further calculations, I explicitly neglect these loss processes, assuming that the coupling  $g$  is much

bigger than the dissipation, i.e.

$$\frac{g^2}{\gamma \lambda} \gg 1. \quad (2.86)$$

This approach is known in the literature as working in the *strong coupling regime*. This regime has already been shown to be experimentally feasible in many different setups [66, 82, 83, 86, 93, 94, 102, 104, 106, 111, 117, 140, 141]. From equation (2.85), I deduce that, this regime can be established by maximizing the electronic-transition dipole moment and choosing a small cavity volume. For completeness, I mention that there also exists some calculations [140, 142–145] and experiments [88, 115], that explicitly describe and test the dissipative regime by taking loss processes into account.

Hitherto, I thoroughly derived and justified the basic constituents of the form of the Jaynes-Cummings Hamiltonian as I will consider it. Therefore, I can now write down the full Hamiltonian, which reads

$$\hat{H}^{\text{JC}} = \hat{H}_{\text{field}} + \hat{H}_{\text{atom}} + \hat{H}_{\text{int}}. \quad (2.87)$$

Shifting the energy of the system by  $\frac{1}{2}\hbar\omega$  in order to get rid of the zero-point energy contribution arising from the electromagnetic field Hamiltonian, one finds the following form for the Jaynes-Cummings Hamiltonian in the rotating wave approximation:

$$\hat{H}^{\text{JC}} = \hbar\omega \hat{a}^\dagger \hat{a} + \hbar\varepsilon \hat{\sigma}^+ \hat{\sigma}^- + \hbar g (\hat{a} \hat{\sigma}^+ + \hat{a}^\dagger \hat{\sigma}^-). \quad (2.88)$$

One can further transform this expression to a more convenient form, by introducing the composed occupation number operator

$$\hat{n} = \hat{a}^\dagger \hat{a} + \hat{\sigma}^+ \hat{\sigma}^-, \quad (2.89)$$

and the detuning parameter

$$\Delta = \varepsilon - \omega, \quad (2.90)$$

which is a measure for the detuning between the monochromatic photon field frequency and the two-level transition frequency. The resulting Hamiltonian reads

$$\hat{H}^{\text{JC}} = \hbar\omega \hat{n} + \hbar\Delta \hat{\sigma}^+ \hat{\sigma}^- + \hbar g (\hat{a} \hat{\sigma}^+ + \hat{a}^\dagger \hat{\sigma}^-), \quad (2.91)$$

which I will use within the further calculations.

First, I notice some general properties of this Hamiltonian. One thing I observe is that in the case of resonant pumping, i.e.  $\Delta = 0$  the second term vanishes, leaving just the contribution proportional to  $\hbar\omega$  and the interaction term, which is proportional to  $g$ . Considering the latter, I place emphasis on the fact that, this term describes the conversion of atomic excitations to photonic excitations and vice versa. The next step to analyse the Jaynes-Cummings model is to determine the eigenstates and eigenvalues of the Hamiltonian (2.91). It turns out that to perform these

calculations, the rotating wave approximation introduced in Section 2.3 is absolutely crucial. Within this approximation it is possible to analytically diagonalize the Hamiltonian. However, as proposed by Feranchuk et. al. [146] and others [122, 147–150] it is also possible to analytically solve the Jaynes-Cummings model without the RWA, but within this thesis, I explicitly make use of this simplification.

In order to diagonalize Hamiltonian (2.91), one has to investigate its commutator with the occupation number operator  $\hat{n}$ , which leads to

$$\left[ \hat{n}, \hat{H}^{\text{JC}} \right] = \hbar \omega [\hat{n}, \hat{n}] + \hbar \Delta [\hat{n}, \hat{\sigma}^+ \hat{\sigma}^-] + \hbar g \left( [\hat{n}, \hat{a} \hat{\sigma}^+] + [\hat{n}, \hat{a}^\dagger \hat{\sigma}^-] \right). \quad (2.92)$$

Remembering that, each operator commutes with itself and noticing that the following relations have to hold

$$[\hat{a}, \hat{\sigma}^+] = [\hat{a}, \hat{\sigma}^-] = [\hat{a}^\dagger, \hat{\sigma}^+] = [\hat{a}^\dagger, \hat{\sigma}^-] = 0, \quad (2.93)$$

since the appearing operators  $\hat{a}^\dagger$ ,  $\hat{a}$  and  $\hat{\sigma}^+$ ,  $\hat{\sigma}^-$  operate on independent subspaces, one can immediately conclude that

$$[\hat{n}, \hat{\sigma}^+ \hat{\sigma}^-] = [\hat{n}, \hat{a}^\dagger \hat{a}] = 0. \quad (2.94)$$

Hence, the commutator (2.92) simplifies to

$$\left[ \hat{n}, \hat{H}^{\text{JC}} \right] = \hbar g \left( [\hat{n}, \hat{a} \hat{\sigma}^+] + [\hat{n}, \hat{a}^\dagger \hat{\sigma}^-] \right). \quad (2.95)$$

Using the fundamental commutator relations for the photonic ladder operators defined in (2.38), as well as the commutator relation of the Pauli matrices:

$$[\hat{\sigma}^+, \hat{\sigma}^-] = \hat{\sigma}_z, \quad (2.96)$$

one can easily calculate the remaining commutators, which results in the following relations

$$\begin{aligned} [\hat{\sigma}^+ \hat{\sigma}^-, \hat{a} \hat{\sigma}^+] &= \hat{a} \hat{\sigma}^+, & [\hat{a}^\dagger \hat{a}, \hat{a} \hat{\sigma}^+] &= -\hat{\sigma}^+ \hat{a}, \\ [\hat{a}^\dagger \hat{a}, \hat{a}^\dagger \hat{\sigma}^-] &= \hat{a}^\dagger \hat{\sigma}^-, & [\hat{\sigma}^+ \hat{\sigma}^-, \hat{a}^\dagger \hat{\sigma}^-] &= -\hat{\sigma}^- \hat{a}^\dagger, \end{aligned} \quad (2.97)$$

which yields for the commutators in equation (2.95)

$$[\hat{n}, \hat{a} \hat{\sigma}^+] = [\hat{n}, \hat{a}^\dagger \hat{\sigma}^-] = 0. \quad (2.98)$$

Thus, I found the very important property, that the Jaynes-Cummings Hamiltonian  $\hat{H}^{\text{JC}}$  commutes with the bosonic occupation number operator  $\hat{n}$ :

$$\left[ \hat{n}, \hat{H}^{\text{JC}} \right] = 0. \quad (2.99)$$

This result has two essential implications. The first one is that  $\hat{n}$  obviously describes a conserved quantity in the Jaynes-Cummings model. This quantity is the number of so called *polaritons* in the system. In the present model, a polariton is basically a

coupled excitation of the atomic and the photonic system.

The second important implication is, that  $\hat{H}^{\text{JC}}$  and  $\hat{n}$  share a common set of eigenstates, in which both operators are diagonal. In order to find these states, it is advisable to have a closer look at the occupation number operator. As introduced in (2.89), this operator is the sum of the occupation number operators for the intracavity photon field  $\hat{n}_p = \hat{a}^\dagger \hat{a}$  and the occupation number operator  $\hat{n}_a = \hat{\sigma}^+ \hat{\sigma}^-$  of the two-level system, respectively. Because these operators commute as well, they also share a set of common eigenstates. Nevertheless, since they operate in different subspaces and, therefore, have distinct sets of eigenvalues, the only possible candidate for a common set of eigenstates are the product states of the photonic Fock states and the atomic two-level states. For this reason, I consider the ansatz

$$|n_p, s\rangle = |n_p\rangle \otimes |s\rangle, \quad s \in \{e, g\}, \quad (2.100)$$

where these new states have to satisfy the eigenvalue equations

$$\begin{aligned} \hat{n}_p |n_p, s\rangle &= n_p |n_p, s\rangle, \\ \hat{n}_a |n_p, s\rangle &= n_a |n_p, s\rangle. \end{aligned} \quad (2.101)$$

Furthermore, the new set of product states inherits the completeness and orthogonality relations from the subspaces of its components yielding

$$\sum_{n=0}^{\infty} \sum_{s=e,g} |n_p, s\rangle \langle n_p, s| = 1, \quad (2.102)$$

$$\langle n'_p, s'| \cdot |n_p, s\rangle = \delta_{n_p, n'_p} \delta_{s, s'}. \quad (2.103)$$

Throughout this thesis, I refer to this product states as the *bare basis set* of the Jaynes-Cummings model. The presented set of states leads, according to equations (2.100) and (2.101), to the following eigenvalue equation of the polariton occupation number operator

$$\hat{n} |n_p, s\rangle = (n_p + n_a) |n_p, s\rangle = n |n_p, s\rangle. \quad (2.104)$$

Remembering from Section 2.2 that  $n_a$  can only take on the values 1 and 0, corresponding to the excitation states  $|e\rangle$  and  $|g\rangle$ , one can immediately deduce from (2.104) the important fact that for a fixed number  $n$  of polaritons there exist *two possible micro states*.

Having found a set of eigenstates of the polariton occupation number operator, one can now make use of this result and write down the representation of the Jaynes-Cummings Hamilton operator with respect to the bare basis by using the completeness relation (2.102):

$$\hat{H}^{\text{JC}} = \sum_{n_p, n'_p=0}^{\infty} \sum_{s, s'} |n_p, s\rangle \langle n_p, s| \hat{H}^{\text{JC}} |n'_p, s'\rangle \langle n'_p, s'|. \quad (2.105)$$

Arranging the occurring terms according to the number of polaritons and using the orthogonality relation (2.103), leads to a block-diagonal form of the Hamilton operator. One can see that (2.105) separates into the ground-state contribution and an infinite number of blocks of higher order contributions with fixed polariton number  $n$ :

$$\begin{aligned} \hat{H}^{\text{JC}} = & |0, g\rangle h_{0g,0g} \langle 0, g| \\ & + |1, g\rangle h_{1g,0e} \langle 0, e| + |1, g\rangle h_{1g,1g} \langle 1, g| + |0, e\rangle h_{0e,1g} \langle 1, g| + |0, e\rangle h_{0e,0e} \langle 0, e| \\ & + |2, g\rangle h_{2g,1e} \langle 1, e| + |2, g\rangle h_{2g,2g} \langle 2, g| + |1, e\rangle h_{1e,2g} \langle 2, g| + |1, e\rangle h_{1e,1e} \langle 1, e| \\ & + |3, g\rangle h_{3g,2e} \langle 2, e| + |3, g\rangle h_{3g,3g} \langle 3, g| + |2, e\rangle h_{2e,2e} \langle 2, e| + |2, e\rangle h_{2e,3g} \langle 3, g| \\ & + \dots, \end{aligned} \quad (2.106)$$

where I used the abbreviation  $h_{n s, n' s'} = \langle n, s | \hat{H}^{\text{JC}} | n', s' \rangle$  for the respective matrix elements. This expression can be transformed to a simpler form by introducing  $(2 \times 2)$  matrices for each polariton number, leading to a Hamiltonian of the form

$$\hat{H}^{\text{JC}} = \hat{h}_0 + \sum_{n=1}^{\infty} \hat{h}_n, \quad (2.107)$$

where  $n$  labels the number of polaritons and the operators  $\hat{h}_0, \hat{h}_n$  are defined as

$$\hat{h}_0 = |0, g\rangle \langle 0, g| \hat{H}^{\text{JC}} |0, g\rangle \langle 0, g| = 0, \quad (2.108)$$

$$\hat{h}_n = \begin{pmatrix} \langle n, g | \hat{H}^{\text{JC}} | n, g \rangle & \langle n, g | \hat{H}^{\text{JC}} | n-1, e \rangle \\ \langle n-1, e | \hat{H}^{\text{JC}} | n, g \rangle & \langle n-1, e | \hat{H}^{\text{JC}} | n-1, e \rangle \end{pmatrix}. \quad (2.109)$$

Remembering the analysis of Sections 2.1 and 2.2, one can calculate the matrix entries using the action of the ladder operators on their respective eigenstates. With the properties

$$\begin{aligned} \hat{\sigma}^+ \hat{\sigma}^- |n, g\rangle &= 0, & \hat{\sigma}^+ \hat{\sigma}^- |n-1, e\rangle &= |n-1, e\rangle, \\ \hat{a}^\dagger \hat{a} |n, g\rangle &= n |n, g\rangle, & \hat{a}^\dagger \hat{a} |n-1, e\rangle &= (n-1) |n-1, e\rangle, \\ \hat{a} \hat{\sigma}^+ |n, g\rangle &= \sqrt{n} |n-1, e\rangle, & \hat{a} \hat{\sigma}^+ |n-1, e\rangle &= 0, \\ \hat{a}^\dagger \hat{\sigma}^- |n, g\rangle &= 0, & \hat{a}^\dagger \hat{\sigma}^- |n-1, e\rangle &= \sqrt{n} |n, g\rangle, \end{aligned} \quad (2.110)$$

one finds, that the sub Hamiltonians (2.109) have the following representation in the bare basis

$$\hat{h}_n = \begin{pmatrix} \hbar \omega n & \hbar g \sqrt{n} \\ \hbar g \sqrt{n} & \hbar \omega n + \hbar \Delta \end{pmatrix}. \quad (2.111)$$

Thus, the problem of finding the eigenvalues of the potentially infinite Hamiltonian (2.91) is reduced to the much simpler task of finding the two eigenvalues of matrix (2.111). Mathematically this is a well known situation, which can be solved in

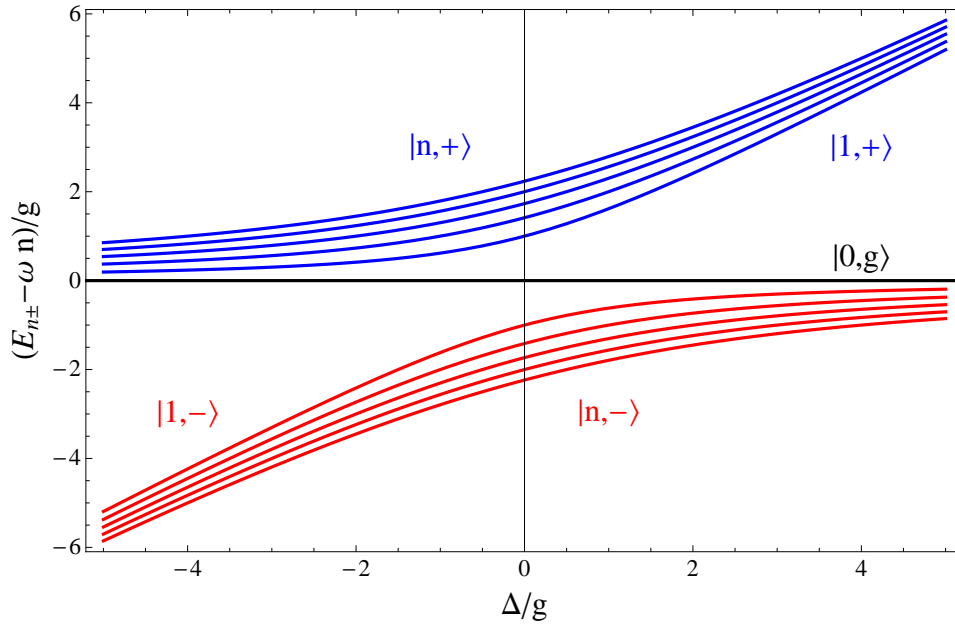


Figure 2.3: **Plot of the energy eigenvalues (2.113) of the Jaynes-Cummings model versus the detuning ( $\hbar = 1$ ).**

general by evaluating the characteristic polynomial of the respective matrix. In the present case this approach yields the following equation

$$(\hbar\omega n - E_n)(\hbar\omega n + \hbar\Delta - E_n) - \hbar^2 g^2 n = 0, \quad (2.112)$$

which immediately gives the eigenvalues as

$$E_{n\pm} = \hbar\omega n + \frac{1}{2}\hbar(\Delta \pm R_n), \quad n > 1 \quad \text{and} \quad E_0 = 0. \quad (2.113)$$

Here, I followed the conventional notation found in the literature (see for example [122, 135–138]) and introduced the *generalized Rabi frequency*

$$R_n(\Delta) = \sqrt{\Delta^2 + 4g^2n}. \quad (2.114)$$

In Figure 2.3, I plot the energy eigenvalues (2.113) versus the detuning. One can see from this picture that for a fixed polariton number  $n$  the spectrum contains a set of two non-degenerated energy eigenvalues. One can see clearly that these eigenvalues naturally separate into so called upper and lower polariton branches, with the vacuum state as the only eigenstate belonging to both of them. Furthermore, one finds that the energy eigenvalues remain completely non-degenerated, even if the system is not in resonance. This fact is quite important for the following Schrödinger perturbation theory.

The splitting between states with the same number of polaritons is, according to equation (2.113), given by

$$\delta E_n = E_{n+} - E_{n-} = R_n(\Delta) = \sqrt{\Delta^2 + 4g^2n}. \quad (2.115)$$

Notice, that this splitting does not only depend on the detuning  $\Delta$ , which is expected, but also on the occupation number  $n$  in a non-linear way. This non-linearity leads to some interesting phenomena, which will be discussed in a little bit more detail within the next section.

Having obtained the energy eigenvalues, I can now calculate the respective eigenvectors by solving the eigenvalue equation

$$\begin{pmatrix} \hbar\omega n & \hbar g\sqrt{n} \\ \hbar g\sqrt{n} & \hbar\omega n + \hbar\Delta \end{pmatrix} \begin{pmatrix} \alpha^\pm \\ \beta^\pm \end{pmatrix} = E_{n^\pm} \begin{pmatrix} \alpha^\pm \\ \beta^\pm \end{pmatrix}. \quad (2.116)$$

To this end I additionally assume that the eigenvectors are normalized and therefore their coefficients have to satisfy the relation

$$(\alpha^\pm)^2 + (\beta^\pm)^2 = 1. \quad (2.117)$$

Hence, the coefficients  $\alpha^\pm$  and  $\beta^\pm$  depend on each other. Because of that, I just have to consider one of the equations described by (2.116). Choosing the first one, I find that the coefficients have to satisfy the relation

$$\hbar\omega n\alpha^+ + \hbar g\sqrt{n}\beta^+ = E_{n+}\alpha^+. \quad (2.118)$$

Inserting (2.117) yields:

$$\begin{aligned} (\hbar\omega n - E_{n+})\alpha^+ + \hbar g\sqrt{n}\sqrt{1 - (\alpha^+)^2} &= 0, \\ \frac{1}{2}\hbar(\Delta + R_n)\alpha^+ &= \hbar g\sqrt{n}\sqrt{1 - (\alpha^+)^2}, \\ (\Delta + R_n)^2(\alpha^+)^2 &= 4g^2n[1 - (\alpha^+)^2]. \end{aligned} \quad (2.119)$$

Hence, one finds for the first coefficient  $\alpha^+$ :

$$\alpha^+ = \frac{2g\sqrt{n}}{\sqrt{(\Delta + R_n)^2 + 4g^2n}}. \quad (2.120)$$

Applying (2.117) once more, the second coefficient  $\beta^+$  becomes:

$$\beta^+ = \frac{\Delta + R_n}{\sqrt{(\Delta + R_n)^2 + 4g^2n}}. \quad (2.121)$$

In principle, one could directly use these expressions. Yet, relation (2.117) implicates, that there should also exist a mapping for the coefficients  $\alpha^+$  and  $\beta^+$  onto the unit circle. This observation justifies the parametrization

$$\sin \theta_n := \alpha^+, \quad \cos \theta_n := \beta^+. \quad (2.122)$$

That does not look like a huge improvement, but using some trigonometric addition theorems, one can show that this approach simplifies the form of the eigenstate coefficients. Using an addition theorem for the cosine leads to:

$$\begin{aligned} \cos(2\theta_n) &= \cos^2 \theta_n - \sin^2 \theta_n = \frac{(\Delta + R_n)^2 - 4g^2n}{(\Delta + R_n)^2 + 4g^2n} \\ &= \frac{\Delta}{\frac{\Delta^2 + \Delta R_n + R_n^2 - \Delta^2}{(\Delta + R_n)}} = \frac{\Delta}{\frac{(\Delta + R_n)R_n}{(\Delta + R_n)}}, \end{aligned} \quad (2.123)$$

which, in turn, leads to the neat relation:

$$\cos(2\theta_n) = \frac{\Delta}{R_n}. \quad (2.124)$$

A corresponding theorem for the sine yields:

$$\begin{aligned} \sin(2\theta_n) &= 2 \sin \theta_n \cos \theta_n = \frac{4g\sqrt{n}(\Delta + R_n)}{(\Delta + R_n)^2 + 4g^2n} \\ &= \frac{4g\sqrt{n}}{\frac{\Delta^2 + 2\Delta R_n + R_n^2 + R_n^2 - \Delta^2}{(\Delta + R_n)}} = \frac{4g\sqrt{n}}{\frac{2R_n(\Delta + R_n)}{(\Delta + R_n)}}, \end{aligned} \quad (2.125)$$

and, thus, one finds:

$$\sin(2\theta_n) = \frac{2g\sqrt{n}}{R_n}. \quad (2.126)$$

The combination of equation (2.124) and equation (2.126) results in the concise expression

$$\tan(2\theta_n) = \frac{2g\sqrt{n}}{\Delta}. \quad (2.127)$$

Performing the same calculations for the second set of probability amplitudes, one finds the analogue relations:

$$\alpha^- = \frac{2g\sqrt{n}}{\sqrt{(\Delta - R_n)^2 + 4g^2n}}, \quad (2.128)$$

$$\beta^- = \frac{\Delta - R_n}{\sqrt{(\Delta - R_n)^2 + 4g^2n}}. \quad (2.129)$$

In order to determine the corresponding expressions in the parametrized picture introduced in relation (2.122), one needs to take a closer look at the squared amplitudes. After some transformations:

$$\begin{aligned}
 (\alpha^-)^2 &= \frac{4g^2n}{(\Delta - R_n)^2 + 4g^2n} = \frac{4g^2n(\Delta + R_n)^2}{(\Delta - R_n)^2(\Delta + R_n)^2 + 4g^2n(\Delta + R_n)^2} \\
 &= \frac{(\Delta + R_n)^2}{\frac{(\Delta^2 - R_n^2)^2}{4g^2n} + (\Delta + R_n)^2} = \frac{(\Delta + R_n)^2}{4g^2n + (\Delta + R_n)^2},
 \end{aligned} \tag{2.130}$$

one gets the important relation:

$$(\alpha^-)^2 = (\beta^+)^2. \tag{2.131}$$

Following the same argumentation for  $\beta^-$ , yields:

$$\begin{aligned}
 (\beta^-)^2 &= \frac{(\Delta - R_n)^2}{(\Delta - R_n)^2 + 4g^2n} = \frac{(\Delta - R_n)^2 4g^2n}{4g^2n(\Delta - R_n)^2 + (4g^2n)^2} \\
 &= \frac{(\Delta - R_n)^2 4g^2n}{4g^2n(\Delta - R_n)^2 + (R_n^2 - \Delta^2)^2} = \frac{4g^2n}{4g^2n + \frac{(R_n^2 - \Delta^2)^2}{(\Delta - R_n)^2}} \\
 &= \frac{4g^2n}{4g^2n + \frac{(R_n - \Delta)^2(R_n + \Delta)^2}{(\Delta - R_n)^2}} = \frac{4g^2n}{4g^2n + (\Delta + R_n)^2},
 \end{aligned} \tag{2.132}$$

which indicates that

$$(\beta^-)^2 = (\alpha^+)^2. \tag{2.133}$$

However, there is still an uncertainty left. The calculations of the squared amplitudes  $(\alpha^\pm)^2, (\beta^\pm)^2$  harbour the risk to loose some signs. If I consider the case of zero detuning, I find that  $\beta^-$  indeed has to fulfil the relation  $\beta^- = -\alpha^+$ . Now, I finally arrive at the desired form of the Jaynes-Cummings eigenstates, that for  $n > 0$  the polariton eigenstates are given by

$$|n, +\rangle := \sin \theta_n |n, g\rangle + \cos \theta_n |n - 1, e\rangle \tag{2.134a}$$

$$|n, -\rangle := \cos \theta_n |n, g\rangle - \sin \theta_n |n - 1, e\rangle, \tag{2.134b}$$

whereas the vacuum state corresponding to  $n = 0$  takes on the form

$$|0, \pm\rangle \equiv |0, g\rangle = |0\rangle. \tag{2.135}$$

According to (2.127) the occurring mixing angle  $\theta_n$  is defined as:

$$\theta_n = \frac{1}{2} \arctan \left( \frac{2g\sqrt{n}}{\Delta} \right). \tag{2.136}$$

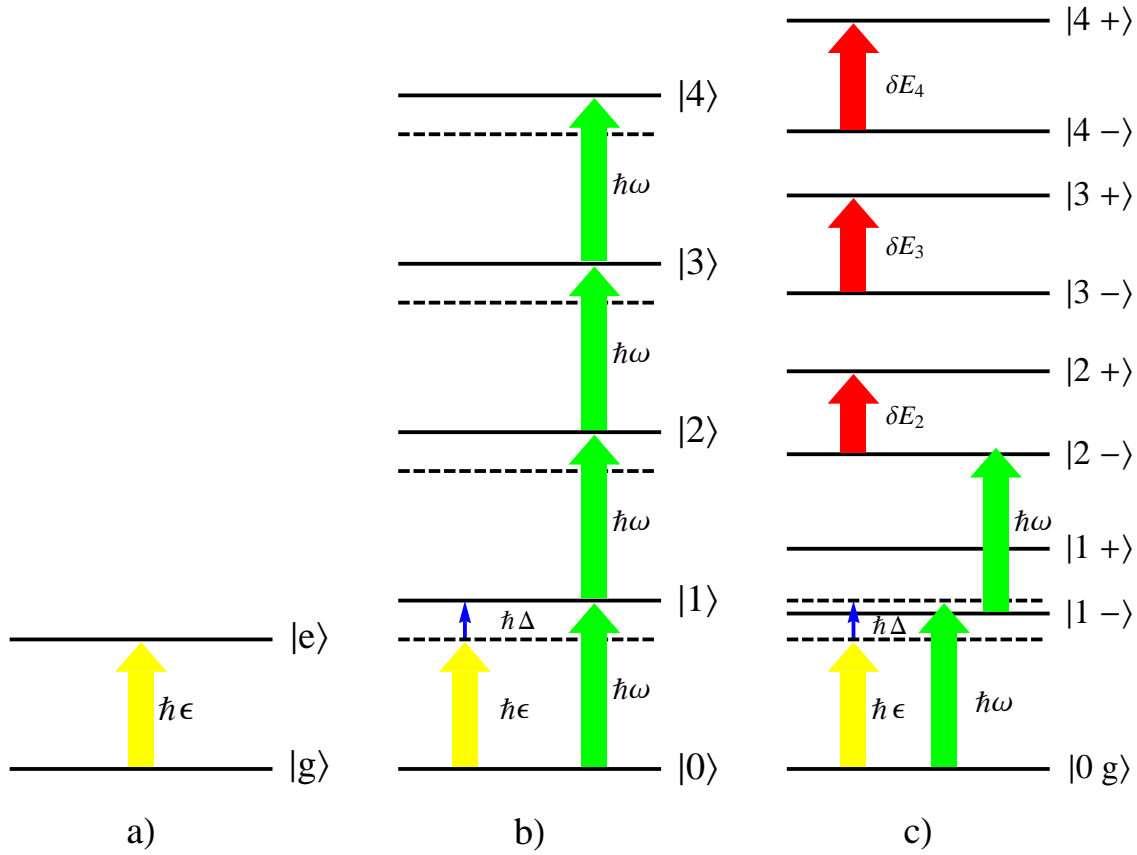


Figure 2.4: **Energy structure of the Jaynes-Cummings model with the parameters:**  $\Delta = 0.3\varepsilon$ ,  $g = 0.2\varepsilon$ . a) Energy spectrum of the two-level system. b) Energy spectrum of the harmonic oscillator corresponding to the intra-cavity field. c) Jaynes-Cummings dressed state ladder. The non-linearity indicated by the red arrows for the splitting as defined by (2.115).

Besides, using the orthogonality relation defined in (2.103), one can show that the Jaynes-Cummings eigenstates are orthonormal and obey the relation

$$\langle m, \alpha | n, \beta \rangle = \delta_{m,n} \delta_{\alpha,\beta}. \quad (2.137)$$

In the following, I refer to this eigenbasis as the *dressed-state basis* of the JC model. Figure 2.4 shows the dressed state energy levels of the Jaynes-Cummings model in comparison to the simple energy levels of the two-level system and the harmonic oscillator levels, corresponding to the energies of the intra-cavity photon field. The most striking difference is that the levels for the single atomic system, as well as for the single photonic system are equally spaced, whereas they are not for the dressed-state energy ladder of the Jaynes-Cummings system. This fact is the direct result of the non-linear dependence of the energy eigenvalues on the polariton number operator, found in (2.113).

## 2.6 Polariton Mapping

Throughout the further calculations, one has to deal with expressions containing expectation values of products of photonic ladder operators  $\hat{a}$  and  $\hat{a}^\dagger$ . Since these expectation values have to be evaluated with respect to the dressed-state basis, the question arises, how the photonic ladder operators act on the dressed states. All that is known so far, is their action on the bare states. However, the analysis in Section 2.5 showed how the dressed states are connected to the bare states, namely

$$\begin{pmatrix} |n, +\rangle \\ |n, -\rangle \end{pmatrix} = \mathcal{R}_n \begin{pmatrix} |n, g\rangle \\ |n-1, e\rangle \end{pmatrix}, \quad \mathcal{R}_n = \begin{pmatrix} a_n^+ & b_n^+ \\ a_n^- & b_n^- \end{pmatrix}, \quad (2.138)$$

where I introduced the matrix  $\mathcal{R}_n$  with entries

$$a_n^\alpha = \begin{cases} \sin \theta_n, & \alpha = + \\ \cos \theta_n, & \alpha = - \end{cases}, \quad b_n^\alpha = \begin{cases} \cos \theta_n, & \alpha = + \\ -\sin \theta_n, & \alpha = - \end{cases}. \quad (2.139)$$

Applying a photonic annihilation operator on one of the dressed states, results in a state vector, which is a superposition of the two dressed states corresponding to the reduced photon number. Thus, in the end, the action of this ladder operator on the dressed states is of the form

$$\hat{a} \begin{pmatrix} |n, +\rangle \\ |n, -\rangle \end{pmatrix} \stackrel{!}{=} \mathcal{T}_n \begin{pmatrix} |n-1, +\rangle \\ |n-1, -\rangle \end{pmatrix} = \begin{pmatrix} t_{n++} & t_{n+-} \\ t_{n-+} & t_{n--} \end{pmatrix} \begin{pmatrix} |n-1, +\rangle \\ |n-1, -\rangle \end{pmatrix}, \quad (2.140)$$

with the transition matrix  $\mathcal{T}_n$ . Using the definition (2.138) and the properties of the annihilation operator on the bare states, one finds that equation (2.140) leads to the following expression in the bare state representation:

$$\hat{a} \begin{pmatrix} |n, +\rangle \\ |n, -\rangle \end{pmatrix} = \hat{a} \mathcal{R}_n \begin{pmatrix} |n, g\rangle \\ |n-1, e\rangle \end{pmatrix}, \quad (2.141)$$

$$\mathcal{T}_n \mathcal{R}_{n-1} \begin{pmatrix} |n-1, g\rangle \\ |n-2, e\rangle \end{pmatrix} = \mathcal{R}_n \begin{pmatrix} \sqrt{n} & 0 \\ 0 & \sqrt{n-1} \end{pmatrix} \begin{pmatrix} |n-1, g\rangle \\ |n-2, e\rangle \end{pmatrix}. \quad (2.142)$$

Therefore, one obtains the following definition of the transition matrix

$$\mathcal{T}_n = \mathcal{R}_n \begin{pmatrix} \sqrt{n} & 0 \\ 0 & \sqrt{n-1} \end{pmatrix} \mathcal{R}_{n-1}^{-1}, \quad (2.143)$$

from which one can immediately deduce the respective transition amplitudes as

$$t_{n\pm-} = \sqrt{n} a_n^\pm b_{n-1}^+ + \sqrt{n-1} b_n^\pm b_{n-1}^-, \quad (2.144a)$$

$$t_{n\pm+} = \sqrt{n} a_n^\pm a_{n-1}^+ + \sqrt{n-1} b_n^\pm a_{n-1}^-. \quad (2.144b)$$

Thus, I find that the action of the photonic annihilation operator on the dressed basis states is given by

$$\hat{a} |m, \beta\rangle = \sum_{\alpha'=\pm} t_{m\beta\alpha'} |m-1, \alpha'\rangle. \quad (2.145)$$

In order to find a representation for  $\hat{a}$ , one needs to rewrite the right-hand side of equation (2.145) in such a way, that it yields an operator acting on  $|m, \beta\rangle$ . Therefore, I insert a suitable identity and use the orthonormal properties of the dressed state basis in (2.137), leading to

$$\hat{a} |m, \beta\rangle = \left( \sum_{n=1}^{\infty} \sum_{\alpha, \alpha'=\pm} t_{n\alpha\alpha'} |n-1, \alpha'\rangle \langle n, \alpha| \right) |m, \beta\rangle. \quad (2.146)$$

In principle, one could now use this result to calculate each emerging action of a photonic ladder operator on a dressed state in this matrix approach. However, I would like to follow an approach suggested in Ref. [49] and introduce an operator formalism to rewrite the projection operator in (2.146). Since I expand the model onto a lattice in the next chapter, I introduce the lattice site index  $j$  at this point and sum over all lattice sites. In order to get this polariton mapping, I start by looking for some operator representation, in which the local Jaynes-Cummings Hamiltonian becomes diagonal, i.e. takes on the form:

$$\hat{H}^{JC} = \sum_j \sum_{n=0}^{\infty} \sum_{\alpha=\pm} E_{n\alpha} \hat{P}_{jn\alpha}^\dagger \hat{P}_{jn\alpha}. \quad (2.147)$$

In this notation the energy eigenvalues  $E_{n\alpha}$  correspond to (2.113). Naturally, the first candidates for such operators are simply the projection operators in the dressed state basis, which are defined as

$$\hat{P}_{jn\alpha}^\dagger = |n, \alpha\rangle_j \langle 0, g|_j, \quad \hat{P}_{jn\alpha} = |0, g\rangle_j \langle n, \alpha|_j, \quad (2.148)$$

with their respective action on arbitrary dressed states

$$\begin{aligned} \hat{P}_{jn\alpha}^\dagger \hat{P}_{jn\alpha} |m, \beta\rangle_i &= \delta_{n,m} \delta_{\alpha,\beta} \delta_{i,j} |n, \alpha\rangle_j, \\ \hat{P}_{jn\alpha} \hat{P}_{jn\alpha}^\dagger |m, \beta\rangle_i &= \delta_{0,m} \delta_{i,j} |0, g\rangle_j. \end{aligned} \quad (2.149)$$

Note that, both operators in (2.148) represent projections of an arbitrarily dressed state with respect to the ground state. This is due to the fact, that the ground state is the only singlet state in the Jaynes-Cummings ladder, which makes it unique and, thus, a perfect candidate to define polariton creation with respect to it.

From the orthogonality relation of the dressed states (2.137) follows that these operators fulfil bosonic commutation relations. In fact, one finds for the commutators the following expressions

$$\left[ \hat{P}_{jn\alpha}, \hat{P}_{in\beta} \right] = 0, \quad (2.150)$$

and

$$\left[ \hat{P}_{jn\alpha}^\dagger, \hat{P}_{in\beta} \right] = \delta_{i,j} \delta_{\alpha,\beta}. \quad (2.151)$$

Therefore these operators represent bosonic annihilation and creation operators. Last but not least, I note that the ground-state projection operators obviously coincide:

$$\hat{P}_{j0}^\dagger = \hat{P}_{j0} = |0, g\rangle_j \langle 0, g|_j. \quad (2.152)$$

Since the introduced operators effectively create and annihilate polaritons from the vacuum, the huge advantage of this mapping is that it allows to express the photonic ladder operators in terms of these projection operators. Regarding equation (2.146) once again and using the derived properties of the polariton projection operators, one finds the following representation of the photonic ladder operators

$$\hat{a}_j = \sum_{n=1}^{\infty} \sum_{\alpha, \alpha'=\pm} t_{n\alpha\alpha'} \hat{P}_{j(n-1)\alpha'}^\dagger \hat{P}_{jn\alpha}, \quad (2.153a)$$

$$\hat{a}_j^\dagger = \sum_{n=0}^{\infty} \sum_{\alpha, \alpha'=\pm} t_{(n+1)\alpha'\alpha} \hat{P}_{j(n+1)\alpha'}^\dagger \hat{P}_{jn\alpha}. \quad (2.153b)$$

Now the action of  $\hat{a}_j$  on an arbitrary polariton dressed state, according to equation (2.153a), is to diminish the polariton number by one and perhaps alter the polariton type. This derived representation of the photonic annihilation and creation operators will be used throughout the whole thesis to calculate expectation values in the dressed-state basis.

# Chapter 3

## Jaynes-Cummings-Hubbard Model

Having thoroughly investigated the physics of the on-site light-matter interaction within the previous chapter, I am now going to expand this system on a  $D$ -dimensional lattice. This transition is performed by making all operators in the Jaynes-Cummings Hamiltonian (2.91) site dependent and sum over all lattice sites. To allow for a photon dynamic on the lattice, an additional Hubbard-like hopping term is included. This kind of approximation of dynamics on a lattice has first been proposed by J. Hubbard [5] for strongly correlated fermionic systems. Later it has been successfully applied to strongly interacting hardcore bosonic particle systems as well [6]. Whereas in these fermionic and hardcore bosonic systems a strong interaction occurs quite naturally, due to Coulomb or contact interaction respectively, the case is not quite so simple for photonic systems. In fact, photons hardly interact with each other and also their interaction with atoms is normally rather weak. As already outlined in the previous chapter, one can prevent the latter, by choosing a micro cavity setup, which enhances the light-matter interaction and, thus, leads to new bosonic quasi particles, the so called polaritons. Fortunately, the non-linearity exhibited in their energy spectrum, provides a mechanism for strong photonic interaction.

Suppose one has a Jaynes-Cummings system in its ground state, in which a cavity photon with exact the right frequency is coupled in, in order to achieve a transition form  $|0\rangle \rightarrow |1, -\rangle$ . Now, one climbed up the Jaynes-Cummings ladder, which leads, due to the non-linearity, to a slightly shifted transition frequency for the next higher transition. Hence, if a second photon, with the same frequency as the first one, tries to enter the cavity, it is detuned from the available transitions. In effect, it can not enter the cavity and gets reflected. This effect is known as the so called photon blockade effect [52, 60, 151]. Recently, it could be shown experimentally, that this effect leads, indeed, to the desired strong photonic interaction [55]. I give a short derivation of the Hubbard-like hopping term for the Jaynes-Cummings model on a lattice within the following section. Note that, in all following calculations I use the convention  $\hbar = 1$ .

### 3.1 Coupled Cavity Lattice

Within this section I present the theoretical description of the coupling of optical cavities in an array. To this end, I follow the ansatz proposed in Refs. [67, 152, 153]. As previously mentioned, I consider the Jaynes-Cummings-Hubbard model to be experimentally realized by a lattice, which is built of coupled micro cavities. Each of this cavities contains a two-level atom and, thus, matter is present in the system. For these reason the Maxwell equations (2.1) have to be modified. The resulting set of equations, for the case that no sources are present, reads

$$\nabla \cdot \mathbf{B}(\mathbf{r}, t) = 0, \quad (3.1a)$$

$$\nabla \cdot \mathbf{D}(\mathbf{r}, t) = 0, \quad (3.1b)$$

$$\nabla \times \mathbf{E}(\mathbf{r}, t) = -\frac{\partial \mathbf{B}(\mathbf{r}, t)}{\partial t}, \quad (3.1c)$$

$$\nabla \times \mathbf{H}(\mathbf{r}, t) = \frac{\partial \mathbf{D}(\mathbf{r}, t)}{\partial t}, \quad (3.1d)$$

where now the fields  $\mathbf{E}(\mathbf{r}, t)$  and  $\mathbf{D}(\mathbf{r}, t)$  are linked via the relation

$$\mathbf{D}(\mathbf{r}, t) = \epsilon_0 \epsilon(\mathbf{r}) \mathbf{E}(\mathbf{r}, t) = \epsilon_0 \epsilon(\mathbf{r}) \frac{\partial \mathbf{A}(\mathbf{r}, t)}{\partial t}. \quad (3.2)$$

Hence, this setup leads to an electrical permittivity  $\epsilon(\mathbf{r})$ , which now shares the periodicity of the lattice. Thus, it has the property

$$\epsilon(\mathbf{r}) = \epsilon(\mathbf{r} + \mathbf{R}), \quad (3.3)$$

where  $\mathbf{R}$  is a lattice vector. The local permittivity centred at lattice site  $\mathbf{R}$  is denoted as  $\epsilon_{\mathbf{R}}(\mathbf{r})$ . The appearance of the electrical permittivity in equation (3.2) leads to the following explicit form of the Maxwell relation (3.1b):

$$\nabla \cdot \left[ \epsilon(\mathbf{r}) \frac{\partial \mathbf{A}(\mathbf{r}, t)}{\partial t} \right] = 0. \quad (3.4)$$

It is too see that, in order to fulfil the above equation, one needs to modify the Coulomb gauge (2.11), which in the presence of matter reads

$$\nabla \cdot [\epsilon(\mathbf{r}) \mathbf{A}(\mathbf{r}, t)] = 0. \quad (3.5)$$

Following the usual procedure, one obtains the wave equation for the vector potential  $\mathbf{A}(\mathbf{r}, t)$ , by inserting equation (3.2) and  $\mathbf{H}(\mathbf{r}, t) / \mu_0 = \nabla \times \mathbf{A}(\mathbf{r}, t)$  into the Maxwell relation (3.1d), which yields

$$0 = \frac{\epsilon(\mathbf{r})}{c^2} \frac{\partial^2 \mathbf{A}(\mathbf{r}, t)}{\partial t^2} + \nabla \times \nabla \times \mathbf{A}(\mathbf{r}, t). \quad (3.6)$$

The periodicity of the permittivity as described by (3.3) leads to the fact that a photon moving in the lattice sees an effective potential with the periodicity of the lattice. This situation is equivalent to an electron moving through a solid, feeling an atomic potential with the periodicity of the crystal lattice. Inspired by this analogy, I apply a tight-binding ansatz for the vector potential, which satisfies the Bloch theorem and, hence, has the property

$$\mathbf{A}(\mathbf{r} + \mathbf{R}, t) = e^{i\mathbf{k}\mathbf{R}} \mathbf{A}(\mathbf{r}, t). \quad (3.7)$$

Therefore, I expand  $\mathbf{A}(\mathbf{r}, t)$  in terms of local on-site mode functions. In specific, I assume that these mode functions are given by Wannier functions  $w_{\mathbf{R}}(\mathbf{r})$ , which are localized around the centre  $\mathbf{R}$  of a lattice site. On each lattice site, these Wannier functions represent the spatial part of the high-Q cavity-mode and, thus, they are characterized by the cavity resonance frequency  $\omega_c$  and the local permittivity  $\epsilon_{\mathbf{R}}(\mathbf{r})$ . Then, follows from the Maxwell equations (3.1) that these local Wannier functions fulfil the eigenvalue equation

$$\epsilon_{\mathbf{R}}(\mathbf{r}) \frac{\omega_c^2}{c^2} w_{\mathbf{R}}(\mathbf{r}) = \nabla \times \nabla \times w_{\mathbf{R}}(\mathbf{r}). \quad (3.8)$$

Additionally, these Wannier functions have to obey locally the normalization condition

$$\int d\mathbf{r} \epsilon_{\mathbf{R}}(\mathbf{r}) w_{\mathbf{R}}^*(\mathbf{r}) w_{\mathbf{R}}(\mathbf{r}) = 1. \quad (3.9)$$

The assumption of localized wave functions leads to an expansion of the vector potential in terms of these Wannier functions. Therefore, in the case of a monochromatic field mode with fixed polarization, the vector potential takes on the following form

$$\mathbf{A}(\mathbf{r}, t) = \sum_n w_{\mathbf{R}}(\mathbf{r} - \mathbf{R}_n) e^{i(\mathbf{k}\mathbf{R}_n - \omega t)}. \quad (3.10)$$

Here, I introduced the lattice vectors  $\mathbf{R}_n = R \mathbf{n}$ , where  $R$  is a constant and  $\mathbf{n}$  a tuple of integers. It is easy to prove that this ansatz, indeed, satisfies (3.7). Inserting the approach (3.10) in the wave equation (3.6) yields

$$\sum_n \epsilon(\mathbf{r}) \frac{\omega^2}{c^2} w_{\mathbf{R}}(\mathbf{r} - \mathbf{R}_n) e^{i(\mathbf{k}\mathbf{R}_n - \omega t)} = \sum_n \nabla \times \nabla \times w_{\mathbf{R}}(\mathbf{r} - \mathbf{R}_n) e^{i(\mathbf{k}\mathbf{R}_n - \omega t)}. \quad (3.11)$$

Using result (3.8), the right-hand side of this expression can further be transformed into

$$\sum_n \epsilon(\mathbf{r}) \frac{\omega^2}{c^2} w_{\mathbf{R}}(\mathbf{r} - \mathbf{R}_n) e^{i\mathbf{k}\mathbf{R}_n} = \sum_n \epsilon_{\mathbf{R}}(\mathbf{r} - \mathbf{R}_n) \frac{\omega_c^2}{c^2} w_{\mathbf{R}}(\mathbf{r} - \mathbf{R}_n) e^{i\mathbf{k}\mathbf{R}_n}. \quad (3.12)$$

Now, multiplying both sides of this equation with  $w_{\mathbf{R}}^*(\mathbf{r})$  and performing a spatial integration, one finds

$$\omega^2 = \omega_c^2 \frac{\sum_n \int d\mathbf{r} \epsilon_{\mathbf{R}}(\mathbf{r} - \mathbf{R}_n) w_{\mathbf{R}}^*(\mathbf{r}) w_{\mathbf{R}}(\mathbf{r} - \mathbf{R}_n) e^{i\mathbf{k}\mathbf{R}_n}}{\sum_n \int d\mathbf{r} \epsilon(\mathbf{r}) w_{\mathbf{R}}^*(\mathbf{r}) w_{\mathbf{R}}(\mathbf{r} - \mathbf{R}_n) e^{i\mathbf{k}\mathbf{R}_n}}. \quad (3.13)$$

Splitting the summation over the lattice sites  $n$  into a term for  $n = 0$  and a sum over  $n \neq 0$  yields

$$\omega^2 = \omega_c^2 \frac{1 + \sum_{n \neq 0} e^{i\mathbf{k}\mathbf{R}_n} \beta_n}{1 + \gamma + \sum_{n \neq 0} e^{i\mathbf{k}\mathbf{R}_n} \alpha_n}, \quad (3.14)$$

where, for  $n \neq 0$ , the tight binding parameters are given by

$$\alpha_n = \int d\mathbf{r} \epsilon(\mathbf{r}) w_{\mathbf{R}}^*(\mathbf{r}) w_{\mathbf{R}}(\mathbf{r} - \mathbf{R}_n), \quad (3.15)$$

$$\beta_n = \int d\mathbf{r} \epsilon_{\mathbf{R}}(\mathbf{r} - \mathbf{R}_n) w_{\mathbf{R}}^*(\mathbf{r}) w_{\mathbf{R}}(\mathbf{r} - \mathbf{R}_n), \quad (3.16)$$

$$\gamma = \int d\mathbf{r} [\epsilon(\mathbf{r}) - \epsilon_{\mathbf{R}}(\mathbf{r})] w_{\mathbf{R}}^*(\mathbf{r}) w_{\mathbf{R}}(\mathbf{r}). \quad (3.17)$$

Here I used (3.9) in order to transform the denominator of equation (3.14).

Now, assuming that the Wannier functions decay sufficiently fast outside the cavity, one can restrict the integrals (3.15) and (3.16) to next neighbouring sites, so that the only surviving contributions belong to  $\alpha_{\pm 1}$  and  $\beta_{\pm 1}$ . Due to the symmetry of the lattice, one furthermore finds that these integrals have to be invariant under a change of sign of  $n$  i.e.  $\alpha_1 = \alpha_{-1}$  and  $\beta_1 = \beta_{-1}$ . Under these assumptions expression (3.14) becomes

$$\omega^2 = \omega_c^2 \frac{1 + 2\beta_1 \cos(\mathbf{k}\mathbf{R})}{1 + \gamma + 2\alpha_1 \cos(\mathbf{k}\mathbf{R})}, \quad (3.18)$$

which can be rewritten to the form

$$\omega^2 = \omega_c^2 \left[ \frac{-\gamma + 2\kappa \cos(\mathbf{k}\mathbf{R})}{1 + \gamma + 2\alpha_1 \cos(\mathbf{k}\mathbf{R})} + 1 \right]. \quad (3.19)$$

In the last equation I introduced the coupling strength  $\kappa = \beta_1 - \alpha_1$  as

$$\kappa = \int d\mathbf{r} [\epsilon_{\mathbf{R}}(\mathbf{r} - \mathbf{R}) - \epsilon(\mathbf{r})] w_{\mathbf{R}}^*(\mathbf{r}) w_{\mathbf{R}}(\mathbf{r} - \mathbf{R}). \quad (3.20)$$

Using the fact that  $\gamma$  and  $\alpha_1$  are small quantities, i.e.  $\gamma \approx 0$ ,  $\alpha_1 \approx 0$ , one finds for the field frequency the approximated expression

$$\omega \approx \omega_c \sqrt{2\kappa \cos(\mathbf{k}\mathbf{R}) + 1}. \quad (3.21)$$

Expanding the square root for small arguments yields the approximation

$$\omega \approx \omega_c [1 + \kappa \cos(\mathbf{k}\mathbf{R})]. \quad (3.22)$$

Finally, in the large wave-length limit, i.e.  $\mathbf{k}\mathbf{R} \approx 0$ , the cosine can be Taylor expanded as well, leading to

$$\omega \approx \omega_c + \omega_c \kappa. \quad (3.23)$$

This result can be interpreted in the way, that the first term on the left-hand side describes the on-site contribution, whereas the second term estimates the correction arising from next neighbour hopping processes. Thus, combining equation (3.23) with expression (2.56) leads to

$$\hat{H}_{\text{field}}^{\text{JCH}} = \sum_{i,j} (\omega \delta_{i,j} + \omega \kappa_{ij}) \hat{a}_i^\dagger \hat{a}_j, \quad (3.24)$$

where I introduced the summation over all lattice sites  $i, j$  and shifted the energies to compensate the ground-state energy of the photon field. Hence if only nearest neighbour couplings are taken into account, one finds the expression

$$\hat{H}_{\text{field}}^{\text{JCH}} = \sum_i \omega \hat{a}_i^\dagger \hat{a}_i + \kappa \sum_{\langle i,j \rangle} \omega \hat{a}_i^\dagger \hat{a}_j, \quad (3.25)$$

with the coupling constant as defined in (3.20). Numerical calculations of this overlap integral for different models have been performed for example in Ref. [154].

## 3.2 Jaynes-Cummings-Hubbard Hamiltonian

Having justified the theoretical Hubbard approach in the previous section, I now state another assumption for my calculations. Since I am going to perform the further calculations for finite temperatures, I work in the grand-canonical ensemble. Therefore, I include a chemical potential term ( $-\mu \hat{N}$ ) in the Hamiltonian as well. The chemical potential  $\mu$  plays the usual role of a Lagrange multiplier, that fixes the mean polariton number on the lattice. The complete Hamiltonian for this lattice model, to which I refer in the following as the Jaynes-Cummings-Hubbard (JCH) model, then takes on the general form

$$\hat{H}^{\text{JCH}} = \sum_j \hat{H}_j^{\text{JC}} + \hat{H}_{\text{hop}} - \mu \hat{N}, \quad (3.26)$$

where the sum runs over all lattice sites and the local Jaynes-Cummings Hamiltonian now reads

$$\hat{H}_j^{\text{JC}} = \omega \hat{n}_j + \Delta \hat{\sigma}_j^+ \hat{\sigma}_j^- + g \left( \hat{a}_j^\dagger \hat{\sigma}_j^- + \hat{a}_j \hat{\sigma}_j^+ \right). \quad (3.27)$$

As shown in the previous section, the hopping term in its standard form, in which it is widely used throughout most Hubbard and Bose-Hubbard models, is given by

$$\hat{H}_{\text{hop}} = -\kappa \sum_{\langle i,j \rangle} \hat{a}_i^\dagger \hat{a}_j = -\kappa \sum_i \sum_{j \in \text{nn}(i)} \hat{a}_i^\dagger \hat{a}_j. \quad (3.28)$$

This hopping term corresponds to the physical situation, that a photon might tunnel from one cavity to a neighbouring one. The probability for such a process is, according to the results obtained in the previous section, proportional to the photon

wave-function overlap between two neighbouring cavities. Within this approach, the hopping probability is measured by the parameter  $\kappa$ . Though it is not explicitly forbidden, it is mostly experimentally justified to restrict oneself to next-neighbour hopping processes only. Therefore, the sum extends only over next neighbouring sites, which is indicated by the expression  $\langle i, j \rangle$ . As shown in equation (3.28), this sum can be decomposed into two sums, where the second summation runs over all next neighbours  $i$ . Since the total polariton number operator is given by

$$\hat{N} = \sum_j \hat{n}_j = \sum_j \left( \hat{a}_j^\dagger \hat{a}_j + \hat{\sigma}_j^+ \hat{\sigma}_j^- \right), \quad (3.29)$$

it is to see from (3.26) together with (2.99) that, the JCH Hamiltonian decomposes into a diagonal on-site contribution and a non-diagonal hopping term contribution. The diagonal term is easy to solve and essentially leads to the same energy eigenvalues as already found for the Jaynes-Cummings model in (2.113). Nevertheless, the presence of the intra-cavity field mode lowers the chemical potential and, hence, leads to a new effective potential  $\mu_{\text{eff}} = \mu - \omega$ . Thus, one finds for each lattice site

$$E_{n\pm}^{(0)} = \frac{1}{2} \left( \Delta \pm \sqrt{\Delta^2 + 4g^2 n} \right) - \mu_{\text{eff}} n, \quad E_0^{(0)} = 0 \quad (3.30)$$

for the on-site potential energy. Unfortunately, the effect of the kinetic energy contribution arising from the hopping term can not be read off right away. However, in the following sections I consider some special limits in order to gain more physical insight in the dynamics of the model described by (3.26).

### 3.3 Atomic Limit

The first limit I investigate within this section, is the so called weak-hopping limit, where  $\kappa \ll g$ . Within this regime, the hopping may be treated perturbatively. Expanding (3.26) for small  $\kappa$  and taking only the lowest order, i.e.  $\mathcal{O}(\kappa^0)$ , into account, completely decouples the Hamiltonian in the site index and, thus, reduces it to the form

$$\hat{H}_{\text{atom}}^{\text{JCH}} = \sum_j \left( \hat{H}_j^{\text{JC}} - \mu \hat{n}_j \right). \quad (3.31)$$

The corresponding *local* eigenvalues of this Hamiltonian are given by Eq. (3.30). Obviously, this corresponds to the physical situation, where no hopping between neighbouring cavities is allowed. In this case, all excitations remain at their respective lattice sites. For this reason, the ground-state wave function of the whole lattice is simply given as a direct product of the local on-site ground-state wave functions:

$$|\Psi_{\text{lattice}}\rangle = |\Psi_{\text{loc}}\rangle_{j=1} \otimes |\Psi_{\text{loc}}\rangle_{j=2} \otimes |\Psi_{\text{loc}}\rangle_{j=3} \otimes \dots \quad (3.32)$$

As derived in Section 2.5, the polariton eigenstates naturally separate into an upper and a lower branch, where the lower-branch states are always lower in energy than the upper-branch states. Thus, the local ground-state wave function for a given system configuration corresponds either to one of the lower-branch states or the vacuum state itself. To specify the ground state of the system more precisely, I take a look at some special limits of expression (3.30).

Let us first consider the case where  $(\omega - \mu) \gg g, |\Delta|$ . In this situation, the ground state is obviously given by the vacuum state with  $n = 0$ . However, decreasing the difference  $(\omega - \mu)$ , one eventually reaches a point where adding an excitation to the system becomes energetically favourable. This point is exactly reached when  $E_{0-}^{(0)} = E_{1-}^{(0)}$ . A successive repetition of this argument leads to a whole set of such degeneracy points, which are characterized by the condition

$$E_{n-}^{(0)} = E_{(n+1)-}^{(0)}. \quad (3.33)$$

Using expression (3.30) yields the explicit relations

$$\frac{(\mu - \omega)}{g} = \frac{1}{2g} [R_n(\Delta) - R_{n+1}(\Delta)], \quad n > 1, \quad (3.34)$$

$$\frac{(\mu - \omega)}{g} = \frac{1}{2g} [\Delta - R_1(\Delta)], \quad n = 0, \quad (3.35)$$

where the generalized Rabi frequency  $R_n(\Delta)$  is given by equation (2.114). The resulting parameter curves for the critical effective chemical potential are shown in Figure 3.1 for the first six polariton states (for comparison see Ref. [48]). One can see from this picture that, in the considered limit the system is characterized by local states with a fixed number of polaritons. When the polariton number equals an integer multiple of the number of cavities, the local polariton number is the same for each lattice site and it remains fixed for a specific set of parameters  $\{\Delta/g, (\mu - \omega)/g\}$ . However, if the parameter set crosses one of the critical curves depicted in Figure 3.1, the local polariton number will increase or decrease by one. An analogue behaviour is known from the Bose-Hubbard model, where it leads to the emergence of so called Mott-lobes, which border on a superfluid phase. I therefore conclude that this critical curves mark the onset of superfluidity for very small hopping and represent the boundary between adjacent Mott lobes for zero hopping. Besides, I notice that the regions of stability become significantly smaller with increasing polariton number. It is easy to see that the states  $|0\rangle$  and  $|1, -\rangle$  are the most stable ones. The size of this stability regions is linked to the width of the Mott lobes in the phase diagram, which is why I expect the lobes for  $n = 0$  and  $n = 1$  to be the biggest, followed by a progression of rapidly shrinking lobes for higher orders of  $n$ . Furthermore, it is to see that all critical curves are symmetric with respect to the detuning, except for the critical curve between  $|0\rangle$  and  $|1, -\rangle$ . The reason for this behaviour lies in the fact, that the ground-state energy is independent of the detuning parameter  $\Delta$ .

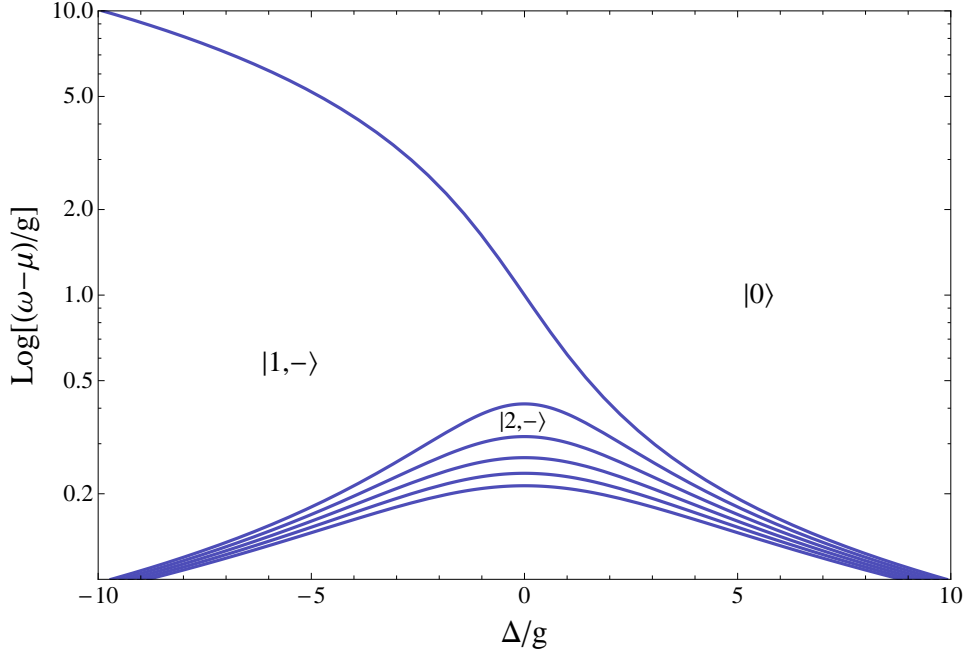


Figure 3.1: **Degeneracy points in the atomic limit.** Plot of the first six critical potentials. The two lowest stable regions correspond to  $|1, -\rangle$  on the left and  $|0\rangle$  on the right. The curve separating these two regions results from equation (3.35). Higher stable regions corresponding to  $|2, -\rangle, |3, -\rangle, \dots$ , are depicted in the central region with their respective critical curves according to equation (3.34).

### 3.4 Hopping Limit

In this section I consider the limit of the JCH model, which corresponds to the situation that the photon hopping overwhelms the coupling between cavity mode and two level atom, i.e.  $\kappa \gg g$ . Using this assumption one can neglect all terms proportional to  $g$  in equation (3.26). This yields the simplified Hamilton operator

$$\hat{H}_{\text{hop}}^{\text{JCH}} = (\omega - \mu) \sum_i \left( \hat{a}_i^\dagger \hat{a}_i + \sigma_i^+ \sigma_i^- \right) + \Delta \sum_i \hat{\sigma}_i^+ \hat{\sigma}_i^- - \kappa \sum_{\langle i,j \rangle} \hat{a}_i^\dagger \hat{a}_j. \quad (3.36)$$

Following the procedure from the previous section, I determine the ground state also for this limit and, thus, I am only interested in the energetically lowest state. Keeping this in mind, I note that the energies, associated with the Hamiltonian (3.36), can be minimized by assuming that no atomic excitations are present within the system. Therefore, I additionally drop all atomic contributions in (3.36), This results in the following hopping-limit ground-state Hamiltonian

$$\hat{H}_{\text{hop}}^{\text{JCH}} = (\omega - \mu) \sum_i \hat{a}_i^\dagger \hat{a}_i - \kappa \sum_{\langle i,j \rangle} \hat{a}_i^\dagger \hat{a}_j. \quad (3.37)$$

Fortunately, this operator can be diagonalized by going into momentum space. For this reason, I perform the following Fourier transformation of the annihilation and creation operators:

$$\hat{a}_i = \frac{1}{\sqrt{N_s}} \sum_{\mathbf{k}} \hat{a}_{\mathbf{k}} e^{-i\mathbf{k}\cdot\mathbf{r}_i}, \quad (3.38)$$

where  $N_s$  corresponds to the total number of cavities in the lattice. The sum runs over all wave vectors in the first Brillouine zone. Inserting this expression into equation (3.37), one finds

$$\hat{H}_{\text{hop}}^{\text{JCH}} = (\omega - \mu) \sum_i \frac{1}{N_s} \sum_{\mathbf{k}, \mathbf{k}'} \hat{a}_{\mathbf{k}}^\dagger \hat{a}_{\mathbf{k}'} e^{i(\mathbf{k}-\mathbf{k}')\cdot\mathbf{r}_i} - \kappa \sum_{\langle i, j \rangle} \frac{1}{N_s} \sum_{\mathbf{k}, \mathbf{k}'} \hat{a}_{\mathbf{k}}^\dagger \hat{a}_{\mathbf{k}'} e^{i(\mathbf{k}\cdot\mathbf{r}_i - \mathbf{k}'\cdot\mathbf{r}_j)}. \quad (3.39)$$

The calculation of the sum over all lattice sites  $i$  in the first term of the above relation, simply yields a delta function for  $\mathbf{k}$  and  $\mathbf{k}'$ . In order too simplify the second term, I introduce the decomposition  $\mathbf{r}_j = \mathbf{r}_i + \mathbf{G}$ , where  $\mathbf{G}$  is a lattice vector, connecting the lattice site  $i$  with its next neighbour site  $j$ . Given that, throughout this thesis, I assume a 3D simple cubic lattice, the lattice vectors  $\mathbf{G}$  explicitly take on the form

$$\mathbf{G} \in \left\{ \left( \begin{array}{c} \pm a \\ 0 \\ 0 \end{array} \right), \left( \begin{array}{c} 0 \\ \pm a \\ 0 \end{array} \right), \left( \begin{array}{c} 0 \\ 0 \\ \pm a \end{array} \right) \right\}, \quad (3.40)$$

where  $a$  is the lattice constant. Inserting this ansatz into (3.39) leads to

$$\hat{H}_{\text{hop}}^{\text{JCH}} = (\omega - \mu) \sum_{\mathbf{k}} \hat{a}_{\mathbf{k}}^\dagger \hat{a}_{\mathbf{k}} - \kappa \sum_i \sum_{\mathbf{G}} \frac{1}{N_s} \sum_{\mathbf{k}, \mathbf{k}'} \hat{a}_{\mathbf{k}}^\dagger \hat{a}_{\mathbf{k}'} e^{i(\mathbf{k}-\mathbf{k}')\cdot\mathbf{r}_i} e^{-i\mathbf{k}'\cdot\mathbf{G}}. \quad (3.41)$$

Now, I can calculate the sum over all lattice sites in the second term as well, which introduces another delta function for  $\mathbf{k}$  and  $\mathbf{k}'$ . Hence I get

$$\hat{H}_{\text{hop}}^{\text{JCH}} = (\omega - \mu) \sum_{\mathbf{k}} \hat{a}_{\mathbf{k}}^\dagger \hat{a}_{\mathbf{k}} - \kappa \sum_{\mathbf{G}} \sum_{\mathbf{k}} \hat{a}_{\mathbf{k}}^\dagger \hat{a}_{\mathbf{k}} e^{-i\mathbf{k}\cdot\mathbf{G}}. \quad (3.42)$$

Calculating the sum over  $\mathbf{G}$ , by using definition (3.40), yields

$$\hat{H}_{\text{hop}}^{\text{JCH}} = \sum_{\mathbf{k}} \left[ (\omega - \mu) - 2\kappa \sum_{i=1}^3 \cos(k_i a) \right] \hat{a}_{\mathbf{k}}^\dagger \hat{a}_{\mathbf{k}}. \quad (3.43)$$

Here, the index  $i$  labels the three components of the wave vector  $\mathbf{k}$ . From this Hamilton operator, one can immediately read off its energy eigenvalues, which are given by the expression

$$\varepsilon(\mathbf{k}) = (\omega - \mu) - J(\mathbf{k}), \quad (3.44)$$

where I defined

$$J(\mathbf{k}) = 2\kappa \sum_{i=1}^3 \cos(k_i a). \quad (3.45)$$

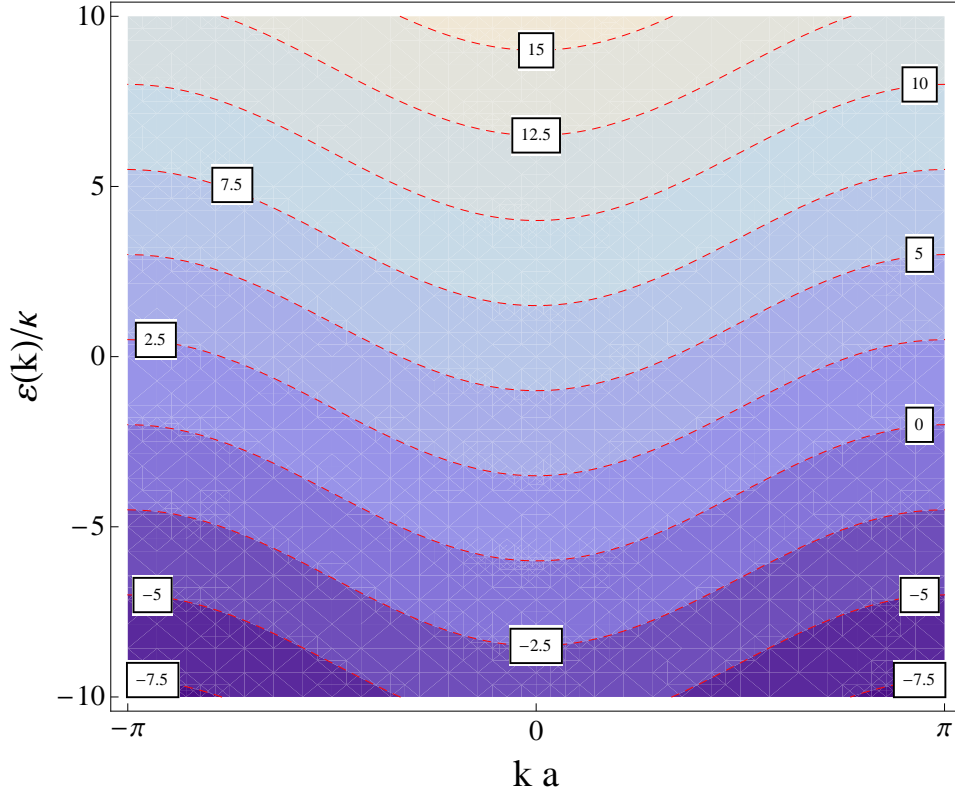


Figure 3.2: **Energy bands in the hopping limit.** Contour plot of the dispersion relation (3.44) for  $\mathbf{k} = k \mathbf{e}_x$ . I plotted  $\varepsilon(k)/\kappa$  versus the wave vector in the first Brillouin zone. The white inset boxes label the value of  $(\omega - \mu)/\kappa$  on their respective red dashed contours.

Figure 3.2 shows a contour plot of the energy bands resulting from equation (3.44). For this plot I assumed the wave vector to have only a non-vanishing component in  $x$ -direction, i.e.  $\mathbf{k} = k \mathbf{e}_x$ .

As a general statement for this consideration, it is to see that the Hamiltonian of the hopping limit (3.43) is local in momentum space. Due to the relation between momentum space and real space, this behaviour is usually accompanied by the fact that the photons are completely delocalised over the lattice in real space. This situation corresponds to the superfluid phase of the system, which is also known from the Bose-Hubbard model.

To sum up, I found within these last two sections that, for the limits of coupling domination and hopping domination, the JCH system shows a completely different behaviour. On the one hand, I observed a pinning of the system excitations to their respective lattice sites in the case of vanishing hopping strength. This situation is especially interesting when the total number of excitations in the system equals an integer multiple of the total number of cavities, because then the excitations spread equally over the lattice and one finds exactly the same number of excitations at each

lattice site. This phase has already been observed in other bosonic many-particle quantum systems and is widely known as Mott-insulator phase. On the other hand, I found that, for the case that the photon hopping dominates the coupling to the two level atom, the JCH ground state consists of photons, which are completely delocalised over the whole lattice. This phase is also known from other bosonic many-particle quantum systems as the superfluid phase. From this observation, one can already deduce that the JCH system undergoes a phase transition from a Mott-insulator to a superfluid, when continuously changing the ratio of hopping strength to coupling strength. Since all considerations so far are completely independent of the temperature, this implies that the occurring phase transition is not driven by thermal fluctuations, but is purely a result of the quantum properties of the system. Therefore, this kind of transition is known as a quantum phase transition [8]. However, up till now I did not develop a theory capable of describing this phase transition properly. In order to derive such a theory from the Hamiltonian (3.26), the easiest and most straightforward way is to calculate a so called mean-field theory. This will be the aim of the next two sections.

### 3.5 Mean-Field Theory

To put it simple, the basic idea behind a mean-field theory is to artificially introduce a so called order parameter, which equals to zero in the Mott-insulator phase and takes on values different from zero, when the system is in the superfluid phase. This order parameter provides a measure to investigate the second-order phase transition as suggested by Landau. The introduction of this order parameter has to be done in a consistent way. Luckily, there exists a well known procedure to derive a mean-field theory for Hamiltonians like the JCH Hamiltonian, where the only off-diagonal contribution is given by the Hubbard hopping term. In order to analytically solve a given Hamiltonian, one has to diagonalize it, with respect to some basis-vector set. To do this for the Hamiltonian of interest, I need to transform the Hubbard-like hopping term to a diagonal form. This can be achieved by decomposing the photonic ladder operators into their respective expectation values plus fluctuations around this mean value. Thus, I decompose the photonic ladder operators as follows

$$\hat{a}_i = \langle \hat{a}_i \rangle + \delta \hat{a}_i, \quad \hat{a}_i^\dagger = \langle \hat{a}_i^\dagger \rangle + \delta \hat{a}_i^\dagger. \quad (3.46)$$

Using these decompositions and neglecting all terms proportional to higher than first order in the fluctuations, I find the mean-field approximation

$$\hat{a}_i^\dagger \hat{a}_j \approx \langle \hat{a}_i^\dagger \rangle \hat{a}_j + \hat{a}_i^\dagger \langle \hat{a}_j \rangle - \langle \hat{a}_i^\dagger \rangle \langle \hat{a}_j \rangle. \quad (3.47)$$

Due to the translational symmetry of the system, the expectation values of the ladder operators have to be site independent. Furthermore, these mean values are the

perfect candidate for the order parameter, since they basically measure on-site fluctuations of the photon number and, hence, are zero in the Mott phase and non zero in the superfluid phase. Therefore, I define the following correspondence

$$\langle \hat{a}_i \rangle = \langle \hat{a}_j \rangle = \Psi, \quad \langle \hat{a}_i^\dagger \rangle = \langle \hat{a}_j^\dagger \rangle = \Psi^* \quad (3.48)$$

where  $\Psi$  is the complex mean-field order parameter. Inserting the above approximation into the Hubbard hopping term yields

$$\hat{H}_1^{\text{MF}} = -\kappa \sum_{\langle i,j \rangle} \left( \Psi^* \hat{a}_j + \hat{a}_i^\dagger \Psi - \Psi^2 \right), \quad (3.49)$$

which can be further simplified by shifting the summation index. Furthermore, due to the  $U(1)$  symmetry of the mean-field Hamiltonian, I can choose the order parameter  $\Psi$  to be a real quantity following an analogue argumentation as in Section 2.4 for the atom-photon coupling  $g$ . This leads to

$$\hat{H}_1^{\text{MF}} = -\kappa z \Psi \sum_j \left( \hat{a}_j + \hat{a}_j^\dagger - \Psi \right), \quad (3.50)$$

where  $z$  is the coordination number of the lattice. Now, following Ref. [155] this mean-field Hamiltonian can consistently be included in the JCH Hamiltonian (3.26) via a variational approach. To do this, one introduces the small parameter  $\eta$  and considers the ansatz

$$\hat{H}^{\text{JCH}}(\eta) = \hat{H}_0 + \hat{H}_1^{\text{MF}} + \eta \left( \hat{H}_{\text{hop}} - \hat{H}_1^{\text{MF}} \right). \quad (3.51)$$

Here, the Hamiltonian of the unperturbed JCH system is given as

$$\hat{H}_0 = \sum_j \left( \hat{H}_j^{\text{JC}} - \mu \hat{n}_j \right), \quad (3.52)$$

where  $\hat{H}_j^{\text{JC}}$  is defined in (3.27). The corresponding eigenvalues of the *local* Hamiltonian (3.52) are given by equation (3.30). The respective eigenstates are given by the dressed polariton states of the lattice  $|i, n, \alpha\rangle$ , which are given by the site dependent form of equation (2.134). These state vectors obey the modified orthogonality relation

$$\langle n, \alpha, i | m, \beta, j \rangle = \delta_{i,j} \delta_{n,m} \delta_{\alpha,\beta} \quad (3.53)$$

Note that, in the limit  $\eta = 1$  this approach yields the JCH Hamiltonian from equation (3.26). Furthermore, the order parameter  $\Psi$  is treated as a variational parameter, like in a variational perturbation theory [7, 156]. Since, the mean-field approximation of the hopping Hamiltonian  $\hat{H}_1^{\text{MF}}$  is supposed to be close to the full expression  $\hat{H}_{\text{hop}}$ , one can Taylor expand expression (3.51) to leading order, which results in

$$\hat{H}^{\text{JCH}}(\eta) \approx \hat{H}_0 + \hat{H}_1^{\text{MF}} =: \hat{H}^{\text{MF}}. \quad (3.54)$$

In principle, this approach allows to calculate higher order corrections, but this accuracy shall be sufficient for now.

Inserting the Hamiltonian of the unperturbed JCH system (3.52) and the mean-field hopping Hamiltonian (3.50) into expression (3.54), leads to the JCH mean-field Hamiltonian:

$$\hat{H}^{\text{MF}} = \sum_j \left[ (\omega - \mu) \hat{n}_j + \Delta \hat{\sigma}_j^+ \hat{\sigma}_j^- + g \left( \hat{a}_j^\dagger \hat{\sigma}_j^- + \hat{a}_j \hat{\sigma}_j^+ \right) - \kappa z \left( \Psi \hat{a}_j + \hat{a}_j^\dagger \Psi - \Psi^2 \right) \right]. \quad (3.55)$$

Unfortunately, one can not straightforwardly calculate the eigenvalues and eigenstates of the JCH mean field Hamiltonian (3.55). However, one can immediately incorporate the term proportional to  $\Psi^2$  into the on site JC eigenvalues, which leads to the shifted energies

$$E_{n\pm}^{(0)} = (\omega - \mu) n + \frac{1}{2} (\Delta \pm R_n) + \kappa z \Psi^2, \quad R_n(\Delta) = \sqrt{\Delta^2 + 4g^2 n}. \quad (3.56)$$

For further calculations, one has to take into account that the mean-field theory I derived is just capable of dealing with a small order parameter and, therefore, I expect it to give reasonable results just in the Mott phase and within a small environment of the phase border. This fact allows us, to treat all terms proportional to  $\Psi$  perturbatively. For this reason I perform a Schrödinger perturbation theory of the mean-field Hamiltonian (3.55) within the following section.

## 3.6 Schrödinger Perturbation Theory

Very often, it is not possible to solve the eigenvalue problem for a given Hamiltonian exactly, even when its explicit form is known. However, if one can split this Hamiltonian into an exactly solvable contribution and a small correction, one might treat this correction to the known problem perturbatively. A standard procedure for such a perturbation calculation is the Schrödinger perturbation theory. In order to apply this procedure, I decompose the mean-field Hamiltonian (3.55) as follows

$$\hat{H}^{\text{MF}} = \sum_j \left( \hat{H}_j^{(0)} + \hat{H}_j^{(1)} \right). \quad (3.57)$$

Here, the second term on the right hand side describes the small correction to the known problem and is in my case explicitly given by

$$\hat{H}^{(1)} = -\kappa z \Psi (\hat{a} + \hat{a}^\dagger) \quad (3.58)$$

where I dropped the site index  $j$ , as I will do for the rest of these calculations.

The first term on the right-hand side of equation (3.57) corresponds to the Hamiltonian of the exactly solvable problem. Dropping the site index  $j$ , this operator takes on the form

$$\hat{H}^{(0)} = (\omega - \mu) \hat{n} + \Delta \hat{\sigma}^+ \hat{\sigma}^- + g (\hat{a}^\dagger \hat{\sigma}^- + \hat{a} \hat{\sigma}^+) + \kappa z \Psi^2 \quad (3.59)$$

and its energy eigenvalues are given by

$$E_{n\pm}^{(0)} = (\omega - \mu) n + \frac{1}{2} \left( \Delta \pm \sqrt{\Delta^2 + 4g^2 n} \right) + \kappa z \Psi^2, \quad n > 1 \quad (3.60a)$$

$$E_0^{(0)} = \kappa z \Psi^2, \quad n = 0. \quad (3.60b)$$

Having found a suitable decomposition of the Hamiltonian of interest, I can now calculate the eigenstate and eigenvalue corrections to the ground state of the known problem up to arbitrary orders in  $\Psi$ . As already discussed within Section 3.3, the ground state of the JCH system is either the vacuum state or one of the lower polariton states. For this reason, I only consider corrections to the lower polariton energies  $E_{n-}$  and their respective eigenstates. In the Schrödinger perturbation theory, the  $p$ -th order correction to the energy eigenvalues can be calculated with the following equation

$$E_{n-}^{(p)} = \left\langle \psi_{n-}^{(0)} \left| \hat{H}^{(1)} \right| \psi_{n-}^{(p-1)} \right\rangle, \quad (3.61)$$

whereas the  $p$ -th order state corrections can be calculated according to

$$\left| \psi_{n-}^{(p)} \right\rangle = \sum_{\{m,\alpha\} \neq \{n,-\}} \left\{ \frac{\left\langle \psi_{m\alpha}^{(0)} \left| \hat{H}^{(1)} \right| \psi_{n-}^{(p-1)} \right\rangle}{E_{n-}^{(0)} - E_{m\alpha}^{(0)}} - \sum_{j=1}^p E_{n-}^{(j)} \frac{\left\langle \psi_{m\alpha}^{(0)} \left| \psi_{n-}^{(p-j)} \right\rangle}{E_{n-}^{(0)} - E_{m\alpha}^{(0)}} \right\} \left| \psi_{m\alpha}^{(0)} \right\rangle. \quad (3.62)$$

From the two equations above, one can see that the difficulty of calculating the perturbation corrections lies solely in the determination of expectation values of the perturbation Hamiltonian  $\hat{H}^{(1)}$ . For this purpose, I define the first-order perturbation matrix  $S_n^m$  as follows:

$$S_n^m := \begin{pmatrix} S_{n+}^{m+} & S_{n-}^{m+} \\ S_{n+}^{m-} & S_{n-}^{m-} \end{pmatrix} = \begin{pmatrix} \langle m, + | \hat{H}^{(1)} | n, + \rangle & \langle m, + | \hat{H}^{(1)} | n, - \rangle \\ \langle m, - | \hat{H}^{(1)} | n, + \rangle & \langle m, - | \hat{H}^{(1)} | n, - \rangle \end{pmatrix}. \quad (3.63)$$

Using the results derived in Section 2.6, I can immediately calculate the perturbation matrix elements to give

$$S_{n\alpha}^{m\beta} = -\kappa z \Psi \left[ t_{n\alpha\beta} \delta_{m,n-1} + t_{(n+1)\alpha\beta} \delta_{m,n+1} \right], \quad (3.64)$$

where the transition amplitudes are defined according to relation (2.144). Knowing the perturbation matrix, one can now go ahead and calculate the energy and state corrections. Due to the  $U(1)$  symmetry of the Hamiltonian, I expect all odd perturbation corrections in the energies to vanish. Indeed, using the orthogonality relation for the polariton states (2.137), it is easy to see that the first-order eigenstate correction is zero:

$$E_{n\pm}^{(1)} = \left\langle \psi_{n\pm}^{(0)} \left| \hat{H}^{(1)} \right| \psi_{n\pm}^{(0)} \right\rangle = -\kappa z \Psi \left\langle \psi_{n\pm}^{(0)} \left| (\hat{a} + \hat{a}^\dagger) \right| \psi_{n\pm}^{(0)} \right\rangle = 0. \quad (3.65)$$

For the first-order state correction, I find, according to (3.62) and using the above results, the following compact formula:

$$|\psi_{n-}^{(1)}\rangle = -\kappa z \Psi \sum_{\alpha=\pm} \left[ |\psi_{(n-1)\alpha}^{(0)}\rangle \frac{t_{n-\alpha}}{E_{n-}^{(0)} - E_{(n-1)\alpha}^{(0)}} + |\psi_{(n+1)\alpha}^{(0)}\rangle \frac{t_{(n+1)-\alpha}}{E_{n-}^{(0)} - E_{(n+1)\alpha}^{(0)}} \right]. \quad (3.66)$$

Here, the first term in (3.66) only contributes to the state correction for the case that  $n > 0$ . Thus, I find for the vacuum state correction

$$|\psi_0^{(1)}\rangle = -\kappa z \Psi \left\{ \frac{\cos \theta_0 \cos \theta_1}{E_0^{(0)} - E_{1-}^{(0)}} |\psi_{1-}^{(0)}\rangle + \frac{\cos \theta_0 \sin \theta_1}{E_0^{(0)} - E_{1+}^{(0)}} |\psi_{1+}^{(0)}\rangle \right\}. \quad (3.67)$$

With the first-order eigenstate correction, I can now calculate the second-order energy correction, following equation (3.61), which leads to

$$E_{n-}^{(2)} = \sum_{\alpha=\pm} \left[ \frac{|S_{(n-1)\alpha}^{n-}|^2}{E_{n-}^{(0)} - E_{(n-1)\alpha}^{(0)}} + \frac{|S_{(n+1)\alpha}^{n-}|^2}{E_{n-}^{(0)} - E_{(n+1)\alpha}^{(0)}} \right]. \quad (3.68)$$

Making use of the perturbation matrix elements  $S_{n\alpha}^{m\beta}$  in (3.64) again, yields the general result for  $n > 0$ :

$$E_{n-}^{(2)} = (\kappa z)^2 \Psi^2 \sum_{\alpha=\pm} \left[ \frac{t_{n-\alpha}^2}{E_{n-}^{(0)} - E_{(n-1)\alpha}^{(0)}} + \frac{t_{(n+1)\alpha-}^2}{E_{n-}^{(0)} - E_{(n+1)\alpha}^{(0)}} \right]. \quad (3.69)$$

I recognize that for  $n = 0$  the first term in (3.68) vanishes. In result I find that, the second-order vacuum energy correction takes on the explicit form

$$E_{0-}^{(2)} = (\kappa z)^2 \Psi^2 \left[ \frac{|\cos \theta_1|^2}{E_{0-}^{(0)} - E_{1-}^{(0)}} + \frac{|\sin \theta_1|^2}{E_{0-}^{(0)} - E_{1+}^{(0)}} \right]. \quad (3.70)$$

The respective denominators can be determined by using the equations (3.60a) and (3.60b), which leads to the following expressions

$$E_{n-}^{(0)} - E_{(n+1)-}^{(0)} = -(\omega - \mu) - \frac{1}{2} (R_n - R_{n+1}), \quad (3.71)$$

$$E_{n-}^{(0)} - E_{(n+1)+}^{(0)} = -(\omega - \mu) - \frac{1}{2} (R_n + R_{n+1}), \quad (3.72)$$

$$E_{n-}^{(0)} - E_{(n-1)-}^{(0)} = (\omega - \mu) - \frac{1}{2} (R_n - R_{n-1}), \quad (3.73)$$

$$E_{n-}^{(0)} - E_{(n-1)+}^{(0)} = (\omega - \mu) - \frac{1}{2} (R_n + R_{n-1}). \quad (3.74)$$

At this point, I used the generalized Rabi frequency, as defined in (2.114). Proceeding with the calculations according to (3.61) and (3.62), I notice that, for the second-order state correction, the second sum in (3.62) vanishes:

$$\sum_{\{m,\alpha\} \neq \{n,-\}} |\psi_{m\alpha}^{(0)}\rangle \frac{\langle \psi_{m\alpha}^{(0)} | \psi_{n-}^{(0)} \rangle}{E_{n-}^{(0)} - E_{m\alpha}^{(0)}} = \sum_{\{m,\alpha\} \neq \{n,-\}} |\psi_{m\alpha}^{(0)}\rangle \frac{\delta_{mn} \delta_{\alpha-}}{E_{n-}^{(0)} - E_{m\alpha}^{(0)}} = 0. \quad (3.75)$$

Therefore, this calculation is simplified to

$$|\psi_{n-}^{(2)}\rangle = \sum_{\{m,\alpha\} \neq \{n,-\}} |\psi_{m\alpha}^{(0)}\rangle \frac{\langle \psi_{m\alpha}^{(0)} | \hat{H}^{(1)} | \psi_{n-}^{(1)} \rangle}{E_{n-}^{(0)} - E_{m\alpha}^{(0)}}. \quad (3.76)$$

Using result (3.66), leads to the equation

$$|\psi_{n-}^{(2)}\rangle = \sum_{\{m,\alpha\} \neq \{n,-\}} \sum_{\gamma=\pm} |\psi_{m\alpha}^{(0)}\rangle \frac{1}{E_{n-}^{(0)} - E_{m\alpha}^{(0)}} \left[ \frac{S_{(n-1)\gamma}^{m\alpha} S_{n-}^{(n-1)\gamma}}{E_{n-}^{(0)} - E_{(n-1)\gamma}^{(0)}} + \frac{S_{(n+1)\gamma}^{m\alpha} S_{n-}^{(n+1)\gamma}}{E_{n-}^{(0)} - E_{(n+1)\gamma}^{(0)}} \right]. \quad (3.77)$$

Finally, performing the sum over  $m$ , yields the following expression for the second-order eigenstate correction:

$$\begin{aligned} |\psi_{n-}^{(2)}\rangle = & \sum_{\alpha,\gamma=\pm} \left\{ |\psi_{(n-2)\alpha}^{(0)}\rangle \frac{S_{(n-1)\gamma}^{(n-2)\alpha} S_{n-}^{(n-1)\gamma}}{(E_{n-}^{(0)} - E_{(n-2)\alpha}^{(0)}) (E_{n-}^{(0)} - E_{(n-1)\gamma}^{(0)})} \right. \\ & + |\psi_{(n+2)\alpha}^{(0)}\rangle \frac{S_{(n+1)\gamma}^{(n+2)\alpha} S_{n-}^{(n+1)\gamma}}{(E_{n-}^{(0)} - E_{(n+2)\alpha}^{(0)}) (E_{n-}^{(0)} - E_{(n+1)\gamma}^{(0)})} \\ & \left. + \frac{\delta_{\alpha,+} (1 - \delta_{n,0})}{(E_{n-}^{(0)} - E_{n\alpha}^{(0)})} |\psi_{n\alpha}^{(0)}\rangle \left[ \frac{S_{(n-1)\gamma}^{n\alpha} S_{n-}^{(n-1)\gamma}}{(E_{n-}^{(0)} - E_{(n-1)\gamma}^{(0)})} + \frac{S_{(n+1)\gamma}^{n\alpha} S_{n-}^{(n+1)\gamma}}{(E_{n-}^{(0)} - E_{(n+1)\gamma}^{(0)})} \right] \right\}. \quad (3.78) \end{aligned}$$

Again, due to the  $U(1)$  symmetry, I already know that, the third-order energy correction has to vanish, i.e.

$$E_{n-}^{(3)} = \langle \psi_{n-}^{(0)} | \hat{H}^{(1)} | \psi_{n-}^{(2)} \rangle = 0. \quad (3.79)$$

It is easy to proof that this is indeed the case. Thus, I immediately continue to derive an expression for the third-order eigenstate correction. Following the same procedure as before yields, according to (3.62), the general expression

$$|\psi_{n-}^{(3)}\rangle = \sum_{\alpha=\pm} \sum_{m \neq n} |\psi_{m\alpha}^{(0)}\rangle \frac{\langle \psi_{m\alpha}^{(0)} | \hat{H}^{(1)} | \psi_{n-}^{(2)} \rangle}{E_{n-}^{(0)} - E_{m\alpha}^{(0)}} - E_{n-}^{(2)} \sum_{\alpha=\pm} \sum_{m \neq n} |\psi_{m\alpha}^{(0)}\rangle \frac{\langle \psi_{m\alpha}^{(0)} | \psi_{n-}^{(1)} \rangle}{E_{n-}^{(0)} - E_{m\alpha}^{(0)}}. \quad (3.80)$$

Using equation (3.66) and the orthogonality relation (2.137), I get

$$\langle \psi_{m\alpha}^{(0)} | \psi_{n-}^{(1)} \rangle = \sum_{\gamma=\pm} \left[ \delta_{m,n-1} \delta_{\alpha\gamma} \frac{S_{n-}^{(n-1)\gamma}}{E_{n-}^{(0)} - E_{(n-1)\gamma}^{(0)}} + \delta_{m,n+1} \delta_{\alpha\gamma} \frac{S_{n-}^{(n+1)\gamma}}{E_{n-}^{(0)} - E_{(n+1)\gamma}^{(0)}} \right]. \quad (3.81)$$

Using this relation, one can derive the following formula

$$\begin{aligned} \sum_{\alpha=\pm} \sum_{m \neq n} |\psi_{m\alpha}^{(0)} \rangle \frac{\langle \psi_{m\alpha}^{(0)} | \psi_{n-}^{(1)} \rangle}{E_{n-}^{(0)} - E_{m\alpha}^{(0)}} &= \sum_{m \neq n} \left( \frac{|\psi_{m-}^{(0)} \rangle}{E_{n-}^{(0)} - E_{m-}^{(0)}} \left[ \frac{\delta_{m,n-1} S_{n-}^{(n-1)-}}{E_{n-}^{(0)} - E_{(n-1)-}^{(0)}} + \frac{\delta_{m,n+1} S_{n-}^{(n+1)-}}{E_{n-}^{(0)} - E_{(n+1)-}^{(0)}} \right] \right. \\ &\quad \left. + |\psi_{m+}^{(0)} \rangle \frac{1}{E_{n-}^{(0)} - E_{m+}^{(0)}} \left[ \delta_{m,n-1} \frac{S_{n-}^{(n-1)+}}{E_{n-}^{(0)} - E_{(n-1)+}^{(0)}} + \delta_{m,n+1} \frac{S_{n-}^{(n+1)+}}{E_{n-}^{(0)} - E_{(n+1)+}^{(0)}} \right] \right) \\ &= \sum_{\alpha=\pm} \left[ |\psi_{(n-1)\alpha}^{(0)} \rangle \frac{S_{n-}^{(n-1)\alpha}}{\left( E_{n-}^{(0)} - E_{(n-1)\alpha}^{(0)} \right)^2} + |\psi_{(n+1)\alpha}^{(0)} \rangle \frac{S_{n-}^{(n+1)\alpha}}{\left( E_{n-}^{(0)} - E_{(n+1)\alpha}^{(0)} \right)^2} \right]. \end{aligned} \quad (3.82)$$

Hence, inserting this result in (3.80) yields

$$\begin{aligned} |\psi_{n-}^{(3)} \rangle &= \sum_{\alpha=\pm} \left\{ \sum_{m \neq n} |\psi_{m\alpha}^{(0)} \rangle \frac{\langle \psi_{m\alpha}^{(0)} | \hat{H}^{(1)} | \psi_{n-}^{(2)} \rangle}{E_{n-}^{(0)} - E_{m\alpha}^{(0)}} \right. \\ &\quad \left. - E_{n-}^{(2)} \left[ \frac{S_{n-}^{(n-1)\alpha} |\psi_{(n-1)\alpha}^{(0)} \rangle}{\left( E_{n-}^{(0)} - E_{(n-1)\alpha}^{(0)} \right)^2} + \frac{S_{n-}^{(n+1)\alpha} |\psi_{(n+1)\alpha}^{(0)} \rangle}{\left( E_{n-}^{(0)} - E_{(n+1)\alpha}^{(0)} \right)^2} \right] \right\}. \end{aligned} \quad (3.83)$$

Since I already calculated the second-order state correction, I can use expression (3.78) and find

$$\begin{aligned} |\psi_{n-}^{(3)} \rangle &= \sum_{\alpha,\nu,\gamma=\pm} \sum_{m \neq n} |\psi_{m\alpha}^{(0)} \rangle \frac{\langle \psi_{m\alpha}^{(0)} | \hat{H}^{(1)} \left[ \frac{S_{(n-1)\nu}^{(n-2)\gamma} S_{n-}^{(n-1)\nu} |\psi_{(n-2)\gamma}^{(0)} \rangle}{\left( E_{n-}^{(0)} - E_{(n-1)\nu}^{(0)} \right) \left( E_{n-}^{(0)} - E_{(n-2)\gamma}^{(0)} \right)} \right. \\ &\quad \left. + \frac{S_{(n+1)\nu}^{(n+2)\gamma} S_{n-}^{(n+1)\nu} |\psi_{(n+2)\gamma}^{(0)} \rangle}{\left( E_{n-}^{(0)} - E_{(n+1)\nu}^{(0)} \right) \left( E_{n-}^{(0)} - E_{(n+2)\gamma}^{(0)} \right)} \right]}{E_{n-}^{(0)} - E_{m\alpha}^{(0)}} \\ &\quad - E_{n-}^{(2)} \sum_{\alpha=\pm} \left[ \frac{S_{n-}^{(n-1)\alpha} |\psi_{(n-1)\alpha}^{(0)} \rangle}{\left( E_{n-}^{(0)} - E_{(n-1)\alpha}^{(0)} \right)^2} + \frac{S_{n-}^{(n+1)\alpha} |\psi_{(n+1)\alpha}^{(0)} \rangle}{\left( E_{n-}^{(0)} - E_{(n+1)\alpha}^{(0)} \right)^2} \right]. \end{aligned} \quad (3.84)$$

Furthermore, inserting the second-order energy correction (3.68), one arrives at the final result for the third-order state correction

$$\begin{aligned}
 |\psi_{n-}^{(3)}\rangle = & \sum_{\alpha,\nu,\gamma=\pm} \left( |\psi_{(n-3)\alpha}^{(0)}\rangle \frac{S_{n-}^{(n-1)\nu} S_{(n-1)\nu}^{(n-2)\gamma} S_{(n-2)\gamma}^{(n-3)\alpha}}{\left(E_{n-}^{(0)} - E_{(n-1)\nu}^{(0)}\right) \left(E_{n-}^{(0)} - E_{(n-2)\gamma}^{(0)}\right) \left(E_{n-}^{(0)} - E_{(n-3)\alpha}^{(0)}\right)} \right. \\
 & + |\psi_{(n+3)\alpha}^{(0)}\rangle \frac{S_{n-}^{(n+1)\nu} S_{(n+1)\nu}^{(n+2)\gamma} S_{(n+2)\gamma}^{(n+3)\alpha}}{\left(E_{n-}^{(0)} - E_{(n+1)\nu}^{(0)}\right) \left(E_{n-}^{(0)} - E_{(n+2)\gamma}^{(0)}\right) \left(E_{n-}^{(0)} - E_{(n+3)\alpha}^{(0)}\right)} \\
 & + |\psi_{(n-1)\alpha}^{(0)}\rangle \left\{ \frac{S_{(n-2)\gamma}^{(n-1)\alpha} S_{(n-1)\nu}^{(n-2)\gamma} S_{n-}^{(n-1)\nu}}{\left(E_{n-}^{(0)} - E_{(n-1)\alpha}^{(0)}\right) \left(E_{n-}^{(0)} - E_{(n-1)\nu}^{(0)}\right) \left(E_{n-}^{(0)} - E_{(n-2)\gamma}^{(0)}\right)} \right. \\
 & - \frac{1}{\left(E_{n-}^{(0)} - E_{(n-1)\alpha}^{(0)}\right)^2} \left[ \frac{S_{n-}^{(n-1)\alpha} |S_{(n-1)\gamma}^{n-}|^2}{\left(E_{n-}^{(0)} - E_{(n-1)\gamma}^{(0)}\right)} + \frac{S_{n-}^{(n-1)\alpha} |S_{(n+1)\gamma}^{n-}|^2}{\left(E_{n-}^{(0)} - E_{(n+1)\gamma}^{(0)}\right)} \right] \left. \right\} \\
 & + |\psi_{(n+1)\alpha}^{(0)}\rangle \left\{ \frac{S_{(n+2)\gamma}^{(n+1)\alpha} S_{(n+1)\nu}^{(n+2)\gamma} S_{n-}^{(n+1)\nu}}{\left(E_{n-}^{(0)} - E_{(n+1)\alpha}^{(0)}\right) \left(E_{n-}^{(0)} - E_{(n+1)\nu}^{(0)}\right) \left(E_{n-}^{(0)} - E_{(n+2)\gamma}^{(0)}\right)} \right. \\
 & - \frac{1}{\left(E_{n-}^{(0)} - E_{(n+1)\alpha}^{(0)}\right)^2} \left[ \frac{S_{n-}^{(n+1)\alpha} |S_{(n-1)\gamma}^{n-}|^2}{\left(E_{n-}^{(0)} - E_{(n-1)\gamma}^{(0)}\right)} + \frac{S_{n-}^{(n+1)\alpha} |S_{(n+1)\gamma}^{n-}|^2}{\left(E_{n-}^{(0)} - E_{(n+1)\gamma}^{(0)}\right)} \right] \left. \right\} \left. \right). \quad (3.85)
 \end{aligned}$$

Having found this result, I am now able to finally calculate the fourth-order energy correction. Making use of equation (3.64) once more leads to

$$\begin{aligned}
 E_{n-}^{(4)} = & \sum_{\alpha,\nu,\gamma=\pm} \left[ \frac{t_{n\alpha-}}{\left(E_{n-}^{(0)} - E_{(n-1)\alpha}^{(0)}\right) \left(E_{n-}^{(0)} - E_{n+}^{(0)}\right)} \right. \\
 & \times \left\{ \frac{t_{n+\alpha} t_{n\nu+} t_{n-\nu}}{\left(E_{n-}^{(0)} - E_{(n-1)\nu}^{(0)}\right)} + \frac{t_{n+\alpha} t_{(n+1)\nu+} t_{(n+1)-\nu}}{\left(E_{n-}^{(0)} - E_{(n+1)\nu}^{(0)}\right)} \right\} \\
 & + \frac{1}{\left(E_{n-}^{(0)} - E_{(n-1)\alpha}^{(0)}\right)} \left\{ \frac{t_{n\alpha-} t_{(n-1)\gamma\alpha} t_{(n-1)\nu\gamma} t_{n-\nu}}{\left(E_{n-}^{(0)} - E_{(n-1)\nu}^{(0)}\right) \left(E_{n-}^{(0)} - E_{(n-2)\gamma}^{(0)}\right)} \right. \\
 & - \frac{t_{n\alpha-}^2}{\left(E_{n-}^{(0)} - E_{(n-1)\alpha}^{(0)}\right)} \left( \frac{t_{n\gamma-}^2}{\left(E_{n-}^{(0)} - E_{(n-1)\gamma}^{(0)}\right)} + \frac{t_{(n+1)\gamma-}^2}{\left(E_{n-}^{(0)} - E_{(n+1)\gamma}^{(0)}\right)} \right) \left. \right\} \\
 & + \left[ \frac{t_{(n+1)\alpha-}}{\left(E_{n-}^{(0)} - E_{(n+1)\alpha}^{(0)}\right) \left(E_{n-}^{(0)} - E_{n+}^{(0)}\right)} \left\{ \frac{t_{(n+1)+\alpha} t_{n\nu+} t_{n-\nu}}{\left(E_{n-}^{(0)} - E_{(n-1)\nu}^{(0)}\right)} + \frac{t_{(n+1)+\alpha} t_{(n+1)\nu+} t_{(n+1)-\nu}}{\left(E_{n-}^{(0)} - E_{(n+1)\nu}^{(0)}\right)} \right\} \right]
 \end{aligned}$$

$$\begin{aligned}
 & + \frac{1}{\left(E_{n-}^{(0)} - E_{(n+1)\alpha}^{(0)}\right)} \left\{ \frac{t_{(n+1)\alpha-} t_{(n+2)\gamma\alpha} t_{(n+2)\nu\gamma} t_{(n+1)-\nu}}{\left(E_{n-}^{(0)} - E_{(n+1)\nu}^{(0)}\right) \left(E_{n-}^{(0)} - E_{(n+2)\gamma}^{(0)}\right)} \right. \\
 & \left. - \frac{t_{(n+1)\alpha-}^2}{\left(E_{n-}^{(0)} - E_{(n+1)\alpha}^{(0)}\right)} \left( \frac{t_{n\gamma-}^2}{\left(E_{n-}^{(0)} - E_{(n-1)\gamma}^{(0)}\right)} + \frac{t_{(n+1)\gamma-}^2}{\left(E_{n-}^{(0)} - E_{(n+1)\gamma}^{(0)}\right)} \right) \right\} (\kappa z)^4 \Psi^4, \quad (3.86)
 \end{aligned}$$

for  $n > 0$ .

In the case that  $n = 0$ , I conclude that the vacuum correction takes on the form

$$\begin{aligned}
 E_{0-}^{(4)} = \sum_{\alpha, \nu, \gamma = \pm} \frac{(\kappa z)^4 |\Psi|^4}{\left(E_{0-}^{(0)} - E_{1\alpha}^{(0)}\right)} \left[ \frac{t_{1\alpha-} t_{2\gamma\alpha} t_{2\nu\gamma} t_{1-\nu}}{\left(E_{0-}^{(0)} - E_{1\nu}^{(0)}\right) \left(E_{0-}^{(0)} - E_{2\gamma}^{(0)}\right)} \right. \\
 \left. - \frac{t_{1\alpha-}^2 t_{1\gamma-}^2}{\left(E_{0-}^{(0)} - E_{1\alpha}^{(0)}\right) \left(E_{0-}^{(0)} - E_{1\gamma}^{(0)}\right)} \right]. \quad (3.87)
 \end{aligned}$$

Now, having found the energy corrections up to fourth order in the order parameter in the framework of the Schrödinger perturbation theory, I can now extract the phase boundary within the next section.

## 3.7 Phase Boundary at Zero Temperature

Up till now, I developed a mean-field theory and introduced an order parameter  $\Psi$  in order to analyse the dynamics of the JCH model. This approach leads to an expression for the energy of the system, which now depends on this order parameter:

$$E_{n\alpha} \rightarrow E_{n\alpha}(\Psi). \quad (3.88)$$

Since the order parameter is small in the vicinity of the phase boundary, I successfully applied the Schrödinger perturbation theory, which eventually leads to the Landau expansion of the ground-state energy:

$$E_{n-}(\Psi) \approx A_0 + A_2 \Psi^2 + A_4 \Psi^4 + \dots \quad (3.89)$$

Now, to extract the phase diagram for the JCH system, it is useful to visualize the behaviour of the ground-state energy in dependence of the order parameter.

The ground-state energy corresponds to the global minimum of the energy perturbation series (3.89). In order to find this extrema, one needs to calculate the first derivative with respect to the order parameter and set it equal to zero. This leads to the equation

$$\frac{\partial E_{n-}}{\partial \Psi} = \Psi (2 A_2 + 4 A_4 \Psi^2) \stackrel{!}{=} 0, \quad (3.90)$$

which has the non-trivial solution

$$\Psi = \sqrt{-\frac{A_2}{2 A_4}}. \quad (3.91)$$

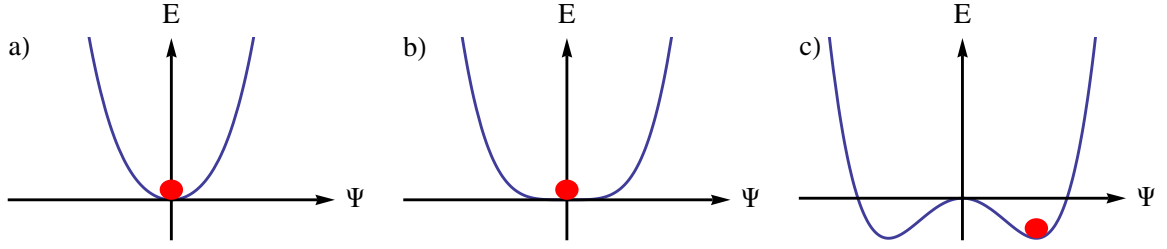


Figure 3.3: **Energy landscape for a second-order phase transition.** I plotted the energy versus the order parameter for 3 different scenarios, following the second-order phase transition. All pictures are projections of a 3D paraboloid on the plane. a) Symmetry is unbroken. One single global minimum corresponding to the Mott insulator ground state. b) Critical point of the quantum phase transition. c) Symmetry is broken. There exists an infinite number of global minima corresponding to the superfluid ground states.

To ensure that this solution describes a minimum, the second derivative with respect to  $\Psi$  has to be positive. Thus, one demands

$$\frac{\partial^2 E_{n-}}{\partial \Psi^2} = 2 A_2 + 12 A_4 \Psi^2 \stackrel{!}{>} 0. \quad (3.92)$$

Combining the two conditions (3.90) and (3.92), yields two possibilities for the ground-state energy minimum. Demanding that  $A_4$  is always positive, these two possibilities are given by

$$\Psi = 0 \text{ if } A_2 > 0, \text{ and } \Psi = \sqrt{-\frac{A_2}{2 A_4}} \text{ if } A_2 < 0. \quad (3.93)$$

A picture of this typical situation for a second-order phase transition is given in Figure 3.3. The first picture *a)* corresponds to the situation that, the second-order expansion coefficient  $A_2$  is positive. In this case, there exists one distinct minimum for the energy of the system at  $\Psi = 0$ , which corresponds to the ground state of the Mott insulator. Picture *c)* shows the situation, when the second-order expansion coefficient is negative. Here, there exists an infinite set of global minima for the energy at finite values of  $\Psi$ , corresponding to the ground states in the superfluid phase. The critical point, when the ground-state symmetry is broken and the transition from the Mott insulator to the superfluid occurs, is depicted in diagram *b)*. At this point, the second-order expansion coefficient exactly vanishes. A necessary condition for the statements made above, is that the fourth-order expansion coefficient  $A_4$  is always positive.

As a consequence, one has to ascertain, that the fourth-order energy correction is always positive. In this case, the boundary of the quantum phase transition can be found, by determining the external parameters of the system from the condition

$$A_2 \stackrel{!}{=} 0. \quad (3.94)$$

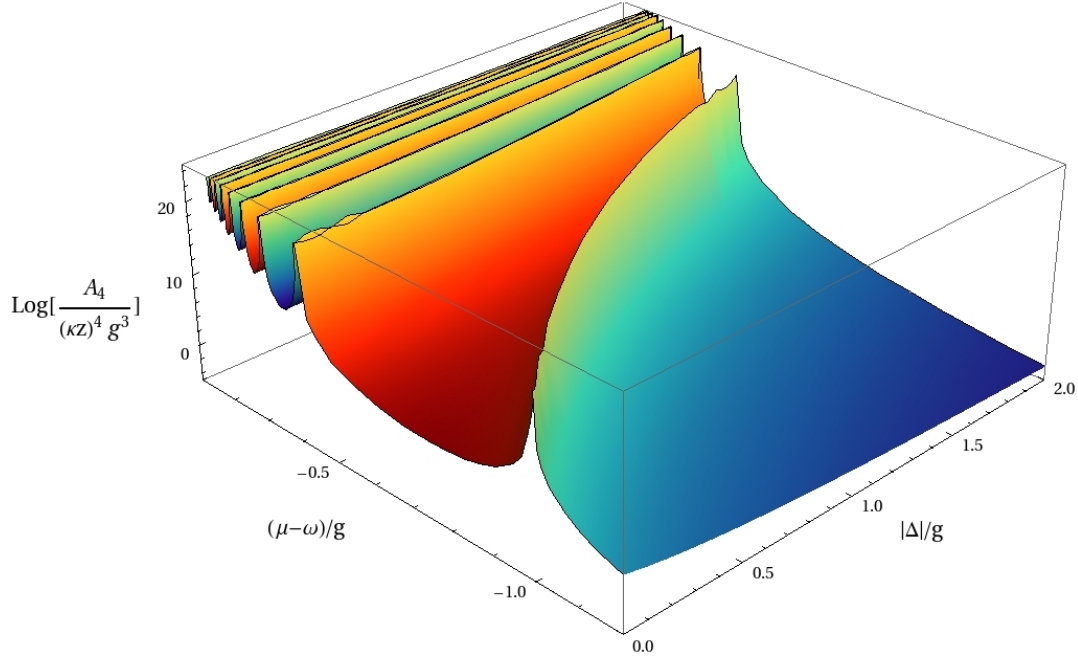


Figure 3.4: **Logarithmic plot of the 4th order Landau coefficient** versus the detuning and the chemical potential for the first six polariton states.

From the results obtained in the previous section, I explicitly find that the Landau coefficients are given by

$$A_2 = \kappa z + (\kappa z)^2 \sum_{\alpha=\pm} \left[ \frac{t_{n-\alpha}^2}{E_{n-}^{(0)} - E_{(n-1)\alpha}^{(0)}} + \frac{t_{(n+1)\alpha-}^2}{E_{n-}^{(0)} - E_{(n+1)\alpha}^{(0)}} \right], \quad (3.95)$$

and

$$A_4 = \frac{E_{n-}^{(4)}}{\Psi^4}. \quad (3.96)$$

Now, the first step is to check whether  $A_4$  fulfils the necessary condition to be positive in all situations. Therefore, I plot the corresponding expression versus the detuning and the effective chemical potential. The resulting diagram is depicted in Figure 3.4. From this picture, one can clearly see that the fourth-order Landau coefficient is always positive, just as expected for a second-order phase transition. Hence, I can go ahead and extract the phase boundary from  $A_2$  according to condition (3.94). Inserting expression (3.95) leads to

$$\kappa z = - \left[ \sum_{\alpha=\pm} \left( \frac{t_{n-\alpha}^2}{E_{n-}^{(0)} - E_{(n-1)\alpha}^{(0)}} + \frac{t_{(n+1)\alpha-}^2}{E_{n-}^{(0)} - E_{(n+1)\alpha}^{(0)}} \right) \right]^{-1}. \quad (3.97)$$

To gain a more insight into the derived expressions, I consider the case of resonance, i.e.  $\Delta = 0$ . First, I notice that within this limit the mixing angle  $\theta_n$  becomes a constant:

$$\lim_{\Delta \rightarrow 0} \theta_n = \lim_{\Delta \rightarrow 0} \left[ \frac{1}{2} \arctan \left( \frac{2g\sqrt{n}}{\Delta} \right) \right] = \frac{\pi}{4}. \quad (3.98)$$

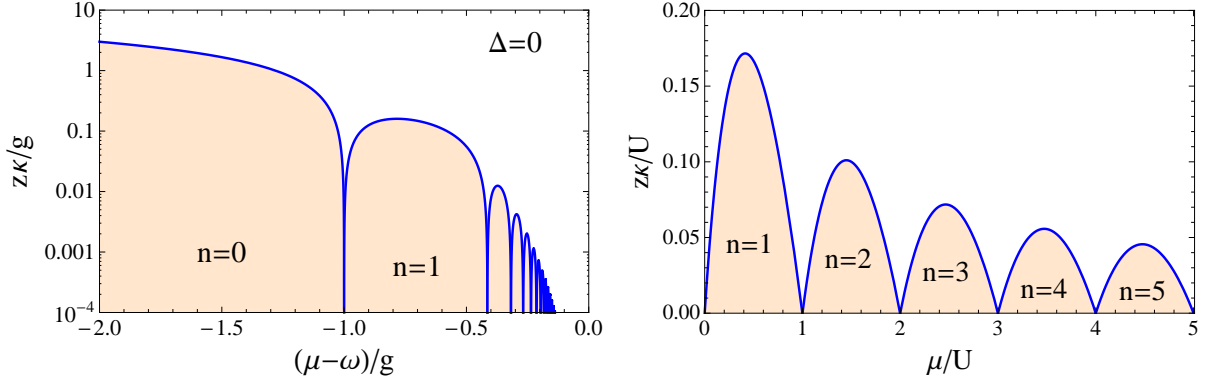


Figure 3.5: **JCH and BH mean-field phase boundary for  $T = 0$  K.** The left figure shows a logarithmic plot of the hopping strength versus the effective chemical potential, which corresponds to the phase border of the JCH model at  $\Delta = 0$  and  $T = 0$  K. For comparison, the right figure shows the mean-field phase diagram for the BH model at  $T = 0$  K. In both systems, the shaded regions below the phase boundary correspond to the Mott insulator and the white region above the lobes corresponds to the superfluid phase.

Using this result in expression (3.95), yields the following equation for the phase boundary at resonance

$$\frac{z\kappa}{g} = \left[ \frac{1}{4} \sum_{\alpha=\pm 1} \frac{(\sqrt{n+1} + \alpha\sqrt{n})^2}{-\frac{(\mu-\omega)}{g} + (\sqrt{n} - \alpha\sqrt{n+1})} + \frac{(\sqrt{n} + \alpha\sqrt{n-1})^2}{\frac{(\mu-\omega)}{g} + (\sqrt{n} - \alpha\sqrt{n-1})} \right]^{-1}, \quad n > 0 \quad (3.99a)$$

$$\frac{z\kappa}{g} = \left[ \frac{1}{2} \sum_{\alpha=\pm 1} \frac{1}{\frac{(\mu-\omega)}{g} + \alpha} \right]^{-1}, \quad n = 0. \quad (3.99b)$$

The respective phase diagram is shown in Figure 3.5. For the purpose of comparison, I also plotted the phase diagram for the hardcore Bose-Hubbard (BH) model [6]. The underlying Hamiltonian of this system is given by equation (1.1), where  $U$  characterizes the particle interaction and  $\kappa$  is the hopping strength. For more details on this system I refer to the standard literature. Additionally, I want to recommend the diploma theses of A. Hoffmann [157], M. Ohliger [158], and T. Grass [159]. In the Bose-Hubbard model, the phase boundary is defined via the equation

$$\frac{z\kappa}{U} = \left[ \frac{n+1}{n - \frac{\mu}{U}} + \frac{n}{(n-1) + \frac{\mu}{U}} \right]^{-1}. \quad (3.100)$$

At first sight, both diagrams in Figure 3.5 look quite different. However, one can see by direct comparison, that the two plots share some common features. Obviously, both phase diagrams consist of lobes, which describe the Mott insulator, and a superfluid phase, that corresponds to the region above the Mott lobes. Furthermore, in both systems the size of

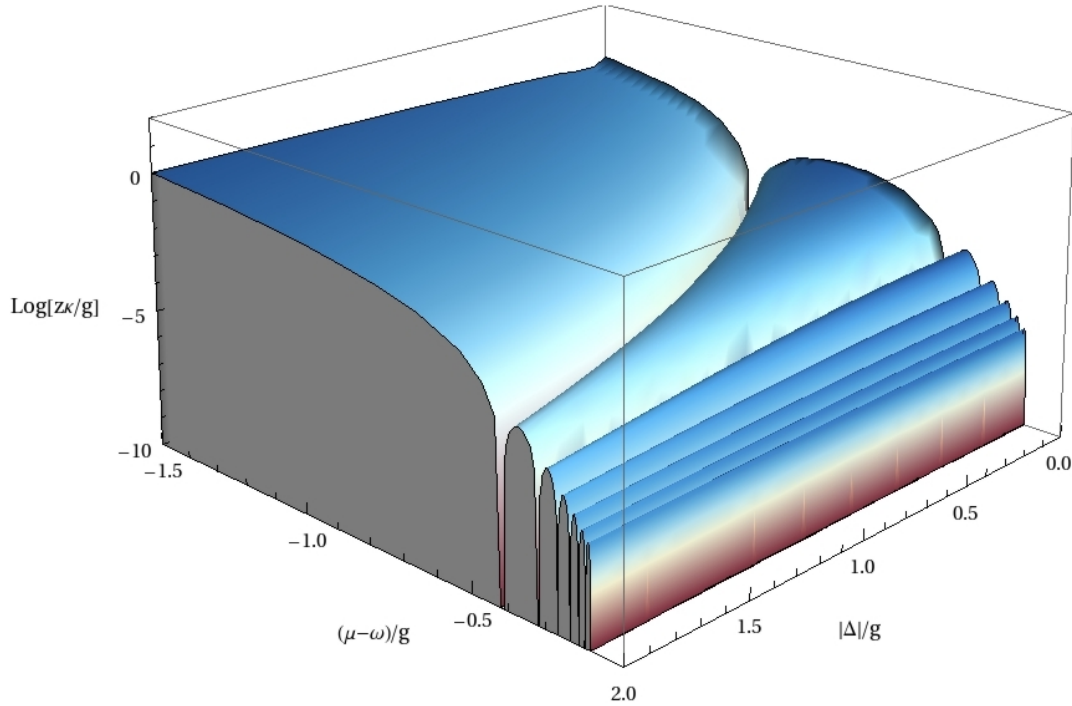


Figure 3.6: **JCH phase boundary for non-zero detuning.** Plot of the logarithm of the hopping strength  $\kappa$  versus the magnitude of the detuning parameter  $|\Delta|$  and the effective chemical potential  $(\mu - \omega)$  according to equation (3.97).

the Mott lobes decreases with increasing particle number  $n$ , but, as indicated by the logarithmic scale, this descent is much stronger in the JCH model. Additionally, another quite striking difference is the fact that, the base widths of the Mott lobes remain constant in the Bose-Hubbard model whereas they rapidly decrease in the JCH model. Worst affected by this feature is the first lobe for  $n = 0$  in the JCH model.

This behaviour can partly be understood by recalling that in the JCH model the effective on-site interaction strength increases non-linear with the polariton number, whereas in the BH case  $U$  is a constant. Note that, the obtained result is in agreement with calculation by other groups, for example see Ref. [160].

For completeness, I also plotted the dependency of the JCH phase boundary from the detuning parameter  $\Delta$  in Figure 3.6. From this plot, one can see the following important properties. First, the phase diagram is obviously symmetric in the detuning parameter, which is why I plotted only  $|\Delta|/g$ . However, the main result, which can be seen in Figure 3.6, is that the width of the Mott lobes, except for  $n = 0$ , shrinks when the detuning parameter increases. Though this is hard to see from the plot, in fact the same thing happens to the height of the lobes. Furthermore, these effects are obviously strongest for the Mott lobe with  $n = 1$ , whereas the higher lobes seem almost unaffected. In contrast, one can see that the opposite is true for the first Mott lobe with  $n = 0$ . This lobe actually increases in size, when the detuning is raised. The shrinking of the Mott lobes is a quite expected behaviour, since getting farther away from resonance, excitations become more and more unstable. This leaves the

Mott state with  $n = 0$  as the only stable one and causes Mott lobes with  $n > 0$  to shrink in size, whereas the lobe for  $n = 0$  extends. The dependence of the phase boundary on the detuning parameter, as depicted in Figure 3.6, is in agreement with investigations by other groups [48, 160].

After this basic insight into the properties and dynamics of the JCH model, I continue and develop a thermodynamic theory for this model within the following chapter.

# Chapter 4

## Thermodynamic Properties

So far I analysed the JCH model by means of a mean-field theory in the zero-temperature limit. Now, the aim of the present chapter is to derive a theoretical description capable to exceed this limitation. In order to build up a theory for the JCH model at finite temperatures I already introduced, at the beginning of the previous chapter, the thermodynamic potential I work with. Namely, I use the grand-canonical ensemble, which allows for energy and particle exchange between the considered system and its environment. To fix the mean polariton number in the system, I introduced the chemical potential  $\mu$  in (3.26). Such a modified Hamiltonian is a suitable starting point to derive a theory for finite temperatures. In general all thermodynamic properties of a system can be derived from the thermodynamic potential corresponding to the chosen statistical ensemble. In the case of the grand-canonical ensemble the potential of choice is the free energy, which is defined as:

$$\mathcal{F}(T, V, \mu) = -\frac{1}{\beta} \ln \mathcal{Z}(T, V, \mu). \quad (4.1)$$

Here  $T$  labels the temperature of the system,  $V$  corresponds to the volume,  $N$  is the particle number and  $\beta$  is the reciprocal temperature defined by

$$\beta = \frac{1}{k_B T}. \quad (4.2)$$

It is clear from equation (4.1), that all thermodynamic information about the system under consideration stems from the partition function  $\mathcal{Z}$ . Therefore, the main problem one always faces in order to derive finite-temperature properties of a given system, is to find this function. In quantum statistics the partition function of a system, described by the Hamiltonian  $\hat{H}$ , is defined as

$$\mathcal{Z}(T, V, \mu) = \text{Tr} \left\{ e^{-\beta \hat{H}(\mu, V)} \right\}. \quad (4.3)$$

At a first glance, calculating the above function does not look very difficult and, in fact, it is not as long as the Hamiltonian is diagonal with respect to some suitable basis. However, in almost all interesting physical situations this is not the case and calculating the partition function (4.3) becomes quite challenging. In general, due to the hopping term in the system Hamiltonian (3.26), there does not exist a basis in which the considered JCH Hamiltonian becomes diagonal. For this reason I developed a mean-field theory at zero temperature in Section 3.5. In this chapter I will at first generalize this mean-field theory to finite temperatures. Afterwards, I will work out a different ansatz to describe the quantum phase transition. Instead of applying a mean-field theory, I am going to use a perturbation approach,

which eventually leads to an approximation of the grand-canonical partition function. To this end I derive a Ginzburg-Landau theory for the JCH model which includes the mean-field result for the phase boundary as a formal special case but allows, in principle, to calculate the phase boundary more accurate. Therefore, the mean-field calculations obtained in the first sections, will mainly serve as a reference for comparison with the Ginzburg-Landau results. Before starting with the perturbation calculation for the partition function, I introduce a reformulation of equation (4.3) in the following section, in order to simplify the further computations.

## 4.1 Dirac Interaction Picture

One can see from equation (4.3) that the definition of the partition function involves the full Hamiltonian of the system. However, as stated before, I do not know the eigenvalues of the full Hamiltonian but instead I found that it is possible to split the full Hamiltonian into a solvable part and a perturbing part. Now, I want to use this fact and switch to the imaginary-time Dirac interaction picture, which will lead to a reformulation of the partition function as a perturbation series, involving just the perturbation part of the full Hamiltonian of the system.

The Dirac picture is, besides the Schrödinger and the Heisenberg picture, one of the three most popular time evolution schemes in quantum mechanics. Their meaning stems from the fact that in quantum mechanics the time evolution can be divided arbitrarily between the states and the operators. In the Schrödinger picture the whole time dependence is associated with the state vectors, whereas all quantum mechanical operators in this picture are time independent. The opposite is true for the Heisenberg picture, where all operators are time dependent and the states are constant in time. The Dirac picture represents a middle course between the other two pictures and is commonly used in situations where the full Hamiltonian can be split in a solvable and a perturbative part. In this picture the time dependence is divided between the states and the operators in such a way, that the unperturbed Hamiltonian determines the time evolution of the operators, whereas the perturbation Hamiltonian governs the time evolution of the state vectors. To see how the transition from one picture into another is performed, I start with the Schrödinger equation in imaginary time. This equation can be obtained from the real-time Schrödinger equation by a so called Wick rotation  $t \rightarrow -i\tau$  which yields with  $\hbar = 1$

$$-\frac{\partial}{\partial\tau}|\psi(\tau)\rangle = \hat{H}(\tau)|\psi(\tau)\rangle. \quad (4.4)$$

In this picture the time evolution of an initial state vector to a final state vector is mediated via the imaginary-time evolution operator

$$|\psi(\tau)\rangle = \hat{U}(\tau, \tau_0)|\psi(\tau_0)\rangle. \quad (4.5)$$

Substituting this new state into equation (4.4) one notices, that the imaginary-time evolution operator has to satisfy the imaginary-time Schrödinger equation as well. Thus the following relation has to hold

$$-\frac{\partial}{\partial\tau}\hat{U}(\tau, \tau_0) = \hat{H}(\tau)\hat{U}(\tau, \tau_0). \quad (4.6)$$

Formally solving the differential equation yields, together with the initial condition  $\hat{U}(\tau, \tau) = 1$ , the following integral equation for the imaginary-time evolution operator

$$\hat{U}(\tau, \tau_0) = 1 - \int_{\tau_0}^{\tau} \hat{H}(\tau') \hat{U}(\tau', \tau) d\tau'. \quad (4.7)$$

Solving this equation iteratively, leads to the Dyson series

$$\hat{U}(\tau, \tau_0) = 1 + \sum_{n=1}^{\infty} (-1)^n \int_{\tau_0}^{\tau} d\tau_1 \int_{\tau_0}^{\tau_1} d\tau_2 \dots \int_{\tau_0}^{\tau_{n-1}} d\tau_n \hat{H}(\tau_1) \hat{H}(\tau_2) \dots \hat{H}(\tau_n). \quad (4.8)$$

Due to ambiguities in the time ordering it is convenient to rewrite this expression with the help of the bosonic imaginary-time ordering operator  $\hat{T}$  which is defined according to

$$\hat{T}[A(\tau_1) B(\tau_2)] = \Theta(\tau_1 - \tau_2) A(\tau_1) B(\tau_2) + \Theta(\tau_2 - \tau_1) B(\tau_2) A(\tau_1), \quad (4.9)$$

where  $\Theta$  is the Heaviside step function. Using this operator allows to rewrite equation (4.8) as

$$\hat{U}_D(\tau, \tau_0) = \hat{T} \left[ 1 + \sum_{n=1}^{\infty} \frac{(-1)^n}{n!} \int_{\tau_0}^{\tau} d\tau_1 \int_{\tau_0}^{\tau_1} d\tau_2 \dots \int_{\tau_0}^{\tau_{n-1}} d\tau_n \hat{H}(\tau_1) \hat{H}(\tau_2) \dots \hat{H}(\tau_n) \right]. \quad (4.10)$$

Here I included an additional pre-factor  $1/n!$  to cancel the imaginary-time variable permutations introduced by the time ordering operator. Comparing this expression with the series expansion of the exponential function, one notices that equation (4.10) can be transformed in an even shorter form, reading

$$\hat{U}(\tau, \tau_0) = \hat{T} e^{-\int_{\tau_0}^{\tau} d\tau' \hat{H}(\tau')}. \quad (4.11)$$

It is easy to prove, that the so defined imaginary-time evolution operator has the properties

$$\hat{U}^\dagger(\tau, \tau_0) \hat{U}(\tau, \tau_0) = 1, \quad (4.12)$$

and

$$\hat{U}^\dagger(\tau, \tau_0) = \hat{U}^{-1}(\tau, \tau_0) = \hat{U}(\tau_0, \tau). \quad (4.13)$$

Now, as stated before, I will assume that the full Hamiltonian can be decomposed in the following form

$$\hat{H}(\tau) = \hat{H}_0 + \hat{H}_1(\tau), \quad (4.14)$$

where  $\hat{H}_0$  describes the exactly solvable part and  $\hat{H}_1(\tau)$  can be treated as a perturbation to the known problem. From this situation one can perform the transition to the Dirac picture, denoted in the following by the label D, by conducting the following steps:

1. Synchronizing the two pictures at a fixed point in time

$$|\psi_D(\tau_0)\rangle = |\psi(\tau_0)\rangle. \quad (4.15)$$

2. Transition to the Dirac picture via

$$|\psi_D(\tau)\rangle = \hat{U}_0(\tau, \tau_0) |\psi(\tau)\rangle, \quad (4.16)$$

where I have

$$\hat{U}_0(\tau, \tau_0) = e^{-\hat{H}_0(\tau-\tau_0)}. \quad (4.17)$$

3. Time evolution for Dirac states via

$$|\psi_D\rangle(\tau) = \hat{U}_D(\tau, \tau') |\psi_D(\tau')\rangle, \quad (4.18)$$

and for Dirac operators via

$$\hat{A}_D = \hat{U}_0^{-1}(\tau, \tau_0) \hat{A} \hat{U}_0(\tau, \tau_0). \quad (4.19)$$

Subsequently, following these steps, it is easy to show that the imaginary-time evolution operator in the Dirac interaction picture is given by

$$\hat{U}_D(\tau, \tau') = \hat{U}_0^{-1}(\tau, \tau_0) \hat{U}(\tau, \tau') \hat{U}_0(\tau', \tau_0), \quad (4.20)$$

Note, that all physical quantities, i.e. all expectation values, are completely independent of the choice of picture.

Using the results obtained above, I can derive the Schrödinger equation in the imaginary Dirac interaction picture and obtain

$$\begin{aligned} \frac{\partial}{\partial \tau} |\psi_D(\tau)\rangle &= \left[ \frac{\partial}{\partial \tau} \hat{U}_0(\tau_0, \tau) \right] |\psi(\tau)\rangle + \hat{U}_0(\tau_0, \tau) \left[ \frac{\partial}{\partial \tau} |\psi(\tau)\rangle \right] \\ &= \left[ \hat{U}_0(\tau_0, \tau) \hat{H}_0 - \hat{U}_0(\tau_0, \tau) \hat{H} \right] |\psi(\tau)\rangle, \end{aligned} \quad (4.21)$$

which reduces to

$$-\frac{\partial}{\partial \tau} |\psi_D(\tau)\rangle = \hat{H}_{1D}(\tau) |\psi_D(\tau)\rangle. \quad (4.22)$$

Analogous to the analysis of the imaginary-time Schrödinger picture, one can determine the form of the imaginary-time Dirac evolution operator by considering its equation of motion:

$$-\frac{\partial}{\partial \tau} \hat{U}_D(\tau, \tau_0) = \hat{H}_{1D}(\tau) \hat{U}_D(\tau, \tau_0). \quad (4.23)$$

Following the same steps as for equation (4.6), eventually leads to the expression

$$\hat{U}_D(\tau, \tau_0) = \hat{T} e^{-\int_{\tau_0}^{\tau} d\tau' \hat{H}_{1D}(\tau')}. \quad (4.24)$$

Thus, I found that the Hamiltonian of the unperturbed system governs the time evolution of the Dirac operators and the perturbation Hamiltonian determines the time evolution of the Dirac state vectors.

In order to see how all the observations presented in this section are of any help for the task of finding a thermodynamic description of the JCH model, I remark that the time-ordered

imaginary Dyson series (4.10) naturally represents a power series with respect to the perturbation Hamiltonian. If one now considers the partition function (4.3) in the imaginary Dirac picture, which takes on the form

$$\mathcal{Z} = \text{Tr} \left\{ \hat{U}(\beta, 0) \right\}, \quad (4.25)$$

with the imaginary-time evolution operator according to equation (4.11) and uses relations (4.17) and (4.20), one finds

$$\mathcal{Z} = \text{Tr} \left\{ e^{-\beta \hat{H}_0} \hat{U}_D(\beta, 0) \right\}. \quad (4.26)$$

This can be further transformed using the definition of the thermal average with respect to the unperturbed system which I introduce as

$$\langle \bullet \rangle_0 = \frac{1}{\mathcal{Z}_0} \text{Tr} \left\{ \bullet e^{-\beta \hat{H}_0} \right\}, \quad (4.27)$$

where the partition function of the unperturbed system is given by

$$\mathcal{Z}_0 = \text{Tr} \left\{ e^{-\beta \hat{H}_0} \right\}. \quad (4.28)$$

Thus, one finds for the grand-canonical partition function the relation

$$\mathcal{Z} = \mathcal{Z}_0 \left\langle \hat{U}_D(\beta, 0) \right\rangle_0, \quad (4.29)$$

where the imaginary-time evolution operator takes on the form

$$\hat{U}_D(\beta, 0) = \hat{T} \exp \left[ - \int_0^\beta d\tau \hat{H}_{1D}(\tau) \right]. \quad (4.30)$$

Hence, I showed that, within the Dirac interaction picture, the partition function can be written as a product of the partition function of the unperturbed system  $\mathcal{Z}_0$  and a thermal average with respect to the unperturbed system over a power series of the perturbation Hamiltonian. This allows for a perturbative calculation of the thermodynamic potential up to arbitrary accuracy in the perturbation Hamiltonian. This result will be the corner stone for the further calculations within this chapter.

## 4.2 Mean-Field Theory for Finite Temperatures

Having outlined the principle idea of a thermodynamic perturbation theory within the previous section, I can straightforwardly use the results obtained therein, as soon as I settle for a specific Hamiltonian. As already shown in Section 3.5, within the mean-field approach the JCH Hamiltonian becomes diagonal and splits locally into an unperturbed part  $\hat{H}_0$  and the term  $\hat{H}_1^{\text{MF}}$ , which I treat as a perturbation. Therefore, I consider the Hamiltonian  $\hat{H}^{\text{MF}}$  which decomposes as stated in equation (3.54). The Hamiltonian of the unperturbed system is given according to equation (3.52). Note that there the sum runs over all lattice sites  $j$ ,

the on-site Hamiltonian  $\hat{H}_j^{\text{JC}}$  being defined by equation (3.27) and the perturbation Hamiltonian reads according to equation (3.50). Here, the appearing order parameter  $\Psi$  is defined as stated in equation (3.48).

In order to investigate the thermodynamic properties of the JCH-Hamiltonian, I start with the determination of the grand-canonical partition function. As outlined within the previous section, in the imaginary-time Dirac interaction picture the partition function is given by (4.29), where the imaginary-time evolution operator now takes on the form

$$\hat{U}_D(\beta, 0) = \hat{T} \exp \left[ - \int_0^\beta d\tau \hat{H}_{1D}^{\text{MF}}(\tau) \right]. \quad (4.31)$$

The pre-factor  $Z_0$  in (4.29) is equivalent to the grand-canonical partition function of the unperturbed system, which is given by

$$Z_0 = \text{Tr} \left\{ e^{-\beta \hat{H}_0} \right\} = \sum_j \sum_{n=0}^{\infty} \sum_{\alpha=\pm} \langle n, \alpha, j | e^{-\beta \hat{H}_0} | n, \alpha, j \rangle = \sum_j \sum_{n=0}^{\infty} \sum_{\alpha=\pm} e^{-\beta E_{jn\alpha}}, \quad (4.32)$$

where the local energy eigenvalues  $E_{jn\alpha}$  correspond to (3.30). Expression (4.29) tells me that I need to calculate the thermal average of the imaginary-time evolution operator in order to obtain the partition function. For this reason, I make use of the series representation of the exponential function to expand expression (4.29) in a power series. The expansion of the imaginary-time evolution operator (4.31) leads to

$$\hat{U}_D(\beta, 0) = \sum_{n=0}^{\infty} \frac{(-1)^n}{n!} \int_0^\beta d\tau_1 \dots \int_0^\beta d\tau_n \hat{T} \left[ \hat{H}_{1D}^{\text{MF}}(\tau_1) \dots \hat{H}_{1D}^{\text{MF}}(\tau_n) \right]. \quad (4.33)$$

Taking into account (3.50), this expression can be rewritten in the form

$$\hat{U}_D(\beta, 0) = \sum_{n=0}^{\infty} \hat{U}_D^{(n)}(\beta, 0), \quad (4.34)$$

with the coefficients

$$\begin{aligned} \hat{U}_D^{(n)}(\beta, 0) = & \frac{(\kappa z)^n}{n!} \sum_{j_1 \dots j_n} \int_0^\beta d\tau_1 \dots \int_0^\beta d\tau_n \hat{T} \left\{ \left[ \Psi \hat{a}_{j_1}(\tau_1) + \hat{a}_{j_1}^\dagger(\tau_1) \Psi - \Psi^2 \right] \dots \right. \\ & \left. \times \left[ \Psi \hat{a}_{j_n}(\tau_n) + \hat{a}_{j_n}^\dagger(\tau_n) \Psi - \Psi^2 \right] \right\}. \end{aligned} \quad (4.35)$$

Note that, here and in the following calculations, I drop the Dirac index D for the ladder operators, since their dependence on the imaginary-time variable  $\tau$  already indicates that they have to be taken in the imaginary-time Dirac interaction picture. The above expression together with relation (4.29) allows to calculate the partition function up to arbitrary orders in the order parameter. As discussed in Section 3.5 one needs to calculate this expansion to at least second order in the order parameter in order to locate the boundary of the quantum

phase transition. Thus, I focus on the first two terms of the expansion (4.35) leading to the following contributions to the partition function

$$\begin{aligned} \mathcal{Z} &\approx \mathcal{Z}_0 \left\langle \hat{U}_D^{(0)}(\beta, 0) + \hat{U}_D^{(1)}(\beta, 0) + \hat{U}_D^{(2)}(\beta, 0) + \dots \right\rangle_0 \\ &= \mathcal{Z}_0 + \mathcal{Z}_0 \left\langle \hat{U}_D^{(1)}(\beta, 0) \right\rangle_0 + \mathcal{Z}_0 \left\langle \hat{U}_D^{(2)}(\beta, 0) \right\rangle_0 + \dots \\ &= \mathcal{Z}_0 + \mathcal{Z}_1 + \mathcal{Z}_2 + \dots \end{aligned} \quad (4.36)$$

Hence, the first-order correction to the grand-canonical partition function is given by

$$\mathcal{Z}_1 = \mathcal{Z}_0 \kappa z \sum_j \int_0^\beta d\tau_1 \left\langle \Psi^* \hat{a}_j(\tau_1) + \hat{a}_j^\dagger(\tau_1) \Psi - \Psi^2 \right\rangle_0, \quad (4.37)$$

which can be evaluated to give

$$\mathcal{Z}_1 = -\beta \kappa z \sum_j \Psi^2. \quad (4.38)$$

Here I used the fact, that all thermal average over photonic ladder operators, where the number of annihilation operators does not match the number creation operators, vanish due to the orthogonality of the dressed states (2.137). In an analogue way one finds for the second-order contribution

$$\begin{aligned} \mathcal{Z}_2 &= \mathcal{Z}_0 \frac{(\kappa z)^2}{2} \sum_{j_1, j_2} \int_0^\beta d\tau_1 \int_0^\beta d\tau_2 \left\langle \hat{T} \left\{ \left[ \Psi \hat{a}_{j_1}(\tau_1) + \hat{a}_{j_1}^\dagger(\tau_1) \Psi - \Psi^2 \right] \right. \right. \\ &\quad \left. \left. \times \left[ \Psi^* \hat{a}_{j_2}(\tau_2) + \hat{a}_{j_2}^\dagger(\tau_2) \Psi - \Psi^2 \right] \right\} \right\rangle_0. \end{aligned} \quad (4.39)$$

Realizing that the action of the time ordering operator yields two expressions which are identical when exchanging the imaginary-time variables  $\tau_1 \longleftrightarrow \tau_2$ , I can just calculate one of the terms, say for instance  $\tau_1 > \tau_2$ , but I have to include a pre-factor 2. Additionally, making use of the orthogonality relation (2.137) again and dropping all terms of higher than second order in the order parameter, yields the following form of the above expression

$$\mathcal{Z}_2 = \mathcal{Z}_0 (\kappa z \Psi)^2 \sum_{j_1, j_2} \int_0^\beta d\tau_1 \int_0^\beta d\tau_2 \Theta(\tau_1 - \tau_2) \left\langle \hat{a}_{j_1}(\tau_1) \hat{a}_{j_2}^\dagger(\tau_2) + \hat{a}_{j_1}^\dagger(\tau_1) \hat{a}_{j_2}(\tau_2) \right\rangle_0. \quad (4.40)$$

Hence, to calculate this contribution to the partition function, one has to determine thermal averages over products of photonic creation and annihilation operators. For this reason, I will use the polariton mapping approach introduced in Section 2.6. The first thing to notice is that, due to the orthogonality relation (2.137), these expectation values do not vanish, only if both operators act on the same lattice side

$$\left\langle \hat{a}_i(\tau) \hat{a}_j^\dagger(\tau') \right\rangle_0 = \delta_{ij} \left\langle \hat{a}_i(\tau) \hat{a}_i^\dagger(\tau') \right\rangle_0. \quad (4.41)$$

Thus, I can rewrite expression (4.40) as a sum over local contributions

$$\mathcal{Z}_2 = \sum_j [\mathcal{Z}_2]_j, \quad (4.42)$$

where the respective coefficients are given by

$$[\mathcal{Z}_2]_j = \mathcal{Z}_0 (\kappa z \Psi)^2 \int_0^\beta d\tau_1 \int_0^\beta d\tau_2 \Theta(\tau_1 - \tau_2) \left\langle \hat{a}(\tau_1) \hat{a}^\dagger(\tau_2) + \hat{a}^\dagger(\tau_1) \hat{a}(\tau_2) \right\rangle_0. \quad (4.43)$$

Note that, here and in the following calculations of the local contribution  $[\mathcal{Z}_2]_j$ , I explicitly skip the site index  $j$  of the photonic ladder operators, as the expectation value is independent of the individual site. The local thermal expectation values occurring in the above expression can be calculated according to (4.27), which yields

$$\begin{aligned} \left\langle \hat{a}(\tau_1) \hat{a}^\dagger(\tau_2) \right\rangle_0 &= \frac{1}{\mathcal{Z}_0} \text{Tr} \left\{ \hat{a}(\tau_1) \hat{a}^\dagger(\tau_2) e^{-\beta \hat{H}_0} \right\} \\ &= \frac{1}{\mathcal{Z}_0} \sum_{n=0}^{\infty} \sum_{\alpha=\pm} \langle n, \alpha | e^{\tau_1 \hat{H}_0} \hat{a} e^{(\tau_2 - \tau_1) \hat{H}_0} \hat{a}^\dagger e^{-\tau_2 \hat{H}_0} e^{-\beta \hat{H}_0} | n, \alpha \rangle. \end{aligned} \quad (4.44)$$

Now, making use of the polariton mapping obtained in Section 2.6 and substituting expressions (2.153) for the photonic annihilation and creation operators, leads to the following calculation:

$$\begin{aligned} \mathcal{Z}_0 \left\langle \hat{a}(\tau_1) \hat{a}^\dagger(\tau_2) \right\rangle_0 &= \sum_{n=0}^{\infty} \sum_{\alpha=\pm} e^{-\beta E_{n\alpha}} e^{(\tau_1 - \tau_2) E_{n\alpha}} \langle n, \alpha | \hat{a} e^{(\tau_2 - \tau_1) \hat{H}_0} \\ &\quad \times \sum_{m=0}^{\infty} \sum_{\beta, \beta'=\pm} t_{(m+1)\beta' \beta} \hat{P}_{(m+1)\beta'}^\dagger \hat{P}_{m\beta} | n, \alpha \rangle \\ &= \sum_{n, m=0}^{\infty} \sum_{\alpha, \beta, \beta'=\pm} e^{-\beta E_{n\alpha}} e^{(\tau_1 - \tau_2) E_{n\alpha}} t_{(m+1)\beta' \beta} \delta_{mn} \delta_{\alpha\beta} \langle n, \alpha | \hat{a} e^{(\tau_2 - \tau_1) \hat{H}_0} | m+1, \beta' \rangle \\ &= \sum_{n, m=0}^{\infty} \sum_{k=1}^{\infty} \sum_{\alpha, \beta, \beta', \gamma, \gamma'=\pm} e^{-\beta E_{n\alpha}} e^{(\tau_1 - \tau_2) (E_{n\alpha} - E_{(m+1)\beta'})} t_{(m+1)\beta' \beta} \delta_{mn} \delta_{\alpha\beta} t_{k\gamma\gamma'} \\ &\quad \times \langle n, \alpha | \hat{P}_{(k-1)\gamma'}^\dagger \hat{P}_{k\gamma} | m+1, \beta' \rangle \\ &= \sum_{n, m=0}^{\infty} \sum_{k=1}^{\infty} \sum_{\alpha, \beta, \beta', \gamma, \gamma'=\pm} e^{-\beta E_{n\alpha}} e^{(\tau_1 - \tau_2) (E_{n\alpha} - E_{(m+1)\beta'})} t_{(m+1)\beta' \beta} t_{k\gamma\gamma'} \\ &\quad \times \delta_{mn} \delta_{\alpha\beta} \delta_{k(m+1)} \delta_{\gamma\beta'} \delta_{n(k-1)} \delta_{\alpha\gamma'} \\ &= \sum_{n=0}^{\infty} \sum_{k=1}^{\infty} \sum_{\alpha, \beta'=\pm} e^{-\beta E_{n\alpha}} e^{(\tau_1 - \tau_2) (E_{n\alpha} - E_{(n+1)\beta'})} t_{(n+1)\beta' \alpha} t_{k\beta' \alpha} \delta_{n(k-1)}, \end{aligned} \quad (4.45)$$

resulting in the final expression

$$\left\langle \hat{a}(\tau_1) \hat{a}^\dagger(\tau_2) \right\rangle_0 = \frac{1}{\mathcal{Z}_0} \sum_{n=0}^{\infty} \sum_{\alpha, \alpha'=\pm} e^{-\beta E_{n\alpha}} e^{(E_{n\alpha} - E_{(n+1)\alpha'}) (\tau_1 - \tau_2)} (t_{(n+1)\alpha' \alpha})^2. \quad (4.46)$$

Performing the same calculations for the remaining expectation value yields

$$\left\langle \hat{a}^\dagger(\tau_1) \hat{a}(\tau_2) \right\rangle_0 = \frac{1}{\mathcal{Z}_0} \sum_{n=1}^{\infty} \sum_{\alpha, \alpha'=\pm} e^{-\beta E_{n\alpha}} e^{(E_{n\alpha} - E_{(n-1)\alpha'}) (\tau_1 - \tau_2)} (t_{n\alpha \alpha'})^2. \quad (4.47)$$

Reinserting these expressions into (4.43) results in the following form of the on-site second-order contribution to the partition function

$$[\mathcal{Z}_2]_j = (\kappa z \Psi)^2 \sum_{\alpha, \alpha' = \pm} \int_0^\beta d\tau_1 \int_0^\beta d\tau_2 \left\{ \sum_{n=0}^{\infty} e^{-\beta E_{n\alpha}} e^{\omega_{n(n+1)\alpha\alpha'}(\tau_1 - \tau_2)} (t_{(n+1)\alpha'\alpha})^2 + \sum_{m=1}^{\infty} e^{-\beta E_{m\alpha}} e^{\omega_{m(m-1)\alpha\alpha'}(\tau_1 - \tau_2)} (t_{m\alpha\alpha'})^2 \right\} \Theta(\tau_1 - \tau_2), \quad (4.48)$$

where I introduced the abbreviation

$$\omega_{nm\alpha\alpha'} = E_{n\alpha} - E_{m\alpha'}. \quad (4.49)$$

After having determined the thermal expectation values, all that remains to do is to evaluate the imaginary-time integrals in the above expression. These integrals pose no problems and are easily calculated using the fact that

$$\int_0^\beta d\tau_1 \int_0^{\tau_1} d\tau_2 e^{\omega_{nm\alpha\alpha'}(\tau_1 - \tau_2)} = \left[ \frac{e^{\beta \omega_{nm\alpha\alpha'}} - 1}{\omega_{nm\alpha\alpha'}^2} - \frac{\beta}{\omega_{nm\alpha\alpha'}} \right]. \quad (4.50)$$

Note, that the integration limits have changed due to the Heaviside step function in expression (4.48). Thus, the expression for the local second-order contribution decomposes into a sum of terms proportional to  $\beta$  and a sum over terms proportional to differences of exponential functions. By shifting the summation index, it can be shown that the latter sum equals zero. Thus, only the terms proportional to  $\beta$  survive and equation (4.48) finally results in

$$[\mathcal{Z}_2]_j = -\beta (\kappa z \Psi)^2 \sum_{\alpha, \alpha' = \pm} \left[ \sum_{n=0}^{\infty} e^{-\beta E_{n\alpha}} \frac{(t_{(n+1)\alpha'\alpha})^2}{\omega_{n(n+1)\alpha\alpha'}} + \sum_{n=1}^{\infty} e^{-\beta E_{n\alpha}} \frac{(t_{n\alpha\alpha'})^2}{\omega_{n(n-1)\alpha\alpha'}} \right]. \quad (4.51)$$

Hence, eventually I obtained all necessary contributions to the partition function in order to find the phase transition. Combining the result calculated above and inserting them together with relation (4.49) into equation (4.36), yields

$$\mathcal{Z} \approx \mathcal{Z}_0 - \beta \sum_j \left\{ (\kappa z) + (\kappa z)^2 \sum_{\alpha, \alpha' = \pm} \left[ \sum_{n=0}^{\infty} e^{-\beta E_{n\alpha}} \frac{(t_{(n+1)\alpha'\alpha})^2}{E_{n\alpha} - E_{(n+1)\alpha'}} + \sum_{m=1}^{\infty} e^{-\beta E_{m\alpha}} \frac{(t_{m\alpha\alpha'})^2}{E_{m\alpha} - E_{(m-1)\alpha'}} \right] \right\} \Psi^2. \quad (4.52)$$

This result allows me to give an approximate expression for the grand-canonical free energy up to second order in the order parameter. Using definition (4.1) and inserting approximation (4.36) for the partition function leads to

$$\mathcal{F} = -\frac{1}{\beta} \ln(\mathcal{Z}_0 + \mathcal{Z}_1 + \mathcal{Z}_2 + \dots) = -\frac{1}{\beta} \ln \mathcal{Z}_0 - \frac{1}{\beta} \ln \left( 1 + \frac{\mathcal{Z}_1 + \mathcal{Z}_2}{\mathcal{Z}_0} + \dots \right). \quad (4.53)$$

One can transform this expression even further, if one uses the Taylor expansion of the logarithm

$$\ln(1+x) = \sum_{n=1}^{\infty} \frac{(-1)^{n+1}}{n} x^n, \quad (4.54)$$

which yields for equation (4.53) up to first order the expression

$$\ln\left(1 + \frac{\mathcal{Z}_1 + \mathcal{Z}_2}{\mathcal{Z}_0}\right) \approx \frac{\mathcal{Z}_1 + \mathcal{Z}_2}{\mathcal{Z}_0}. \quad (4.55)$$

Hence, the grand-canonical free energy is approximately given by

$$\mathcal{F} = \mathcal{F}_0 - \frac{1}{\beta} \left( \frac{\mathcal{Z}_1 + \mathcal{Z}_2}{\mathcal{Z}_0} + \dots \right), \quad (4.56)$$

where the free energy of the unperturbed system is defined as

$$\mathcal{F}_0 = -\frac{1}{\beta} \ln \mathcal{Z}_0. \quad (4.57)$$

In order to finally get the phase boundary, I rearrange the terms in the free energy with respect to the powers of the order parameter  $\Psi$ , resulting in an expansion of the form

$$\mathcal{F} = \mathcal{F}_0 + \sum_j a_2^{\text{MF}} \Psi^2 + O(\Psi^4). \quad (4.58)$$

As I have already reasoned in Section 3.7, one can obtain the phase boundary from the second-order expansion coefficient in (4.58). Using the results (4.38) and (4.51) together with the approximation (4.56), the Landau coefficient turns out to be site independent and takes on the form

$$a_2^{\text{MF}} = \kappa z + \frac{(\kappa z)^2}{\mathcal{Z}_0} \sum_{\alpha, \alpha' = \pm} \left[ \sum_{n=0}^{\infty} e^{-\beta E_{n\alpha}} \frac{(t_{(n+1)\alpha'\alpha})^2}{\omega_{n(n+1)\alpha\alpha'}} + \sum_{m=1}^{\infty} e^{-\beta E_{m\alpha}} \frac{(t_{m\alpha\alpha'})^2}{\omega_{m(m-1)\alpha\alpha'}} \right]. \quad (4.59)$$

The phase border is defined via the condition

$$a_2^{\text{MF}} \stackrel{!}{=} 0, \quad (4.60)$$

which leads to the on-site equation

$$\kappa z = - \frac{\mathcal{Z}_0}{\sum_{\alpha, \alpha' = \pm} \left\{ \frac{(t_{1\alpha'-\alpha})^2}{\omega_{01-\alpha'}} + \sum_{n=1}^{\infty} e^{-\beta E_{n\alpha}} \left[ \frac{(t_{(n+1)\alpha'\alpha})^2}{\omega_{n(n+1)\alpha\alpha'}} + \frac{(t_{n\alpha\alpha'})^2}{\omega_{n(n-1)\alpha\alpha'}} \right] \right\}}. \quad (4.61)$$

I will now check, whether this result is consistent with the one obtained at zero temperature from the Schrödinger perturbation theory in Section 3.6, I take a look at the ground-state  $|n, -\rangle$  of the system. To this end I consider the limit  $\beta \rightarrow \infty$  for the above expression, which immediately leads to

$$a\kappa z = - \left[ \sum_{\alpha = \pm} \frac{(t_{(n+1)\alpha-})^2}{E_{n-} - E_{(n+1)\alpha}} + \frac{(t_{n-\alpha})^2}{E_{n-} - E_{(n-1)\alpha}} \right]^{-1}, \quad n > 0, \quad (4.62)$$

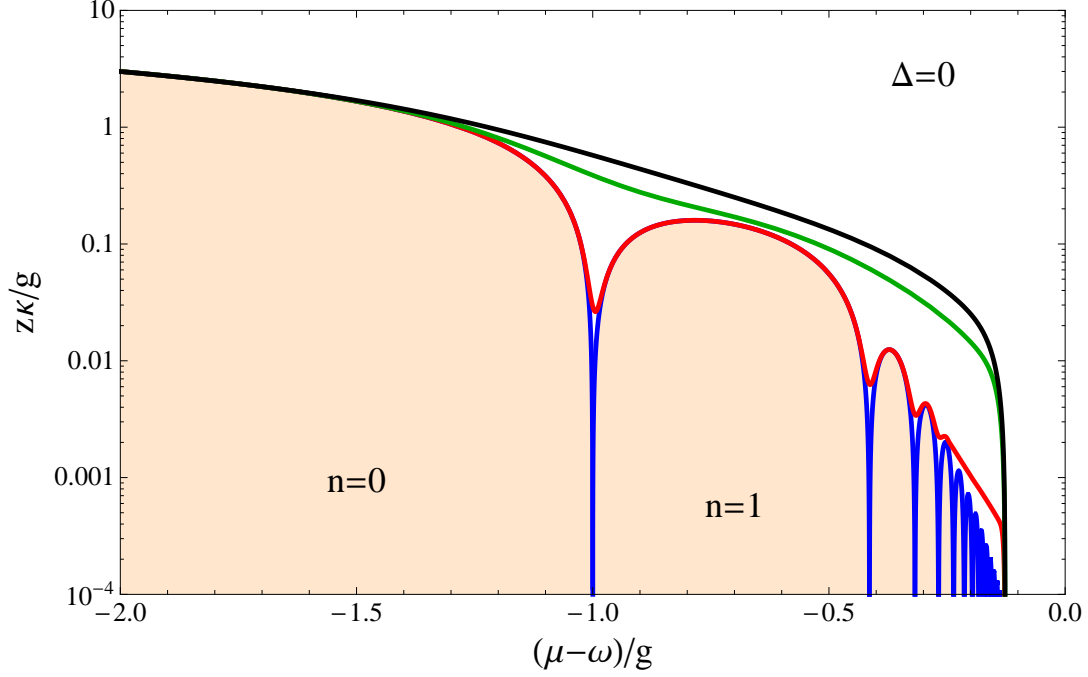


Figure 4.1: **Mean-field phase boundary for finite temperatures** in the case of resonance  $\Delta = 0$ . Depicted are the critical values for the hopping amplitude  $\kappa$ , scaling with the lattice coordination number  $z$ , with respect to the effective chemical potential  $\mu - \omega$ . The blue curve corresponds to  $T = 0$  K, the red curve to  $T = 0.005 g/k_B$ , the green curve to  $T = 0.1 g/k_B$  and the black curve corresponds to  $T = 0.2 g/k_B$ . All quantities are measured in units of the coupling strength  $g$ . The area under the curve represents the Mott-insulator phase, whereas the area above corresponds to the superfluid phase. Note that the rapid decreasing of the phase border at  $(\mu - \omega)/g \approx -0.13$  is a remnant resulting from the summation cut-off in equation (4.64).

and

$$\kappa z = - \left[ \frac{(t_{1--})^2}{E_{0-} - E_{1-}} + \frac{(t_{1+-})^2}{E_{0-} - E_{1+}} \right]^{-1}, \quad n = 0. \quad (4.63)$$

Comparing these phase boundaries with equation (3.97) shows, that the two results are, indeed, identical. On top of simply having reproduced the mean-field phase border for zero temperature, now I also obtained a formula giving the phase border at finite temperatures. Specifically in the case of resonance  $\Delta = 0$  I find for finite temperatures the explicit expres-

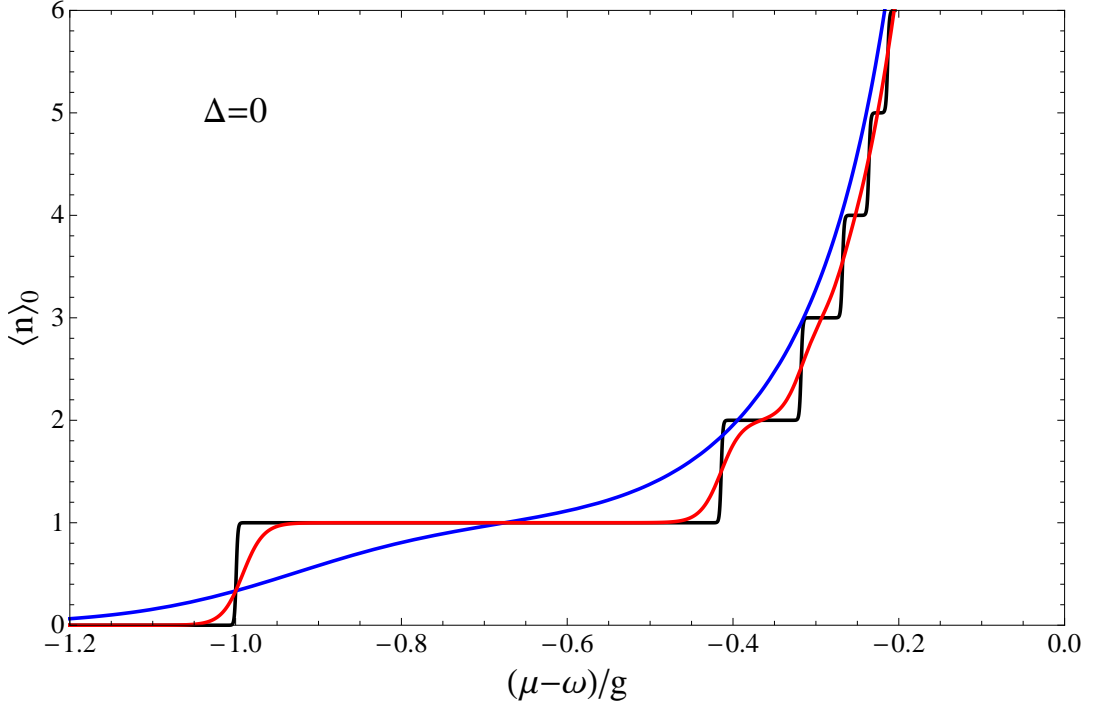


Figure 4.2: **Mean polariton occupation number for finite temperatures** versus the effective chemical potential, in the case of resonance. The black curve corresponds to  $T = 0.001 g/k_B$ , the red curve to  $T = 0.0125 g/k_B$  and the blue curve to  $T = 0.1 g/k_B$ .

sion

$$\kappa z = - \frac{4 \sum_{n=0}^{\infty} \sum_{\alpha=\pm} e^{-\beta E_{n\alpha}}}{\sum_{\alpha, \alpha'=\pm 1} \left\{ \frac{1}{E_{0-} - E_{1\alpha'}} - \sum_{n=1}^{\infty} e^{-\beta E_{n\alpha}} \left[ \frac{(\sqrt{n+1} + \alpha\alpha'\sqrt{n})^2}{E_{n\alpha} - E_{(n+1)\alpha'}} + \frac{(\sqrt{n} + \alpha\alpha'\sqrt{n-1})^2}{E_{n\alpha} - E_{(n-1)\alpha'}} \right] \right\}}. \quad (4.64)$$

In Figure 4.1 I plot the first 15 loops of the resulting phase boundary for a variety of temperatures at  $\Delta = 0$ . Analogue to the phase transition in the Bose-Hubbard model [157], one finds that the phase border smears out with increasing temperature.

One might interpret this result as a decrease of the superfluid phase with increasing temperature. To check whether this is really the case, I analyse the compressibility of the system in the following, which should vanish for a genuine Mott insulator [33]. The isothermal compressibility in the grand-canonical ensemble is defined as

$$\kappa_T = \frac{1}{N_s} \frac{\partial \langle n \rangle_0}{\partial \mu_{\text{eff}}}, \quad (4.65)$$

with the effective chemical potential  $\mu_{\text{eff}} = (\mu - \omega)$ . The quantity  $\langle n \rangle_0$  appearing in the numerator of (4.65) is the mean polariton number per lattice site. It is given as the thermal

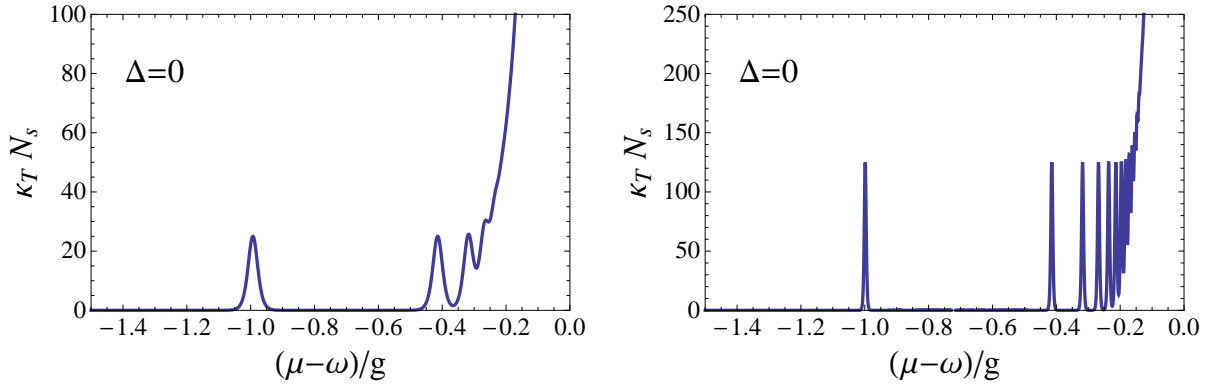


Figure 4.3: **Plot of the isothermal compressibility  $\kappa_T$  at finite temperatures** versus the effective chemical potential  $\mu - \omega$ , without hopping ( $\kappa = 0$ ) and in case of resonance ( $\Delta = 0$ ). The curve in the left diagram corresponds to  $T = 0.01 g/k_B$  and the curve in the right diagram corresponds to  $T = 0.002 g/k_B$ .

average

$$\langle n \rangle_0 = \frac{1}{\mathcal{Z}_0} \sum_{n=0}^{\infty} \sum_{\alpha=\pm} n e^{-\beta E_{n\alpha}}, \quad (4.66)$$

where the index 0 denotes that I am calculating the thermal average with respect to the unperturbed system. Thus this result holds for each on-site Jaynes-Cummings system individually. First, I discuss the local mean polariton occupation number, for which the resulting function in the case of resonance is plotted in Figure 4.2 for several temperatures. Here one can observe that the curves are smeared out for increasing temperatures as well. In the limit of vanishing temperature the function becomes a sequence of integer steps in the occupation number. It is experimentally interesting to realise that with increasing occupation number the system becomes more and more sensitive to small changes in the effective chemical potential. Furthermore, it is to see from Figure 4.2, that for high temperatures just the lowest state can easily be fixed at an integer value, whereas for the higher states the function loses its step character and becomes an exponential.

Knowing the mean occupation number, one can go ahead and calculate the isothermal compressibility according to equation (4.65). The resulting curve is plotted in Figure 4.3 for different temperatures. Having a look at the compressibility of the system one finds, that it does not vanish anymore in the smeared out regions but has positive finite values. Thus, one can not interpret these new regions in the phase diagram as a pure Mott insulator. As shown for example in Ref. [161, 162] the quantum phase transition between Mott-insulator and superfluid phase occurs strictly only for  $T = 0$ . For finite temperatures one finds a “classical” phase transition between the superfluid phase and a normal phase, driven by thermal fluctuations. There is only a crossover between the normal phase and a Mott-insulator. One can also see from Figure 4.3 that in the zero-temperature limit the compressibility becomes delta function like and thus, is zero everywhere except at the border between neighbouring Mott lobes, just as expected for a proper Mott insulator, which is incompressible by definition.

However, as can be seen in Figure 4.3, even for finite temperatures there are regions with a compressibility very close to zero, which justifies to call these regions a Mott-insulator for all practical purposes. Furthermore, it can be seen that these Mott-insulator regions shrink in size with increasing temperature and hence I conclude that, contrary to the first impression mediated by the phase diagram 4.1, the Mott-lobes become smaller with increasing temperature. This conclusion is in qualitative agreement with numerical results obtained for 1D and 2D systems [163].

### 4.3 Strong-Coupling Perturbation Theory

So far I successfully derived a mean-field theory for the JCH model for zero and finite temperatures. I also showed that this approach leads to a Landau theory with a site-dependent Landau order parameter  $\Psi$ . However, the focus of this thesis is a different approach which will be presented within the following sections. Basically, instead of using a mean-field theory in order to diagonalize the hopping term I will rather utilize a field-theoretic approach, which is well known in the investigation of thermal second-order phase transitions [7]. Namely, I introduce additional source currents  $j_i(\tau), j_i^*(\tau)$  in the original Jaynes-Cummings-Hubbard Hamiltonian, that break the global  $U(1)$  symmetry. This approach eventually leads to a Ginzburg-Landau theory, where the order parameter  $\Psi(\tau)$  now depends on space as well as on imaginary time. The starting point to derive the Ginzburg-Landau theory is the same as in the previous section. Thus, I first decompose the JCH Hamiltonian into the following terms

$$\hat{H}^{\text{SC}}(\tau) = \hat{H}_0 + \hat{H}_1^{\text{SC}}(\tau), \quad (4.67)$$

with the Hamiltonian of the unperturbed system given by (3.52) and the perturbation Hamiltonian by

$$\hat{H}_{1\text{D}}^{\text{SC}}(\tau) [j, j^*] = - \sum_{ij} \kappa_{ij} \hat{a}_i^\dagger(\tau) \hat{a}_j(\tau) + \sum_i \left[ j_i^*(\tau) \hat{a}_i(\tau) + j_i(\tau) \hat{a}_i^\dagger(\tau) \right]. \quad (4.68)$$

Note that, I dropped the Dirac index D again, using the convention that all operators, which depend on imaginary-time variables, are implicitly given in the imaginary-time Dirac interaction picture. Furthermore, in the above equation, I rewrite the hopping constant in the form

$$\kappa_{ij} = \begin{cases} \kappa, & \text{if } i, j \text{ are next neighbors} \\ 0, & \text{else} \end{cases}, \quad (4.69)$$

and introduced an additional term over the symmetry-breaking source currents coupling to the photonic creation and annihilation operators. Following the same procedure as in Section 4.2, I insert the perturbation Hamiltonian (4.68) into (4.29), which yields the following expression for the grand-canonical partition function

$$\mathcal{Z} [j, j^*] = \mathcal{Z}_0 \sum_{n=0}^{\infty} \frac{(-1)^n}{n!} \int_0^\beta d\tau_1 \dots \int_0^\beta d\tau_n \left\langle \hat{T} \left[ \hat{H}_{1\text{D}}^{\text{SC}}(\tau_1) [j, j^*] \dots \hat{H}_{1\text{D}}^{\text{SC}}(\tau_n) [j, j^*] \right] \right\rangle_0, \quad (4.70)$$

where the partition function is now a functional of the currents  $j$  and  $j^*$ . Splitting the grand-canonical partition functional into

$$\mathcal{Z}[j, j^*] = \mathcal{Z}_0 + \mathcal{Z}_0 \sum_{n=1}^{\infty} \mathcal{Z}_n[j, j^*], \quad (4.71)$$

where the latter part is defined as

$$\mathcal{Z}_n[j, j^*] = \frac{(-1)^n}{n!} \int_0^\beta d\tau_1 \dots \int_0^\beta d\tau_n \left\langle \hat{T} \left[ \hat{H}_{\text{ID}}^{\text{SC}}(\tau_1)[j, j^*] \dots \hat{H}_{\text{ID}}^{\text{SC}}(\tau_n)[j, j^*] \right] \right\rangle_0, \quad (4.72)$$

the free energy becomes

$$\mathcal{F}[j, j^*] = -\frac{1}{\beta} \ln \mathcal{Z}[j, j^*] = \mathcal{F}_0 - \frac{1}{\beta} \ln \left\{ 1 + \sum_{n=1}^{\infty} \mathcal{Z}_n[j, j^*] \right\}. \quad (4.73)$$

Using the series expansion (4.54) for the logarithm, one can approximate the free energy up to second order in  $\mathcal{Z}_n$  leading to

$$\mathcal{F}[j, j^*] \approx \mathcal{F}_0 - \frac{1}{\beta} \left\{ \sum_{n=1}^{\infty} \mathcal{Z}_n[j, j^*] - \frac{1}{2} \left( \sum_{n=1}^{\infty} \mathcal{Z}_n[j, j^*] \right)^2 \right\}. \quad (4.74)$$

For clarity, I will skip mentioning the explicit dependence of the perturbation Hamiltonian  $\hat{H}_{\text{ID}}^{\text{SC}}(\tau)[j, j^*]$  from the currents  $j, j^*$  in the following, and rather use the shorter form  $\hat{H}_{\text{ID}}^{\text{SC}}(\tau)$ . Collecting all terms up to fourth order in the currents and first order in the hopping in equation (4.74) leads to the following contribution from the second term

$$\begin{aligned} \sum_{n=1}^5 \mathcal{Z}_n[j, j^*] = & \left\{ - \int_0^\beta d\tau_1 \left\langle \hat{H}_{\text{ID}}^{\text{SC}}(\tau_1) \right\rangle_0 + \frac{1}{2} \int_0^\beta d\tau_1 \int_0^\beta d\tau_2 \left\langle \hat{T} \left[ \hat{H}_{\text{ID}}^{\text{SC}}(\tau_1) \hat{H}_{\text{ID}}^{\text{SC}}(\tau_2) \right] \right\rangle_0 \right. \\ & - \frac{1}{6} \int_0^\beta d\tau_1 \dots \int_0^\beta d\tau_3 \left\langle \hat{T} \left[ \hat{H}_{\text{ID}}^{\text{SC}}(\tau_1) \hat{H}_{\text{ID}}^{\text{SC}}(\tau_2) \hat{H}_{\text{ID}}^{\text{SC}}(\tau_3) \right] \right\rangle_0 \\ & + \frac{1}{24} \int_0^\beta d\tau_1 \dots \int_0^\beta d\tau_4 \left\langle \hat{T} \left[ \hat{H}_{\text{ID}}^{\text{SC}}(\tau_1) \hat{H}_{\text{ID}}^{\text{SC}}(\tau_2) \hat{H}_{\text{ID}}^{\text{SC}}(\tau_3) \hat{H}_{\text{ID}}^{\text{SC}}(\tau_4) \right] \right\rangle_0 \\ & \left. - \frac{1}{120} \int_0^\beta d\tau_1 \dots \int_0^\beta d\tau_5 \left\langle \hat{T} \left[ \hat{H}_{\text{ID}}^{\text{SC}}(\tau_1) \hat{H}_{\text{ID}}^{\text{SC}}(\tau_2) \hat{H}_{\text{ID}}^{\text{SC}}(\tau_3) \hat{H}_{\text{ID}}^{\text{SC}}(\tau_4) \hat{H}_{\text{ID}}^{\text{SC}}(\tau_5) \right] \right\rangle_0 \right\}. \quad (4.75) \end{aligned}$$

Furthermore, for the third term in equation (4.74), the only contributing terms are given by

$$\begin{aligned} \left( \sum_{n=1}^3 \mathcal{Z}_n[j, j^*] \right)^2 = & \left\{ - \int_0^\beta d\tau_1 \left\langle \hat{H}_{\text{ID}}^{\text{SC}}(\tau_1) \right\rangle_0 + \frac{1}{2} \int_0^\beta d\tau_1 \int_0^\beta d\tau_2 \left\langle \hat{T} \left[ \hat{H}_{\text{ID}}^{\text{SC}}(\tau_1) \hat{H}_{\text{ID}}^{\text{SC}}(\tau_2) \right] \right\rangle_0 \right. \\ & \left. - \frac{1}{6} \int_0^\beta d\tau_1 \dots \int_0^\beta d\tau_3 \left\langle \hat{T} \left[ \hat{H}_{\text{ID}}^{\text{SC}}(\tau_1) \hat{H}_{\text{ID}}^{\text{SC}}(\tau_2) \hat{H}_{\text{ID}}^{\text{SC}}(\tau_3) \right] \right\rangle_0 \right\}^2 \quad (4.76) \end{aligned}$$

Inserting the definition of the perturbation Hamiltonian (4.68) and making use of the orthonormality relation for the dressed state basis (2.137), one finds that the occurring thermal averages become

$$\begin{aligned}
 \sum_{n=1}^5 \mathcal{Z}_n [j, j^*] &= \sum_{i_1, i_2} \int_0^\beta d\tau_1 \int_0^\beta d\tau_2 \left\{ j_{i_1}(\tau_1) j_{i_2}^*(\tau_2) \left\langle \hat{T} \left[ \hat{a}_{i_1}^\dagger(\tau_1) \hat{a}_{i_2}(\tau_2) \right] \right\rangle_0 \right. \\
 &+ \sum_{i_3, j_3} \kappa_{i_3 j_3} \int_0^\beta d\tau_1 \dots \int_0^\beta d\tau_3 j_{i_1}(\tau_1) j_{i_2}^*(\tau_2) \left\langle \hat{T} \left[ \hat{a}_{i_1}^\dagger(\tau_1) \hat{a}_{i_2}(\tau_2) \hat{a}_{i_3}^\dagger(\tau_3) \hat{a}_{j_3}(\tau_3) \right] \right\rangle_0 \\
 &+ \frac{1}{4} \sum_{i_3, i_4} \int_0^\beta d\tau_1 \dots \int_0^\beta d\tau_4 j_{i_1}(\tau_1) j_{i_2}^*(\tau_2) j_{i_3}(\tau_3) j_{i_4}^*(\tau_4) \left\langle \hat{T} \left[ \hat{a}_{i_1}^\dagger(\tau_1) \hat{a}_{i_2}(\tau_2) \hat{a}_{i_3}^\dagger(\tau_3) \hat{a}_{i_4}(\tau_4) \right] \right\rangle_0 \\
 &+ \frac{1}{4} \sum_{i_3, i_4, i_5, j_5} \kappa_{i_5 j_5} \int_0^\beta d\tau_1 \dots \int_0^\beta d\tau_5 j_{i_1}(\tau_1) j_{i_2}^*(\tau_2) j_{i_3}(\tau_3) j_{i_4}^*(\tau_4) \\
 &\times \left\langle \hat{T} \left[ \hat{a}_{i_1}^\dagger(\tau_1) \hat{a}_{i_2}(\tau_2) \hat{a}_{i_3}^\dagger(\tau_3) \hat{a}_{i_4}(\tau_4) \hat{a}_{i_5}^\dagger(\tau_5) \hat{a}_{j_5}(\tau_5) \right] \right\rangle_0 + \mathcal{O}(j^6) \mathcal{O}(\kappa^2) \left. \right\}, \quad (4.77)
 \end{aligned}$$

and

$$\begin{aligned}
 \left( \sum_{n=1}^3 \mathcal{Z}_n [j, j^*] \right)^2 &= \left( \sum_{i_1, i_2} \int_0^\beta d\tau_1 \int_0^\beta d\tau_2 j_{i_1}(\tau_1) j_{i_2}^*(\tau_2) \left\langle \hat{T} \left[ \hat{a}_{i_1}^\dagger(\tau_1) \hat{a}_{i_2}(\tau_2) \right] \right\rangle_0 \right)^2 \\
 &+ \left( \sum_{i_3, j_3} \kappa_{i_3 j_3} \int_0^\beta d\tau_1 \dots \int_0^\beta d\tau_3 j_{i_1}(\tau_1) j_{i_2}^*(\tau_2) \left\langle \hat{T} \left[ \hat{a}_{i_1}^\dagger(\tau_1) \hat{a}_{i_2}(\tau_2) \hat{a}_{i_3}^\dagger(\tau_3) \hat{a}_{j_3}(\tau_3) \right] \right\rangle_0 \right) \\
 &\times \left( \sum_{i_1, i_2} \int_0^\beta d\tau_1 \int_0^\beta d\tau_2 j_{i_1}(\tau_1) j_{i_2}^*(\tau_2) \left\langle \hat{T} \left[ \hat{a}_{i_1}^\dagger(\tau_1) \hat{a}_{i_2}(\tau_2) \right] \right\rangle_0 \right). \quad (4.78)
 \end{aligned}$$

Hence, the expansion of the grand-canonical partition functional leads to a sum of integrals over  $n$ -particle thermal Green's functions of the unperturbed system, which are defined as

$$G_n^{(0)} (\tau'_1, i'_1; \dots; \tau'_n, i'_n | \tau_1, i_1; \dots; \tau_n, i_n) = \left\langle \hat{T} \left[ \hat{a}_{i'_1}^\dagger(\tau'_1) \hat{a}_{i_1}(\tau_1) \dots \hat{a}_{i'_n}^\dagger(\tau'_n) \hat{a}_{i_n}(\tau_n) \right] \right\rangle_0, \quad (4.79)$$

where the upper index corresponds to the order in the hopping parameter  $\kappa$  and the lower index corresponds to two times the order in the symmetry-breaking currents  $j$ .

Furthermore, I point out that one can see from (4.77) that the Ginzburg-Landau approach (4.68) does not only lead to a perturbation series in the source currents  $j, j^*$  but also in  $\kappa$ . Thus, this ansatz is far more powerful than the mean-field approach, because it allows to calculate corrections due to photon hopping up to arbitrary orders in  $\kappa$ . Inserting the results (4.77) and (4.78) into the approximation (4.74) for the free energy, leads to the following

relation for the free energy

$$\begin{aligned} \mathcal{F}[j, j^*] = \mathcal{F}_0 - \frac{1}{\beta} \sum_{i_1, i_2} \int_0^\beta d\tau_1 d\tau_2 \left\{ \left[ a_2^{(0)}(i_1, \tau_1 | i_2, \tau_2) + \sum_{i_3, j_3} \kappa_{i_3 j_3} a_2^{(1)}(i_1, \tau_1; i_3 | i_2, \tau_2; j_3) \right] \right. \\ \times j_{i_1}(\tau_1) j_{i_2}^*(\tau_2) + \frac{1}{4} \sum_{i_3, i_4} \int_0^\beta d\tau_3 d\tau_4 \left[ a_4^{(0)}(i_1, \tau_1; i_2, \tau_2 | i_3, \tau_3; i_4, \tau_4) \right. \\ \left. \left. + \sum_{i_5, j_5} \kappa_{i_5 j_5} a_4^{(1)}(i_1, \tau_1; i_2, \tau_2; i_5 | i_3, \tau_3; i_4, \tau_4; j_5) \right] j_{i_1}(\tau_1) j_{i_2}(\tau_2) j_{i_3}^*(\tau_3) j_{i_4}^*(\tau_4) \right\}, \end{aligned} \quad (4.80)$$

where the introduced expansion coefficients are defined as

$$a_2^{(0)}(i_1, \tau_1 | i_2, \tau_2) = G_1^{(0)}(i_1, \tau_1 | i_2, \tau_2), \quad (4.81)$$

$$a_2^{(1)}(i_1, \tau_1; i_3 | i_2, \tau_2; j_3) = \int_0^\beta d\tau_3 G_2^{(0)}(i_1, \tau_1; i_3, \tau_3 | i_2, \tau_2; j_3, \tau_3), \quad (4.82)$$

$$\begin{aligned} a_4^{(0)}(i_1, \tau_1; i_2, \tau_2 | i_3, \tau_3; i_4, \tau_4) &= G_2^{(0)}(i_1, \tau_1; i_2, \tau_2 | i_3, \tau_3; i_4, \tau_4) \\ &\quad - 2 G_1^{(0)}(i_1, \tau_1 | i_3, \tau_3) G_1^{(0)}(i_2, \tau_2 | i_4, \tau_4), \end{aligned} \quad (4.83)$$

$$\begin{aligned} a_4^{(1)}(i_1, \tau_1; i_2, \tau_2; i_5 | i_3, \tau_3; i_4, \tau_4; j_5) &= \int_0^\beta d\tau_5 \left[ G_3^{(0)}(i_1, \tau_1; i_2, \tau_2; i_5, \tau_5 | i_3, \tau_3; i_4, \tau_4; j_5, \tau_5) \right. \\ &\quad \left. - 2 G_2^{(0)}(i_1, \tau_1; i_5, \tau_5 | i_3, \tau_3; j_5, \tau_5) G_1^{(0)}(i_3, \tau_3 | i_4, \tau_4) \right]. \end{aligned} \quad (4.84)$$

In principle, one could now make use of the definition (4.79) and calculate the expansion coefficients of the free energy straightforwardly. However, with increasing order of the thermal Green's function the calculation becomes more and more complex due to the increasing number of space- and time-index permutations. Therefore, I want to introduce another approach to calculate the thermal Green's functions, which automatically takes care of the emerging problems. Namely, I decompose the thermal Green's functions into cumulants.

## 4.4 Cumulant Expansion

In the following I apply the approach proposed in reference [164] and expand the thermal Green's functions of the unperturbed system diagrammatically using cumulants. I will show that each Green's function decomposes into a sum of products of cumulants. Furthermore, these cumulants can be mapped on suitably defined Feynman diagrams. This approach allows to formulate some easy diagrammatic rules, to write down the correct cumulant decomposition for every Green's function without calculations.

To find these cumulants one needs to define a generating functional from which all higher cumulants can be derived. Therefore, I consider a Hamiltonian of the form

$$\hat{H}(\tau)[j, j^*] = \hat{H}_0 - \sum_i \left[ j_i(\tau) \hat{a}_i^\dagger + j_i^*(\tau) \hat{a}_i \right], \quad (4.85)$$

with the Hamiltonian  $\hat{H}_0 = \sum_i \hat{H}_{0i}$  of the unperturbed system, which decomposes into a sum over local Hamiltonians  $\hat{H}_{0i}$ , and a perturbation arising from the currents  $j, j^*$ . I showed in Section 4.1, that in the Dirac interaction picture the corresponding imaginary-time evolution operator is given by

$$\hat{U}_D [j, j^*] (\tau, \tau_0) = \hat{T} \exp \left\{ \int_{\tau_0}^{\tau} d\tau_1 \sum_i \left[ j_i(\tau_1) \hat{a}_i^\dagger(\tau_1) + j_i^*(\tau_1) \hat{a}_i(\tau_1) \right] \right\}, \quad (4.86)$$

and hence, the partition function becomes according to (4.29)

$$\mathcal{Z}^{(0)} [j, j^*] = \mathcal{Z}_0 \left\langle \hat{T} \exp \left\{ \int_0^\beta d\tau \sum_i \left[ j_i(\tau) \hat{a}_i^\dagger(\tau) + j_i^*(\tau) \hat{a}_i(\tau) \right] \right\} \right\rangle_0. \quad (4.87)$$

Calculating the functional derivatives of the above expression, one finds

$$\frac{1}{\mathcal{Z}^{(0)}} \frac{\delta^2 \mathcal{Z}_0 [j, j^*]}{\delta j_{n'}(\tau') \delta j_n^*(\tau)} = \left\langle \hat{T} \left\{ \hat{a}_{n'}^\dagger(\tau') \hat{a}_n(\tau) e^{\int_0^\beta d\tau'' \sum_i \left[ j_i(\tau'') \hat{a}_i^\dagger(\tau'') + j_i^*(\tau'') \hat{a}_i(\tau'') \right]} \right\} \right\rangle_0, \quad (4.88)$$

which, in the situation of vanishing currents, gives exactly the two-point thermal Green's function of the unperturbed system i.e.

$$\frac{1}{\mathcal{Z}^{(0)}} \frac{\delta^2 \mathcal{Z}_0 [j, j^*]}{\delta j_{n'}(\tau') \delta j_n^*(\tau)} \Big|_{j=j^*=0} = \left\langle \hat{T} \left[ \hat{a}_{n'}^\dagger(\tau') \hat{a}_n(\tau) \right] \right\rangle_0 = G_1^{(0)} (n', \tau' | n, \tau). \quad (4.89)$$

It is clear to see that, this procedure works as well for the higher Green's functions and, thus, one finds that all thermal  $n$ -point Green's functions can be obtained from (4.87) by performing  $2n$  functional derivatives with respect to the source currents. Therefore, the thermal Green's functions can be expressed by

$$G_n^{(0)} (\tau'_1, i'_1; \dots; \tau'_n, i'_n | \tau_1, i_1; \dots; \tau_n, i_n) = \frac{1}{\mathcal{Z}_0} \frac{\delta^{2n} \mathcal{Z}^{(0)} [j, j^*]}{\delta j_{i'_1}(\tau'_1) \delta j_{i'_1}^*(\tau'_1) \dots \delta j_{i'_n}(\tau'_n) \delta j_{i'_n}^*(\tau'_n)} \Big|_{j=j^*=0}. \quad (4.90)$$

Normally one would apply Wick's theorem to decompose the  $n$ -point correlation function (4.90) into sums of products of 2-point correlation functions [165]. Unfortunately, this is not possible for the considered system, since Wick's theorem just holds for systems, where the unperturbed Hamiltonian is linear in the occupation number operator. Instead, one has to use the so called *cluster expansion* introduced by Metzner [166], which states that the logarithm of the partition function is given by the sum of all connected Green's. In fact equation (4.90) leads to a decomposition into connected *and* disconnected diagrams. Using the logarithm on this decomposition cancels all disconnected diagrams and leaves only the connected ones. For this reason and inspired by the result (4.90), one defines the generating functional as

$$\begin{aligned} C_0^{(0)} [j, j^*] &= \log \left( \frac{\mathcal{Z}^{(0)} [j, j^*]}{\mathcal{Z}_0} \right) \\ &= \log \left\langle \hat{T} \exp \left\{ \int_0^\beta d\tau \sum_i \left[ j_i(\tau) \hat{a}_i^\dagger(\tau) + j_i^*(\tau) \hat{a}_i(\tau) \right] \right\} \right\rangle_0. \end{aligned} \quad (4.91)$$

Due to the properties of the logarithm and the fact that the unperturbed Hamiltonian decomposes into a sum over local contributions, the generating functional decomposes into a sum over local cumulants as well

$$C_0^{(0)} [j, j^*] = \sum_i {}_i C_0^{(0)} [j, j^*], \quad (4.92)$$

where the local cumulants are defined via

$${}_i C_0^{(0)} [j, j^*] = \log \left\langle \hat{T} \exp \left\{ \int_0^\beta d\tau \left[ j_i(\tau) \hat{a}_i^\dagger(\tau) + j_i^*(\tau) \hat{a}_i(\tau) \right] \right\} \right\rangle_{0,i}. \quad (4.93)$$

Note, that the index  $i$  associated with the thermal average now indicates, that it has to be calculated with respect to the local unperturbed Hamiltonian  $\hat{H}_{0i}$ . Since I work in a homogeneous system, where all lattice sites are equivalent, I drop the site index right away and work in the following with local cumulants defined by the generating functional

$$C_0^{(0)} [j, j^*] = \log \left\langle \hat{T} \exp \left\{ \int_0^\beta d\tau \left[ j(\tau) \hat{a}^\dagger(\tau) + j^*(\tau) \hat{a}(\tau) \right] \right\} \right\rangle_0. \quad (4.94)$$

One finds the higher order cumulants from this expression by calculating the functional derivatives with respect to the symmetry-breaking currents, just as I did in (4.90) for the  $n$ -point Green's functions. Thus, one finds

$$C_n^{(0)} (i'_1, \tau'_1; \dots; i'_n, \tau'_n | i_1, \tau_1; \dots; i_n, \tau_n) = \frac{\delta^{2n} C_0^{(0)} [j, j^*]}{\delta j_{i'_1}(\tau'_1) \dots \delta j_{i'_n}(\tau'_n) \delta j_{i_1}^*(\tau_1) \dots \delta j_{i_n}^*(\tau_n)} \Big|_{j=j^*=0}. \quad (4.95)$$

Since according to equation (4.92) the cumulants are local quantities, I introduce a shorter notation for the  $n$ -th order cumulant, which reads

$$C_n^{(0)} (i'_1, \tau'_1; \dots; i'_n, \tau'_n | i_1, \tau_1; \dots; i_n, \tau_n) = C_n^{(0)} (i_1; \tau'_1, \dots, \tau'_n | \tau_1, \dots, \tau_n) \delta_{i_1, i_2} \dots \delta_{i_{n-1}, i_n} \\ \times \delta_{i'_1, i'_2} \dots \delta_{i'_{n-1}, i'_n} \delta_{i_1, i'_1}. \quad (4.96)$$

Performing the calculations according to this formula, always leads to the thermal Green's function of the same order and a sum over products of lower order cumulants. Rearranging the results from this calculations, one finds the respective cumulant decomposition for each thermal Green's function. For the Green's functions up to 2nd order one finds explicitly

$$G_1^{(0)} (i_1, \tau_1 | i_2, \tau_2) = \frac{1}{\mathcal{Z}^{(0)} [j, j^*]} \frac{\delta^2 \mathcal{Z}^{(0)} [j, j^*]}{\delta j_{i_1}(\tau_1) \delta j_{i_2}^*(\tau_2)} \Big|_{j=j^*=0} = \frac{\delta^2 C_0^{(0)} [j, j^*]}{\delta j_{i_1}(\tau_1) \delta j_{i_2}^*(\tau_2)} \Big|_{j=j^*=0} \\ = \delta_{i_1, i_2} C_1^{(0)} (i_1; \tau_1 | \tau_2), \quad (4.97)$$

and

$$G_2^{(0)} (i_1, \tau_1; i_2, \tau_2 | i_3, \tau_3; i_4, \tau_4) = \delta_{i_3 i_4} \delta_{i_3 i_1} \delta_{i_4 i_2} C_2^{(0)} (i_1; \tau_1, \tau_2 | \tau_3, \tau_4) \\ + \delta_{i_3 i_1} \delta_{i_4 i_2} C_1^{(0)} (i_1; \tau_1 | \tau_3) C_1^{(0)} (i_2; \tau_2 | \tau_4) + \delta_{i_3 i_2} \delta_{i_4 i_1} C_1^{(0)} (i_1; \tau_1 | \tau_4) C_1^{(0)} (i_2; \tau_2 | \tau_3). \quad (4.98)$$

Comparing these results with the expansion (4.80) and expansion coefficients (4.81) – (4.84) leads to the following important observation: The logarithm transforms the grand-canonical partition function, which is sum over connected and disconnected thermal  $n$ -point Green's functions, into the grand-canonical free energy, that turns out to be a sum over cumulants representing the connected Green's functions only. This is due to the fact that the expansion of the logarithm introduces additional corrections to the expansion coefficients (4.83) and (4.84) of the free energy, which exactly cancel the disconnected diagrams of the thermal Green's functions. However, the straightforward calculation according to equation (4.95) is still rather tricky and the number of contributing terms rises very quickly with the order of the considered Green's function. Furthermore, many of the terms are identical due to symmetry reasons or do not contribute to the free energy functional and, thus, these calculations are not very efficient. For this reason, I will introduce some rules within the next section, which will provide the basis for a diagrammatic expansion of the  $n$ -point Green's function. This approach will yield a much simpler access to the cumulant decomposition.

## 4.5 Diagrammatic Expansion

Within this section I introduce some diagrammatic rules in order to calculate the perturbation series of the free energy. This approach will prove to be completely analogue to the cumulant expansion, derived in the previous section, but much easier to calculate. The rules for this decomposition are presented in the following subsection.

### 4.5.1 Diagrammatic Rules

The diagrammatic expansion can be obtained by applying the following rules:

1. A vertex with  $n$  ingoing and  $n$  outgoing lines corresponds to a  $n$ -th order cumulant  $C_n^{(0)}$ .

$$C_1^{(0)}(\tau_1|\tau_2) = \tau_1 \longrightarrow \overset{i}{\bullet} \longrightarrow \tau_2 \quad , \quad (4.99)$$

$$C_2^{(0)}(\tau_1, \tau_2|\tau_3, \tau_4) = \begin{array}{c} \tau_1 \quad \tau_3 \\ \swarrow \quad \searrow \\ \overset{i}{\bullet} \\ \nearrow \quad \nwarrow \\ \tau_2 \quad \tau_4 \end{array} \quad . \quad (4.100)$$

2. Each vertex is labelled with a site index and each line with an imaginary-time index.
3. Each entering line is associated with a factor  $j_i(\tau)$  and each leaving line is associated with a factor  $j_i^*(\tau)$ :

$$\square \xrightarrow{\tau} = j_i(\tau), \quad \xrightarrow{\tau} \square = j_i^*(\tau) \quad (4.101)$$

4. All internal lines starting in one vertex and ending in another correspond to hopping processes and are associated with a factor  $\kappa_{ij}$ :

$$\begin{array}{c} i \qquad \tau \qquad j \\ \bullet \longrightarrow \bullet \end{array} = \kappa_{ij} \quad (4.102)$$

5. For a connected Green's function of a given order draw all inequivalent connected diagrams.

6. Integrate over all time variables and sum over all site indices.

The above rules allow to construct the diagram for each cumulant and Green's function. However, in order to get the correct expansion of the partition function the following additional rules are necessary

7. Multiply by the multiplicity and divide by the symmetry factor.

Following these rules, one does not need to calculate the cumulant decomposition but, instead, one can just write down the necessary contributions right away.

Subsequently, one can deduce the thermal Green's functions, which correspond to the expansion coefficients of the free energy defined in (4.81) – (4.84). Applying the diagrammatic rules and afterwards rewriting the result in terms of cumulants yields:

$$\begin{aligned} a_2^{(0)}(i, \tau_1 | i_2, \tau_2) &= G_1^{(0)}(i, \tau_1 | i_2, \tau_2) = \begin{array}{c} i \\ \tau_1 \longrightarrow \bullet \longrightarrow \tau_2 \end{array} \\ &= \delta_{i,i_2} C_1^{(0)}(i; \tau_1 | \tau_2), \end{aligned} \quad (4.103)$$

$$\begin{aligned} a_2^{(1)}(i_1, \tau_1; i | i_2, \tau_2; j) &= \int_0^\beta d\tau G_2^{(0)}(i_1, \tau_1; i, \tau | i_2, \tau_2; j, \tau) = \begin{array}{c} i \qquad \tau \qquad j \\ \tau_1 \longrightarrow \bullet \longrightarrow \bullet \longrightarrow \tau_2 \end{array} \\ &= \delta_{i_1,j} \delta_{i_2,i} \int_0^\beta d\tau C_1^{(0)}(i; \tau_1 | \tau) C_1^{(0)}(j; \tau | \tau_2), \end{aligned} \quad (4.104)$$

$$\begin{aligned} a_4^{(0)}(i, \tau_1; i_2, \tau_2 | i_3, \tau_3; i_4, \tau_4) &= \begin{array}{c} \tau_1 \qquad \tau_3 \\ \searrow \qquad \nearrow \\ \bullet \qquad \bullet \\ \nearrow \qquad \searrow \\ \tau_2 \qquad \tau_4 \end{array} \\ &= \delta_{i,i_2} \delta_{i_2,i_3} \delta_{i_3,i_4} C_2^{(0)}(i; \tau_1, \tau_2 | \tau_3, \tau_4), \end{aligned} \quad (4.105)$$

$$a_4^{(1)}(i_1, \tau_1; i_2, \tau_2; i | i_3, \tau_3; i_4, \tau_4; j) = \begin{array}{c} \tau_1 \qquad \tau_3 \\ \searrow \qquad \nearrow \\ \bullet \qquad \bullet \\ \nearrow \qquad \searrow \\ \tau_2 \qquad \tau_4 \end{array} + \begin{array}{c} \tau_1 \qquad \tau_3 \\ \searrow \qquad \nearrow \\ \bullet \qquad \bullet \\ \nearrow \qquad \searrow \\ \tau_2 \qquad \tau_4 \end{array}$$

$$\begin{aligned}
 &= \delta_{i_1, j} \delta_{i_2, i} \delta_{i_3, i_4} \delta_{i_3, i} \int_0^\beta d\tau C_2^{(0)}(i; \tau_2, \tau | \tau_3, \tau_4) C_1^{(0)}(j, \tau_1 | \tau) \\
 &+ \delta_{i_1, i_2} \delta_{i_4, i} \delta_{i_1, i} \delta_{i_3, j} \int_0^\beta d\tau C_2^{(0)}(i; \tau_1, \tau_2 | \tau, \tau_4) C_1^{(0)}(j; \tau | \tau_3) .
 \end{aligned} \tag{4.106}$$

Having found the diagrammatic expressions for the thermal connected Green's functions up to fourth order in the symmetry-breaking currents and first order in the hopping parameter, one can proceed in deriving the diagrammatic expansion of the free energy.

### 4.5.2 Diagram Weights

As stated in Section 4.5.1 the results obtained in the previous subsection are not sufficient to write down the diagrammatic expansion of the grand-canonical free energy. According to rule 7, one needs to know the weights of the emerging diagrams in order to find the correct decomposition. To calculate these weights is the aim of the present subsection.

The weight of a given diagram in the expansion basically consists of two contributions. On the one side each diagram has a symmetry factor associated with it, which accounts for the possible permutations of equal imaginary-time variables. This symmetry can be read of each diagram simply by noticing that its form remains invariant when equal time labels at the external in going and out going lines at hopping elements are interchanged respectively. For example diagram (4.100) is obviously symmetric if one interchanges  $\tau_1 \longleftrightarrow \tau_2$  and  $\tau_3 \longleftrightarrow \tau_4$ . In fact for each  $n$ th order cumulant of 0th order in the hopping parameter there are  $n!$  of such permutations. On the other side, not all of these permutations might contribute to the cumulant decomposition for higher hopping orders. Thus, one introduces another quantity, called the symmetry factor, which counts all possible permutations of equivalent time variables *and* equivalent vertex indices, which do not change the topological structure of the diagram. Taking these observations into consideration and additionally including the factor  $1/n!$  from the Taylor series, one defines the weight of each diagram as follows:

$$\text{weight} = \frac{1}{n!} \frac{n!}{\text{symmetry factor}} . \tag{4.107}$$

Since obviously the number of time variable permutations is cancelled by the Taylor expansion coefficient, all that one needs to determine is the symmetry factor for a given diagram.

## 4.6 Expansion of the Free Energy

Applying the results obtained in the previous paragraphs, I am now able to write down the diagrammatic expansion of the grand-canonical free energy. Up to first order in the hopping parameter and the fourth order in the symmetry-breaking currents this yields

$$\begin{aligned}
 \mathcal{F}[j, j^*] = & \square \longrightarrow \bullet \longrightarrow \square + \square \longrightarrow \bullet \longrightarrow \bullet \longrightarrow \square \\
 & + \frac{1}{4} \left( \begin{array}{c} \square \quad \square \\ \searrow \quad \nearrow \\ \bullet \\ \nearrow \quad \searrow \\ \square \quad \square \end{array} \right) + \frac{1}{2} \left( \begin{array}{c} \square \quad \square \\ \searrow \quad \nearrow \\ \bullet \\ \nearrow \quad \searrow \\ \square \quad \square \end{array} + \begin{array}{c} \square \quad \square \\ \searrow \quad \nearrow \\ \bullet \\ \nearrow \quad \searrow \\ \square \quad \square \end{array} \right). \quad (4.108)
 \end{aligned}$$

Here, I dropped all imaginary-time and vertex indices in order to indicate that, following rule 6 from Section 4.5.1, all space-time variables have been integrated out. The appearing pre-factors correspond to the symmetry factors of the respective diagrams as discussed in the previous subsection. This diagrammatic expression can be translated into the respective cumulants, which subsequently can be calculated according to equation (4.95).

In order to sketch how to derive these expressions explicitly, I will consider the local first order cumulant. Using definition (4.87) together with (4.95) yields

$$C_1^{(0)}(\tau'_1, i'_1 | \tau_1, i_1) = \frac{\delta^2 C_0^{(0)}[j, j^*]}{\delta j_{i'_1}(\tau'_1) \delta j_{i_1}^*(\tau_1)} \Bigg|_{j=j^*=0} \quad (4.109)$$

$$= \frac{\delta}{\delta j_{i'_1}(\tau'_1)} \frac{\langle \hat{T} \hat{a}_i(\tau_1) \exp[-\int_0^\beta d\tau \hat{H}_{\text{ID}}^{\text{SC}}(\tau)] \rangle_0 \delta_{ii_1}}{\langle \hat{T} \exp[-\int_0^\beta d\tau \hat{H}_{\text{ID}}^{\text{SC}}(\tau)] \rangle_0} \Bigg|_{j=j^*=0} \quad (4.110)$$

$$= \left[ -\langle \hat{a}_i^\dagger(\tau'_1) \rangle_0 \langle \hat{a}_i(\tau_1) \rangle_0 + \langle \hat{T} \hat{a}_i(\tau_1) \hat{a}_i^\dagger(\tau'_1) \rangle_0 \right] \delta_{ii'_1} \delta_{ii_1} \quad (4.111)$$

$$= \delta_{ii'_1} \delta_{ii_1} \langle \hat{T} \hat{a}_i(\tau_1) \hat{a}_i^\dagger(\tau'_1) \rangle_0 = \delta_{ii'_1} \delta_{ii_1} C_1^{(0)}(i; \tau'_1 | \tau_1). \quad (4.112)$$

Using the definition of the time-ordering operator, the definition of the thermal average (4.27) and the operator representation in the Dirac picture (4.19) yields

$$\begin{aligned}
 C_1^{(0)}(\tau'_1 | \tau_1) = & \frac{1}{\mathcal{Z}_0} \sum_{n=0}^{\infty} \sum_{\alpha=\pm} \left[ \Theta(\tau_1 - \tau_2) \langle n, \alpha | \hat{a}_i^\dagger e^{\hat{H}_0(\tau_2 - \tau_1)} \hat{a}_i | n, \alpha \rangle e^{-E_{n\alpha}(\tau_2 - \tau_1)} \right. \\
 & \left. + \Theta(\tau_2 - \tau_1) \langle n, \alpha | \hat{a}_i e^{\hat{H}_0(\tau_1 - \tau_2)} \hat{a}_i^\dagger | n, \alpha \rangle e^{E_{n\alpha}(\tau_2 - \tau_1)} \right] e^{-\beta E_{n\alpha}}. \quad (4.113)
 \end{aligned}$$

The further calculation of the above expression can be performed analogues to Section 4.2 by using the polariton mapping (2.153). However, one can further simplify these derivations by going into frequency space. Therefore, I use a Matsubara transformation, which is defined as follows

$$g(\omega_m) = \frac{1}{\sqrt{\beta}} \int_0^\beta d\tau g(\tau) e^{i\omega_m \tau}, \quad (4.114)$$

$$g(\tau) = \frac{1}{\sqrt{\beta}} \sum_{m=-\infty}^{\infty} g(\omega_m) e^{-i\omega_m \tau}, \quad (4.115)$$

with Matsubara frequencies

$$\omega_m = \frac{2\pi m}{\beta}, \quad m \in \mathbb{Z}. \quad (4.116)$$

Performing this transformation for the photonic annihilation and creation operators yields

$$\hat{a}_i(\omega_m) = \frac{1}{\sqrt{\beta}} \int_0^\beta d\tau \hat{a}_i(\tau) e^{i\omega_m\tau}, \quad (4.117a)$$

$$\hat{a}_i^\dagger(\omega_m) = \frac{1}{\sqrt{\beta}} \int_0^\beta d\tau \hat{a}_i^\dagger(\tau) e^{-i\omega_m\tau}. \quad (4.117b)$$

One can use these expressions in the further considerations to calculate all cumulants in the free energy expansion (4.108) in Matsubara space. The resulting expansion coefficients are explicitly derived within the following two subsections.

### 4.6.1 Second Order in the Currents

In the present subsection I derive the exact expression in frequency space for the second-order contribution in the currents of equation (4.108). Therefore, I consider the grand-canonical free energy in the form

$$\begin{aligned} \mathcal{F}[j, j^*] = & \mathcal{F}_0 - \frac{1}{\beta} \sum_{i_1, i_2} \int_0^\beta d\tau_1 d\tau_2 \left\{ A_2(\tau_1|\tau_2) j_{i_1}(\tau_1) j_{i_2}^*(\tau_2) \right. \\ & \left. + \frac{1}{4} \sum_{i_3, i_4} \int_0^\beta d\tau_3 d\tau_4 A_4(\tau_1, \tau_3|\tau_2, \tau_4) j_{i_1}(\tau_1) j_{i_2}^*(\tau_2) j_{i_3}(\tau_3) j_{i_4}^*(\tau_4) \right\}, \end{aligned} \quad (4.118)$$

where I introduced the abbreviations

$$A_2(i_1, \tau_1|i_2, \tau_2) = a_2^{(0)}(i_1, \tau_1|i_2, \tau_2) + \sum_{i, j} \kappa_{ij} a_2^{(1)}(i_1, \tau_1; i|i_2, \tau_2; j), \quad (4.119)$$

$$\begin{aligned} A_4(i_1, \tau_1; i_2, \tau_2|i_3, \tau_3; i_4, \tau_4) = & a_4^{(0)}(i_1, \tau_1; i_2, \tau_2|i_3, \tau_3; i_4, \tau_4) \\ & + \sum_{i, j} \kappa_{ij} a_4^{(1)}(i_1, \tau_1; i_2, \tau_2; i|i_3, \tau_3; i_4, \tau_4; j). \end{aligned} \quad (4.120)$$

First, I start by calculating the coefficient  $a_2^{(0)}(i_1, \omega_{m1}|i_2, \omega_{m2})$  in Matsubara space. Due to frequency conservation and the locality of the cumulants the following relation has to hold

$$a_2^{(0)}(i_1, \omega_{m1}|i_2, \omega_{m2}) = a_2^{(0)}(i_1, \omega_{m1}) \delta_{i_1, i_2} \delta_{\omega_{m1}, \omega_{m2}}. \quad (4.121)$$

This cumulant can be derived from the expression (4.103) with the help of relations (4.112) and (4.9), by performing the Matsubara transformation according to equations (4.117). This

approach yields the following relation:

$$\begin{aligned}
 a_2^{(0)}(i, \omega_m) &= \frac{1}{\beta} \int_0^\beta d\tau_1 \int_0^\beta d\tau_2 a_2^{(0)}(i, \tau_1 | i, \tau_2) e^{-i\omega_m(\tau_1 - \tau_2)} \\
 &= \frac{1}{\beta} \int_0^\beta d\tau_1 \int_0^\beta d\tau_2 \left\langle \hat{T} \left[ \hat{a}_i^\dagger(\tau_1) \hat{a}_i(\tau_2) \right] \right\rangle_0 e^{-i\omega_m(\tau_1 - \tau_2)} \\
 &= \frac{1}{\beta} \int_0^\beta d\tau_1 \int_0^\beta d\tau_2 \left[ \Theta(\tau_1 - \tau_2) \left\langle \hat{a}_i^\dagger(\tau_1) \hat{a}_i(\tau_2) \right\rangle_0 \right. \\
 &\quad \left. + \Theta(\tau_2 - \tau_1) \left\langle \hat{a}_i(\tau_2) \hat{a}_i^\dagger(\tau_1) \right\rangle_0 \right] e^{-i\omega_m(\tau_1 - \tau_2)}. \tag{4.122}
 \end{aligned}$$

The respective thermal averages occurring in the above equation have been already calculated in Section 4.2. Using the results (4.46) and (4.47) and dropping the site index again, the second-order expansion coefficient  $a_2^{(0)}(i, \omega_m)$  from (4.122) reduces to

$$\begin{aligned}
 a_2^{(0)}(i, \omega_m) &= \frac{1}{\beta \mathcal{Z}_0} \int_0^\beta d\tau_1 \left[ \int_0^{\tau_1} d\tau_2 \sum_{n=1}^{\infty} \sum_{\alpha, \alpha' = \pm} e^{-\beta E_{n\alpha}} e^{(E_{n\alpha} - E_{(n-1)\alpha'} - i\omega_m)(\tau_1 - \tau_2)} (t_{n\alpha\alpha'})^2 \right. \\
 &\quad \left. + \int_{\tau_1}^\beta d\tau_2 \sum_{n=0}^{\infty} \sum_{\alpha, \alpha' = \pm} e^{-\beta E_{n\alpha}} e^{(E_{n\alpha} - E_{(n+1)\alpha'} + i\omega_m)(\tau_2 - \tau_1)} (t_{(n+1)\alpha'\alpha})^2 \right]. \tag{4.123}
 \end{aligned}$$

Additionally, making use of the fact that the imaginary-time integrals have the general solution

$$\int_0^\beta d\tau_1 \int_{\tau_1}^\beta d\tau_2 e^{(\omega_{nm\alpha\alpha'} \pm i\omega_p)(\tau_2 - \tau_1)} = \frac{e^{\beta(\omega_{nm\alpha\alpha'} \pm i\omega_p)} - 1}{(\omega_{nm\alpha\alpha'} \pm i\omega_p)^2} - \frac{\beta}{\omega_{nm\alpha\alpha'} \pm i\omega_p}, \tag{4.124}$$

with the abbreviation

$$\omega_{nm\alpha\alpha'} = E_{n\alpha} - E_{m\alpha'}, \tag{4.125}$$

leads to the following expression

$$\begin{aligned}
 a_2^{(0)}(i, \omega_p) &= \frac{1}{\beta \mathcal{Z}_0} \sum_{\alpha, \alpha' = \pm} \left\{ \sum_{n=0}^{\infty} e^{-\beta E_{n\alpha}} \left[ \frac{e^{\beta(\omega_{n(n+1)\alpha\alpha'} + i\omega_p)} - 1}{(\omega_{n(n+1)\alpha\alpha'} + i\omega_p)^2} - \frac{\beta}{\omega_{n(n+1)\alpha\alpha'} + i\omega_p} \right] \right. \\
 &\quad \left. \times (t_{(n+1)\alpha'\alpha})^2 + \sum_{m=1}^{\infty} e^{-\beta E_{m\alpha}} \left[ \frac{e^{\beta(\omega_{m(m-1)\alpha\alpha'} - i\omega_p)} - 1}{(\omega_{m(m-1)\alpha\alpha'} - i\omega_p)^2} - \frac{\beta}{\omega_{m(m-1)\alpha\alpha'} - i\omega_p} \right] (t_{m\alpha\alpha'})^2 \right\} \\
 &= \frac{1}{\beta \mathcal{Z}_0} \sum_{\alpha, \alpha' = \pm} \left\{ \sum_{n=0}^{\infty} \left[ \frac{e^{-\beta(E_{(n+1)\alpha'} - i\omega_p)} - e^{-\beta E_{n\alpha}}}{(\omega_{n(n+1)\alpha\alpha'} + i\omega_p)^2} + \frac{e^{-\beta(E_{n\alpha} + i\omega_p)} - e^{-\beta E_{(n+1)\alpha'}}}{(\omega_{(n+1)n\alpha'\alpha} - i\omega_p)^2} \right] (t_{(n+1)\alpha'\alpha})^2 \right. \\
 &\quad \left. - \left[ \sum_{n=0}^{\infty} \frac{\beta e^{-\beta E_{n\alpha}}}{\omega_{n(n+1)\alpha\alpha'} + i\omega_p} (t_{(n+1)\alpha'\alpha})^2 + \sum_{m=1}^{\infty} \frac{\beta e^{-\beta E_{m\alpha}}}{(\omega_{m(m-1)\alpha\alpha'} - i\omega_p)} (t_{m\alpha\alpha'})^2 \right] \right\}. \tag{4.126}
 \end{aligned}$$

Noticing that  $\omega_{n(n+1)\alpha\alpha'} = -\omega_{(n+1)n\alpha'\alpha}$  and  $e^{\pm i\beta\omega_p} = e^{\pm i\beta\frac{2\pi p}{\beta}} = e^{\pm i2\pi p} = 1$ , due to the definition of the Matsubara frequencies (4.116), the above expression can be simplified to

$$\begin{aligned} a_2^{(0)}(i, \omega_p) &= -\frac{1}{\beta \mathcal{Z}_0} \sum_{\alpha, \alpha'=\pm} \left[ \sum_{n=0}^{\infty} \frac{\beta e^{-\beta E_{n\alpha}} (t_{(n+1)\alpha'\alpha})^2}{\omega_{n(n+1)\alpha\alpha'} + i\omega_p} + \sum_{m=1}^{\infty} \frac{\beta e^{-\beta E_{m\alpha}} (t_{m\alpha\alpha'})^2}{\omega_{m(m-1)\alpha\alpha'} - i\omega_p} \right] \\ &= \frac{1}{\mathcal{Z}_0} \sum_{\alpha, \alpha'=\pm} \left\{ \frac{(t_{1\alpha'})^2}{E_{1\alpha'} - i\omega_m} - \sum_{n=1}^{\infty} \left[ \frac{e^{-\beta E_{n\alpha}} (t_{(n+1)\alpha'\alpha})^2}{E_{n\alpha} - E_{(n+1)\alpha'} + i\omega_m} - \frac{e^{-\beta E_{n\alpha}} (t_{n\alpha\alpha'})^2}{E_{(n-1)\alpha'} - E_{n\alpha} + i\omega_m} \right] \right\}. \end{aligned} \quad (4.127)$$

Going ahead, one can calculate the first-order hopping correction for this expression

$$a_2^{(1)}(i_1, \tau_1; j|i_2, \tau_2; i) = \delta_{i,i_1} \delta_{i_2,j} \int_0^\beta d\tau_3 C_1^{(0)}(i; \tau_1|\tau_3) C_1^{(0)}(j; \tau_3|\tau_2), \quad (4.128)$$

by using frequency conservation again and make use of the cumulant multiplicity properties in frequency space, which leads to the restriction

$$a_2^{(1)}(i_1, \omega_{m1}; j|i_2, \omega_{m2}, i) = a_2^{(0)}(i, \omega_{m1}) a_2^{(0)}(j, \omega_{m2}) \delta_{i,i_1} \delta_{i_2,j} \delta_{\omega_{m1}, \omega_{m2}}. \quad (4.129)$$

Thus, one finds that the expansion coefficient correction under consideration takes on the form

$$\begin{aligned} a_2^{(1)}(i_1, \omega_{m1}; j|i_2, \omega_{m2}, i) &= \frac{1}{\mathcal{Z}_0^2} \sum_{\alpha, \alpha'=\pm} \left\{ \frac{(t_{1\alpha'})^2}{E_{1\alpha'} - i\omega_{m1}} - \sum_{n=1}^{\infty} e^{-\beta E_{n\alpha}} \left[ \frac{(t_{(n+1)\alpha'\alpha})^2}{E_{n\alpha} - E_{(n+1)\alpha'} + i\omega_{m1}} \right. \right. \\ &\quad \left. \left. + \frac{(t_{n\alpha\alpha'})^2}{E_{n\alpha} - E_{(n-1)\alpha'} - i\omega_{m1}} \right] \right\}_i \times \sum_{\gamma, \gamma'=\pm} \left\{ \frac{(t_{1\gamma'\gamma})^2}{E_{1\gamma'} - i\omega_{m2}} - \sum_{n=1}^{\infty} e^{-\beta E_{n\gamma}} \right. \\ &\quad \left. \times \left[ \frac{(t_{(n+1)\gamma'\gamma})^2}{E_{n\gamma} - E_{(n+1)\gamma'} + i\omega_{m2}} + \frac{(t_{n\gamma\gamma'})^2}{E_{n\gamma} - E_{(n-1)\gamma'} - i\omega_{m2}} \right] \right\}_j \delta_{i,i_1} \delta_{i_2,j} \delta_{\omega_{m1}, \omega_{m2}}. \end{aligned} \quad (4.130)$$

Hence, I derived the complete expression for the coefficient (4.119) in Matsubara space, which now takes on the form

$$A_2(i_1, \omega_{m1}|i_2, \omega_{m2}) = \left[ a_2^{(0)}(i_1, \omega_{m1}) \delta_{i_1, i_2} + \sum_{i,j} \kappa_{ij} a_2^{(0)}(i, \omega_{m1}) a_2^{(0)}(j, \omega_{m2}) \delta_{i,i_1} \delta_{i_2,j} \right] \delta_{\omega_{m1}, \omega_{m2}}. \quad (4.131)$$

Therefore, the second order in the symmetry-breaking currents is solely dependent on suitable combinations of expression (4.127). In the next subsection, I derive the analogue expression for  $A_4(i_1, \tau_1; i_3, \tau_3|i_2, \tau_2; i_4, \tau_4)$  in frequency space.

## 4.6.2 Fourth Order in the Currents

To derive the contribution up to fourth order in the currents I will proceed analogously to the previous subsection. First, I consider the zeroth order hopping term. Going into frequency

space again yields

$$a_4^{(0)}(i_1, \omega_{m1}; i_3, \omega_{m3} | i_2, \omega_{m2}; i_4, \omega_{m4}) = \frac{1}{\beta^2} \delta_{i_1, i_3} \delta_{i_2, i_4} \delta_{i_1, i_2} \int_0^\beta d\tau_1 \dots d\tau_4 C_2^{(0)}(i_1; \tau_1, \tau_3 | \tau_2, \tau_4) \times e^{i(-\omega_{m1}\tau_1 + \omega_{m2}\tau_2 - \omega_{m3}\tau_3 + \omega_{m4}\tau_4)}. \quad (4.132)$$

The combination of relation (4.132) it with the equation (4.98) leads to

$$a_4^{(0)}(i_1, \omega_{m1}; i_3, \omega_{m3} | i_2, \omega_{m2}; i_4, \omega_{m4}) = \frac{1}{\beta^2} \int_0^\beta d\tau_1 \dots d\tau_4 \left\{ \left\langle \hat{T} \left[ \hat{a}_{i_1}^\dagger(\tau_1) \hat{a}_{i_3}^\dagger(\tau_3) \hat{a}_{i_2}(\tau_2) \hat{a}_{i_4}(\tau_4) \right] \right\rangle_0 - \delta_{i_1, i_2} \delta_{i_3, i_4} C_1^{(0)}(i_1; \tau_1 | \tau_2) C_1^{(0)}(i_3; \tau_3 | \tau_4) - \delta_{i_1, i_4} \delta_{i_3, i_2} C_1^{(0)}(i_1; \tau_1 | \tau_4) C_1^{(0)}(i_3; \tau_3 | \tau_2) \right\} \times e^{i(-\omega_{m1}\tau_1 + \omega_{m2}\tau_2 - \omega_{m3}\tau_3 + \omega_{m4}\tau_4)}. \quad (4.133)$$

As seen in the previous paragraph the respective Matsubara frequencies are restricted by frequency conservation. Therefore, the following relation has to be satisfied:

$$\omega_{m1} + \omega_{m3} = \omega_{m2} + \omega_{m4} \quad (4.134)$$

Using the frequency conservation and the results from the previous subsection, leads to the expression

$$a_4^{(0)}(i_1, \omega_{m1}; i_3, \omega_{m3} | i_2, \omega_{m2}; i_4, \omega_{m4}) = \frac{1}{\beta^2} \delta_{\omega_{m1} + \omega_{m3}, \omega_{m2} + \omega_{m4}} \left\{ -a_2^{(0)}(i_1, \omega_{m1}) \times a_2^{(0)}(i_3, \omega_{m3}) [\delta_{i_1, i_2} \delta_{i_3, i_4} \delta_{\omega_1, \omega_2} \delta_{\omega_3, \omega_4} + \delta_{i_1, i_4} \delta_{i_3, i_2} \delta_{\omega_1, \omega_4} \delta_{\omega_3, \omega_2}] + \int_0^\beta d\tau_1 \dots d\tau_4 \left\langle \hat{T} \left[ \hat{a}_{i_1}^\dagger(\tau_1) \hat{a}_{i_3}^\dagger(\tau_3) \hat{a}_{i_2}(\tau_2) \hat{a}_{i_4}(\tau_4) \right] \right\rangle_0 e^{i(-\omega_{m1}\tau_1 + \omega_{m2}\tau_2 - \omega_{m3}\tau_3 + \omega_{m4}\tau_4)} \right\}. \quad (4.135)$$

Since, the expressions in the first two terms have already been calculated, all one needs to derive is the integral over the time-ordered thermal average. First I notice that, for the time-ordered product of the annihilation and creation operators, there are 6 distinct permutations leading to different expectation values. Each of these orderings itself has 4 time variable permutations corresponding to  $\tau_1 \leftrightarrow \tau_2$  and  $\tau_3 \leftrightarrow \tau_4$ . Thus, overall one finds 24 terms for the above expectation value. Luckily, the integrals over different time-variable permutations yield the same result, and thus, they just lead to a fixed pre-factor 4. For this reason, one just needs to determine the 6 different thermal averages for one specific time-ordering. Furthermore, due to the orthogonality relation (3.53), these expectation values are local quantities and, therefore, I drop the site indices in the following calculations. Thus, one has to solve the following expressions:

$$\left\langle \hat{a}^\dagger(\tau_1) \hat{a}^\dagger(\tau_3) \hat{a}(\tau_2) \hat{a}(\tau_4) \right\rangle_0, \quad \left\langle \hat{a}^\dagger(\tau_1) \hat{a}(\tau_2) \hat{a}^\dagger(\tau_3) \hat{a}(\tau_4) \right\rangle_0, \quad (4.136)$$

$$\left\langle \hat{a}(\tau_4) \hat{a}^\dagger(\tau_1) \hat{a}^\dagger(\tau_3) \hat{a}(\tau_2) \right\rangle_0, \quad \left\langle \hat{a}(\tau_4) \hat{a}(\tau_2) \hat{a}^\dagger(\tau_1) \hat{a}^\dagger(\tau_3) \right\rangle_0, \quad (4.137)$$

$$\left\langle \hat{a}(\tau_4) \hat{a}^\dagger(\tau_1) \hat{a}(\tau_2) \hat{a}^\dagger(\tau_3) \right\rangle_0, \quad \left\langle \hat{a}^\dagger(\tau_1) \hat{a}(\tau_4) \hat{a}(\tau_2) \hat{a}^\dagger(\tau_3) \right\rangle_0, \quad (4.138)$$

where I dropped here and in the following calculations the site indices of the photonic creation and annihilation operators, because these expectation values are all local quantities due to the orthogonality of the dressed state basis (2.137). With the help of the polariton mapping from Section 2.6, one can calculate these averages which yields:

$$\begin{aligned}
 \langle \hat{a}^\dagger(\tau_1) \hat{a}(\tau_2) \hat{a}^\dagger(\tau_3) \hat{a}(\tau_4) \rangle_0 &= \frac{1}{\mathcal{Z}_0} \sum_{n=1}^{\infty} \sum_{\alpha} \langle n, \alpha | \hat{a}^\dagger(\tau_1) \hat{a}(\tau_2) \hat{a}^\dagger(\tau_3) \hat{a}(\tau_4) e^{-\beta \hat{H}_0} | n, \alpha \rangle \\
 &= \frac{1}{\mathcal{Z}_0} \sum_{n=1}^{\infty} \sum_{\alpha} e^{-\beta E_{n\alpha}} \langle n, \alpha | e^{\tau_1 \hat{H}_0} \hat{a}^\dagger e^{(\tau_2 - \tau_1) \hat{H}_0} \hat{a} e^{(\tau_3 - \tau_2) \hat{H}_0} \hat{a}^\dagger e^{(\tau_4 - \tau_3) \hat{H}_0} \hat{a} e^{-\tau_4 \hat{H}_0} | n, \alpha \rangle \\
 &= \frac{1}{\mathcal{Z}_0} \sum_{n,m=1}^{\infty} \sum_{\alpha\gamma\gamma'} e^{-\beta E_{n\alpha}} e^{(\tau_1 - \tau_4) E_{n\alpha}} \langle n, \alpha | \hat{a}^\dagger e^{(\tau_2 - \tau_1) \hat{H}_0} \hat{a} e^{(\tau_3 - \tau_2) \hat{H}_0} \hat{a}^\dagger | m - 1, \gamma' \rangle \\
 &\quad \times e^{(\tau_4 - \tau_3) E_{m-1\gamma'}} t_{m\gamma\gamma'} \delta_{mn} \delta_{\alpha\gamma} \\
 &= \frac{1}{\mathcal{Z}_0} \sum_{n,m=1}^{\infty} \sum_{p=0}^{\infty} \sum_{\alpha\gamma\gamma'\nu\nu'} e^{-\beta E_{n\alpha}} e^{(\tau_1 - \tau_4) E_{n\alpha}} \langle n, \alpha | \hat{a}^\dagger e^{(\tau_2 - \tau_1) \hat{H}_0} \hat{a} | p + 1, \nu' \rangle e^{(\tau_3 - \tau_2) E_{(p+1)\nu'}} \\
 &\quad \times e^{(\tau_4 - \tau_3) E_{m-1\gamma'}} t_{(p+1)\nu'\nu} t_{m\gamma\gamma'} \delta_{mn} \delta_{\alpha\gamma} \delta_{p(m-1)} \delta_{\gamma'\nu} \\
 &= \frac{1}{\mathcal{Z}_0} \sum_{n,m,r=1}^{\infty} \sum_{p=0}^{\infty} \sum_{\alpha\gamma\gamma'\nu\nu'\rho\rho'} e^{-\beta E_{n\alpha}} e^{(\tau_1 - \tau_4) E_{n\alpha}} \langle n, \alpha | \hat{a}^\dagger | r - 1, \rho' \rangle e^{(\tau_2 - \tau_1) E_{(r-1)\rho'}} e^{(\tau_3 - \tau_2) E_{(p+1)\nu'}} \\
 &\quad \times e^{(\tau_4 - \tau_3) E_{m-1\gamma'}} t_{r\rho\rho'} t_{(p+1)\nu'\nu} t_{m\gamma\gamma'} \delta_{mn} \delta_{\alpha\gamma} \delta_{p(m-1)} \delta_{\gamma'\nu} \delta_{(p+1)r} \delta_{\rho\nu'} \\
 &= \frac{1}{\mathcal{Z}_0} \sum_{n,m,r=1}^{\infty} \sum_{p,q=0}^{\infty} \sum_{\alpha\gamma\gamma'\nu\nu'\rho\rho'\pi\pi'} e^{-\beta E_{n\alpha}} \left[ e^{(\tau_1 - \tau_4) E_{n\alpha}} e^{(\tau_2 - \tau_1) E_{(r-1)\rho'}} e^{(\tau_3 - \tau_2) E_{(p+1)\nu'}} e^{(\tau_4 - \tau_3) E_{m-1\gamma'}} \right] \\
 &\quad \times [t_{(q+1)\pi'\pi} t_{r\rho\rho'} t_{(p+1)\nu'\nu} t_{m\gamma\gamma'}] \times [\delta_{n(q+1)} \delta_{q(r-1)} \delta_{r(p+1)} \delta_{p(m-1)} \delta_{mn}] \times [\delta_{\alpha\pi'} \delta_{\rho'\pi} \delta_{\rho\nu'} \delta_{\nu\gamma'} \delta_{\gamma\alpha}]. \tag{4.139}
 \end{aligned}$$

Hence, I find the following expectation value

$$\begin{aligned}
 \langle \hat{a}^\dagger(\tau_1) \hat{a}(\tau_2) \hat{a}^\dagger(\tau_3) \hat{a}(\tau_4) \rangle_0 &= \frac{1}{\mathcal{Z}_0} \sum_{n=1}^{\infty} \sum_{\alpha,\nu,\rho,\pi=\pm} e^{-\beta E_{n\alpha}} e^{(E_{n\alpha} - E_{(n-1)\pi})\tau_1} e^{(E_{(n-1)\pi} - E_{n\rho})\tau_2} \\
 &\quad \times e^{(E_{n\rho} - E_{(n-1)\nu})\tau_3} e^{(E_{(n-1)\nu} - E_{n\alpha})\tau_4} (t_{n\alpha\pi} \times t_{n\rho\pi} \times t_{n\rho\nu} \times t_{n\alpha\nu}). \tag{4.140}
 \end{aligned}$$

Subsequently performing the same procedure for the remaining expectation values, leads to the following expressions:

$$\begin{aligned}
 \langle \hat{a}(\tau_4) \hat{a}^\dagger(\tau_1) \hat{a}^\dagger(\tau_3) \hat{a}(\tau_2) \rangle_0 &= \frac{1}{\mathcal{Z}_0} \sum_{n=1}^{\infty} \sum_{\alpha,\nu,\rho,\pi=\pm} e^{-\beta E_{n\alpha}} e^{(E_{(n+1)\pi} - E_{n\rho})\tau_1} e^{(E_{(n-1)\nu} - E_{n\alpha})\tau_2} \\
 &\quad \times e^{(E_{n\rho} - E_{(n-1)\nu})\tau_3} e^{(E_{n\alpha} - E_{(n+1)\pi})\tau_4} (t_{(n+1)\alpha\pi} \times t_{(n+1)\rho\pi} \times t_{n\rho\nu} \times t_{n\alpha\nu}), \tag{4.141}
 \end{aligned}$$

$$\langle \hat{a}^\dagger(\tau_1) \hat{a}(\tau_4) \hat{a}(\tau_2) \hat{a}^\dagger(\tau_3) \rangle_0 = \frac{1}{\mathcal{Z}_0} \sum_{n=1}^{\infty} \sum_{\alpha,\nu,\rho,\pi=\pm} e^{-\beta E_{n\alpha}} e^{(E_{n\alpha} - E_{(n-1)\pi})\tau_1} e^{(E_{n\rho} - E_{(n+1)\nu})\tau_2}$$

$$\times e^{(E_{(n+1)\nu}-E_{n\alpha})\tau_3} e^{(E_{(n-1)\pi}-E_{n\rho})\tau_4} (t_{n\alpha\pi} \times t_{n\rho\pi} \times t_{(n+1)\nu\rho} \times t_{(n+1)\nu\alpha}), \quad (4.142)$$

$$\begin{aligned} \langle \hat{a}(\tau_4) \hat{a}(\tau_2) \hat{a}^\dagger(\tau_1) \hat{a}^\dagger(\tau_3) \rangle_0 &= \frac{1}{\mathcal{Z}_0} \left[ \sum_{\nu,\rho,\pi=\pm} e^{(E_{2\rho}-E_{1\nu})\tau_1} e^{(E_{1\pi}-E_{2\rho})\tau_2} e^{E_{1\nu}\tau_3} e^{-E_{1\pi}\tau_4} \right. \\ &\times (t_{1\pi-} \times t_{2\rho\pi} \times t_{2\rho\nu} \times t_{1\nu-}) + \sum_{n=1}^{\infty} \sum_{\alpha,\nu,\rho,\pi=\pm} e^{-\beta E_{n\alpha}} e^{(E_{(n+2)\rho}-E_{(n+1)\nu})\tau_1} e^{(E_{(n+1)\pi}-E_{(n+2)\rho})\tau_2} \\ &\times e^{(E_{(n+1)\nu}-E_{n\alpha})\tau_3} e^{(E_{n\alpha}-E_{(n+1)\pi})\tau_4} (t_{(n+1)\pi\alpha} \times t_{(n+2)\rho\pi} \times t_{(n+2)\rho\nu} \times t_{(n+1)\nu\alpha}) \left. \right], \quad (4.143) \end{aligned}$$

$$\begin{aligned} \langle \hat{a}(\tau_4) \hat{a}^\dagger(\tau_1) \hat{a}(\tau_2) \hat{a}^\dagger(\tau_3) \rangle_0 &= \frac{1}{\mathcal{Z}_0} \left[ \sum_{\nu,\pi=\pm} e^{E_{1\pi}\tau_1} e^{-E_{1\nu}\tau_2} e^{E_{1\nu}\tau_3} e^{-E_{1\pi}\tau_4} (t_{1\pi-}^2 \times t_{1\nu-}^2) \right. \\ &+ \sum_{n=1}^{\infty} \sum_{\alpha,\nu,\rho,\pi=\pm} e^{-\beta E_{n\alpha}} e^{(E_{(n+1)\pi}-E_{n\rho})\tau_1} e^{(E_{n\rho}-E_{(n+1)\nu})\tau_2} e^{(E_{(n+1)\nu}-E_{n\alpha})\tau_3} \\ &\times e^{(E_{n\alpha}-E_{(n+1)\pi})\tau_4} (t_{(n+1)\pi\alpha} \times t_{(n+1)\pi\rho} \times t_{(n+1)\nu\rho} \times t_{(n+1)\nu\alpha}) \left. \right], \quad (4.144) \end{aligned}$$

$$\begin{aligned} \langle \hat{a}^\dagger(\tau_1) \hat{a}^\dagger(\tau_3) \hat{a}(\tau_2) \hat{a}(\tau_4) \rangle_0 &= \frac{1}{\mathcal{Z}_0} \sum_{n=2}^{\infty} \sum_{\alpha,\nu,\rho,\pi=\pm} e^{-\beta E_{n\alpha}} e^{(E_{n\alpha}-E_{(n-1)\pi})\tau_1} e^{(E_{(n-2)\rho}-E_{(n-1)\nu})\tau_2} \\ &\times e^{(E_{(n-1)\pi}-E_{(n-2)\rho})\tau_3} e^{(E_{(n-1)\nu}-E_{n\alpha})\tau_4} (t_{n\alpha\pi} \times t_{(n-1)\pi\rho} \times t_{(n-1)\nu\rho} \times t_{n\alpha\nu}). \quad (4.145) \end{aligned}$$

Note, that due to the order in which the annihilation and creation operators act on the polariton states, the polariton number has a minimum threshold for each average. Thus, expression (4.145) just contributes if  $n > 1$ , expressions (4.140) to (4.142) just contribute if  $n > 0$  and only the last two expressions (4.143) and (4.144) contribute for every polariton number.

Following the same procedure as for the second-order expansion coefficient, I now perform a Matsubara transformation according to equations (4.117). For this purpose, I make use of the fact that the elementary integral

$$I = \gamma \int_0^\beta dt e^{at} \int_0^t dt_1 e^{bt_1} \int_0^{t_1} dt_2 e^{ct_2} \int_0^{t_2} dt_3 e^{dt_3}, \quad (4.146)$$

has the general solution

$$\begin{aligned} I = \gamma \left( \frac{e^{(a+b+c+d)\beta} - 1}{(a+b+c+d)(b+c+d)(c+d)d} - \frac{e^{(a+b+c)\beta} - 1}{(a+b+c)(b+c)cd} \right. \\ \left. + \frac{-1 + e^{(a+b)\beta}}{b(a+b)c(c+d)} - \frac{-1 + e^{a\beta}}{ab(b+c)(b+c+d)} \right). \quad (4.147) \end{aligned}$$

Applying this result to the expressions (4.145) – (4.144), one finds that the variable combination corresponding to  $a + b + c + d$  in (4.147) always vanishes. Therefore, one additionally

needs the limit:

$$\lim_{a+b+c+d \rightarrow 0} \frac{e^{(a+b+c+d)\beta} - 1}{(a+b+c+d)(b+c+d)(c+d)d} = \frac{\beta}{(b+c+d)(c+d)d}, \quad (4.148)$$

leading to the adapted solution of (4.147), which reads

$$I = \gamma \left( \frac{\beta}{(b+c+d)(c+d)d} - \frac{e^{(a+b+c)\beta} - 1}{(a+b+c)(b+c)d} + \frac{-1 + e^{(a+b)\beta}}{b(a+b)c(c+d)} - \frac{-1 + e^{a\beta}}{ab(b+c)(b+c+d)} \right). \quad (4.149)$$

Now, one can use this result to perform the Matsubara transformation leading to the following expressions:

$$\begin{aligned} \langle \hat{a}^\dagger(\omega_{m1}) \hat{a}^\dagger(\omega_{m3}) \hat{a}(\omega_{m2}) \hat{a}(\omega_{m4}) \rangle_0 &= \frac{1}{\mathcal{Z}_0 \beta^2} \sum_{n=2}^{\infty} \sum_{\alpha, \nu, \rho, \lambda = \pm} (t_{n\alpha\lambda} t_{(n-1)\lambda\rho} t_{(n-1)\nu\rho} t_{n\alpha\nu}) \\ &\times \left\{ \frac{1}{(i(\omega_{m1} + \omega_{m3}) + E_{(n-2)\rho} - E_{n\alpha})} \left[ \frac{\beta}{(i(\omega_{m1} + E_{(n-1)\lambda} - E_{n\alpha}) (i\omega_{m4} + E_{(n-1)\nu} - E_{n\alpha})} \right. \right. \\ &\quad \left. \left. - \frac{-1 + e^{\beta(-i(\omega_{m1} + \omega_{m3}) - E_{(n-2)\rho} + E_{n\alpha})}}{(-i\omega_{m3} - E_{(n-2)\rho} + E_{(n-1)\lambda}) (i(\omega_{m1} + \omega_{m3} - \omega_{m4}) + E_{(n-2)\rho} - E_{(n-1)\nu})} \right] \right. \\ &\times \frac{1}{(i(\omega_{m1} + \omega_{m3}) + E_{(n-2)\rho} - E_{n\alpha})} \left. \right] + \frac{1}{(i(\omega_{m1} - \omega_{m4}) + E_{(n-1)\lambda} - E_{(n-1)\nu})} \\ &\times \left[ \frac{-1 + e^{\beta(-i\omega_{m1} - E_{(n-1)\lambda} + E_{n\alpha})}}{(-i\omega_{m3} - E_{(n-2)\rho} + E_{(n-1)\lambda}) (i\omega_{m1} + E_{(n-1)\lambda} - E_{n\alpha})^2} + \right. \\ &\quad \left. + \frac{-1 + e^{\beta(-i\omega_{m4} - E_{(n-1)\nu} + E_{n\alpha})}}{(i(\omega_{m1} + \omega_{m3} - \omega_{m4}) + E_{(n-2)\rho} - E_{(n-1)\nu}) (i\omega_{m4} + E_{(n-1)\nu} - E_{n\alpha})^2} \right] \left. \right\} e^{-\beta E_{n\alpha}}, \quad (4.150) \end{aligned}$$

$$\begin{aligned} \langle \hat{a}^\dagger(\omega_{m1}) \hat{a}(\omega_{m2}) \hat{a}^\dagger(\omega_{m3}) \hat{a}(\omega_{m4}) \rangle_0 &= \frac{1}{\mathcal{Z}_0 \beta^2} \sum_{n=1}^{\infty} \sum_{\alpha, \nu, \rho, \lambda = \pm} e^{-\beta E_{n\alpha}} (t_{n\alpha\lambda} t_{n\rho\lambda} t_{n\rho\nu} t_{n\alpha\nu}) \\ &\times \left\{ \frac{1}{(i(\omega_{m1} - \omega_{m4}) + E_{(n-1)\lambda} - E_{(n-1)\nu})} \left[ \frac{-1 + e^{\beta(-i\omega_{m1} - E_{(n-1)\lambda} + E_{n\alpha})}}{(i(\omega_{m1} + \omega_{m3} - \omega_{m4}) + E_{(n-1)\lambda} - E_{n\rho})} \right. \right. \\ &\quad \left. \left. + \frac{-1 + e^{\beta(-i\omega_{m4} - E_{(n-1)\nu} + E_{n\alpha})}}{(i\omega_{m4} + E_{(n-1)\nu} - E_{n\alpha})^2 (-i\omega_{m3} - E_{(n-1)\nu} + E_{n\rho})} \right] \right. \\ &\quad \left. - \frac{1}{(i(\omega_{m3} - \omega_{m4}) + E_{n\alpha} - E_{n\rho})} \left[ \frac{-1 + e^{\beta(i(\omega_{m3} - \omega_{m4}) + E_{n\alpha} - E_{n\rho})}}{(i(\omega_{m3} - \omega_{m4}) + E_{n\alpha} - E_{n\rho})} \right] \right. \\ &\quad \left. \times \frac{1}{(-i\omega_{m3} - E_{(n-1)\nu} + E_{n\rho}) (i(\omega_{m1} + \omega_{m3} - \omega_{m4}) + E_{(n-1)\lambda} - E_{n\rho})} \right\} \end{aligned}$$

$$+ \left. \frac{\beta}{(i\omega_{m1} + E_{(n-1)\lambda} - E_{n\alpha})(i\omega_{m4} + E_{(n-1)\nu} - E_{n\alpha})} \right\}, \quad (4.151)$$

$$\begin{aligned} \langle \hat{a}(\omega_{m4}) \hat{a}^\dagger(\omega_{m1}) \hat{a}^\dagger(\omega_{m3}) \hat{a}(\omega_{m2}) \rangle_0 &= \frac{1}{\mathcal{Z}_0 \beta^2} \sum_{n=1}^{\infty} \sum_{\alpha, \nu, \rho, \lambda = \pm} (t_{(n+1)\alpha\lambda} t_{(n+1)\rho\lambda} t_{n\rho\nu} t_{n\alpha\nu}) \\ &\times e^{-\beta E_{n\alpha}} \left\{ \frac{-1}{(i(\omega_{m1} + \omega_{m3}) + E_{(n-1)\nu} - E_{(n+1)\lambda})} \right. \\ &\times \left[ \frac{-1 + e^{\beta(i\omega_{m4} + E_{n\alpha} - E_{(n+1)\lambda})}}{(i\omega_{m4} + E_{n\alpha} - E_{(n+1)\lambda})^2 (-i\omega_{m1} - E_{n\rho} + E_{(n+1)\lambda})} \right. \\ &\left. \left. + \frac{-1 + e^{\beta(-i(\omega_{m1} + \omega_{m3} - \omega_{m4}) - E_{(n-1)\nu} + E_{n\alpha})}}{(i(\omega_{m1} + \omega_{m3} - \omega_{m4}) + E_{(n-1)\nu} - E_{n\alpha})^2 (-i\omega_{m3} - E_{(n-1)\nu} + E_{n\rho})} \right] \right. \\ &+ \frac{1}{(i(\omega_{m1} - \omega_{m4}) - E_{n\alpha} + E_{n\rho})} \left[ \frac{1 - e^{\beta(-i(\omega_{m1} - \omega_{m4}) + E_{n\alpha} - E_{n\rho})}}{(-i\omega_{m3} - E_{(n-1)\nu} + E_{n\rho})} \right. \\ &\times \frac{1}{(i(\omega_{m1} - \omega_{m4}) - E_{n\alpha} + E_{n\rho}) (-i\omega_{m1} - E_{n\rho} + E_{(n+1)\lambda})} \\ &\left. \left. + \frac{\beta}{(i(\omega_{m1} + \omega_{m3} - \omega_{m4}) + E_{(n-1)\nu} - E_{n\alpha}) (-i\omega_{m4} - E_{n\alpha} + E_{(n+1)\lambda})} \right] \right\}, \quad (4.152) \end{aligned}$$

$$\begin{aligned} \langle \hat{a}(\omega_{m4}) \hat{a}(\omega_{m2}) \hat{a}^\dagger(\omega_{m1}) \hat{a}^\dagger(\omega_{m3}) \rangle_0 &= \frac{1}{\mathcal{Z}_0 \beta^2} \sum_{n=0}^{\infty} \sum_{\alpha, \nu, \rho, \lambda = \pm} e^{-\beta E_{n\alpha}} (t_{(n+1)\lambda\alpha} t_{(n+2)\rho\lambda}) \\ &\times (t_{(n+2)\rho\nu} t_{(n+1)\nu\alpha}) \left\{ \frac{1}{(i(\omega_{m3} - \omega_{m4}) + E_{(n+1)\lambda} - E_{(n+1)\nu})} \right. \\ &\times \left[ \frac{1 - e^{\beta(i\omega_{m3} + E_{n\alpha} - E_{(n+1)\nu})}}{(i\omega_{m3} + E_{n\alpha} - E_{(n+1)\nu})^2 (i\omega_{m1} + E_{(n+1)\nu} - E_{(n+2)\rho})} \right. \\ &\left. \left. + \frac{-1 + e^{\beta(i\omega_{m4} + E_{n\alpha} - E_{(n+1)\lambda})}}{(i\omega_{m4} + E_{n\alpha} - E_{(n+1)\lambda})^2 (i(\omega_{m1} + \omega_{m3} - \omega_{m4}) + E_{(n+1)\lambda} - E_{(n+2)\rho})} \right] \right. \\ &- \frac{1}{(i(\omega_{m1} + \omega_{m3}) + E_{n\alpha} - E_{(n+2)\rho})} \left[ \frac{-1 + e^{\beta(i(\omega_{m1} + \omega_{m3}) + E_{n\alpha} - E_{(n+2)\rho})}}{(-i\omega_{m1} - E_{(n+1)\nu} + E_{(n+2)\rho})} \right. \\ &\times \frac{1}{(i(\omega_{m1} + \omega_{m3} - \omega_{m4}) + E_{(n+1)\lambda} - E_{(n+2)\rho}) (i(\omega_{m1} + \omega_{m3}) + E_{n\alpha} - E_{(n+2)\rho})} \\ &\left. \left. + \frac{\beta}{(-i\omega_{m4} - E_{n\alpha} + E_{(n+1)\lambda}) (-i\omega_{m3} - E_{n\alpha} + E_{(n+1)\nu})} \right] \right\}, \quad (4.153) \end{aligned}$$

$$\begin{aligned}
 \left\langle \hat{a}(\omega_{m4}) \hat{a}^\dagger(\omega_{m1}) \hat{a}(\omega_{m2}) \hat{a}^\dagger(\omega_{m3}) \right\rangle_0 &= \frac{1}{\mathcal{Z}_0 \beta^2} \sum_{n=0}^{\infty} \sum_{\alpha, \nu, \rho, \lambda = \pm} e^{-\beta E_{n\alpha}} (t_{(n+1)\lambda\alpha} t_{(n+1)\lambda\rho} t_{(n+1)\nu\rho}) \\
 &\left\{ \frac{1}{(i(\omega_{m1} - \omega_{m4}) - E_{n\alpha} + E_{n\rho})} \left[ \frac{\beta}{(-i\omega_{m4} - E_{n\alpha} + E_{(n+1)\lambda}) (-i\omega_{m3} - E_{n\alpha} + E_{(n+1)\nu})} \right. \right. \\
 &\quad \left. \left. + \frac{-1 + e^{\beta(-i(\omega_{m1} - \omega_{m4}) + E_{n\alpha} - E_{n\rho})}}{(-i(\omega_{m1} - \omega_{m4}) + E_{n\alpha} - E_{n\rho}) (i(\omega_{m1} + \omega_{m3} - \omega_{m4}) + E_{n\rho} - E_{(n+1)\nu})} \right] \right. \\
 &\times \frac{1}{(-i\omega_{m1} - E_{n\rho} + E_{(n+1)\lambda})} + \frac{1}{(i(\omega_{m3} - \omega_{m4}) + E_{(n+1)\lambda} - E_{(n+1)\nu})} \\
 &\times \left[ \frac{-1 + e^{\beta(i\omega_{m4} + E_{n\alpha} - E_{(n+1)\lambda})}}{(i\omega_{m4} + E_{n\alpha} - E_{(n+1)\lambda})^2 (-i\omega_{m1} - E_{n\rho} + E_{(n+1)\lambda})} + \right. \\
 &\quad \left. + \frac{-1 + e^{\beta(i\omega_{m3} + E_{n\alpha} - E_{(n+1)\nu})}}{(i\omega_{m3} + E_{n\alpha} - E_{(n+1)\nu})^2 (i(\omega_{m1} + \omega_{m3} - \omega_{m4}) + E_{n\rho} - E_{(n+1)\nu})} \right] \left. \right\} (t_{(n+1)\nu\alpha}), \quad (4.154)
 \end{aligned}$$

$$\begin{aligned}
 \left\langle \hat{a}^\dagger(\omega_{m1}) \hat{a}(\omega_{m4}) \hat{a}(\omega_{m2}) \hat{a}^\dagger(\omega_{m3}) \right\rangle_0 &= \frac{1}{\mathcal{Z}_0 \beta^2} \sum_{n=0}^{\infty} \sum_{\alpha, \nu, \rho, \lambda = \pm} e^{-\beta E_{n\alpha}} (t_{n\alpha\lambda} t_{n\rho\lambda} t_{(n+1)\nu\rho} t_{(n+1)\nu\alpha}) \\
 &\left\{ \frac{1}{(i(\omega_{m1} + \omega_{m3}) + E_{(n-1)\lambda} - E_{(n+1)\nu})} \left[ \frac{-1 + e^{\beta(-i\omega_{m1} - E_{(n-1)\lambda} + E_{n\alpha})}}{(i\omega_{m1} + E_{(n-1)\lambda} - E_{n\alpha})^2 (i\omega_{m4} + E_{(n-1)\lambda} - E_{n\rho})} \right. \right. \\
 &\quad \left. \left. + \frac{-1 + e^{\beta(i\omega_{m3} + E_{n\alpha} - E_{(n+1)\nu})}}{(i\omega_{m3} + E_{n\alpha} - E_{(n+1)\nu})^2 (i(\omega_{m1} + \omega_{m3} - \omega_{m4}) + E_{n\rho} - E_{(n+1)\nu})} \right] \right. \\
 &+ \frac{1}{(i(\omega_{m1} - \omega_{m4}) - E_{n\alpha} + E_{n\rho})} \left[ \frac{\beta}{(i\omega_{m1} + E_{(n-1)\lambda} - E_{n\alpha}) (-i\omega_{m3} - E_{n\alpha} + E_{(n+1)\nu})} \right. \\
 &\quad \left. - \frac{-1 + e^{\beta(-i(\omega_{m1} - \omega_{m4}) + E_{n\alpha} - E_{n\rho})}}{(i\omega_{m4} + E_{(n-1)\lambda} - E_{n\rho}) (i(\omega_{m1} - \omega_{m4}) - E_{n\alpha} + E_{n\rho})} \right. \\
 &\quad \left. \left. \times \frac{1}{(i(\omega_{m1} + \omega_{m3} - \omega_{m4}) + E_{n\rho} - E_{(n+1)\nu})} \right] \right\}. \quad (4.155)
 \end{aligned}$$

Using these results together with the definition (4.135), one finally finds the following expression for the 4th order coefficient

$$\begin{aligned}
 a_4^{(0)}(\omega_{m1}, \omega_{m3} | \omega_{m2}, \omega_{m4}) &= \frac{1}{\beta \mathcal{Z}_0} \sum_{n=0}^{\infty} \sum_{\alpha, \nu, \rho, \lambda = \pm} e^{-\beta E_{n\alpha}} \left( \left\{ \frac{t_{(n-1)\lambda\rho} t_{(n-1)\nu\rho} t_{n\alpha\lambda} t_{n\alpha\nu}}{i(\omega_{m1} - \omega_{m4}) + E_{(n-1)\lambda} - E_{(n-1)\nu}} \right. \right. \\
 &\times \left[ \frac{e^{\beta(-i\omega_{m4} - E_{(n-1)\nu} + E_{n\alpha})} - 1}{(i(\omega_{m1} + \omega_{m3} - \omega_{m4}) + E_{(n-2)\rho} - E_{(n-1)\nu}) (i\omega_{m4} + E_{(n-1)\nu} - E_{n\alpha})^2} \right. \\
 &\quad \left. \left. - \frac{e^{\beta(-i\omega_{m1} - E_{(n-1)\lambda} + E_{n\alpha})} - 1}{(i\omega_{m3} + E_{(n-2)\rho} - E_{(n-1)\lambda}) (i\omega_{m1} + E_{(n-1)\lambda} - E_{n\alpha})^2} \right] \right)
 \end{aligned}$$

$$\begin{aligned}
 & + \frac{t_{(n-1)\lambda\rho} t_{(n-1)\nu\rho} t_{n\alpha\lambda} t_{n\alpha\nu}}{i(\omega_{m1} + \omega_{m3}) + E_{(n-2)\rho} - E_{n\alpha}} \left[ \frac{\beta}{(i\omega_{m1} + E_{(n-1)\lambda} - E_{n\alpha})(i\omega_{m4} + E_{(n-1)\nu} - E_{n\alpha})} \right. \\
 & + \frac{e^{\beta(-i(\omega_{m1} + \omega_{m3}) - E_{(n-2)\rho} + E_{n\alpha})} - 1}{(i\omega_{m3} + E_{(n-2)\rho} - E_{(n-1)\lambda})(i(\omega_{m1} + \omega_{m3}) + E_{(n-2)\rho} - E_{n\alpha})} \\
 & \left. \times \frac{1}{(i(\omega_{m1} + \omega_{m3} - \omega_{m4}) + E_{(n-2)\rho} - E_{(n-1)\nu})} \right] \left. \right\} (1 - \delta_{n,0})(1 - \delta_{n,1}) \\
 & + (1 - \delta_{n,0}) \left\{ - \frac{\beta}{(i\omega_{m1} + E_{(n-1)\lambda} - E_{n\alpha})(i(\omega_{m3} - \omega_{m4}) + E_{n\alpha} - E_{n\rho})} \right. \\
 & \times \frac{1}{(i\omega_{m4} + E_{(n-1)\nu} - E_{n\alpha})} + \frac{-1 + e^{\beta(i(\omega_{m3} - \omega_{m4}) + E_{n\alpha} - E_{n\rho})}}{(i(\omega_{m3} - \omega_{m4}) + E_{n\alpha} - E_{n\rho})(i(\omega_{m3} - \omega_{m4}) + E_{n\alpha} - E_{n\rho})} \\
 & \times \frac{1}{(i(\omega_{m1} + \omega_{m3} - \omega_{m4}) + E_{(n-1)\lambda} - E_{n\rho})(i\omega_{m3} + E_{(n-1)\nu} - E_{n\rho})} \\
 & + \frac{1}{i(\omega_{m1} - \omega_{m4}) + E_{(n-1)\lambda} - E_{(n-1)\nu}} \left[ - \frac{e^{\beta(-i\omega_{m4} - E_{(n-1)\nu} + E_{n\alpha})} - 1}{(i\omega_{m4} + E_{(n-1)\nu} - E_{n\alpha})^2 (i\omega_{m3} + E_{(n-1)\nu} - E_{n\rho})} \right. \\
 & \left. + \frac{e^{\beta(-i\omega_{m1} - E_{(n-1)\lambda} + E_{n\alpha})} - 1}{(i\omega_{m1} + E_{(n-1)\lambda} - E_{n\alpha})^2 (i(\omega_{m1} + \omega_{m3} - \omega_{m4}) + E_{(n-1)\lambda} - E_{n\rho})} \right] \left. \right\} t_{n\alpha\lambda} t_{n\alpha\nu} t_{n\rho\lambda} t_{n\rho\nu} \\
 & + (1 - \delta_{n,0}) \left\{ - \frac{\beta}{(i\omega_{m1} + E_{(n-1)\lambda} - E_{n\alpha})(i(\omega_{m1} - \omega_{m4}) - E_{n\alpha} + E_{n\rho})} \right. \\
 & \times \frac{1}{(i\omega_{m3} + E_{n\alpha} - E_{(n+1)\nu})} + \frac{1 - e^{\beta(-i(\omega_{m1} + \omega_{m4}) + E_{n\alpha} - E_{n\rho})}}{(i\omega_{m4} + E_{(n-1)\lambda} - E_{n\rho})(i(\omega_{m1} - \omega_{m4}) - E_{n\alpha} + E_{n\rho})} \\
 & \times \frac{1}{(i(\omega_{m1} - \omega_{m4}) - E_{n\alpha} + E_{n\rho})(i(\omega_{m1} + \omega_{m3} - \omega_{m4}) + E_{n\rho} - E_{(n+1)\nu})} \\
 & + \frac{1}{i(\omega_{m1} + \omega_{m3}) + E_{(n-1)\lambda} - E_{(n+1)\nu}} \left[ \frac{e^{\beta(-i\omega_{m1} - E_{(n-1)\lambda} + E_{n\alpha})} - 1}{(i\omega_{m1} + E_{(n-1)\lambda} - E_{n\alpha})^2 (i\omega_{m4} + E_{(n-1)\lambda} - E_{n\rho})} \right. \\
 & \left. + \frac{e^{\beta(i\omega_{m3} + E_{n\alpha} - E_{(n+1)\nu})} - 1}{(i\omega_{m3} + E_{n\alpha} - E_{(n+1)\nu})^2 (i(\omega_{m1} + \omega_{m3} - \omega_{m4}) + E_{n\rho} - E_{(n+1)\nu})} \right] \left. \right\} t_{n\alpha\lambda} t_{n\rho\lambda} t_{(n+1)\nu\alpha} t_{(n+1)\nu\rho} \\
 & + (1 - \delta_{n,0}) \left\{ - \frac{\beta}{(i(\omega_{m1} + \omega_{m3} - \omega_{m4}) + E_{(n-1)\nu} - E_{n\alpha})(i\omega_{m4} + E_{n\alpha} - E_{(n+1)\lambda})} \right. \\
 & \times \frac{1}{(i(\omega_{m1} - \omega_{m4}) - E_{n\alpha} + E_{n\rho})} - \frac{-1 + e^{\beta(-i(\omega_{m1} - \omega_{m4}) + E_{n\alpha} - E_{n\rho})}}{(i\omega_{m3} + E_{(n-1)\nu} - E_{n\rho})} \\
 & \times \frac{1}{(i(\omega_{m1} - \omega_{m4}) - E_{n\alpha} + E_{n\rho})(i(\omega_{m1} - \omega_{m4}) - E_{n\alpha} + E_{n\rho})(i\omega_{m1} + E_{n\rho} - E_{(n+1)\lambda})} \\
 & + \frac{1}{i(\omega_{m1} + \omega_{m3}) + E_{(n-1)\nu} - E_{(n+1)\lambda}} \left[ \frac{e^{\beta(i\omega_{m4} + E_{n\alpha} - E_{(n+1)\lambda})} - 1}{(i\omega_{m4} + E_{n\alpha} - E_{(n+1)\lambda})^2 (i\omega_{m1} + E_{n\rho} - E_{(n+1)\lambda})} \right.
 \end{aligned}$$

$$\begin{aligned}
 & + \left. \frac{e^{\beta(-i\omega_{m1}-i\omega_{m3}+i\omega_{m4}-E_{(n-1)\nu}+E_{n\alpha})} - 1}{(i(\omega_{m1} + \omega_{m3} - \omega_{m4}) + E_{(n-1)\nu} - E_{n\alpha})^2 (i\omega_{m3} + E_{(n-1)\nu} - E_{n\rho})} \right\} t_{n\alpha\nu} t_{n\rho\nu} t_{(n+1)\alpha\lambda} t_{(n+1)\nu\rho} \\
 & + \left\{ \frac{\beta}{(i\omega_{m4} + E_{n\alpha} - E_{(n+1)\lambda}) (i(\omega_{m1} - \omega_{m4}) - E_{n\alpha} + E_{n\rho}) (i\omega_{m3} + E_{n\alpha} - E_{(n+1)\nu})} \right. \\
 & + \frac{e^{\beta(-i\omega_{m1}+i\omega_{m4}+E_{n\alpha}-E_{n\rho})} - 1}{(i(\omega_{m1} - \omega_{m4}) - E_{n\alpha} + E_{n\rho}) (i\omega_{m1} + E_{n\rho} - E_{(n+1)\lambda})} \\
 & \left. \frac{1}{(i(\omega_{m1} - \omega_{m4}) - E_{n\alpha} + E_{n\rho}) (i(\omega_{m1} + \omega_{m3} - \omega_{m4}) + E_{n\rho} - E_{(n+1)\nu})} \right. \\
 & - \frac{e^{\beta(i\omega_{m4}+E_{n\alpha}-E_{(n+1)\lambda})} - 1}{(i\omega_{m4} + E_{n\alpha} - E_{(n+1)\lambda})^2 (i\omega_{m1} + E_{n\rho} - E_{(n+1)\lambda}) (i(\omega_{m3} - \omega_{m4}) + E_{(n+1)\lambda} - E_{(n+1)\nu})} \\
 & + \frac{e^{\beta(i\omega_{m3}+E_{n\alpha}-E_{(n+1)\nu})} - 1}{(i(\omega_{m3} - \omega_{m4}) + E_{(n+1)\lambda} - E_{(n+1)\nu}) (i(\omega_{m1} + \omega_{m3} - \omega_{m4}) + E_{n\rho} - E_{(n+1)\nu})} \\
 & \left. \times \frac{1}{(i\omega_{m3} + E_{n\alpha} - E_{(n+1)\nu})^2} \right\} t_{(n+1)\lambda\alpha} t_{(n+1)\lambda\rho} t_{(n+1)\nu\alpha} t_{(n+1)\nu\rho} \\
 & + \left\{ \frac{-\beta}{(i\omega_{m4} + E_{n\alpha} - E_{(n+1)\lambda}) (i(\omega_{m1} + \omega_{m3}) + E_{n\alpha} - E_{(n+2)\rho}) (i\omega_{m3} + E_{n\alpha} - E_{(n+1)\nu})} \right. \\
 & + \frac{e^{\beta(i\omega_{m1}+i\omega_{m3}+E_{n\alpha}-E_{(n+2)\rho})} - 1}{(i(\omega_{m1} + \omega_{m3}) + E_{n\alpha} - E_{(n+2)\rho}) (i\omega_{m1} + E_{(n+1)\nu} - E_{(n+2)\rho})} \\
 & \left. \times \frac{1}{(i(\omega_{m1} + \omega_{m3}) + E_{n\alpha} - E_{(n+2)\rho}) (i(\omega_{m1} + \omega_{m3} - \omega_{m4}) + E_{(n+1)\lambda} - E_{(n+2)\rho})} \right. \\
 & + \frac{1}{(i(\omega_{m3} - \omega_{m4}) + E_{(n+1)\lambda} - E_{(n+1)\nu})} \left[ \frac{i(-1 + e^{\beta(i\omega_{m4}+E_{n\alpha}-E_{(n+1)\lambda})})}{(\omega_{m4} - iE_{n\alpha} + iE_{(n+1)\lambda})^2} \right. \\
 & \left. \times \frac{1}{(\omega_{m1} + \omega_{m3} - \omega_{m4} - iE_{(n+1)\lambda} + iE_{(n+2)\rho})} + \frac{1}{(i\omega_{m1} + E_{(n+1)\nu} - E_{(n+2)\rho})} \right. \\
 & \left. \times \frac{e^{\beta(i\omega_{m3}+E_{n\alpha}-E_{(n+1)\nu})} - 1}{(\omega_{m3} - iE_{n\alpha} + iE_{(n+1)\nu})^2} \right\} t_{(n+1)\lambda\alpha} t_{(n+1)\nu\alpha} t_{(n+2)\rho\lambda} t_{(n+2)\rho\nu} \Bigg\}_{\omega_{m1} \leftrightarrow \omega_{m3}} \\
 & - \left\{ a_2^{(0)}(\omega_{m1}|\omega_{m2}) a_2^{(0)}(\omega_{m3}|\omega_{m4}) \right\}_{\omega_{m1} \leftrightarrow \omega_{m3}}, \tag{4.156}
 \end{aligned}$$

where the label  $\omega_{m1} \leftrightarrow \omega_{m3}$  means a symmetrisation with respect to the respective Matsubara frequencies. Note, that the above expression for  $a_4^{(0)}(\omega_{m1}, \omega_{m3}|\omega_{m2}, \omega_{m4})$  only holds in case that  $\omega_{m1}, \omega_{m3}, \omega_{m4} \neq 0$  because otherwise new poles arise for suitable polariton-index combinations.

In order to validate the correctness of the above result, I consider the mean-field approach (3.54) again. Comparing equations (3.54) and (3.50) with expressions (4.67) and (4.68), one finds that the mean-field Hamiltonian can be rewritten in the form

$$\hat{H}^{\text{MF}} = \hat{H}_0 + \hat{H}_1^{\text{SC}}|_{\kappa_{ij}=0} + \kappa z \sum_i |\Psi_i|^2, \tag{4.157}$$

when using the formal identification

$$j_i(\tau) = -\kappa z \Psi_i. \quad (4.158)$$

Now, one can use the approach introduced in Section 4.4 to perform an expansion of  $\mathcal{F}$  to leading order. This ansatz leads to an expansion of the mean-field free energy  $\mathcal{F}_{\text{MF}}$  in powers of the order parameter  $\Psi_i$ , provided one notices that the term proportional to  $|\Psi_i|$  in equation (4.157) contributes only a constant term to  $\mathcal{F}_{\text{MF}}$ . With these considerations in mind, one finds the explicit result

$$\mathcal{F}_{\text{MF}} = \mathcal{F}_0 - \sum_i \left( a_2^{\text{MF}} |\Psi_i|^2 + \frac{1}{4} \beta a_4^{\text{MF}} |\Psi_i|^4 \right), \quad (4.159)$$

where the mean-field Landau coefficients are defined via the relations

$$a_2^{\text{MF}} = a_2^{(0)}(0|0) (\kappa z)^2 - \kappa z, \quad (4.160)$$

$$a_4^{\text{MF}} = a_4^{(0)}(0, 0|0, 0) (\kappa z)^4. \quad (4.161)$$

Hence, the mean-field result can directly be obtained from the free energy expansion coefficients  $a_2^{(0)}$  and  $a_4^{(0)}$ . Thus, in order to check if the result derived for  $a_4^{(0)}$  is correct, I will first calculate the low-temperature limit, which should coincide with the mean-field result for  $\omega_{m1} = \omega_{m2} = \omega_{m3} = \omega_{m4} = 0$  according to equation (4.161). Thus, calculating the limits for frequencies equal to zero and rearranging the terms in an analogous way as I did for the second-order coefficient, I find the following limit

$$\begin{aligned} \lim_{\beta \rightarrow \infty} a_4^{(0)}(0, 0|0, 0) &= 4 \sum_{n=0}^{\infty} \sum_{\alpha, \nu, \rho = \pm} \left[ \frac{(1 - \delta_{n,0}) t_{n-\alpha}}{(E_{(n-1)\alpha} - E_{n-}) (E_{n-} - E_{n+})} \right. \\ &\times \left( \frac{t_{n-\nu} t_{n+\alpha} t_{n+\nu}}{(E_{n-} - E_{(n-1)\nu})} + \frac{t_{n+\alpha} t_{(n+1)\nu-} t_{(n+1)\nu+}}{(E_{n-} - E_{(n+1)\nu})} \right) - \frac{(1 - \delta_{n,0}) t_{(n+1)-\alpha}}{(E_{n-} - E_{(n+1)\alpha}) (E_{n-} - E_{n+})} \\ &\times \left( \frac{t_{(n+1)\alpha+} t_{(n+1)\nu-} t_{(n+1)\nu+}}{(E_{n-} - E_{(n+1)\nu})} + \frac{t_{n-\nu} t_{n+\nu} t_{(n+1)\alpha+}}{(E_{n-} - E_{(n-1)\nu})} \right) \\ &- \frac{t_{(n+1)-\alpha} t_{(n+1)\nu-} t_{(n+1)\alpha+} t_{(n+2)\rho\nu}}{(E_{n-} - E_{(n+1)\alpha}) (E_{n-} - E_{(n+1)\nu}) (E_{n-} - E_{(n+2)\rho})} \\ &\left. + \frac{(1 - \delta_{n,0}) (1 - \delta_{n,1}) t_{(n-1)-\rho} t_{(n-1)\nu\rho} t_{n-\alpha} t_{n-\nu}}{(E_{(n-1)\nu} - E_{n-}) (-E_{(n-2)\rho} + E_{n-}) (-E_{(n-1)\alpha} + E_{n-})} \right] - \lim_{\beta \rightarrow \infty} \left[ 2 a_2^{(0)}(0|0) a_2^{(0)}(0|0) \right]. \end{aligned} \quad (4.162)$$

Calculating the remaining limit yields

$$\begin{aligned} \lim_{\beta \rightarrow \infty} a_2^{(0)}(0|0) a_2^{(0)}(0|0) &= 2 \sum_{n=0}^{\infty} \sum_{\alpha, \lambda, \nu, \rho = \pm} \left[ - \frac{(1 - \delta_{n,0}) t_{n\alpha\rho}^2 t_{n\alpha\rho}^2}{(-E_{(n-1)\rho} + E_{n\alpha})^2 (E_{(n-1)\nu} - E_{n\lambda})} \right. \\ &- \frac{(1 - \delta_{n,0}) t_{n\lambda\nu}^2 t_{n\lambda\nu}^2}{(E_{(n-1)\nu} - E_{n\lambda}) (E_{n\alpha} - E_{(n+1)\rho})^2} + \frac{t_{(n+1)\nu\lambda}^2 t_{n\lambda\nu}^2}{(E_{n\lambda} - E_{(n+1)\nu}) (E_{n\alpha} - E_{(n+1)\rho})^2} \\ &\left. + \frac{(1 - \delta_{n,0}) t_{n\alpha\rho}^2 t_{(n+1)\nu\lambda}^2}{(-E_{(n-1)\rho} + E_{n\alpha})^2 (E_{n\lambda} - E_{(n+1)\nu})} \right]. \end{aligned} \quad (4.163)$$

Inserting this result into equation (4.162) leads to the final result for the zero-temperature limit

$$\begin{aligned}
 a_4^{(0)}(0, 0|0, 0) = & 4 \sum_{n=0}^{\infty} \sum_{\alpha, \nu, \rho = \pm} \left[ \frac{(1 - \delta_{n,0})(1 - \delta_{n,1}) t_{(n-1)-\rho} t_{(n-1)\nu\rho} t_{n-\alpha} t_{n-\nu}}{(E_{(n-1)\nu} - E_{n-}) (-E_{(n-2)\rho} + E_{n-}) (-E_{(n-1)\alpha} + E_{n-})} \right] \\
 & - \frac{t_{(n+1)-\alpha} t_{(n+1)\nu-} t_{(n+1)+\alpha} t_{(n+2)\rho\nu}}{(E_{n-} - E_{(n+1)\alpha}) (E_{n-} - E_{(n+1)\nu}) (E_{n-} - E_{(n+2)\rho})} \\
 & + \frac{(1 - \delta_{n,0}) t_{n-\alpha}}{(E_{(n-1)\alpha} - E_{n-}) (E_{n-} - E_{n+})} \left( \frac{t_{n-\nu} t_{n+\alpha} t_{n+\nu}}{(E_{n-} - E_{(n-1)\nu})} + \frac{t_{n+\alpha} t_{(n+1)\nu-} t_{(n+1)\nu+}}{(E_{n-} - E_{(n+1)\nu})} \right) \\
 & - \frac{(1 - \delta_{n,0}) t_{(n+1)-\alpha}}{(E_{n-} - E_{(n+1)\alpha}) (E_{n-} - E_{n+})} \left( \frac{t_{(n+1)\alpha+} t_{(n+1)\nu-} t_{(n+1)\nu+}}{(E_{n-} - E_{(n+1)\nu})} + \frac{t_{n-\nu} t_{n+\nu} t_{(n+1)+\alpha}}{(E_{n-} - E_{(n-1)\nu})} \right) \\
 & - \frac{(1 - \delta_{n,0}) t_{n-\rho}^2}{(E_{n-} - E_{(n-1)\rho})^2} \left\{ \frac{t_{n-\nu}^2}{(E_{n-} - E_{(n-1)\nu})} + \frac{t_{(n+1)\nu-}^2}{(E_{n-} - E_{(n+1)\nu})} \right\} \\
 & - \frac{t_{(n+1)\rho-}^2}{(E_{n-} - E_{(n+1)\rho})^2} \left\{ \frac{(1 - \delta_{n,0}) t_{n-\nu}^2}{(E_{n-} - E_{(n-1)\nu})} + \frac{t_{(n+1)\nu-}^2}{(E_{n-} - E_{(n+1)\nu})} \right\}. \tag{4.164}
 \end{aligned}$$

If one now compares this result with expressions (3.96) and (3.86) obtained from Rayleigh-Schrödinger perturbation theory, one finds the correspondence

$$a_4^{\text{MF}} = a_4^{(0)}(0, 0|0, 0) (\kappa z)^4, \tag{4.165}$$

and thus I confirmed that the calculated fourth-order contribution is consistent within the zero-temperature limit. Next, I determine the first-order hopping correction  $a_4^{(1)}$ . In order to determine this correction in Matsubara space, I can use the integral properties and frequency conservation again, which leads to the relation

$$a_4^{(1)}(i, \omega_{m1}; i, \omega_{m3}|j, \omega_{m2}; i, \omega_{m4}) = a_4^{(0)}(i, \omega_{m1}; i, \omega_{m3}|i, \omega_{m4}) a_2^{(0)}(j, \omega_{m2}) \delta_{\omega_{m1} + \omega_{m3}, \omega_{m2} + \omega_{m4}}. \tag{4.166}$$

Hence the first-order hopping correction for the fourth-order current coefficient is given by expressions I already calculated and can therefore be included right away.

Finally, I derived the complete equation for the grand-canonical free energy in Matsubara space up to fourth order in the symmetry-breaking currents and first order in the hopping strength. However, this still is not the desired Ginzburg-Landau theory. Since the free energy is a functional of the currents  $j, j^*$ , which are no physical quantities, it is not a proper thermodynamic potential. Fortunately, there exists a well-known mathematical procedure to map this functional into a genuine thermodynamic potential. This procedure will be presented within the next section.

## 4.7 Ginzburg-Landau Action

Within this section I finally derive the Ginzburg-Landau action for the JCH model, which is the proper thermodynamic potential for this system. Since the symmetry-breaking currents  $j, j^*$  are no physical quantities, one has to transform them into physical fields. This

transformation can be accomplished by means of a Legendre transformation of the free-energy functional to an effective action. In order to do this in a neat way, I first rewrite the grand-canonical free energy in Matsubara space in the following form

$$\mathcal{F}[j, j^*] = \mathcal{F}_0 - \frac{1}{\beta} \sum_{i,j} \sum_{\omega_{m1}, \omega_{m2}} \left\{ M_{ij}(\omega_{m1}, \omega_{m2}) j_i(\omega_{m1}) j_j^*(\omega_{m2}) + \sum_{k,l} \sum_{\omega_{m3}, \omega_{m4}} N_{ijkl}(\omega_{m1}, \omega_{m2}, \omega_{m3}, \omega_{m4}) j_i(\omega_{m1}) j_j(\omega_{m2}) j_k^*(\omega_{m3}) j_l^*(\omega_{m4}) \right\}, \quad (4.167)$$

where the new introduced coefficients are defined as

$$M_{ij}(\omega_{m1}, \omega_{m2}) = \left[ a_2^{(0)}(i, \omega_{m1}) \delta_{i,j} + \kappa_{ij} a_2^{(0)}(i, \omega_{m1}) a_2^{(0)}(j, \omega_{m2}) \right] \delta_{\omega_{m1}, \omega_{m2}}, \quad (4.168)$$

and

$$N_{ijkl}(\omega_{m1}, \omega_{m2}, \omega_{m3}, \omega_{m4}) = \frac{1}{4} a_4^{(0)}(i, \omega_{m1}; i, \omega_{m3} | i, \omega_{m4}) \left[ \delta_{i,j} \delta_{k,l} \delta_{i,k} + \kappa_{ik} a_2^{(0)}(k, \omega_{m2}) \delta_{i,j} \delta_{i,l} + \kappa_{ij} a_2^{(0)}(j, \omega_{m3}) \delta_{i,k} \delta_{k,l} \right] \delta_{\omega_{m1} + \omega_{m3}, \omega_{m2} + \omega_{m4}}. \quad (4.169)$$

Now I define the Legendre transformation by self-consistently introducing the order parameter field  $\psi_i(\omega_m)$  according to

$$\psi_i(\omega_m) = \langle \hat{a}_i(\omega_m) \rangle_0 = \beta \frac{\delta \mathcal{F}}{\delta j_i^*(\omega_m)}. \quad (4.170)$$

Note, that this Ginzburg-Landau order parameter field differs from the Landau order parameter (3.48) by being space *and* time dependent. Inserting expression (4.167) into equation (4.170) yields the following relation for the Ginzburg-Landau order parameter field

$$\psi_i(\omega_m) = - \sum_p \sum_{\omega_{m1}} \left\{ M_{pi}(\omega_{m1}, \omega_m) j_p(\omega_{m1}) - 2 \sum_{k,l} \sum_{\omega_{m2}, \omega_{m3}} N_{lpki}(\omega_{m1}, \omega_{m2}, \omega_{m3}, \omega_m) j_l(\omega_{m1}) j_p(\omega_{m2}) j_k^*(\omega_{m3}) \right\}. \quad (4.171)$$

The Legendre transformation (4.170) defines the new Ginzburg-Landau action  $\Gamma$ , which takes on the following form

$$\Gamma[\psi_i(\omega_m), \psi_i^*(\omega_m)] = \mathcal{F}[j, j^*] - \frac{1}{\beta} \sum_i \sum_{\omega_m} [\psi_i(\omega_m) j_i^*(\omega_m) + \psi_i^*(\omega_m) j_i(\omega_m)], \quad (4.172)$$

where  $\psi$  and  $j$  are conjugate variables satisfying the Legendre relations

$$j_i(\omega_m) = -\beta \frac{\delta \Gamma}{\delta \psi_i^*(\omega_m)}, \quad j_i^*(\omega_m) = -\beta \frac{\delta \Gamma}{\delta \psi_i(\omega_m)}. \quad (4.173)$$

Using the fact, that physical situations correspond to  $j = j^* = 0$ , together with the above relations, defines the following equations of motion

$$\frac{\delta\Gamma}{\delta\psi_i^*(\omega_m)} = \frac{\delta\Gamma}{\delta\psi_i(\omega_m)} = 0. \quad (4.174)$$

Thus, the equilibrium order parameter  $\psi_{\text{eq}}$  is defined by the condition that the Ginzburg-Landau action is stationary with respect to fluctuations around it. Furthermore, comparing with equation (4.172) it is clear to see that, evaluating the effective action for the equilibrium field  $\psi_{\text{eq}}$  yields the physical grand-canonical free energy:

$$\Gamma|_{\psi=\psi_{\text{eq}}} = \lim_{j \rightarrow 0} \mathcal{F}. \quad (4.175)$$

Since I want the effective action to be a functional only of the order parameter field I still need to get rid of residual currents. In order to achieve this, I can use expression (4.171) to define the currents as functionals of the order parameter field. Eventually, this relation can be recursively inserted to obtain the thermodynamic potential as a functional of only the order parameter field. Unfortunately this is quite complicated because of the inner structure of the coefficients  $M_{pi}$  and  $N_{lpki}$ . However, if one knows the inverse matrix  $M_{qi}^{-1}(\omega_{m1}, \omega_m)$  one can determine an expression for  $j$  in dependence of  $\Psi$  recursively. Therefore, I first consider expression (4.168) and calculate its inverse using the ansatz

$$M_{ij}^{-1}(\omega_{m1}, \omega_{m2}) = m_{ij}^{(0)} + m_{ij}^{(1)} \kappa_{ij} + \mathcal{O}(\kappa_{ij}^2), \quad (4.176)$$

and demand that the following relation has to be satisfied

$$\sum_k M_{ik}^{-1}(\omega_{m1}, \omega_{m2}) M_{kj}(\omega_{m1}, \omega_{m2}) \stackrel{!}{=} \delta_{i,j}. \quad (4.177)$$

Using definition (4.168) this ansatz leads to

$$\begin{aligned} \delta_{i,j} = & \left[ m_{ij}^{(0)} a_2^{(0)}(j, \omega_{m1}) + \sum_k m_{ik}^{(0)} \kappa_{kj} a_2^{(0)}(k, \omega_{m1}) a_2^{(0)}(j, \omega_{m2}) \right. \\ & \left. + m_{ij}^{(1)} \kappa_{ij} a_2^{(0)}(j, \omega_{m1}) \right] \delta_{\omega_{m1}, \omega_{m2}}. \end{aligned} \quad (4.178)$$

Since this relation has to be true for all possible values of  $\kappa$ , I find the condition

$$\delta_{ij} = m_{ij}^{(0)} a_2^{(0)}(j, \omega_{m1}) \delta_{\omega_{m1}, \omega_{m2}}, \quad (4.179)$$

from which follows that

$$m_{ij}^{(0)} = \frac{\delta_{i,j} \delta_{\omega_{m1}, \omega_{m2}}}{a_2^{(0)}(j, \omega_{m1})}. \quad (4.180)$$

Furthermore, one finds the condition

$$0 = \left[ \sum_k m_{ik}^{(0)} \kappa_{kj} a_2^{(0)}(k, \omega_{m1}) a_2^{(0)}(j, \omega_{m2}) + m_{ij}^{(1)} \kappa_{ij} a_2^{(0)}(j, \omega_{m1}) \right] \delta_{\omega_{m1}, \omega_{m2}}, \quad (4.181)$$

which is solved by

$$m_{ij}^{(1)} = -\frac{a_2^{(0)}(j, \omega_{m2})}{a_2^{(0)}(j, \omega_{m1})} \delta_{\omega_{m1}, \omega_{m2}}. \quad (4.182)$$

Combining result (4.180) and equation (4.182) leads to the following relation for the inverse matrix  $M_{ij}^{-1}$ :

$$M_{ij}^{-1}(\omega_{m1}, \omega_{m2}) = \frac{1}{a_2^{(0)}(j, \omega_{m1})} \left[ \delta_{i,j} - a_2^{(0)}(j, \omega_{m2}) \kappa_{ij} \right] \delta_{\omega_{m1}, \omega_{m2}}. \quad (4.183)$$

Having obtained this inverse matrix, I can use it to transform equation (4.171) into recursive equation for the currents  $j, j^*$ . Simply rearranging the terms in equation (4.171) and multiplying with the inverse matrix  $M_{ip}^{-1}$  yields

$$j_i(\omega_m) = - \sum_p \sum_{\omega_{m1}} M_{ip}^{-1}(\omega_m, \omega_{m1}) \left[ \psi_p(\omega_{m1}) - 2 \sum_{q,k,l} \sum_{\omega_{m2}, \omega_{m3}} N_{lqkp}(\omega_{m1}, \omega_{m2}, \omega_{m3}, \omega_m) j_l(\omega_{m1}) j_q(\omega_{m2}) j_k^*(\omega_{m3}) \right]. \quad (4.184)$$

Reinserting expression (4.184) into itself and keeping just contributions up to first order in the hopping leads to the relation

$$j_i(\omega_m) = - \sum_p \sum_{\omega_{m1}} M_{ip}^{-1}(\omega_m, \omega_{m1}) \left[ \psi_p(\omega_{m1}) - 2 \sum_{q,k,l} \sum_{\omega_{m2}, \omega_{m3}} N_{lqkp}(\omega_{m1}, \omega_{m2}, \omega_{m3}, \omega_m) J_l(\omega_{m1}) J_q(\omega_{m2}) J_k^*(\omega_{m3}) \right], \quad (4.185)$$

where I defined the abbreviation

$$J_i(\omega_m) = - \sum_p \sum_{\omega_{m1}} M_{ip}^{-1}(\omega_{m1}, \omega_m) \psi_p(\omega_{m1}). \quad (4.186)$$

Using result (4.185) and inserting it into equation (4.172) leads to the expression

$$\Gamma[\psi_i(\omega_m), \psi_i^*(\omega_m)] = \mathcal{F}[J, J^*] + \frac{1}{\beta} \sum_{i,p} \sum_{\omega_m, \omega_{m1}} \psi_i(\omega_m) M_{ip}^{-1}(\omega_m, \omega_{m1}) \left[ \psi_p^*(\omega_{m1}) - 2 \sum_{q,k,l} \sum_{\omega_{m2}, \omega_{m3}} N_{lqkp}(\omega_{m1}, \omega_{m2}, \omega_{m3}, \omega_m) J_l^*(\omega_{m1}) J_q^*(\omega_{m2}) J_k(\omega_{m3}) \right] + c.c. \quad (4.187)$$

The next step is to insert expansion (4.167) for the free energy into equation (4.187). Using equation (4.185) once again and keeping just the contributions up to first order in the

hopping strength, one arrives at the final expression for the Ginzburg-landau action which reads

$$\Gamma [\psi_i (\omega_m), \psi_i^* (\omega_m)] \approx \mathcal{F}_0 + \frac{1}{\beta} \sum_i \sum_{\omega_{m1}} \left\{ \frac{|\psi_i (\omega_{m1})|^2}{a_2^{(0)} (i, \omega_{m1})} - \sum_j \kappa_{ij} \psi_j (\omega_{m1}) \psi_i^* (\omega_{m1}) \right. \\ \left. - \sum_{\omega_{m2}, \omega_{m3}, \omega_{m4}} \frac{a_4^{(0)} (i; \omega_{m1}, \omega_{m3} | \omega_{m2}, \omega_{m4}) \psi_i (\omega_{m1}) \psi_i (\omega_{m3}) \psi_i^* (\omega_{m2}) \psi_i^* (\omega_{m4})}{4 a_2^{(0)} (i, \omega_{m1}) a_2^{(0)} (i, \omega_{m2}) a_2^{(0)} (i, \omega_{m3}) a_2^{(0)} (i, \omega_{m4})} \right\}. \quad (4.188)$$

Formally comparing this result with the expansion of the free energy (4.108) it is to see that the two terms in the Ginzburg-Landau action corresponding to the coefficient  $a_4^{(1)}$  of the free energy expansion vanish. Considering the diagrammatic expansion, this result means, that the one-particle reducible diagrams vanish. Thus, it is to see that the Legendre transformation of the grand-canonical free energy, which is given by the sum over all connected diagrams, leads to an effective action, which is given by the sum over all one-particle irreducible diagrams.

In order to obtain physical results from equation (4.188), I insert this expression in the stationary condition (4.174), which then takes on the following form

$$0 = \left[ \frac{1}{a_2^{(0)} (i, \omega_m)} - \sum_j \kappa_{ij} \right] \psi_i (\omega_m) \\ - \sum_{\omega_{m1}, \omega_{m2}, \omega_{m3}} \frac{a_4^{(0)} (i, \omega_{m1}; i, \omega_{m3} | i, \omega_{m2}; i, \omega_m) \psi_i (\omega_{m1}) \psi_i (\omega_{m3}) \psi_i^* (\omega_{m2})}{2 a_2^{(0)} (i, \omega_{m1}) a_2^{(0)} (i, \omega_{m2}) a_2^{(0)} (i, \omega_{m3}) a_2^{(0)} (i, \omega_m)} \quad (4.189)$$

Equation (4.188) is in fact the proper thermodynamic potential for the JCH model up to the desired accuracy in the order parameter and the hopping parameter. However, as should be clear from the approximations performed so far, this expression can be extended to include higher order corrections. In the next chapter this result is used to analyse the thermodynamic properties of the considered system.

# Chapter 5

## Results from Ginzburg-Landau Action

Having derived the Ginzburg-Landau action in the previous chapter, I now use this result to extract some thermodynamic properties of the JCH model. The starting point for these calculations is the physical stationarity condition defined in equation (4.189). The results following from this ansatz are examined in the following sections for both static and dynamic order fields  $\psi_i(\omega_m)$ .

### 5.1 Static Case

First, I consider an equilibrium situation, where the order parameter field is constant in space and time

$$\psi_i(\omega_m) = \sqrt{\beta} \psi_{\text{eq}} \delta_{\omega_m, 0}. \quad (5.1)$$

Inserting this ansatz in the stationarity condition (4.189) yields for the equilibrium order parameter the following relation

$$|\psi|_{\text{eq}}^2 = \frac{2}{\beta} \frac{[a_2^{(0)}(0|0)]^3}{a_4^{(0)}(0, 0|0, 0)} [1 - a_2^{(0)}(0|0) \kappa z]. \quad (5.2)$$

Note that this expression is strictly local and site independent. For this reason I dropped the site index  $i$  of the coefficients  $a_2^{(0)}(i; 0|0)$  and  $a_4^{(0)}(i; 0, 0|0, 0)$ .

On the one hand, this expression is an estimate for the condensate density in the static case. On the other side, it is to see that, according to relation (4.175), all physical quantities can be obtained by calculating the derivatives of the effective Ginzburg-Landau action evaluated at the equilibrium field  $\psi_{\text{eq}}$ . Thus, for example the average polariton number per lattice site and the compressibility can be calculated following the relations

$$\langle n \rangle = -\frac{1}{N_s} \left. \frac{\partial \Gamma}{\partial \mu} \right|_{\psi=\psi_{\text{eq}}}, \quad (5.3)$$

and

$$\kappa_T = -\frac{1}{N_s} \left. \frac{\partial^2 \Gamma}{\partial \mu^2} \right|_{\psi=\psi_{\text{eq}}}. \quad (5.4)$$

Note that, due to relation (4.175), all relations which normally can be derived from the grand-canonical free energy  $\mathcal{F}$ , can analogously be calculated from the Ginzburg-Landau

action  $\Gamma$ , if evaluated at  $\psi_{\text{eq}}$  in the end.

Furthermore, one can read off from equation (5.2) the location of the quantum phase transition. The condition that the equilibrium order parameter vanishes, yields

$$0 = \frac{1}{a_2^{(0)}(0|0)} - \kappa z. \quad (5.5)$$

Inserting equation (4.127) and comparing this with formula (4.61) one finds that expression (5.5) is exactly the mean-field result for finite temperatures.

## 5.2 Dynamic Case

Within this section I analyse the 2-point Matsubara Green's function for the case of a dynamic order field  $\psi_i(\omega_m)$  in the Mott phase. In particular, I determine the dispersion relations for this correlation function in the Mott phase. These correlation functions describe the system response to an external disturbance. It is well known from the studies of critical phenomena that correlation functions become arbitrarily strong at the critical values [7]. Thus, the dispersion relations can be obtained from the poles of the real-time Green's functions [165].

In Section 4.4 I showed that the imaginary-time Green's functions can be obtained from the grand-canonical free energy by means of functional derivatives with respect to the symmetry-breaking currents. For example the 2-point Green's function reads

$$\left. \frac{\delta^2 \mathcal{F}[j_i(\omega_m), j_i^*(\omega_m)]}{\delta j_{i_1}(\omega_{m1}) \delta j_{i_2}^*(\omega_{m2})} \right|_{j=j^*=0} = G_1^{(0)}(i_1, \omega_{m1} | i_2, \omega_{m2}). \quad (5.6)$$

In a similar manner one can obtain the *inverse* Green's function in the Mott phase [159] from the effective action  $\Gamma$  given in (4.172) via

$$\left. \frac{\delta^2 \Gamma[\psi_i(\omega_m), \psi_i^*(\omega_m)]}{\delta \psi_{i_1}(\omega_{m1}) \delta \psi_{i_2}^*(\omega_{m2})} \right|_{\psi=\psi^*=0} = \left[ G_1^{(0)}(i_1, \omega_{m1} | i_2, \omega_{m2}) \right]^{-1}. \quad (5.7)$$

From equation (4.188) I see that this yields the following expression

$$\left[ G_1^{(0)}(i_1, \omega_{m1} | i_2, \omega_{m2}) \right]^{-1} \equiv \frac{1}{\beta} \left[ \frac{\delta_{i_1, i_2}}{a_2^{(0)}(i_1, \omega_{m1})} - \kappa_{i_1, i_2} \right] \delta_{\omega_{m1}, \omega_{m2}}. \quad (5.8)$$

This inverse Green's function obviously depends just on one Matsubara frequency and, due to the definition of  $\kappa_{i,j}$  in (4.69), on the distance between the lattice sites  $i_1, i_2$ . Therefore, one can rewrite this functions as follows:

$$\left[ G_1^{(0)}(i_1, \omega_{m1} | i_2, \omega_{m2}) \right]^{-1} = \left[ G_1^{(0)}(i_1 - i_2, \omega_{m1}) \right]^{-1} \delta_{\omega_{m1}, \omega_{m2}}. \quad (5.9)$$

The property, that this function only depends on the distance between neighbouring sites, suggests to further evaluate it in Fourier space. Thus, I perform a Fourier transformation

which reads

$$\begin{aligned}
 \left[ \tilde{G}_1^{(0)}(\omega_{m1}, \mathbf{k}) \right]^{-1} &= \frac{1}{N_s} \sum_{i_1, i_2} \left[ G_1^{(0)}(i_1 - i_2, \omega_{m1}) \right]^{-1} e^{-i\mathbf{k}(\mathbf{r}_{i_1} - \mathbf{r}_{i_2})} \\
 &= \frac{1}{\beta N_s} \sum_{i_1, i_2} \left[ \frac{\delta_{i_1, i_2}}{a_2^{(0)}(i_1, \omega_{m1})} - \kappa_{i_1, i_2} \right] e^{-i\mathbf{k}(\mathbf{r}_{i_1} - \mathbf{r}_{i_2})} \\
 &= \frac{1}{\beta} \left[ \frac{1}{a_2^{(0)}(\omega_{m1})} - \frac{1}{N_s} \sum_{i_1, i_2} \kappa_{i_1, i_2} e^{-i\mathbf{k}(\mathbf{r}_{i_1} - \mathbf{r}_{i_2})} \right]. \tag{5.10}
 \end{aligned}$$

Here I dropped the site index of the coefficient  $a_2^{(0)}(i_1, \omega_{m1})$  in the last equivalence because this coefficient is a local and site independent quantity and, thus, the sum over the lattice sites simply yields

$$\sum_{i_1} \frac{1}{a_2^{(0)}(i_1, \omega_{m1})} = \frac{N_s}{a_2^{(0)}(\omega_{m1})}. \tag{5.11}$$

In order to further calculate the expression (5.10) I make use of the definition (4.69) again and introduce the relation

$$\mathbf{r}_{i_2} = \mathbf{r}_{i_1} + \mathbf{G}, \tag{5.12}$$

where the lattice vector  $\mathbf{G}$  is defined by equation (3.40). Inserting this relation into (5.10) leads to

$$\begin{aligned}
 \left[ \tilde{G}_1^{(0)}(\omega_{m1}, \mathbf{k}) \right]^{-1} &= \frac{1}{\beta} \left[ \frac{1}{a_2^{(0)}(\omega_{m1})} - \kappa \sum_{\mathbf{G}} e^{i\mathbf{k}\mathbf{G}} \right] \\
 &= \frac{1}{\beta} \left[ \frac{1}{a_2^{(0)}(\omega_{m1})} - J(\mathbf{k}) \right], \tag{5.13}
 \end{aligned}$$

where  $J(\mathbf{k})$  is defined according to equation (3.45) as

$$J(\mathbf{k}) = 2\kappa \sum_{i=1}^3 \cos(k_i a). \tag{5.14}$$

Rearranging the terms in relation (5.13) and renaming the occurring Matsubara frequency  $\omega_{m1} \rightarrow \omega_m$  leads to the following expression for the 2-point Green's function in Fourier space:

$$\tilde{G}_1^{(0)}(\omega_m, \mathbf{k}) = \frac{\beta a_2^{(0)}(\omega_m)}{1 - J(\mathbf{k}) a_2^{(0)}(\omega_m)}, \tag{5.15}$$

However, since one needs the real-time Green's function in order to extract the dispersion relations, I furthermore perform an analytic continuation to real frequencies

$$i\omega_m \rightarrow \omega + i0^+. \tag{5.16}$$

Using the above transformation and multiplying with a factor  $-i$  leads to the real-time 2-point Green's function [158] which then takes on the form

$$\tilde{G}_1^{(0)}(\omega, \mathbf{k}) = \frac{-i\beta a_2^{(0)}(\omega)}{1 - J(\mathbf{k}) a_2^{(0)}(\omega)}. \tag{5.17}$$

The pole of this function is obviously given by the relation

$$1 = J(\mathbf{k}) a_2^{(0)}(\omega) . \quad (5.18)$$

Inserting equation (4.127) leads to the following, explicit form for this pole:

$$1 \stackrel{!}{=} \frac{J(\mathbf{k})}{Z_0} \sum_{\alpha, \alpha'} \left\{ \frac{t_{1\alpha'}^2}{E_{1\alpha'} - \omega} - \sum_{n=1}^{\infty} e^{-\beta E_{n\alpha}} \left[ \frac{t_{(n+1)\alpha'}^2}{E_{n\alpha} - E_{(n+1)\alpha'} + \omega} + \frac{t_{n\alpha'}^2}{E_{n\alpha} - E_{(n-1)\alpha'} - \omega} \right] \right\} . \quad (5.19)$$

Thus, I successfully derived the pole of the 2-point correlation function. The further investigation of this equation leads to polariton excitation spectra and will be performed in the next section.

### 5.3 Excitation Spectra in the Mott Phase

To gain more insight into expression (5.19), I first consider the special limit for zero temperature  $T = 0$ . Therefore, I consider just the lowest excitations and thus fix the polariton species to  $\alpha = -$ . Using these assumptions one finds that, for polariton numbers  $n > 0$ , equation (5.19) reduces to the simplified formula

$$1 = J(\mathbf{k}) \sum_{\alpha'} \left[ \frac{t_{(n+1)\alpha'}^2}{E_{(n+1)\alpha'} - E_{n-} - \omega} - \frac{t_{n-\alpha'}^2}{E_{n-} - E_{(n-1)\alpha'} - \omega} \right] . \quad (5.20)$$

Solving this equation for  $\omega$  yields the following two dispersion relations

$$\begin{aligned} \omega_1 = \frac{1}{2} \left[ E_{(n+1)-} - E_{(n-1)-} + J(\mathbf{k}) \left( t_{n--}^2 - t_{(n+1)--}^2 \right) - \left( \{ E_{(n-1)-} - E_{(n+1)-} \right. \right. \\ \left. \left. - J(\mathbf{k}) \left[ t_{n--}^2 - t_{(n+1)--}^2 \right] \right)^2 - 4 \{ J(\mathbf{k}) E_{(n+1)-} t_{n--}^2 - E_{n-}^2 + E_{(n-1)-} (E_{n-} - E_{(n+1)-} \right. \right. \\ \left. \left. + J(\mathbf{k}) t_{(n+1)--}^2 \right) + E_{n-} \left[ E_{(n+1)-} - J(\mathbf{k}) \left( t_{n--}^2 + t_{(n+1)--}^2 \right) \right] \right]^{\frac{1}{2}} \Bigg] , \quad (5.21) \end{aligned}$$

and

$$\begin{aligned} \omega_2 = \frac{1}{2} \left[ E_{(n+1)-} - E_{(n-1)-} + J(\mathbf{k}) \left( t_{n--}^2 - t_{(n+1)--}^2 \right) + \left( \{ E_{(n-1)-} - E_{(n+1)-} \right. \right. \\ \left. \left. - J(\mathbf{k}) \left[ t_{n--}^2 + t_{(n+1)--}^2 \right] \right)^2 - 4 \{ J(\mathbf{k}) E_{(n+1)-} t_{n--}^2 - E_{n-}^2 + E_{(n-1)-} (E_{n-} - E_{(n+1)-} \right. \right. \\ \left. \left. + J(\mathbf{k}) t_{(n+1)--}^2 \right) + E_{n-} \left[ E_{(n+1)-} - J(\mathbf{k}) \left( t_{n--}^2 + t_{(n+1)--}^2 \right) \right] \right]^{\frac{1}{2}} \Bigg] . \quad (5.22) \end{aligned}$$

Putting now  $J(\mathbf{k}) = 0$  in order to clarify the physical meaning of the equations (5.21) and (5.22), yields the very simple relations:

$$\omega_{h-}^{(0)} := \omega_1 = E_{n-} - E_{(n-1)-} , \quad (5.23)$$

$$\omega_{p-}^{(0)} := \omega_2 = E_{(n+1)-} - E_{n-} . \quad (5.24)$$

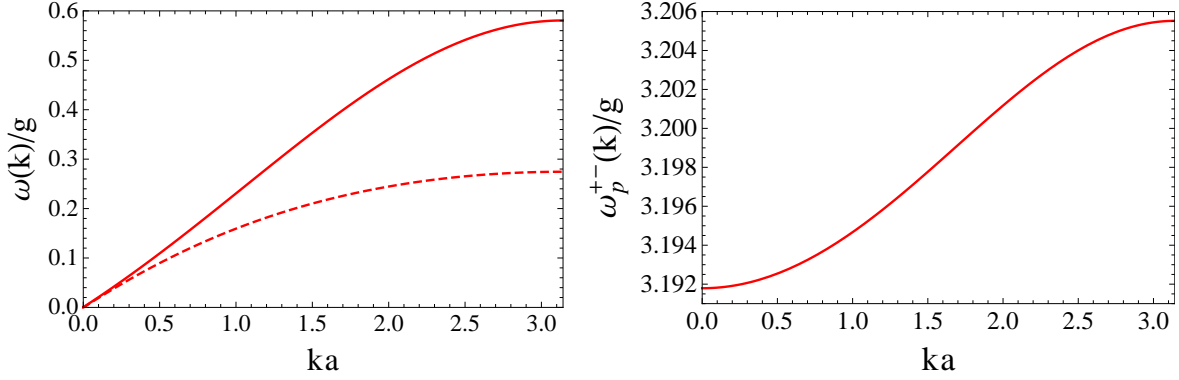


Figure 5.1: **Excitation spectra at  $T = 0$  K,  $\Delta = 0$  for  $n = 1$ ,  $\mu_{\text{eff}} = \mu_{\text{crit}} \approx -0.78g$ ,  $\kappa = \kappa_{\text{crit}} \approx 0.16g/z$ .** The left figure shows particle- (solid line) and hole excitations (dashed line) corresponding to  $\omega_p^{--} \hat{=} E_{2-} - E_{1-}$  and  $\omega_h^{--} \hat{=} E_{1-} - E_{0-}$ . The right figure shows the particle excitation spectrum for  $\omega_p^{+-} \hat{=} E_{2+} - E_{1-}$ .

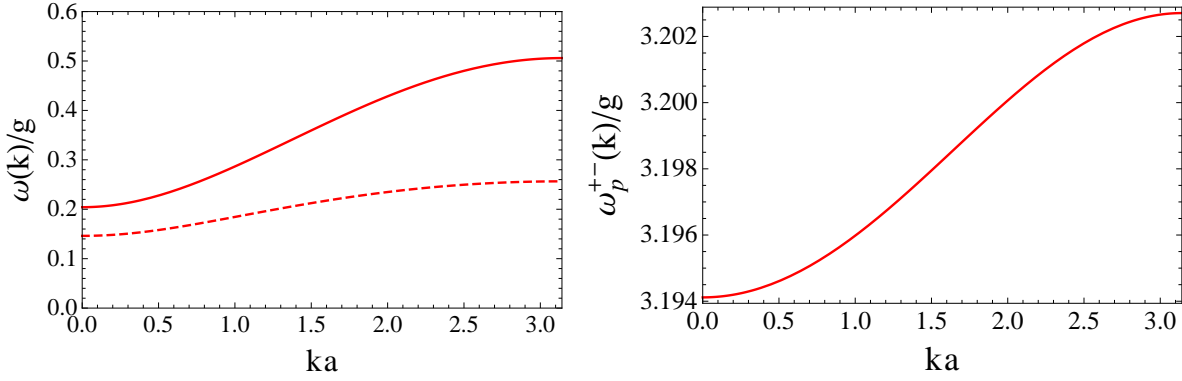


Figure 5.2: **Excitation spectra at  $T = 0$  K,  $\Delta = 0$  for  $n = 1$ ,  $\mu_{\text{eff}} = \mu_{\text{crit}} \approx -0.78g$ ,  $\kappa z/g = 0.1$ .** The left figure shows the lower-polariton particle- (solid line) and hole excitations (dashed line). The right figure shows mixed-particle excitation spectrum for  $\omega_p^{+-}$ .

From these relations it is clear to see that  $\omega_{h-}$  is the energy needed to remove a lower-branch polariton from a lattice site occupied by  $n$  lower-branch polaritons. For this reason I refer to this energy as a *lower-branch-hole* excitation. In contrast the frequency  $\omega_{p-}$  describes the energy required to add a lower-branch polariton to a site that is already occupied by  $n$  lower-branch polaritons. Therefore, I refer to it as a *lower-branch-particle* excitation. With this result in mind one can interpret the relations which I subsequently derive.

Note that, the dispersion relations (5.21) and (5.22) are not exact, since the terms with  $\alpha = +$  in (5.19) significantly contribute to the excitation spectrum as well. In order to get the

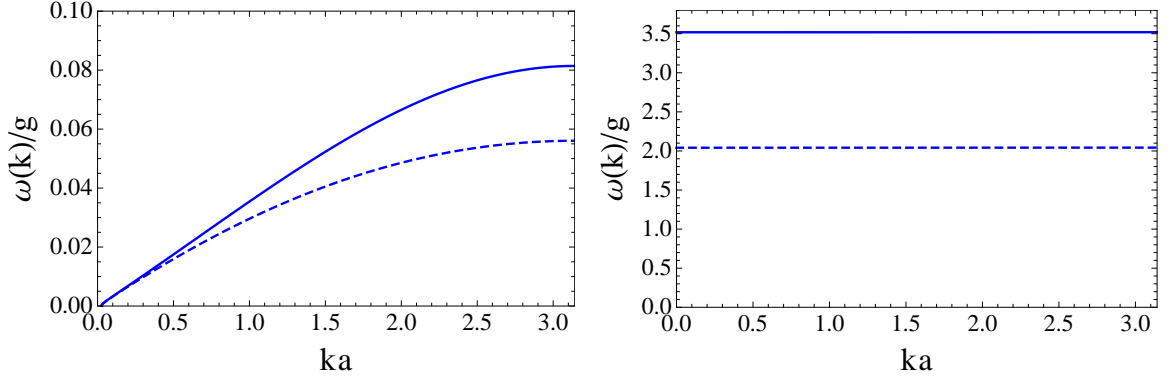


Figure 5.3: **Excitation spectra at  $T = 0$  K,  $\Delta = 0$  for  $n = 2$ ,  $\mu_{\text{eff}} = \mu_{\text{crit}} \approx -0.37 g$ ,  $\kappa = \kappa_{\text{crit}} \approx 0.0125 g/z$ .** The left figure shows particle- (solid line) and hole excitations (dashed line) corresponding to  $\omega_p^{--} \hat{=} E_{3-} - E_{2-}$  and  $\omega_h^{--} \hat{=} E_{2-} - E_{1-}$ . The right figure shows particle- (solid line) and hole (dashed line) excitations corresponding to  $\omega_p^{+-} \hat{=} E_{3+} - E_{2-}$  and  $\omega_h^{-+} \hat{=} E_{2-} - E_{1+}$ .

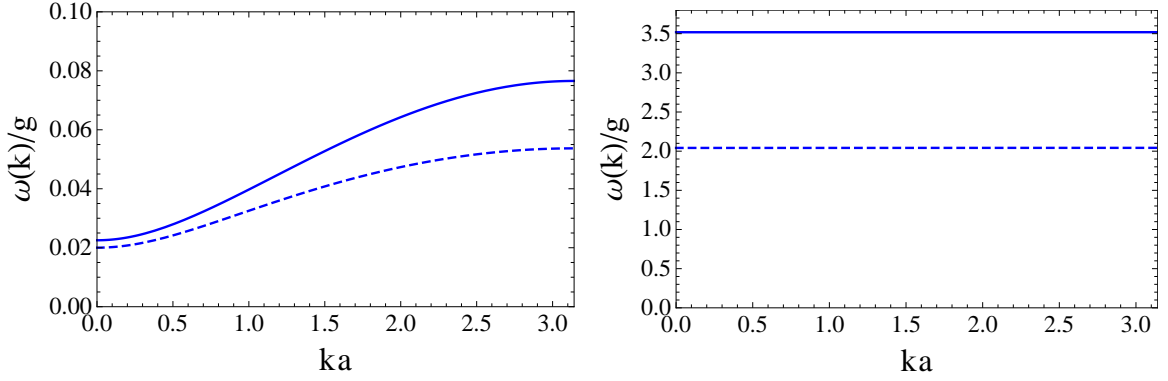


Figure 5.4: **Excitation spectra at  $T = 0$  K,  $\Delta = 0$  for  $n = 2$ ,  $\mu_{\text{eff}} = \mu_{\text{crit}} \approx -0.37 g$ ,  $\kappa z/g = 0.1$ .** The left figure shows the lower-polariton particle- (solid line) and hole excitations (dashed line). The right figure shows the mixed particle- (solid line) and hole (dashed line) excitations.

correct dispersion relations for the case of vanishing temperature and  $n > 0$  one needs to analyse the full expression

$$1 = -J(\mathbf{k}) \sum_{\alpha, \alpha'} \left[ \frac{t_{(n+1)\alpha'\alpha}^2}{E_{n\alpha} - E_{(n+1)\alpha'} + \omega} + \frac{t_{n\alpha\alpha'}^2}{E_{n\alpha} - E_{(n-1)\alpha'} - \omega} \right]. \quad (5.25)$$

The dispersion relations resulting from this equation have been calculated numerically. For the case of resonance ( $\Delta = 0$ ) the spectra are depicted in the Figures 5.1 – 5.4 for different sets of parameters. All these pictures show the dispersion  $\omega(\mathbf{k})$  divided by the coupling strength  $g$  in the first Brillouin zone.

In Figure 5.1 I plot the spectra for  $n = 1$  at the tip of the lobe. For the case of  $n = 1$  one always finds three excitation branches due to the involvement of the ground state. Two of these branches, depicted in the left diagram of Figure 5.1, lie significantly lower in energy than the third branch depicted in the right diagram. These two branches describe particle- (solid line) and hole excitations (dashed line) between lower-polariton states corresponding to  $\omega_p^{--} \hat{=} E_{2-} - E_{1-}$  and  $\omega_h^{--} \hat{=} E_{1-} - E_{0-}$ . In contrast, the single branch in the right diagram in Figure 5.1 describes a mixed particle excitation between a lower- and an upper-polariton state corresponding to  $\omega_p^{+-} \hat{=} E_{2+} - E_{1-}$ . Comparing Figure 5.1 and Figure 5.2 one finds an additional property of this mixed state particle excitation, which is, that it remains almost constant at  $\omega(\mathbf{k})/g \approx 3.2$  over the whole Brillouin zone.

Figure 5.3 shows the same relations as Figure 5.1 but for the polariton number  $n = 2$ . It is clear to see that in this case the particle excitations  $\omega_p^{--} \hat{=} E_{3-} - E_{2-}$  and hole excitations  $\omega_h^{--} \hat{=} E_{2-} - E_{1-}$ , depicted in the left diagram, formally show the same behaviour as for  $n = 1$ , but at much lower energies. The right diagram in Figure 5.3 shows the mixed particle- and hole excitations. By comparison one finds that here the particle excitation  $\omega_p^{+-} \hat{=} E_{3+} - E_{2-}$  have higher energies than  $\omega_p^{+-} \hat{=} E_{2+} - E_{1-}$  in the case of  $n = 1$ .

The changes, which the excitation spectra experience inside the Mott lobes, can be observed in the Figures 5.2 and 5.4. These diagrams show the same situation as Figures 5.1 and 5.3 but for  $\kappa < \kappa_{\text{crit}}$ . In general, this results in a shift to higher energies for small values of  $ka \approx 0$  and a shift to lower energies for high values of  $ka \approx \pi$ . This effect is almost negligible for the mixed excitations but quite strong for the lower-polariton excitations. Considering the latter, one can see from Figures 5.2 and 5.4 that, a lower-polariton particle- or hole excitation needs a finite amount of energy even in the long-wavelength limit, i.e.  $k = 0$ . Furthermore, one can see that within the Mott lobe, i.e. for  $\kappa < \kappa_{\text{crit}}$ , the lower-polariton particle- and hole excitations are always gaped in the whole Brillouin zone. This situation is opposite to the one found at the tip of the lobe, i.e.  $\mu_{\text{eff}} = \mu_{\text{crit}}$ ,  $\kappa = \kappa_{\text{crit}}$ , where the gap between the two branches vanishes for  $ka = 0$ .

At this point it is worth noticing that the excitation spectra discussed so far can, in principle, be experimentally observed using photoluminescence spectroscopy [63, 89, 167]. However, in the considered system the number of excitations is conserved, but this condition is violated by the fact, that the above excitation spectra describe the addition or removal of particles and holes from the outside, which is why they still depend on the chemical potential  $\mu$ . Therefore, it is convenient to consider the simultaneous creation of particle-hole pairs, which can be detected by means of transmission spectroscopy [97, 168, 169]. Their respective dispersion relations are given by relations of the form

$$\omega_{\text{pair}}^{\alpha\alpha'} = \omega_p^{\alpha\gamma} - \omega_h^{\gamma\alpha'}. \quad (5.26)$$

Since these pair-excitations do not change the number of polaritons in the system, they do not depend on the chemical potential anymore. The resulting dispersion relations have been obtained numerically and are depicted in the Figures 5.5 – 5.7 in the case of resonance ( $\Delta = 0$ ) for zero temperature ( $T = 0$  K) and various values for  $\kappa$ . For each polariton number I plot all possible particle-hole excitations, which leads in general to four different dispersion relations, except for  $n = 1$ , where, due to the involved ground state, only two dispersion relations emerge. All particle-hole excitations share the common property, that, for vanishing hopping strength, their dispersion relation is constant over the first Brillouin zone. This

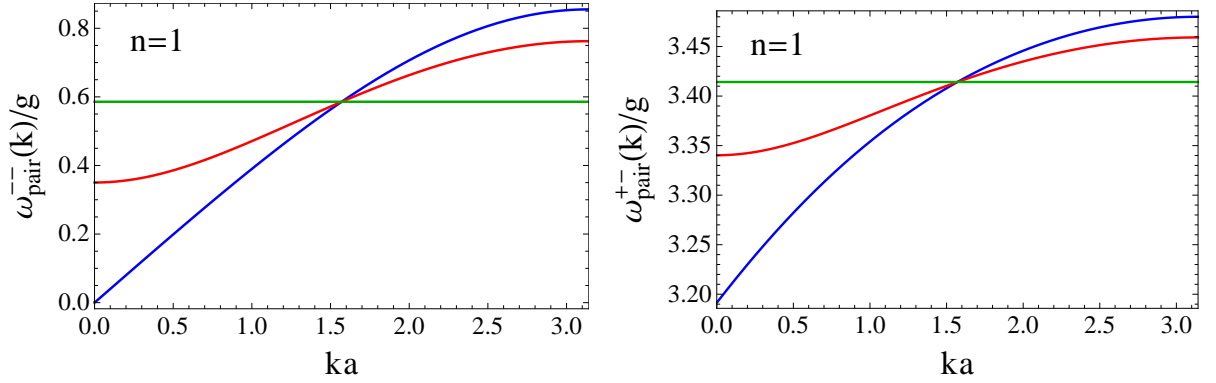


Figure 5.5: **Pair excitation at  $T = 0$  K,  $\Delta = 0$  for  $n = 1$ ,  $\mu_{\text{eff}} = \mu_{\text{crit}}$  and different values for  $\kappa$ .** The green line corresponds to  $\kappa = 0$ , the red line corresponds to  $\kappa z/g = 0.1$  and the blue line corresponds to  $\kappa = \kappa_{\text{crit}}$ .

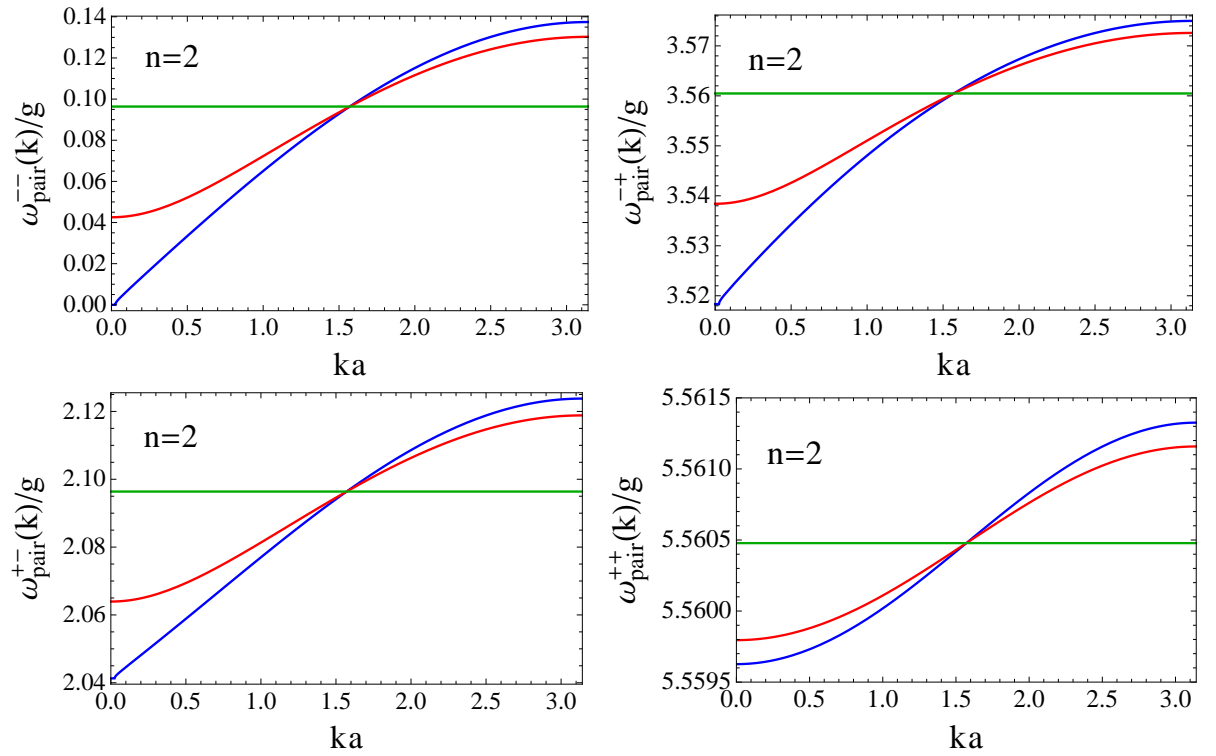


Figure 5.6: **Pair excitation at  $T = 0$  K,  $\Delta = 0$  for  $n = 2$ ,  $\mu_{\text{eff}} = \mu_{\text{crit}} \approx -0.37g$  and different values for  $\kappa$ .** The green line corresponds to  $\kappa = 0$ , the red line corresponds to  $\kappa z/g = 0.1$  and the blue line corresponds to  $\kappa = \kappa_{\text{crit}} \approx 0.0125g/z$ .

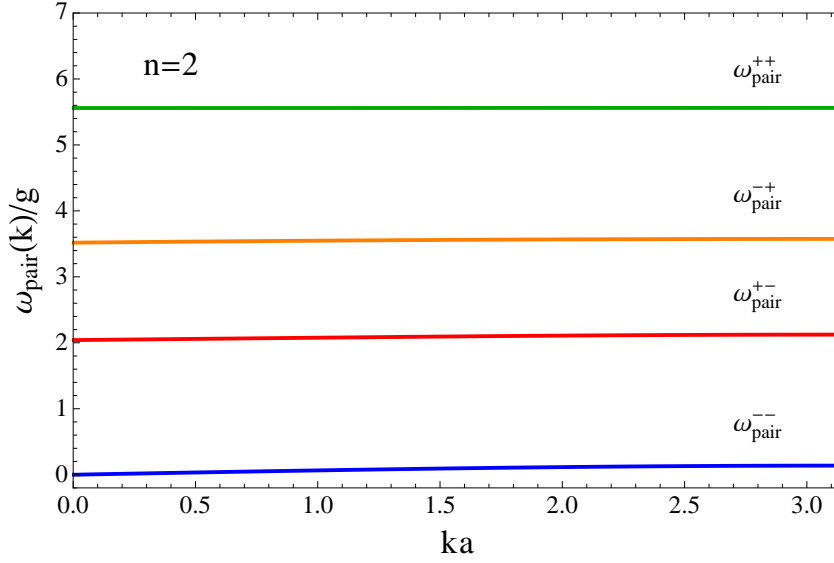


Figure 5.7: **All pair excitations at  $T = 0$  K,  $\Delta = 0$  for  $n = 2$ ,  $\mu_{\text{eff}} = \mu_{\text{crit}}$  and  $\kappa = \kappa_{\text{crit}}$ .**

reflects the fact that, in this deep Mott limit, a constant finite energy is necessary to overcome the pinning of a particle on one site and a different finite energy is needed to create a hole on another site. The sum of these energies for the different particle and hole species defines the energy of the green line in Figures 5.5 – 5.7. Increasing the parameter  $\kappa$ , and therefore enabling photons to move on the lattice, allows to diminish the pair-excitation energy. This situation corresponds to the red line in these figures. However, it also can be seen that, as long as one remains in the Mott phase, a finite energy is necessary in order to create particle-hole pairs. This situation changes only for the lower-polariton-pair excitations, when the tip of the lobe is reached, corresponding to the blue lines in Figure 5.5 and Figure 5.6. At this point the creation of particle and hole excitations does not cost any energy anymore and, thus, this point marks the onset of superfluidity. In fact one often makes use of this property to define a Mott insulator via the energy gap in the excitation spectra. From this approach follows that the phase boundary can be defined as the points where this excitation gap vanishes for the first time. Therefore, regarding the above diagrams, it becomes also evident that only the lower polaritons undergo a quantum phase transition from a Mott insulator to a superfluid, whereas all other polariton species excitations remain gaped. This fact becomes even more obvious in Figure 5.7, where I plot all pair excitation for  $n = 2$  and  $\kappa = \kappa_{\text{crit}}$  in one diagram. From this graphic it is clear to see that  $\omega_{\text{pair}}^{--}$  lies lowest in energy and all other excitations need considerably more energy. This observation justifies a posteriori that the Schrödinger perturbation theory was only investigated for the lowest polariton branch within Section 3.6 and Section 3.7. As a result I will henceforth focus my considerations on the lower polaritons, as they have the most physical impact in this model. Finally, I evaluate equation (5.19) numerically, in order to obtain the temperature depended dispersion relations. The resulting diagrams are depicted in Figure 5.8 at different fractional fillings  $\mu_{\text{eff}}$  for three different temperatures. In general, temperature fluctuations increase the particle-hole excitation energies. This effect is larger near the chemical potential that

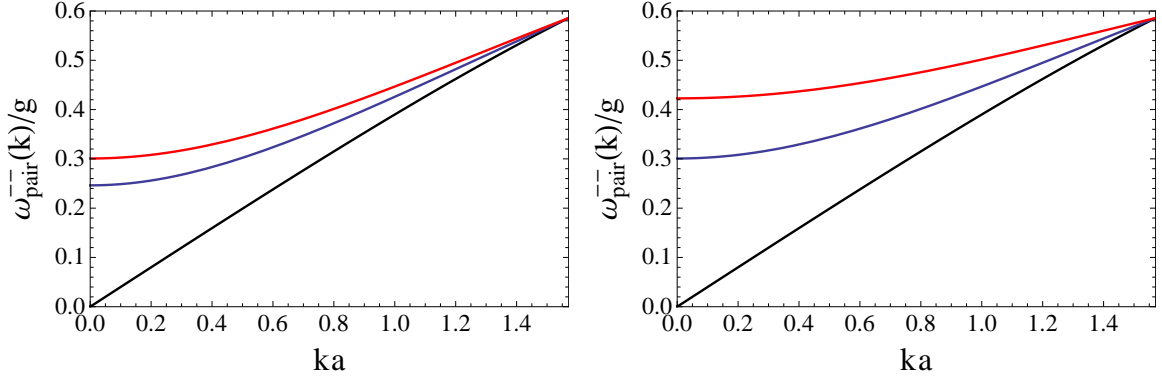


Figure 5.8: **Pair excitations at  $T > 0$  K for  $\Delta = 0$ ,  $\kappa = \kappa_{\text{crit}}|_{T=0}$  and  $n = 1$ .** Left diagram at  $\mu_{\text{eff}}/g = -0.8$ , right diagram at  $\mu_{\text{eff}}/g = -0.98$  for  $T = 0$  K (black curve),  $T = 0.01 k_B/g$  (blue curve) and  $T = 0.1 k_B/g$  (red curve).

determines the deep Mott boundaries of the lobe and weaker at the tip of the lobe, which is in agreement with the behaviour of the phase boundary at finite temperatures 4.1.

Note that the results obtained within this section are in good qualitative agreement with recent numerical simulations in 1D based on Monte-Carlo simulations [170], variational-cluster approaches [163, 171] and density-matrix-renormalization-group approaches [172] and have been also obtained in Ref. [173].

## 5.4 Energy Gap

In the previous section I found that the energy gap in the excitation spectrum of polariton particle-hole pairs is an intrinsic property of the Mott insulator can be used to define this phase and the transition to the superfluid phase. For this reason I investigate this excitation gap at  $k = 0$  more thoroughly within the present section. The easiest way to derive an analytic expression for this gap from the dispersion relations obtained in the previous section, is a Taylor expansion up to zeroth order in  $k$  with respect to  $k_0 = 0$ . This approach directly yields the energy gap:

$$\omega_{\text{p,h}}(\mathbf{k}) \approx E_{\text{gap}} + \mathcal{O}(\mathbf{k}^2). \quad (5.27)$$

The resulting dependencies for the energy gap found from the numerical evaluation are presented in Figures 5.9 and 5.10. In the left diagram of Figure 5.9 one can compare the excitation gaps for the different Mott lobes  $n = 1$  and  $n = 2$  at zero temperature. Corresponding to the size of their respective Mott lobes the energy gap for  $n = 2$  is much smaller and closes much faster than for  $n = 1$  and thus the superfluid phase is reached at much smaller values of the hopping strength. Note that, both curves for  $n = 1$  and  $n = 2$  are plotted for their respective critical chemical potential  $\mu_{\text{eff}} = \mu_{\text{crit}}$ . These results are in agreement with the energy gap as found by Ref. [173]. Note, choosing a different chemical potential only leads to a homogeneous linear shift of the curves along the y-axis. In order to observe *when* the pair excitation gap vanishes, it is therefore recommendable to investigate rather the pair excitation energy gap  $E_{\text{gap}}^{\text{pair}} = E_{\text{gap}}^{\text{p}} - E_{\text{gap}}^{\text{h}}$ . For zero temperature the resulting gap for the first

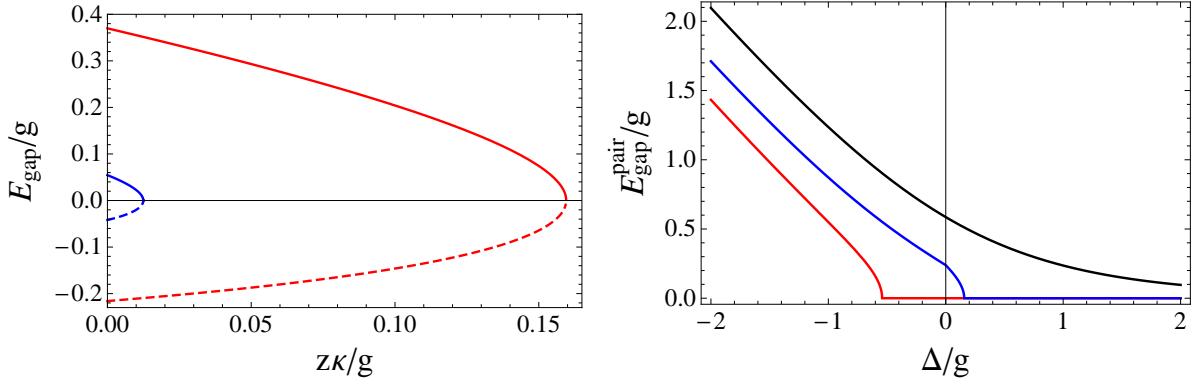


Figure 5.9: **Energy gap for  $T = 0$  K.** The left diagram shows  $E_{\text{gap}}$  for  $n = 1$  (red curve) and  $n = 2$  (blue curve) at their respective critical chemical potentials  $\mu_{\text{crit}}$ . The gap of lower-polariton particle excitation corresponds to the solid lines and the hole excitation corresponds to the dashed lines. The right diagram shows the dependence of the lower-polariton pair-excitation gap  $E_{\text{gap}}^{\text{pair}}$  for  $n = 1$  from the detuning for different hopping parameters  $\kappa z$ . The red curve corresponds to  $\kappa = \kappa_{\text{crit}}$ , the blue curve corresponds to  $\kappa z/g = 0.1$  and the black curve to  $\kappa = 0$ .

lobe  $n = 1$  is depicted in the the right diagram in Figure 5.9 in dependence of the detuning and for different values of the hopping strength  $\kappa$ . As expected, the system always remains in the Mott phase if hopping is forbidden, i.e.  $\kappa = 0$ . On the other hand, for a finite hopping probability the energy gap can also vanish depending on the detuning  $\Delta$ . From this fact it is clear to see that the detuning between cavity mode frequency and atomic transition frequency provides a perfect experimental knob to tune the system from the superfluid to Mott phase.

The temperature dependence of the particle-hole pair excitation gap is depicted in Figure 5.10. The general tendency is obviously that the energy gap for a fixed hopping strength increases with temperature. It can be seen that this effect is strongest at the tip of the Mott lobe, i.e.  $\kappa = \kappa_{\text{crit}}$ , and that it decreases when the hopping gets smaller. If hopping is strictly forbidden, the energy gap is not altered by temperature at all. Now, at a first glance, the fact that the energy gap increases with rising temperature, seems counter-intuitive. However, as shown in Section 3.7, one can not conclude from this fact that the Mott phase is increasing. Strictly speaking, there is no proper Mott insulator at finite temperature but a crossover between a phase with very small compressibility and a normal phase. Nevertheless, this effect is also known from ultra-cold atoms in optical lattices [161] and is interpreted as thermal tunnelling blockade. This would also explain why the energy gap remains unaffected for vanishing hopping strength  $\kappa = 0$ .

Furthermore, since the energy gap of lower-polariton particle-hole excitation is experimentally accessible via transmission spectroscopy, one might use this effect as a thermometer to determine the temperature of the system.

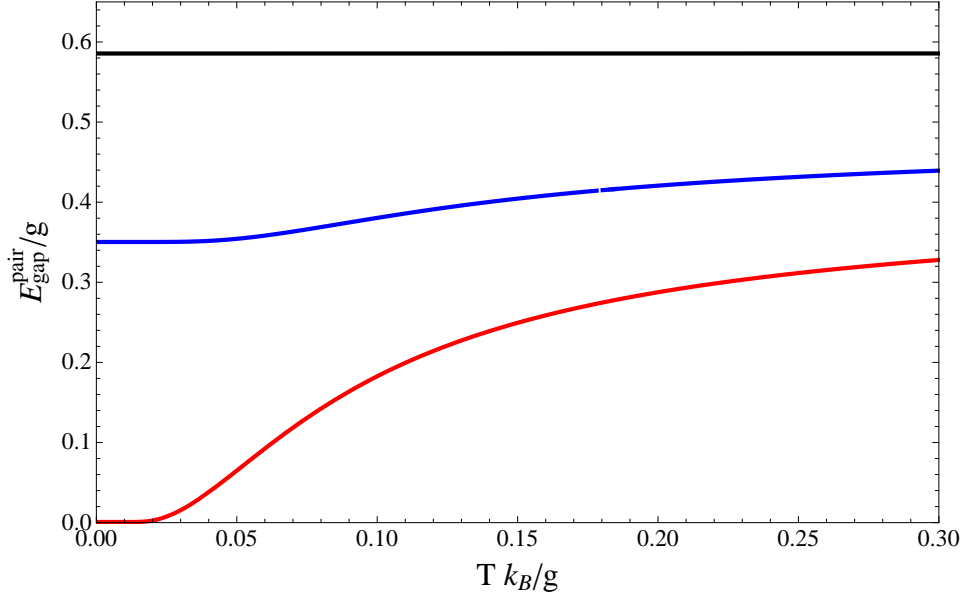


Figure 5.10: **Temperature dependence of the energy gap for  $n = 1$  and  $\Delta = 0$ .** The black line corresponds to  $\kappa = 0$ , the blue line corresponds to  $\kappa z/g = 0.1$  and the red line corresponds to the critical value  $\kappa_{\text{crit}} \approx 0.16 g/z$ .

## 5.5 Effective Mass

From the study of electronic bands in solid-state systems it is known that excitations of the system form quasi-particles, which can freely move through the solid with a motion governed by their effective mass. This effective mass is proportional to the respective energy band curvature. Motivated by this analogy, one can further investigate the dispersion relations of the polariton-holes and -particles in order to extract their effective masses. Therefore, I extend the expansion (5.27) to second order in  $\mathbf{k}$ . This yields

$$\omega_{\text{p,h}}(\mathbf{k}) \approx E_{\text{gap}} + \frac{\mathbf{k}^2}{2M_{\text{p,h}}} + \mathcal{O}(\mathbf{k}^4). \quad (5.28)$$

Hence, it is to see that the introduced effective mass for particle and holes is given by

$$M_{\text{p,h}} = \left( \left. \frac{\partial^2 \omega_{\text{p,h}}(\mathbf{k})}{\partial \mathbf{k}^2} \right|_{\mathbf{k}=0} \right)^{-1} \quad (5.29)$$

The numerically obtained results for the effective masses are presented in the Figures 5.11 and 5.12, respectively. In the left diagram in Figure 5.11 it can be seen that, the effective mass of the polariton-hole excitations is always higher than for the particle excitations. For both species the effective mass is maximal if the tunnel probability vanishes, i.e.  $\kappa = 0$ . With increasing hopping strength the effective mass of both excitations decreases almost linear. At the tip of the lobe, i.e. at  $\kappa = \kappa_{\text{crit}}$ , the effective mass for particle and hole excitations vanish simultaneously. This result is quite expected since it is a consequence of the Nambu-Goldstone theorem [174, 175]. So called Goldstone bosons naturally emerge in systems that

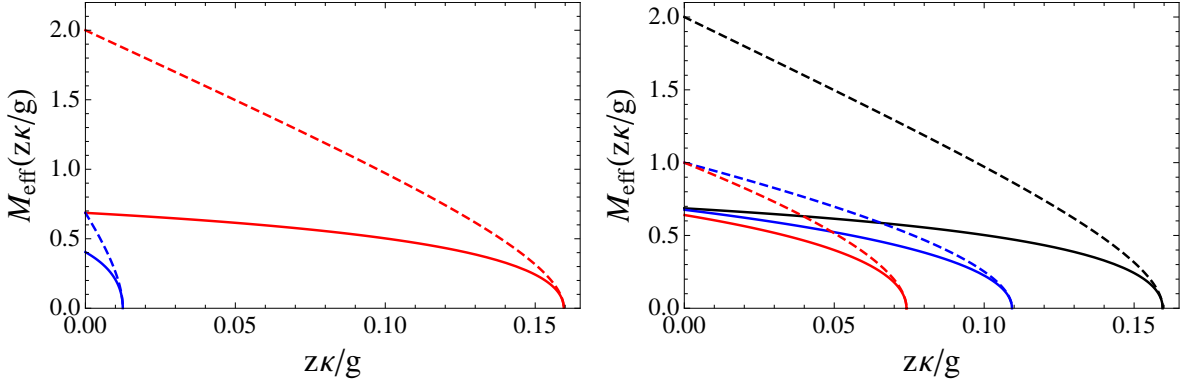


Figure 5.11: **Effective mass at  $T = 0$  K for  $\mu_{\text{eff}} = \mu_{\text{crit}}$ .** The left diagram shows the effective mass for  $n = 1$  (red) and  $n = 2$  (blue). The dashed lines correspond to the effective mass of the hole excitations and the solid lines correspond to the effective mass of the particle excitations. The right diagram shows the effective mass for  $n = 1$  at different detuning: black lines correspond to  $\Delta/g = 0$ , blue lines correspond to  $\Delta/g = 0.1$  and red lines correspond to  $\Delta/g = 0.5$ .

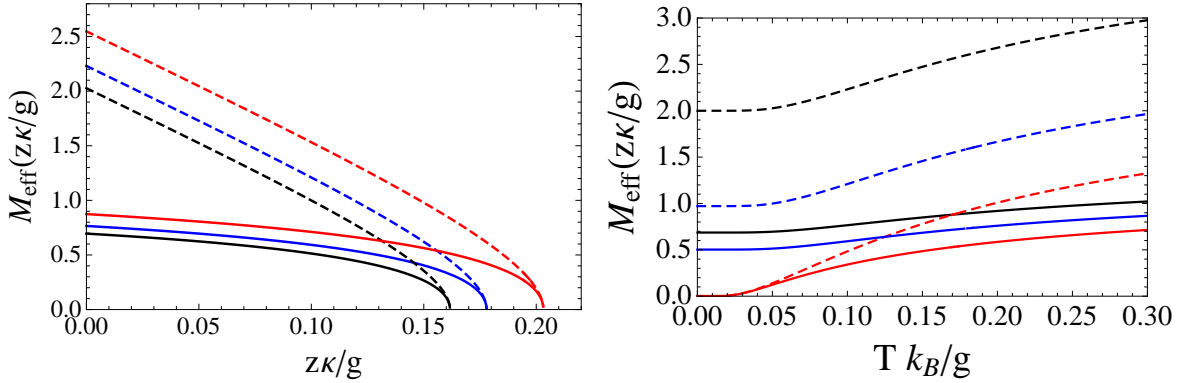


Figure 5.12: **Effective mass for finite temperatures at  $\Delta = 0$  and  $n = 1$ .** Plotted are the effective masses of particle (solid lines) and hole-excitations (dashed lines). The left diagram shows the effective masses for  $T = 0$  corresponding to the black lines,  $T = 0.1 k_B/g$  corresponding to the blue lines and  $T \approx 0.167 (k_B/g)$  corresponding to the red lines. The right diagram shows the effective masses in dependence of the temperature for different values of the hopping strength: red lines correspond to  $\kappa = \kappa_{\text{crit}}$ , blue lines correspond to  $\kappa z/g = 0.1$  and black lines correspond to  $\kappa z/g = 0.00001$ .

exhibit a spontaneous symmetry breakdown. These spin- and massless quasi particles correspond to the generators of the spontaneously broken symmetry. As shown so far, the JCH model undergoes a spontaneous symmetry breakdown during the quantum phase transition from a Mott insulator to a superfluid and, thus, lead to the Goldstone modes. These results are in agreement with the effective mass as found in Ref. [176].

In the right diagram in Figure 5.11 one can observe that non-vanishing detuning reduces the effective masses. The temperature dependence for the effective masses is shown in Figure 5.12. From the left diagram in Figure 5.12 it is to see that a rise in temperature causes an increase of the effective masses and shifts the critical hopping strength, where the masses vanishes, to higher values. The right diagram shows the exact temperature dependence for different hopping probabilities. Obviously, in general the effective masses increase with rising temperature for a fixed hopping strength, quite similar to the energy gap. Note that the effective mass of the holes is stronger affected and increases much faster with temperature than the mass of the particle excitations. For hopping probabilities beyond the critical value  $\kappa_{\text{crit}}$  the effective masses are always finite and the particle- and hole-masses are gaped. Furthermore, the gap between the particle and the hole branch increases with temperature as well, though this effect becomes weaker the smaller  $\kappa$  gets.

# Chapter 6

## Summary and Outlook

In the present thesis I investigated the thermodynamic properties of polaritons in a lattice of micro cavities filled with two-level atoms. Contrary to Bose-Einstein condensed ultra-cold atoms in optical lattices, these polaritons are quasi-particles corresponding to combined excitations of the electromagnetic cavity mode and the two-level atom. The theoretical model describing this local on-site interaction is the Jaynes-Cummings model, which I derived and discussed within the second chapter of this thesis. By showing that a non-vanishing overlap of the cavity-photon wave function leads to a Hubbard-like hopping of the photons between neighbouring cavities and encouraged by the photon blockade effect, which provides an repulsive on-site interaction, I subsequently expanded this model to the Jayne-Cummings-Hubbard model in Chapter 3. This JCH model provides the theoretical basis for the considered lattice system.

Investigating the respective Hamiltonian for the limits of on-site pinning and hopping domination, I could show qualitatively, that the examined system exhibits a quantum phase transition from a Mott insulator to a superfluid, similar to the one known for the Bose-Hubbard model. In the following, I applied two different theoretical approaches in order to analyse the thermodynamic properties of this model. On the one side, I used a standard mean-field ansatz which enabled me to extract the mean-field phase boundary for both zero and finite temperatures. The resulting phase diagram turned out to be qualitatively similar to the one found for Bose-Hubbard systems and is in agreement with results obtained by other groups [48, 160, 163]. It shows an analogue Mott-lobe structure that mainly deviates from the Bose-Hubbard case by the exponentially shrinking size of the Mott-lobes with increasing polariton number and the fact that their width depends on the mean polariton number per lattice site.

For finite temperatures, I find that the phase border is shifted to higher values of the hopping strength. This effect of finite temperatures turned out be strongest at the borders of the Mott lobes and weakest at their tip. However, investigating the compressibility at finite temperatures, I also argued that this effective reduction of the superfluid phase cannot be interpreted as a growth of the Mott-phase regime. In fact for finite temperatures there does not exist a genuine Mott insulator but instead a mixture of a Mott-like phase with an exponentially small compressibility and a normal phase with finite compressibility.

In Chapter 4 I introduced another theoretical approach. Following the procedure outlined in Reference [164], I applied an effective action ansatz, which is well-known in the investigation of classical thermodynamic phase transitions of second order. Introducing artificial symmetry-breaking currents in the JCH Hamiltonian and using the linked-cluster theorem [166] eventually led to a diagrammatic expansion of the grand-canonical free energy of the

system. I explicitly calculated this expression for the free energy up to first order in the hopping strength and to fourth order in the symmetry-breaking currents. Subsequently, I performed a Legendre transformation, mapping the unphysical symmetry-breaking currents onto physical time- and space-dependent order parameter fields. Consequently, the free energy is hereby transformed to an effective Ginzburg-Landau action.

In Chapter 5 I started investigating the implications of this theoretical approach. Evaluating the resulting physical stability conditions for a static equilibrium order parameter field I found up to the calculated level of accuracy that, this procedure exactly reproduces the mean-field phase boundary. Furthermore, for a dynamic order parameter field, I analysed the thermodynamic two-point density correlation function. From its poles I could successfully extract the dispersion relations of polariton particle- and hole-excitations in the Mott phase, as well as their energy gap and effective masses. From this analysis I found that the single-particle excitation spectra in the Mott phase are dominated by lower-polariton particle and hole bands separated by a Mott gap, which vanishes at the tip of the lobe and, hence, provides an experimental signature for the onset of superfluidity. Additionally, I observed the existence of massless Goldstone bosons at this critical point in accordance with the Nambu-Goldstone theorem.

Thus, I could show that this theoretical approach is in general capable to describe second-order quantum phase transitions [8]. Moreover this approach is, in principle, not only restricted on reproducing mean-field results but instead can be extended to include higher-order corrections with respect to the hopping. Therefore, it is advisable for a future analysis to further investigate these higher-order corrections. Specially, I would suggest to spend further attention on the calculation of quantum corrections, which become of striking importance at the tip of each Mott-lobe. Additionally, one could go ahead and calculate the excitation spectra in the superfluid phase, from which one eventually could extract the sound velocity of light on the lattice [164, 173].

In general I find the experimental idea of the JCH model quite appealing and, considering the latest advances in the fabrication and control of micro-cavity systems, I think it is a very good candidate for a possible quantum-information processing architecture. Likewise, the JCH model turns out to be very well suited as a quantum simulator for strongly correlated many-body systems. Especially the possibility to work at higher temperatures, compared to ultra-cold atoms in optical lattices, and the experimentally accessible intrinsic detuning parameter, are important advantages of this system. The latter is an essential improvement over normal Bose-Hubbard models, since it allows on one side to alter the polariton species and it provides on the other side an additional parameter which can move the system through the quantum phase transition. For this reason I would also recommend to study the JCH model without the rotating-wave approximation as suggested by the Refs. [100, 129, 146, 148, 150, 177] which turns out to be of crucial importance in far-off-resonance situation [178, 179] and allows to investigate the ultra-strong coupling regime [180–182].

Last but not least, motivated by the latest experimental approaches to implement such micro-cavity based many-body systems, I suggest to apply the theoretical approach presented within this thesis to the Tavis-Cummings [123–127] and Dicke-Bose-Hubbard model [119–121] as well. In particular, the Tavis-Cummings model would fit best for the actual experimental setup, whereas the Dicke-Bose-Hubbard model is supposed to show an even richer variety of quantum phases. Furthermore, the inclusion of disorder should result in

---

many new interesting phenomena in all these models. The same holds for going into the dispersive regime by including loss processes in the so called *bad-cavity limit* [143, 144, 151, 183–185].



# Bibliography

- [1] A. Kay and J. K. Pachos, *Quantum computation in optical lattices via global laser addressing*, *New Journal of Physics* **6** (2004) 126.
- [2] P. Treutlein, T. Steinmetz, Y. Colombe, B. Lev, P. Hommelhoff, J. Reichel, M. Greiner, O. Mandel, A. Widera, T. Rom, I. Bloch, and T. Hänsch, *Quantum information processing in optical lattices and magnetic microtraps*, *Fortschritte der Physik* **54** (2006) 702.
- [3] J. J. García-Ripoll and J. I. Cirac, *Quantum computation with cold bosonic atoms in an optical lattice*, *Philosophical transactions. Series A, Mathematical, physical, and engineering sciences* **361** (2003) 1537.
- [4] R. P. Feynman, *Simulating physics with computers*, *International Journal of Theoretical Physics* **21** (1982) 467.
- [5] J. Hubbard, *Electron correlations in narrow energy bands*, *Proceedings of the Royal Society of London. Series A*, **276** (1963) 238.
- [6] M. Fisher, P. Weichman, G. Grinstein, and D. Fisher, *Boson localization and the superfluid-insulator transition*, *Physical Review B* **40** (1989) 546.
- [7] H. Kleinert and V. Schulte-Frohlinde, *Critical properties of  $\Phi^4$  theories*. World Scientific, Singapore, 2001.
- [8] S. Sachdev, *Quantum Phase Transitions*. Cambridge University Press, Cambridge, 1999.
- [9] H. van Der Zant, F. Fritschy, W. Elion, L. Geerligs, and J. Mooij, *Field-induced superconductor-to-insulator transitions in Josephson-junction arrays*, *Physical Review Letters* **69** (1992) 2971.
- [10] A. van Oudenaarden and J. E. Mooij, *One-Dimensional Mott Insulator Formed by Quantum Vortices in Josephson Junction Arrays*, *Physical Review Letters* **76** (1996) 4947.
- [11] M. Fisher, G. Grinstein, and S. M. Girvin, *Presence of quantum diffusion in two dimensions: Universal resistance at the superconductor-insulator transition*, *Physical Review Letters* **64** (1990) 587.
- [12] S. N. Bose, *Plancks Gesetz und Lichtquantenhypothese*, *Zeitschrift für Physik* **26** (1924) 178.

- [13] A. Einstein, *Quantentheorie des einatomigen idealen Gases*, *Sitzungsberichte der preussischen Akademie der Wissenschaften* **1** (1925) 3.
- [14] M. H. Anderson, J. R. Ensher, M. R. Matthews, C. E. Wieman, and E. A. Cornell, *Observation of Bose-Einstein Condensation in a Dilute Atomic Vapor*, *Science (New York)* **269** (1995) 198.
- [15] K. B. Davis, M.-O. Mewes, M. R. Andrews, N. J. van Druten, D. S. Durfee, D. M. Kurn, and W. Ketterle, *Bose-Einstein Condensation in a Gas of Sodium Atoms*, *Physical Review Letters* **75** (1995) 3969.
- [16] M. Naraschewski, H. Wallis, A. Schenzle, J. Cirac, and P. Zoller, *Interference of Bose condensates*, *Physical Review A* **54** (1996) 2185.
- [17] M. R. Andrews, *Observation of Interference Between Two Bose Condensates*, *Science* **275** (1997) 637.
- [18] K. W. Madison, F. Chevy, W. Wohlleben, and J. Dalibard, *Vortex Formation in a Stirred Bose-Einstein Condensate*, *Physical Review Letters* **84** (2000) 806.
- [19] J. R. Abo-Shaeer, C. Raman, J. M. Vogels, and W. Ketterle, *Observation of vortex lattices in Bose-Einstein condensates*, *Science (New York)* **292** (2001) 476.
- [20] D. M. Stamper-Kurn, M. R. Andrews, A. P. Chikkatur, S. Inouye, H.-J. Miesner, J. Stenger, and W. Ketterle, *Optical Confinement of a Bose-Einstein Condensate*, *Physical Review Letters* **80** (1998) 2027.
- [21] F. Schreck, L. Khaykovich, K. Corwin, G. Ferrari, T. Bourdel, J. Cubizolles, and C. Salomon, *Quasipure Bose-Einstein Condensate Immersed in a Fermi Sea*, *Physical Review Letters* **87** (2001) 080403.
- [22] T. van Zoest, N. Gaaloul, Y. Singh, H. Ahlers, W. Herr, S. T. Seidel, W. Ertmer, E. Rasel, M. Eckart, E. Kajari, S. Arnold, G. Nandi, W. P. Schleich, R. Walser, A. Vogel, K. Sengstock, K. Bongs, W. Lewoczko-Adamczyk, M. Schiemangk, T. Schuldt, A. Peters, T. Könemann, H. Müntinga, C. Lämmerzahl, H. Dittus, T. Steinmetz, T. W. Hänsch, and J. Reichel, *Bose-Einstein condensation in microgravity*, *Science (New York)* **328** (2010) 1540.
- [23] D. Jaksch, C. Bruder, J. Cirac, C. Gardiner, and P. Zoller, *Cold Bosonic Atoms in Optical Lattices*, *Physical Review Letters* **81** (1998) 3108.
- [24] M. Greiner, O. Mandel, T. Esslinger, T. W. Hänsch, and I. Bloch, *Quantum phase transition from a superfluid to a Mott insulator in a gas of ultracold atoms*, *Nature* **415** (2002) 39.
- [25] A. Micheli, G. K. Brennen, and P. Zoller, *A toolbox for lattice-spin models with polar molecules*, *Nature Physics* **2** (2006) 341.
- [26] D. Jaksch, H.-J. Briegel, J. Cirac, C. Gardiner, and P. Zoller, *Entanglement of Atoms via Cold Controlled Collisions*, *Physical Review Letters* **82** (1999) 1975.

- 
- [27] O. Mandel, M. Greiner, A. Widera, T. Rom, T. W. Hänsch, and I. Bloch, *Controlled collisions for multi-particle entanglement of optically trapped atoms*, *Nature* **425** (2003) 937.
- [28] M. Riebe, H. Häffner, C. F. Roos, W. Hänsel, J. Benhelm, G. P. T. Lancaster, T. W. Körber, C. Becher, F. Schmidt-Kaler, D. F. V. James, and R. Blatt, *Deterministic quantum teleportation with atoms*, *Nature* **429** (2004) 734.
- [29] C. Roos, G. Lancaster, M. Riebe, H. Häffner, W. Hänsel, S. Gulde, C. Becher, J. Eschner, F. Schmidt-Kaler, and R. Blatt, *Bell States of Atoms with Ultralong Lifetimes and Their Tomographic State Analysis*, *Physical Review Letters* **92** (2004) 220402.
- [30] L. Sanchez-Palencia and L. Santos, *Bose-Einstein condensates in optical quasicrystal lattices*, *Physical Review A* **72** (2005) 053607.
- [31] V. Ahufinger, L. Sanchez-Palencia, A. Kantian, A. Sanpera, and M. Lewenstein, *Disordered ultracold atomic gases in optical lattices: A case study of Fermi-Bose mixtures*, *Physical Review A* **72** (2005) 063616.
- [32] D. Clément, A. Varón, M. Hugbart, J. Retter, P. Bouyer, L. Sanchez-Palencia, D. Gangardt, G. Shlyapnikov, and A. Aspect, *Suppression of Transport of an Interacting Elongated Bose-Einstein Condensate in a Random Potential*, *Physical Review Letters* **95** (2005) 170409.
- [33] K. V. Krutitsky, A. Pelster, and R. Graham, *Mean-field phase diagram of disordered bosons in a lattice at nonzero temperature*, *New Journal of Physics* **8** (2006) 187.
- [34] V. Yurovsky, A. Ben-Reuven, P. Julienne, and C. Williams, *Atom loss and the formation of a molecular Bose-Einstein condensate by Feshbach resonance*, *Physical Review A* **62** (2000) 043605.
- [35] S. Kokkelmans, H. Vissers, and B. Verhaar, *Formation of a Bose condensate of stable molecules via a Feshbach resonance*, *Physical Review A* **63** (2001) 031601.
- [36] M. Nomura, *A photonic crystal nanocavity laser with ultralow threshold*, *SPIE Newsroom* (2007).
- [37] K. J. Vahala, *Optical microcavities*, *Nature* **424** (2003) 839.
- [38] J. F. Sherson, C. Weitenberg, M. Endres, M. Cheneau, I. Bloch, and S. Kuhr, *Single-atom-resolved fluorescence imaging of an atomic Mott insulator*, *Nature* **467** (2010) 68.
- [39] K. Gheri and H. Ritsch, *Single-atom quantum gate for light*, *Physical Review A* **56** (1997) 3187.
- [40] L. DiCarlo, J. M. Chow, J. M. Gambetta, L. S. Bishop, B. R. Johnson, D. I. Schuster, J. Majer, A. Blais, L. Frunzio, S. M. Girvin, and R. J. Schoelkopf, *Demonstration of two-qubit algorithms with a superconducting quantum processor*, *Nature* **460** (2009) 240.

## Bibliography

---

- [41] S. Olmschenk, K. C. Younge, D. L. Moehring, D. N. Matsukevich, P. Maunz, and C. Monroe, *Manipulation and detection of a trapped Yb+ hyperfine qubit*, *Physical Review A* **76** (2007) 052314.
- [42] G. Khitrova, H. M. Gibbs, M. Kira, S. W. Koch, and A. Scherer, *Vacuum Rabi splitting in semiconductors*, *Nature Physics* **2** (2006) 81.
- [43] T. M. Benson, S. V. Boriskina, P. Sewell, A. Vukovic, S. C. Greedy, and A. I. Nosich, *Micro-optical resonators for microlasers and integrated optoelectronics: recent advances and future challenges*, *Frontiers of Planar Lightwave Circuit Technology: Design, Simulation and Fabrication* (2006) 32.
- [44] P. Grangier, G. Reymond, and N. Schlosser, *Implementations of Quantum Computing Using Cavity Quantum Electrodynamics Schemes*, *Fortschritte der Physik* **48** (2000) 859.
- [45] M. Bayindir, B. Temelkuran, and E. Ozbay, *Propagation of photons by hopping: A waveguiding mechanism through localized coupled cavities in three-dimensional photonic crystals*, *Physical Review B* **61** (2000) R11855.
- [46] M. D. Lukin, M. Fleischhauer, and A. Imamoglu, *Quantum information processing based on cavity QED with mesoscopic systems*, *Lecture Notes in Physics* **561** (2001) 193.
- [47] M. J. Hartmann, F. G. S. L. Brandão, and M. B. Plenio, *Strongly interacting polaritons in coupled arrays of cavities*, *Nature Physics* **2** (2006) 849.
- [48] A. D. Greentree, C. Tahan, J. H. Cole, and L. C. L. Hollenberg, *Quantum phase transitions of light*, *Nature Physics* **2** (2006) 856.
- [49] D. Angelakis, M. Santos, and S. Bose, *Photon-blockade-induced Mott transitions and XY spin models in coupled cavity arrays*, *Physical Review A* **76** (2007) 031805.
- [50] S. Ates, S. Ulrich, S. Reitzenstein, A. Löffler, A. Forchel, and P. Michler, *Post-Selected Indistinguishable Photons from the Resonance Fluorescence of a Single Quantum Dot in a Microcavity*, *Physical Review Letters* **103** (2009) 167402.
- [51] J. Clarke and F. K. Wilhelm, *Superconducting quantum bits*, *Nature* **453** (2008) 1031.
- [52] A. Imamoglu, H. Schmidt, G. Woods, and M. Deutsch, *Strongly Interacting Photons in a Nonlinear Cavity*, *Physical Review Letters* **79** (1997) 1467.
- [53] P. Grangier, D. Walls, and K. Gheri, *Comment on "Strongly Interacting Photons in a Nonlinear Cavity"*, *Physical Review Letters* **81** (1998) 2833.
- [54] K. Gheri, W. Alge, and P. Grangier, *Quantum analysis of the photonic blockade mechanism*, *Physical Review A* **60** (1999) R2673.
- [55] K. M. Birnbaum, A. Boca, R. Miller, A. D. Boozer, T. E. Northup, and H. J. Kimble, *Photon blockade in an optical cavity with one trapped atom*, *Nature* **436** (2005) 87.

- 
- [56] N. Didier, S. Pugnetti, Y. M. Blanter, and R. Fazio, *Detecting phonon blockade with photons*, eprint arXiv:1007.4714.
- [57] S. E. Harris, J. E. Field, and A. Imamoglu, *Nonlinear optical processes using electromagnetically induced transparency*, *Physical Review Letters* **64** (1990) 1107.
- [58] H. Schmidt and A. Imamoglu, *Giant Kerr nonlinearities obtained by electromagnetically induced transparency*, *Optics Letters* **21** (1996) 1936.
- [59] M. Werner and A. Imamoglu, *Photon-photon interactions in cavity electromagnetically induced transparency*, *Physical Review A* **61** (1999) 011801.
- [60] M. Fleischhauer, A. Imamoglu, and J. Marangos, *Electromagnetically induced transparency: Optics in coherent media*, *Reviews of Modern Physics* **77** (2005) 633.
- [61] M. Mücke, E. Figueroa, J. Bochmann, C. Hahn, K. Murr, S. Ritter, C. J. Villas-Boas, and G. Rempe, *Electromagnetically induced transparency with single atoms in a cavity*, *Nature* **465** (2010) 755–8.
- [62] H. Deng, G. Weihs, C. Santori, J. Bloch, and Y. Yamamoto, *Condensation of semiconductor microcavity exciton polaritons*, *Science (New York)* **298** (2002) 199.
- [63] J. Kasprzak, M. Richard, S. Kundermann, A. Baas, P. Jeambrun, J. M. J. Keeling, F. M. Marchetti, M. H. Szymanska, R. André, J. L. Staehli, V. Savona, P. B. Littlewood, B. Deveaud, and L. S. Dang, *Bose-Einstein condensation of exciton polaritons*, *Nature* **443** (2006) 409.
- [64] R. Balili, V. Hartwell, D. Snoke, L. Pfeiffer, and K. West, *Bose-Einstein condensation of microcavity polaritons in a trap*, *Science (New York)* **316** (2007) 1007.
- [65] A. Amo, D. Sanvitto, F. P. Laussy, D. Ballarini, E. del Valle, M. D. Martin, A. Lemaître, J. Bloch, D. N. Krizhanovskii, M. S. Skolnick, C. Tejedor, and L. Viña, *Collective fluid dynamics of a polariton condensate in a semiconductor microcavity*, *Nature* **457** (2009) 291.
- [66] A. Amo, J. Lefrère, S. Pigeon, C. Adrados, C. Ciuti, I. Carusotto, R. Houdré, E. Giacobino, and A. Bramati, *Superfluidity of polaritons in semiconductor microcavities*, *Nature Physics* **5** (2009) 805.
- [67] M. J. Hartmann, F. G. S. L. Brandão, and M. B. Plenio, *Quantum many-body phenomena in coupled cavity arrays*, *Laser & Photonics Review* **2** (2008) 527.
- [68] A. Z. Muradyan and G. A. Muradyan, *Stationary states of the Jaynes Cummings model with atomic centre-of-mass quantum motion: analytical approximation to transfer counterpropagating waves into a standing wave in a large photon number limit*, *Journal of Physics B: Atomic, Molecular and Optical Physics* **35** (2002) 3995.
- [69] L. Tan, Z.-h. Zhu, and Y. Zhang, *Entanglement dynamics of a moving multi-photon Jaynes-Cummings model in mixed states*, eprint arXiv:0907.3798.

- [70] L. Sun, S. Sun, H. Dong, W. Xie, M. Richard, L. Zhou, L. S. Dang, X. Shen, and Z. Chen, *Room temperature one-dimensional polariton condensate in a ZnO microwire*, eprint *arXiv:1007.4686*.
- [71] F. P. Laussy, E. del Valle, A. Gonzalez-Tudela, E. Cancellieri, D. Sanvitto, and C. Tejedor, *Linear and nonlinear coupling of quantum dots in microcavities*, *18th Int. Symp. "Nanostructures: Physics and Technology"* **298** (2010).
- [72] A. Laucht, J. M. Villas-Bôas, S. Stobbe, N. Hauke, F. Hofbauer, G. Böhm, P. Lodahl, M. C. Amann, M. Kaniber, and J. J. Finley, *Mutual Coupling of two Semiconductor Quantum Dots via an Optical Nanocavity Mode*, eprint *arXiv:0912.3685*.
- [73] T. Carmon, T. J. Kippenberg, L. Yang, H. Rokhsari, S. Spillane, and K. J. Vahala, *Feedback control of ultra-high-Q microcavities: application to micro-Raman lasers and microparametric oscillators*, *Optics Express* **13** (2005) 3558.
- [74] E. Wertz, L. Ferrier, D. D. Solnyshkov, R. Johné, D. Sanvitto, A. Lemaître, I. Sagnes, R. Grousson, A. V. Kavokin, P. Senellart, G. Malpuech, and J. Bloch, *Spontaneous formation and optical manipulation of extended polariton condensates*, *Nature Physics* **1** (2010) 1339.
- [75] J. M. Gérard, D. Barrier, J. Y. Marzin, R. Kuszelewicz, L. Manin, E. Costard, V. Thierry-Mieg, and T. Rivera, *Quantum boxes as active probes for photonic microstructures: The pillar microcavity case*, *Applied Physics Letters* **69** (1996) 449.
- [76] J. M. Gérard, B. Sermage, B. Gayral, B. Legrand, E. Costard, and V. Thierry-Mieg, *Enhanced Spontaneous Emission by Quantum Boxes in a Monolithic Optical Microcavity*, *Physical Review Letters* **81** (1998) 1110.
- [77] M. Kahl, T. Thomay, V. Kohnle, K. Beha, J. Merlein, M. Hagner, A. Halm, J. Ziegler, T. Nann, Y. Fedutik, U. Woggon, M. Artemyev, F. Pérez-Willard, A. Leitenstorfer, and R. Bratschitsch, *Colloidal quantum dots in all-dielectric high-Q pillar microcavities*, *Nano letters* **7** (2007) 2897.
- [78] G. Ctistis, A. Hartsuiker, E. Van Der Pol, and J. Claudon, *Selective addressing of the optical modes of a micropillar cavity with a white light beam*, eprint *arXiv:1007.0344*.
- [79] M. Maragkou, A. J. D. Grundy, E. Wertz, A. Lemaître, I. Sagnes, P. Senellart, J. Bloch, and P. G. Lagoudakis, *Spontaneous non-ground state polariton condensation in pillar microcavities*, eprint *arXiv:0907.3424*.
- [80] M. Cai, O. Painter, K. J. Vahala, and P. C. Sercel, *Fiber-coupled microsphere laser*, *Optics letters* **25** (2000) 1430.
- [81] B. Möller, U. Woggon, and M. V. Artemyev, *Photons in coupled microsphere resonators*, *Journal of Optics A: Pure and Applied Optics* **8** (2006) S113.
- [82] S. Spillane, T. Kippenberg, O. Painter, and K. Vahala, *Ideality in a Fiber-Taper-Coupled Microresonator System for Application to Cavity Quantum Electrodynamics*, *Physical Review Letters* **91** (2003) 043902.

- 
- [83] Y. Akahane, T. Asano, B.-S. Song, and S. Noda, *High-Q photonic nanocavity in a two-dimensional photonic crystal*, *Nature* **425** (2003) 944.
- [84] H. Altug and J. Vuckovic, *Two-dimensional coupled photonic crystal resonator arrays*, *Applied Physics Letters* **84** (2004) 161.
- [85] A. Badolato, K. Hennessy, M. Atatüre, J. Dreiser, E. Hu, P. M. Petroff, and A. Imamoglu, *Deterministic coupling of single quantum dots to single nanocavity modes.*, *Science (New York)* **308** (2005) 1158.
- [86] B.-S. Song, S. Noda, T. Asano, and Y. Akahane, *Ultra-high-Q photonic double-heterostructure nanocavity*, *Nature Materials* **4** (2005) 207.
- [87] K. Hennessy, A. Badolato, M. Winger, D. Gerace, M. Atatüre, S. Gulde, S. Fält, E. L. Hu, and A. Imamoglu, *Quantum nature of a strongly coupled single quantum dot-cavity system*, *Nature* **445** (2007) 896.
- [88] Y.-F. Xiao, J. Gao, X.-B. Zou, J. F. McMillan, X. Yang, Y.-L. Chen, Z.-F. Han, G.-C. Guo, and C. W. Wong, *Coupled quantum electrodynamics in photonic crystal cavities towards controlled phase gate operations*, *New Journal of Physics* **10** (2008) 123013.
- [89] W. C. Stumpf, T. Asano, T. Kojima, M. Fujita, Y. Tanaka, and S. Noda, *Spectral reflectance measurement of two-dimensional photonic nanocavities with embedded quantum dots*, *2008 IEEE/LEOS International Conference on Optical MEMs and Nanophotonics* (2008) 3.
- [90] K. Ishizaki and S. Noda, *Manipulation of photons at the surface of three-dimensional photonic crystals.*, *Nature* **460** (2009) 367.
- [91] R. Johnes, N. Gippius, and G. Malpuech, *Entangled photons from a strongly coupled quantum dot-cavity system*, *Physical Review B* **79** (2009) 155317.
- [92] A. H. Safavi-Naeini and O. Painter, *Design of optomechanical cavities and waveguides on a simultaneous bandgap phononic-photonic crystal slab*, *Optics Express* **18** (2010) 14926.
- [93] F. S. F. Brossard, X. L. Xu, D. A. Williams, M. Hadjipanayi, M. Hopkinson, X. Wang, and R. A. Taylor, *Strongly coupled single quantum dot in a photonic crystal waveguide cavity*, *eprint arXiv:1003.5185*.
- [94] A. Wallraff, D. I. Schuster, A. Blais, L. Frunzio, R. S. Huang, J. Majer, S. Kumar, S. M. Girvin, and R. J. Schoelkopf, *Strong coupling of a single photon to a superconducting qubit using circuit quantum electrodynamics*, *Nature* **431** (2004) 162.
- [95] S. M. Girvin, M. H. Devoret, and R. J. Schoelkopf, *Circuit QED and engineering charge-based superconducting qubits*, *Physica Scripta* **T137** (2009) 014012.
- [96] J. Majer, J. M. Chow, J. M. Gambetta, J. Koch, B. R. Johnson, J. A. Schreier, L. Frunzio, D. I. Schuster, A. A. Houck, A. Wallraff, A. Blais, M. H. Devoret, S. M. Girvin, and R. J. Schoelkopf, *Coupling superconducting qubits via a cavity bus*, *Nature* **449** (2007) 443.

## Bibliography

---

- [97] J. M. Fink, M. Göppl, M. Baur, R. Bianchetti, P. J. Leek, A. Blais, and A. Wallraff, *Climbing the Jaynes-Cummings ladder and observing its nonlinearity in a cavity QED system*, *Nature* **454** (2008) 315.
- [98] M. A. Sillanpää, J. I. Park, and R. W. Simmonds, *Coherent quantum state storage and transfer between two phase qubits via a resonant cavity*, *Nature* **449** (2007) 438.
- [99] J. M. Fink, L. Steffen, P. Studer, L. S. Bishop, M. Baur, R. Bianchetti, D. Bozyigit, C. Lang, S. Filipp, P. J. Leek, and A. Wallraff, *Quantum-to-Classical Transition in Cavity Quantum Electrodynamics (QED)*, *eprint arXiv:1003.1161*.
- [100] C. Sabín, J. J. García-Ripoll, E. Solano, and J. León, *Dynamics of entanglement via propagating microwave photons*, *Physical Review B* **81** (2010) 6.
- [101] A. Abdumalikov, O. Astafiev, Y. Nakamura, Y. Pashkin, and J. Tsai, *Vacuum Rabi splitting due to strong coupling of a flux qubit and a coplanar-waveguide resonator*, *Physical Review B* **78** (2008) 180502.
- [102] T. Niemczyk, F. Deppe, H. Huebl, E. P. Menzel, F. Hocke, M. J. Schwarz, J. J. García-Ripoll, D. Zueco, T. Hümmer, E. Solano, A. Marx, and R. Gross, *Circuit quantum electrodynamics in the ultrastrong-coupling regime*, *Nature Physics* (2010).
- [103] Y. Makhlin, G. Schön, and A. Shnirman, *Quantum-state engineering with Josephson-junction devices*, *Reviews of Modern Physics* **73** (2001) 357.
- [104] P. E. Barclay, K. Srinivasan, O. Painter, B. Lev, and H. Mabuchi, *Integration of fiber-coupled high-Q SiN microdisks with atom chips*, *Applied Physics Letters* **89** (2006) 131108.
- [105] A. M. Armani, A. Srinivasan, and K. J. Vahala, *Soft lithographic fabrication of high Q polymer microcavity arrays.*, *Nano Letters* **7** (2007) 1823.
- [106] S. M. Spillane, T. J. Kippenberg, and K. J. Vahala, *Ultra-high- Q toroidal microresonators for cavity quantum electrodynamics*, *Physical Review A* **71** (2005) 013817.
- [107] T. J. Kippenberg, S. M. Spillane, D. K. Armani, and K. J. Vahala, *Fabrication and coupling to planar high-Q silica disk microcavities*, *Applied Physics Letters* **83** (2003) 797.
- [108] T. J. Kippenberg, S. M. Spillane, and K. J. Vahala, *Demonstration of ultra-high-Q small mode volume toroid microcavities on a chip*, *Applied Physics Letters* **85** (2004) 6113.
- [109] T. J. Kippenberg, S. M. Spillane, D. K. Armani, and K. J. Vahala, *Ultralow-threshold microcavity Raman laser on a microelectronic chip*, *Optics Letters* **29** (2004) 1224.
- [110] D. K. Armani, T. J. Kippenberg, S. M. Spillane, and K. J. Vahala, *Ultra-high-Q toroid microcavity on a chip*, *Nature* **421** (2003) 925.

- 
- [111] T. Aoki, B. Dayan, E. Wilcut, W. P. Bowen, A. S. Parkins, T. J. Kippenberg, K. J. Vahala, and H. J. Kimble, *Observation of strong coupling between one atom and a monolithic microresonator*, *Nature* **443** (2006) 671.
- [112] M. Bajcsy, S. Hofferberth, V. Balic, T. Peyronel, M. Hafezi, A. Zibrov, V. Vuletic, and M. D. Lukin, *Efficient All-Optical Switching Using Slow Light within a Hollow Fiber*, *Physical Review Letters* **102** (2009) 203902.
- [113] A. Dawes, *Optical switching with cold atoms*, *Physics* **2** (2009) 41.
- [114] M. Trupke, E. A. Hinds, S. Eriksson, E. A. Curtis, Z. Moktadir, E. Kukhareuka, and M. Kraft, *Microfabricated high-finesse optical cavity with open access and small volume*, *Applied Physics Letters* **87** (2005) 211106.
- [115] M. Trupke, J. Goldwin, B. Darquié, G. Dutier, S. Eriksson, J. P. Ashmore, and E. A. Hinds, *Atom Detection and Photon Production in a Scalable, Open, Optical Microcavity*, *Physical Review Letters* **99** (2007) 63601.
- [116] G. N. Lewis, Z. Moktadir, C. Gollasch, M. Kraft, S. Pollock, F. Ramirez-Martinez, J. P. Ashmore, A. Laliotis, M. Trupke, and E. A. Hinds, *Fabrication of Magneto-optical Atom Traps on a Chip*, *Journal of Microelectromechanical Systems* **18** (2009) 347.
- [117] Y. Colombe, T. Steinmetz, G. Dubois, F. Linke, D. Hunger, and J. Reichel, *Strong atom-field coupling for Bose-Einstein condensates in an optical cavity on a chip*, *Nature* **450** (2007) 272.
- [118] D. Leibfried, B. DeMarco, V. Meyer, D. Lucas, M. Barrett, J. Britton, W. M. Itano, B. Jelenković, C. Langer, T. Rosenband, and D. J. Wineland, *Experimental demonstration of a robust, high-fidelity geometric two ion-qubit phase gate*, *Nature* **422** (2003) 412.
- [119] R. Dicke, *Coherence in Spontaneous Radiation Processes*, *Physical Review* **93** (1954) 99.
- [120] Y. Wang and F. Hioe, *Phase Transition in the Dicke Model of Superradiance*, *Physical Review A* **7** (1973) 831.
- [121] W. Mallory, *Superradiant phase transition in the Dicke Hamiltonian*, *Physical Review A* **11** (1975) 1088.
- [122] B. Shore and P. Knight, *The Jaynes-Cummings Model*, *Journal of Modern Optics* **40** (1993) 1195.
- [123] M. Tavis and F. Cummings, *Exact Solution for an N-Molecule-Radiation-Field Hamiltonian*, *Physical Review* **170** (1968) 379.
- [124] A. Retzker, E. Solano, and B. Reznik, *Tavis-Cummings model and collective multiqubit entanglement in trapped ions*, *Physical Review A* **75** (2007) 022312.

## Bibliography

---

- [125] C. López, H. Christ, J. Retamal, and E. Solano, *Effective quantum dynamics of interacting systems with inhomogeneous coupling*, *Physical Review A* **75** (2007) 033818.
- [126] J. Fink, R. Bianchetti, M. Baur, M. Göppl, L. Steffen, S. Filipp, P. Leek, A. Blais, and A. Wallraff, *Dressed Collective Qubit States and the Tavis-Cummings Model in Circuit QED*, *Physical Review Letters* **103** (2009) 083601.
- [127] M. Knap, E. Arrigoni, and W. von Der Linden, *Quantum phase transition and excitations of the Tavis-Cummings lattice model*, *Physical Review B* **82** (2010) 045126.
- [128] S.-C. Lei and R.-K. Lee, *Quantum phase transitions of light in the Dicke-Bose-Hubbard model*, *Physical Review A* **77** (2008) 033827.
- [129] B. M. Rodríguez-Lara and R.-K. Lee, *Quantum phase transition of nonlinear light in the finite size Dicke Hamiltonian*, eprint arXiv:1005.3884.
- [130] K. Baumann, C. Guerlin, F. Brennecke, and T. Esslinger, *The Dicke Quantum Phase Transition with a Superfluid Gas in an Optical Cavity*, *Nature* **464** (2009) 1301.
- [131] F. W. Cummings and E. T. Jaynes, *Comparison of quantum and semiclassical radiation theories with application to the beam maser*, *Proceedings of the IEEE* **51** (1963) 89.
- [132] W. Neuhauser, M. Hohenstatt, P. Toschek, and H. Dehmelt, *Optical-Sideband Cooling of Visible Atom Cloud Confined in Parabolic Well*, *Physical Review Letters* **41** (1978) 233.
- [133] D. Wineland, R. Drullinger, and F. Walls, *Radiation-Pressure Cooling of Bound Resonant Absorbers*, *Physical Review Letters* **40** (1978) 1639.
- [134] A. Ashkin, *Optical trapping and manipulation of neutral particles using lasers*, *Proceedings of the National Academy of Sciences of the United States of America* **94** (1997) 4853.
- [135] C. C. Gerry and P. L. Knight, *Introduction to Quantum Optics*. Cambridge University Press, New York, 2005.
- [136] C. L. Tang, *Fundamentals of Quantum Mechanics For Solid State Electronics and Optics*. Cambridge University Press, New York, 2005.
- [137] V. Vedral, *Modern Foundations of Quantum Optics*. Imperial College Press, Leeds, UK, 2005.
- [138] P. Meystre and M. Sargent, *Elements of Quantum Optics*. Springer, Berlin, 4 ed., 2007.
- [139] J. D. Jackson, *Classical Electrodynamics*. Walter de Gruyter, Berlin, 2 ed., 1999.
- [140] F. P. Laussy, E. del Valle, M. R. Singh, and R. H. Lipson, *Optical Spectra of the Jaynes-Cummings Ladder*, *AIP Conference Proceedings* **1147** (2009) 46.

- 
- [141] J. Lisenfeld, C. Müller, J. H. Cole, P. Bushev, A. Lukashenko, A. Shnirman, and A. V. Ustinov, *Rabi spectroscopy of a qubit-fluctuator system*, *Physical Review B* **81** (2010) 100511.
- [142] A. Tomadin, V. Giovannetti, R. Fazio, D. Gerace, I. Carusotto, H. Türeci, and A. Imamoglu, *Signatures of the superfluid-insulator phase transition in laser-driven dissipative nonlinear cavity arrays*, *Physical Review A* **81** (2010) 061801.
- [143] A. Sørensen and K. Mølmer, *Entangling atoms in bad cavities*, *Physical Review A* **66** (2002) 022314.
- [144] L. S. Bishop, E. Ginossar, and S. M. Girvin, *Response of the Strongly Driven Jaynes-Cummings Oscillator*, *Physical Review Letters* **105** (2010) 100505.
- [145] M. Leib and M. J. Hartmann, *Bose-Hubbard dynamics of polaritons in a chain of circuit QED cavities*, eprint *arXiv:1006.2935*.
- [146] I. D. Feranchuk, L. I. Komarov, and A. P. Ulyanenko, *Two-level system in a one-mode quantum field: numerical solution on the basis of the operator method*, *Journal of Physics A: Mathematical and General* **29** (1996) 4035.
- [147] J. Q. Shen, *An approach to the time-dependent Jaynes-Cummings model without the rotating wave approximation*, eprint *arXiv:quant-ph/0311140*.
- [148] M.-F. Fang and P. Zhou, *Multiphoton Jaynes-Cummings Model without the Rotating-wave Approximation*, *Journal of Modern Optics* **42** (1995) 1199.
- [149] A. Kurcz, A. Capolupo, A. Beige, E. Del Giudice, and G. Vitiello, *Energy concentration in composite quantum systems*, *Physical Review A* **81** (2010) 063821.
- [150] A. Kurcz, A. Capolupo, A. Beige, E. Del Giudice, and G. Vitiello, *Rotating wave approximation and entropy*, eprint *arXiv:1001.3944*.
- [151] S. Ferretti, L. C. Andreani, H. E. Türeci, and D. Gerace, *Photon correlations in a two-site non-linear cavity system under coherent drive and dissipation*, eprint *arXiv:1007.0384*.
- [152] R. Glauber and M. Lewenstein, *Quantum optics of dielectric media*, *Physical Review A* **43** (1991) 467.
- [153] K. Liu and L. Tan, *Dissipation Properties of Coupled Cavity Arrays*, eprint *arXiv:1006.4412*.
- [154] N. Marzari and D. Vanderbilt, *Maximally localized generalized Wannier functions for composite energy bands*, *Physical Review B* **56** (1997) 12847.
- [155] F. E. A. dos Santos and A. Pelster, *Quantum phase diagram of bosons in optical lattices*, *Physical Review A* **79** (2009) 013614.

## Bibliography

---

- [156] H. Kleinert, *Path integrals in Quantum Mechanics, Statistics, Polymer Physics, and Financial Markets*. World Scientific, Singapore, 4th ed., 2006.
- [157] A. Hoffmann, *Bosonen im optischen Gitter*. Diploma thesis, Freie Universität Berlin, 2007.
- [158] M. Ohliger, *Thermodynamic Properties of Spinor Bosons in Optical Lattices*. Diploma thesis, Freie Universität Berlin, 2008.
- [159] T. D. Grass, *Real-Time Ginzburg-Landau Theory for Bosonic Gases in Optical Lattices*. Diploma thesis, Freie Universität Berlin, 2009.
- [160] J. Koch and K. Le Hur, *Superfluid-Mott-insulator transition of light in the Jaynes-Cummings lattice*, *Physical Review A* **80** (2009) 023811.
- [161] D. Dickerscheid, D. van Oosten, P. Denteneer, and H. Stoof, *Ultracold atoms in optical lattices*, *Physical Review A* **68** (2003) 043623.
- [162] L. Plimak, M. Olsen, and M. Fleischhauer, *Occupation number and fluctuations in the finite-temperature Bose-Hubbard model*, *Physical Review A* **70** (2004) 013611.
- [163] M. Aichhorn, M. Hohenadler, C. Tahan, and P. B. Littlewood, *Quantum Fluctuations, Temperature, and Detuning Effects in Solid-Light Systems*, *Physical Review Letters* **100** (2008) 216401.
- [164] B. Bradlyn, F. E. A. Dos Santos, and A. Pelster, *Effective action approach for quantum phase transitions in bosonic lattices*, *Physical Review A* **79** (2009) 013615.
- [165] J. W. Negele and H. Orland, *Quantum many-particle systems*. Westview Press, 1998.
- [166] W. Metzner, *Linked-cluster expansion around the atomic limit of the Hubbard model*, *Physical Review B* **43** (1991) 8549.
- [167] A. N. Poddubny, M. M. Glazov, and N. S. Averkiev, *Non-linear emission spectra of quantum dots strongly coupled to photonic mode*, eprint *arXiv:1007.0244*.
- [168] A. Niskanen, K. Harrabi, F. Yoshihara, Y. Nakamura, and J. Tsai, *Spectroscopy of three strongly coupled flux qubits*, *Physical Review B* **74** (2006) 220503.
- [169] F. Deppe, M. Mariani, E. P. Menzel, A. Marx, S. Saito, K. Kakuyanagi, H. Tanaka, T. Meno, K. Semba, H. Takayanagi, E. Solano, and R. Gross, *Two-photon probe of the Jaynes-Cummings model and controlled symmetry breaking in circuit QED*, *Nature Physics* **4** (2008) 686.
- [170] P. Phipps, H. Evertz, and M. Hohenadler, *Excitation spectra of strongly correlated lattice bosons and polaritons*, *Physical Review A* **80** (2009) 033612.
- [171] M. Knap, E. Arrigoni, and W. von Der Linden, *Spectral properties of coupled cavity arrays in one dimension*, *Physical Review B* **81** (2010) 104303.

- 
- [172] A. Mering, M. Fleischhauer, P. Ivanov, and K. Singer, *Analytic approximations to the phase diagram of the Jaynes-Cummings-Hubbard model*, *Physical Review A* **80** (2009) 053821.
- [173] S. Schmidt and G. Blatter, *Excitations of Strongly Correlated Lattice Polaritons*, *Physical Review Letters* **104** (2010) 216402.
- [174] Y. Nambu, *Quasi-Particles and Gauge Invariance in the Theory of Superconductivity*, *Physical Review* **117** (1960) 648.
- [175] J. Goldstone, A. Salam, and S. Weinberg, *Broken Symmetries*, *Physical Review* **127** (1962) 965.
- [176] S. Schmidt and G. Blatter, *Strong Coupling Theory for the Jaynes-Cummings-Hubbard Model*, *Physical Review Letters* **103** (2009) 086403.
- [177] T. Werlang, A. Dodonov, E. Duzzioni, and C. Villas-Bôas, *Rabi model beyond the rotating-wave approximation: Generation of photons from vacuum through decoherence*, *Physical Review A* **78** (2008) 053805.
- [178] A. Santana, J. Llorente, and V. Vedral, *Semiclassical dressed states of two-level quantum systems driven by non-resonant and/or strong laser fields*, *Journal of Physics B* **34** (2001) 2371.
- [179] C. Ogden, E. Irish, and M. Kim, *Dynamics in a coupled-cavity array*, *Physical Review A* **78** (2008) 063805.
- [180] J. Casanova, G. Romero, I. Lizuain, J. J. Garcia-Ripoll, and E. Solano, *Deep Ultrastrong Coupling Regime of the Jaynes-Cummings model*, eprint arXiv:1008.1240.
- [181] J. Hausinger and M. Grifoni, *The qubit-oscillator system: an analytical treatment of the ultra-strong coupling regime*, eprint arXiv:1007.5437.
- [182] Q.-H. Chen, L. Li, T. Liu, and K.-L. Wang, *Theory of Spectrum in Qubit-Oscillator Systems in the Ultrastrong Coupling Regime*, eprint arXiv:1007.1747.
- [183] D. I. Schuster, A. A. Houck, J. A. Schreier, A. Wallraff, J. M. Gambetta, A. Blais, L. Frunzio, J. Majer, B. Johnson, M. H. Devoret, S. M. Girvin, and R. J. Schoelkopf, *Resolving photon number states in a superconducting circuit*, *Nature* **445** (2007) 515.
- [184] J. M. Gambetta, A. Blais, D. Schuster, A. Wallraff, L. Frunzio, J. Majer, M. Devoret, S. M. Girvin, and R. Schoelkopf, *Qubit-photon interactions in a cavity: Measurement-induced dephasing and number splitting*, *Physical Review A* **74** (2006) 042318.
- [185] Z. Fang, R. Guo, X. Zhou, and X. Chen, *Atomic spatial coherence with spontaneous emission in a strong coupling cavity*, eprint arXiv:1007.0794.



# List of Figures

1.1	Micro cavity lattice . . . . .	3
1.2	Experimental setups (1) . . . . .	4
1.3	Experimental setups (2) . . . . .	5
1.4	Experimental setups (3) . . . . .	5
1.5	Experimental setups (4) . . . . .	6
2.1	Energy structure of two-level system . . . . .	19
2.2	Two-level system in micro cavity . . . . .	24
2.3	Energy eigenvalues of Jaynes-Cummings model . . . . .	29
2.4	Energy structure of Jaynes-Cummings model . . . . .	33
3.1	Critical chemical potential . . . . .	44
3.2	Energy bands in hopping limit . . . . .	46
3.3	Energy landscape for second-order phase transition. . . . .	56
3.4	4th order Landau coefficient versus detuning . . . . .	57
3.5	JCH and BH mean-field phase boundary for $T = 0$ K. . . . .	58
3.6	JCH phase boundary for non-zero detuning. . . . .	59
4.1	Mean-field phase diagram at finite temperatures . . . . .	71
4.2	Polariton occupation number at finite temperatures . . . . .	72
4.3	Isothermal compressibility at finite temperatures . . . . .	73
5.1	Excitation spectra: $T = 0$ K, $\Delta = 0$ , $n = 1$ , $\mu_{\text{eff}} = \mu_{\text{crit}}$ , $\kappa = \kappa_{\text{crit}}$ . . . . .	105
5.2	Excitation spectra: $T = 0$ K, $\Delta = 0$ , $n = 1$ , $\mu_{\text{eff}} = \mu_{\text{crit}}$ , $\kappa Z/g = 0.1$ . . . . .	105
5.3	Excitation spectra: $T = 0$ K, $\Delta = 0$ , $n = 2$ , $\mu_{\text{eff}} = \mu_{\text{crit}}$ , $\kappa = \kappa_{\text{crit}}$ . . . . .	106
5.4	Excitation spectra: $T = 0$ K, $\Delta = 0$ , $n = 2$ , $\mu_{\text{eff}} = \mu_{\text{crit}}$ , $\kappa Z/g = 0.1$ . . . . .	106
5.5	Pair excitation: $T = 0$ K, $\Delta = 0$ , $n = 1$ , $\mu_{\text{eff}} = \mu_{\text{crit}}$ . . . . .	108
5.6	Pair excitation: $T = 0$ K, $\Delta = 0$ , $n = 2$ , $\mu_{\text{eff}} = \mu_{\text{crit}}$ . . . . .	108
5.7	All pair excitations: $T = 0$ K, $\Delta = 0$ , $n = 2$ , $\mu_{\text{eff}} = \mu_{\text{crit}}$ <b>and</b> $\kappa = \kappa_{\text{crit}}$ . . . . .	109
5.8	Pair excitations at $T > 0$ K for $\Delta = 0$ , $\kappa = \kappa_{\text{crit}}$ <b>and</b> $n = 1$ . . . . .	110
5.9	Energy gap at $T = 0$ K. . . . .	111
5.10	Temperature dependence of the energy gap for $n = 1$ and $\Delta = 0$ . . . . .	112
5.11	Effective mass at $T = 0$ K for $\mu_{\text{eff}} = \mu_{\text{crit}}$ . . . . .	113
5.12	Effective mass for finite temperatures at $\Delta = 0$ and $n = 1$ . . . . .	113



# Danksagung

Die hier vorgelegte Arbeit bildet den Abschluss meines Diplomstudiums. Eine so umfangreiche Arbeit lässt sich nur schwer alleine verwirklichen. Daher möchte ich an dieser Stelle die Gelegenheit nutzen und mich bei all jenen Personen bedanken, die mir beim Erreichen dieses Zieles geholfen haben.

An erster Stelle gebührt dieser Dank meiner Mutter, die mir dieses Studium erst ermöglichte und mich immer voll unterstützt und an mich geglaubt hat. Sie hat mir oft den Rücken frei gehalten und ohne Sie wäre ich nicht da, wo ich jetzt bin.

Besonders herzlich danke ich Herrn PD Dr. Axel Pelster für seine hervorragende Betreuung und Unterstützung während dieser Zeit. Obwohl er den letzten Monat in Duisburg arbeitet, war er für mich jederzeit erreichbar und fand immer die Zeit, sich um meine Probleme zu kümmern. Vor allem sein intensives Korrekturlesen dieser Arbeit hat mich vor vielen Rechtschreibfehlern und einige inhaltlichen Fehlern bewahrt. Ohne seine Anleitung und Erklärungen wäre es mir nicht möglich gewesen, diese Diplomarbeit anzufertigen.

Bei Herrn Prof. Kleinert möchte ich mich dafür bedanken, dass er mir ermöglicht hat diese Diplomarbeit in seiner Arbeitsgruppe anzufertigen.

Weiterhin möchte ich mich bei Mathias Hayn für die interessanten Diskussionen und Anregungen sowie für seine Hilfe bei der Fehlerkorrektur bedanken. Ednilson dos Santos danke ich dafür, dass ich immer mit meinen Fragen zu ihm kommen konnte wenn ich nicht mehr weiter wusste. Für die angenehme Atmosphäre in der Arbeitsgruppe während der letzten 12 Monate und für die vielen interessanten Gespräche danke ich allen Gruppenmitgliedern, insbesondere Florian Linder, der mir über lange Strecken als einziger im Büro Gesellschaft geleistet hat, Hendrik Ludwig, der mit seinen lustigen Anekdoten immer wieder für Heiterkeit gesorgt hat und Victor Bezerra und Aristeu Lima, die mir immer mit Rat und Tat zur Seite standen.

Zum Schluss geht noch ein ganz dickes Dankeschön an Tobias Homberg und Alex Krüger, ohne sie wäre das Studium nur halb so lustig gewesen. Ich kann mich glücklich schätzen, dass es mir gelungen ist so gute Freunde zu finden.